Imaging Myelin Basic Protein expression in a model of remyelination by Magnetic Resonance Imaging using an Organic Anion Transporter Protein gene reporter system

Myfanwy F.E. Hill

Pembroke College

University of Cambridge

Supervisors:

Professor Robin J.M. Franklin

Wellcome Trust-MRC Cambridge Stem Cell Institute

Professor Kevin M. Brindle

Cambridge Institute, Cancer Research UK

This dissertation is submitted for the Degree of *Doctor of Philosophy*

October 2018

Declaration

This dissertation is the result of my own work and includes nothing which is the outcome of work done in collaboration except as declared in the Preface and specified in the text. It is not substantially the same as any that I have submitted, or, is being concurrently submitted for a degree or diploma or other qualification at the University of Cambridge or any other University or similar institution except as declared in the Preface and specified in the text. I further state that no substantial part of my dissertation has already been submitted, or, is being concurrently submitted for any such degree, diploma or other qualification at the University of Cambridge or any other University or similar institution except as declared in the Preface and specified in the text. It does not exceed the word limit of 60,000 words as prescribed by the Degree Committee for the Department of Clinical Neuroscience, University of Cambridge School of Clinical Medicine.

Myfanwy Frances Elizabeth Hill

May 2019

Summary

Demyelination occurs in several CNS diseases. If demyelinated axons are not remyelinated they become vulnerable to irreversible degeneration. There is, therefore, a clinical need for therapies that enhance remyelination. This can be achieved by 1) pharmacologically targeting endogenous oligodendrocyte progenitor cells (OPCs) responsible for remyelination or 2) transplantation of myelinogenic cells (including OPCs). The first approach is appropriate for diseases with no defect in the myelinating cells, such as multiple sclerosis (MS), while the second approach is suitable for genetic disorders of myelination such as Pelizaeus Merzbacher disease (PMD). Translation into the clinic has or will shortly begin for both approaches. However, there are no current outcome measures providing direct evidence of OPCs differentiation to assess the efficacy of a remyelination therapy.

This thesis presents data which it is hoped will form the foundation of a novel outcome measure for such therapies.

It demonstrates that, by using a novel MRI gene reporter system; OATP, and controlling its expression under a Myelin Basic Protein promoter, OPCs can take up gadolinium based contrast, and be detected using T_1 weighted MRI imaging *in vitro* and *ex vivo*. Using a constitutively active promoter, transplanted cells can be detected by an *in vivo* model of remyelination.

It is hoped that this data will form the foundation for the development of an outcome measure for assessing the efficacy of new, pro-remyelination therapies, and provide a non-invasive, longitudinal, and translational imaging technique for use in drug discovery, or even personalised medicine.

Acknowledgements

I would first like to acknowledge the generous support of the The Wellcome Trust who awarded me the Research Training Fellowship in 2015 which has funded my PhD studies. I would also like to thank them for their support of Veterinary Surgeon clinicians in general, and for all the work they do to promote our role as basic scientists; without their financial support and guidance, my research carrier would not have been possible.

I must next thank my primary supervisor; Professor Robin Franklin, who has been so much more to me than just an academic guide; he has been an inspiration for over a decade. It is because of him that I have a passion for science and research, and that I was able to see a path in to a research career from my beginnings as a veterinary surgeon. Robin's support has gone beyond all hope or expectation and I am hugely grateful for all he has done, not least the lone of the *The Eagles Nest* during the period of my write up.

Next, I would like to thank my second supervisor Professor Kevin Brindle who believed in me and my work, and guided my collaborations with his group. In particular, I must acknowledge the support of Dr Alan Wright, Dr Andre Neves, Dr Susana Ros, Ms Sarah McGuire, and Ms Lyn Ansat-Ansari who have guided my work and welcomed me on my various sojourns over to *their place*.

It goes without saying that Pembroke College has contributed hugely to my three years of study. The friends I have made there and the community it provided me with, have offered love, support, and boundless friendship. I cannot express how much joy my association with

my college has brought me over these years, most particularly in the latter days of my thesis the availability of the '*procrastabath*' was an indispensable innovation. There are not thanks enough in the world to fully acknowledge the gratitude I feel for this place or its people. Most notably Greg, Barry, Joe, Quintin, Courtney, Steph, Emma Marius and Lewis – you have tolerated me, inspired me, comforted me, taught me, and made me laugh on countless occasions.

I must make special mention of those closest to me, whose constant love and support has never wavered. Firstly, my family who have supported me unquestioningly throughout my life. My lab friends, who have shared experimental joys and failures, and have lifted my spirits in and out of the lab: Sarah, Ludo, Natalia, Roey, Mikey, and Björn, you have been the bedrock of my life in Cambridge. Thomas, who has provided support and distraction in equal measure, and who will never allow my ego to go unchecked. Sally who has been the best Cat-Wife I could have dreamed of, and who has been a constant reminder that it is possible to make it through to the other side of PhD life. And lastly to those friends and colleagues, unnamed here, whom I have gained along the way. You are largely scattered around the world, but though you are distant in geography, you are all close to my heart.

Finally, I should acknowledge and give thanks to the endeavours of Mr Steve Jobs, Ms J.K. Rowling, and Messers Ben and Jerry, without whose innovations my sanity might have departed long ago.

Table of Contents

Abbreviations

> *– less than*

< *– more than*

°C *– Degrees Celsius*

2D *– Two dimensional*

3D *– Three dimensional*

Å *– Angstrom*

AD *– axial diffusivity*

ADEM *– Acute Demyelinating Encephalomyelitis*

B *– A magnetic field*

BBB *– Blood Brain Barrier*

CC *– Corpus Callosum*

CCP *– Caudal Cerebellar Peduncle*

CD *– Cluster of Differentiation*

CL2 *– Biological Containment Level 2*

CO_2 *– Carbon Dioxide*

CNS *– Central Nervous System*

CRUK *– Cancer Research UK*

CRISPR *– Clustered Regularly Interspaced Short Palindromic Repeats*

CSCs *– Cerebellar Slice Cultures*

CSF *– Cerebrospinal Fluid*

dH_2O *– deionised water*

DMSO *– Dimethyl sulfoxide*

DNA *– Deoxyribonucleic Acid*

dpl *– days post lesion*

DTI *– Diffusion Tensor Imaging*

e *– embryonic day*

EAE *– Experimental Autoimmune Encephalomyelitis*

E.coli *– Escherichia coli*

EB *– Ethidium Bromide*

ECF *– Extra Cellular Fluid*

FA *– Fractional Anisotropy*

FACS *– Fluorescent Antibody Cell Sorting*

FBS *– Fetal Bovine Serum*

FGF *– Fibroblast Growth Factor*

FLAIR *– Fluid Attenuation Inversion Recovery*

FLASH *– Fast Low Angle SHot*

fr *– french*

g *– g force*

γ *– gyromagnetic ratio*

GalC *– Galactoserebrosidase*

GE *– Gradient Echo*

GFAP *– Glial Fibrillary Acidic Protein*

GFP *– Green Fluorescent Protein*

h *– Plank's constant*

ICP-MS *– Inductively Coupled Plasma Mass Spectrometry*

IGF *– Insulin Like Growth Factor*

IVM *– intravital microscopy*

Js *– Joule seconds*

kg *– kilograms*

m^2 *– metres squared*

MACS *– Magentic Associated Cell Sorting*

MAG *– Myelin Associated Glycoprotein*

MBP – Myelin Basic Protein

MGC *– Mixed Glia Culture*

MGSO *– Mixed Glia Shake Off*

µg *– micro grams*

MHC *– Major Histocompatibility Complex*

MHz *– mega hertz*

µL *– micro litres*

mL *– milli litres*

µM *– micro Moles*

mm *– milli metre*

MOG *– Myelin Oligodendrocyte Glycoprotein*

ms *– milli second*

MR *– Magnetic Resonance*

MRI *– Magnetic Resonance Image(es/ing)*

MS *– Multiple Sclerosis*

MTR *– Magnetisation Transfer Ratio*

MWF *– Myelin Water Fraction*

ng *– nano gram*

NG2 *– Nerve Glial antigen 2*

nL *– nano litres*

nm *– nano metres*

nM *– nano Moles*

NAWM *– Normal Appearing White Matter*

NMR *– Nuclear Magnetic Resonance*

nOPC *– neonatal Oligodendrocyte Progenitor Cell(s)*

NMODS *– Neuromyelitis Optica Disease Syndromes*

OATP *– Organic Anion Transporter Protein*

OEC *– Olfactory Ensheathing Cells*

OPC *– Oligodendrocyte Progenitor Cell(s)*

p *– post natal day*

PBS *– Phosphate Buffered Saline*

PCR *– Polymerase Chain Reaction*

PDGF *– Platelet Derived Growth Factor*

PDGFRα *– Platelet Derived Growth Factor Receptor Alpha*

PDL *– poly-d-lysine*

PET *– Positron Emission Tomography*

PFA *– Paraformaldehyde*

PGK *– Phosphoglycerate Kinase*

PLP *– Proteolipid Protein*

PMD *– Pelezieus Merzbacher's Disease*

PNS *– Peripheral Nervous System*

PPMS *– Primary Progressive Multiple Sclerosis*

rpm *– rotations per minute*

RC *– Receiver Coil*

RF *– Radio Frequency*

RFP *– Red Fluorescent Protein*

RRMS *– Relapsing Remitting Multiple Sclerosis*

SCI *– Spinal Cord Injury*

SPIO *– Super Paramagnetic Iron Oxide*

SPMS *– Secondary Progressive Multiple Sclerosis*

T *– Tesla*

T_1 *– T1 weighted*

T_2 *– T1 weighted*

T_2^* *– T2 star*

T4 *– Thyroxine/Thyroid Hormone*

TE *– Echo Time*

TR *– Relaxation Time*

T_{relax} *– Scan Repeat Time*

TUNEL *– Terminal deoxynucleotidyl transferase dUTP nick end labelling*

USPIO *– Ultra small Super Paramagnetic Iron Oxide*

ω *– Lamour Frequency*

List of Figures

List of Tables

Summary

Demyelination occurs in several CNS diseases. If demyelinated axons are not remyelinated they become vulnerable to irreversible degeneration. There is, therefore, a clinical need for therapies that enhance remyelination. This can be achieved by 1) pharmacologically targeting endogenous oligodendrocyte progenitor cells (OPCs) responsible for remyelination or 2) transplantation of myelinogenic cells (including OPCs). The first approach is appropriate for diseases with no defect in the myelinating cells, such as multiple sclerosis (MS), while the second approach is suitable for genetic disorders of myelination such as Pelizaeus Merzbacher disease (PMD). Translation into the clinic has or will shortly begin for both approaches. However, there are no current outcome measures providing direct evidence of OPCs differentiation to assess the efficacy of a remyelination therapy.

This thesis presents data which it is hoped will form the foundation of a novel outcome measure for such therapies.

It demonstrates that, by using a novel MRI gene reporter system; OATP, and controlling its expression under a Myelin Basic Protein promoter, OPCs can take up gadolinium based contrast, and be detected using T_1 weighted MRI imaging *in vitro* and *ex vivo*. Using a constitutively active promoter, transplanted cells can be detected by an *in vivo* model of remyelination.

It is hoped that this data will form the foundation for the development of an outcome measure for assessing the efficacy of new, pro-remyelination therapies, and provide a non-invasive, longitudinal, and translational imaging technique for use in drug discovery, or even personalised medicine.

1. Introduction

In multicellular bilaterally symmetrical organisms such as mammals, fish, birds, and reptiles, coordination of body movements and functions is organised, regulated and elicited by the central nervous system (CNS). Jelly fish, for example, which are radially symmetrical multicellular organisms, do not have a CNS, instead they have a neural net located across their epidermis which coordinates movements, and to a more limited extent, homeostasis. The role, structure and functions of the CNS are distinct from those of the peripheral nervous system (PNS), and despite its highly conserved structure throughout all vertebrate life, it shows significant specialisation and variation across species. A diagrammatic representation of the structure of the CNS is shown in Figure 1.

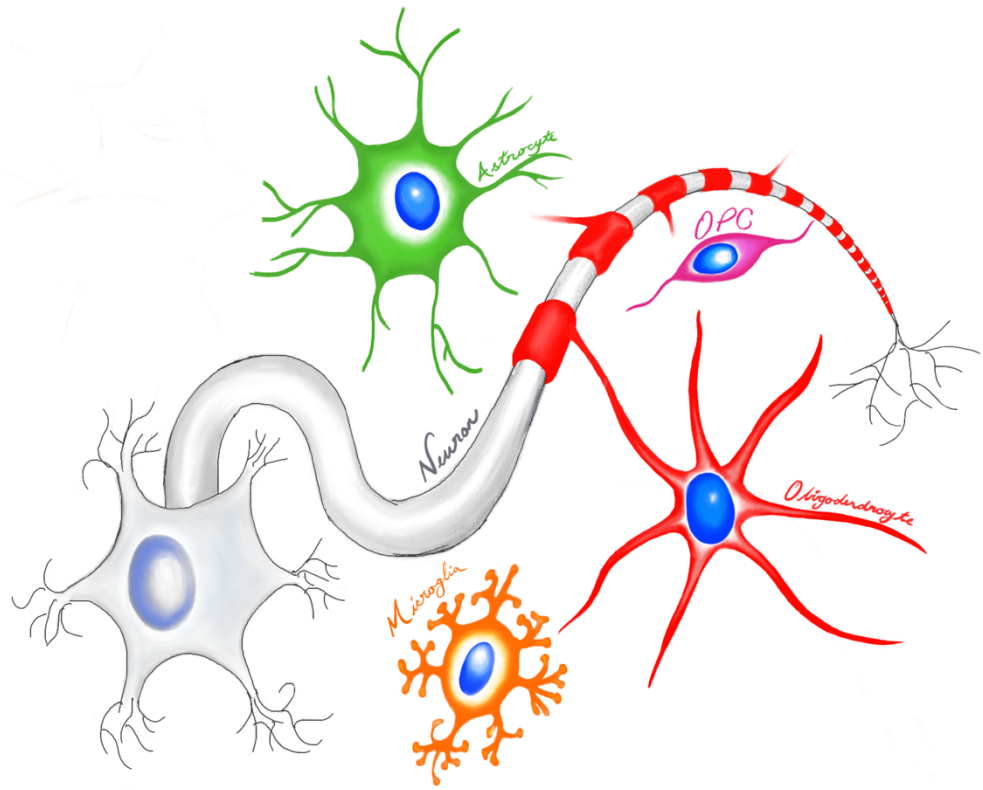

Figure 1: The components of the Central Nervous System.
The CNS is divided in to the White and Grey Matter, this distinction is based on the location of cell bodies of neurons which are found in Grey, but not White Matter. White Matter is characterised by the presence of myelinated axons. Myelin is formed by Oligodendrocytes. The Oligodendrocyte precursor is found in both White and Grey Matter, as is the Astrocyte and the tissue resident immune cell of the CNS; the microglia. Not to scale.

The CNS is one of the most complex systems in the body, and despite centuries of investigations, a full understanding of its functions still eludes us, and may well continue to do so. We have, however, made great progress since the nineteenth century, when only the neuron, alone of the cells of the CNS, was known. It was Virchow, in 1846, who first described the cells between neurons; naming them neuroglia, he drew on the Latin term for glue in this moniker, thinking these cells a form of connective tissue. The current delineation of this neuroglia in to its constituent cells types; astrocytes, oligodendrocytes, and microglia, was established variously by, *inter alia*, the work of Ramon y Cajal, and his student Del Rio Hortega.

Whilst the precise functions of these cell types and their progenitors is still a matter of significant investigation, our current understanding suggests that there is significant communication and interplay between the four cell types.

It has been clear for centuries that neurons are largely responsible for the conduction of action potentials within both the peripheral and the central nervous system. These action potentials form the foundation of homeostatic coordination throughout the body and are the basis for cognition, memory, and movement. In the CNS, the major anatomical distinction is made between regions of grey matter and regions of white matter. This is based the localisation of the neuron cell bodies and their axons respectively. Beyond this broad distinction of white and grey matter there are differences between grey matter regions in their function and in the nature of these neurons. The grey matter in the brain stem, the phylogenetically oldest part of the brain, also known as the paleo cortex, are known as nuclei, these nuclei have distinct properties and functions when compared to the neurons found in the phylogenetically

youngest part of the brain; the cerebral, or neo cortex. The differences in these neuronal populations is expansive and complex and will not be further addressed here.

Astrocytes are the most abundant cell type in the mammalian brain, they have a range of functions within the CNS including synaptic regulation (Chung *et al.* 2013), they play a crucial role in forming and maintaining the blood brain barrier (Sofroniew and Vinters 2009), in providing trophic and metabolic support (Allaman, Bélanger, and Magistretti 2011) to neurons, and in neurotransmitter metabolism (Hamilton and Attwell 2010). They derive from the neuroepithelia, and are morphologically divided in to two main types in the adult mammalian brain; fibrous and protoplasmic, and are found in the white and grey matter respectively (Rowitch and Kriegstein 2010).

Oligodendrocytes form the myelin sheath, they arise from a population of stem like cells (Crawford *et al.* 2014) which are initially responsible for the developmental myelination of the CNS, but remain resident within the tissue and activate in instances of injury, differentiating in to the mature oligodendrocyte in a process known as remyelination.

The function of the oligodendrocyte is, at its simplest, to provide trophic support to the neuron and to facilitate salutatory conduction (Jeffery *et al.* 1999; Baumann and Pham-Dinh 2001; Nave 2010), however work by many groups over the years since the cell was first identified has demonstrated a far wider variety of functions (McKenzie *et al.* 2014; Young *et al.* 2013; Cassoli *et al.* 2015).

Microglia are of mesodermal, specifically haematopoetic, origins and are the tissue resident monocytes of the CNS, they make up around 10% of the cells of the CNS (Kreutzberg 1996). They are, perhaps, somewhat mis-named, as they are neither small, nor truly glia, like other innate immune cells they play a regulatory role in tissue homeostasis. They cross in to the CNS prior to closure of the blood brain barrier (BBB)(Ginhoux 2013) during embryological development. Once within the CNS they play a regulatory role in synaptic plasticity, and a phagocytic role, clearing debris and infectious agents. Upon encountering a stimulus indicative of injury or infection they become activated, this state of activation is characterised by a distinct profile of cytokine production, morphology and behaviour (McMurran *et al.* 2016).

1.1 Oligodendrocyte lineage cells

The oligodendrocyte was first identified by Rio del Hortega (Pérez-Cerdá, Sánchez-Gómez, and Matute 2015), but it was not until the 1980s when Raff and colleagues identified its precursor naming it the O-2A. They were later renamed Oligodendrocyte Precursor Cell, and later still have been re termed Oligodendrocyte Progenitor Cell (OPC). The distinction being that the progenitor cell is now thought not to be restricted to the oligodendrocyte lineage alone, and in fact to have a multipotent, stem like quality (Crawford, Chambers, and Franklin 2013).

OPCs arise in several discrete waves from the embryological neuroepithelium migrating throughout the CNS (Cai *et al.* 2005; Fogarty 2005; Vallstedt, Klos, and Ericson 2005). They account for approximately 5% of the cells of the CNS in the adult.

The OPC is characterised by the expression of various defined markers as outlined in Figure 2. The cell surface proteoglycan Nerve-Glial antigen 2 (NG2), also known as CSPG4, Platelet Derived Growth Factor Receptor Alpha (PDGFRa), and A2B5 are the most reliable and commonly used markers. However, it is not clear that these markers necessarily identify exactly the same population of cells. The transcription factor Olig 2 is expressed by the OPC and throughout differentiation through the lineage to the oligodendrocyte (Fancy, Zhao, and Franklin 2004). There is a significant degree of heterogeneity within the population of adult OPCs, this may represent inherent differences in the cells themselves, or it may represent populations of OPCs at different points along the continuum of differentiation from progenitor cell to myelinating oligodendrocyte.

Despite their potential to make a variety of different cell types, there is indirect evidence that, in vivo, the oligodendrocyte progenitor cell is the major source of remyelinating oligodendrocytes. It has been shown that, following demyelination, OPCs repopulate the lesion prior to remyelination (Sim *et al.* 2002; Fancy, Zhao, and Franklin 2004; Aguirre *et al.* 2007). Transplanted OPCs readily differentiate in to myelinating oligodendrocytes in regions of demyelination (Groves *et al.* 1993), and their differentiation from OPC in to oligodendrocyte has been demonstrated by a variety of different cell tracing experiments (Fancy, Zhao, and Franklin 2004; Gensert and Goldman 1997), including genetic fate mapping using OPC specific promoters which demonstrate more directly OPC derived oligodendrogliogenesis (Tripathi *et al.* 2011; Zawadzka *et al.* 2010; Nakatani *et al.* 2013).

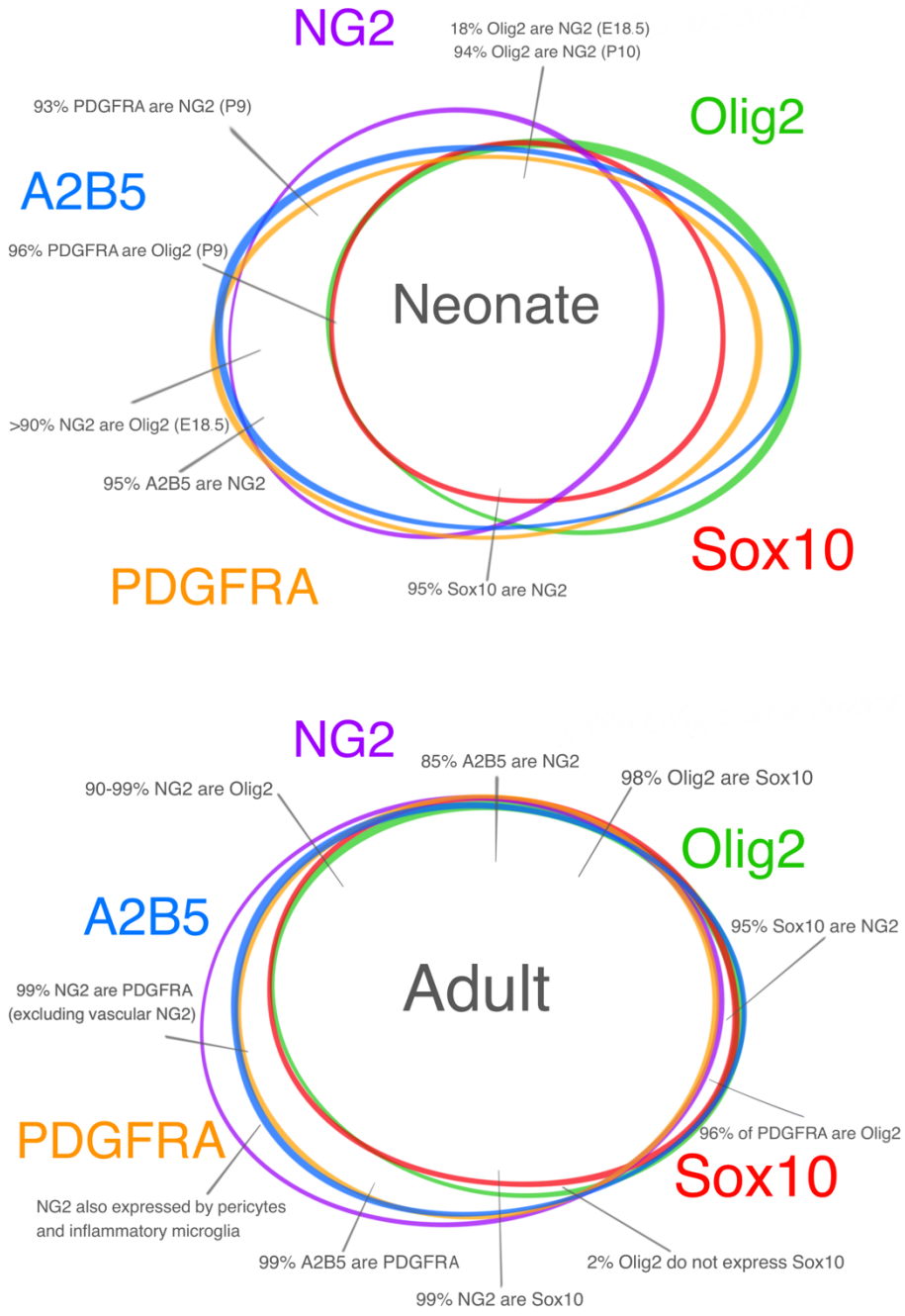

Figure 2: *Oligodendrocyte Progenitor Cell Markers expressed in the neonate and adult brain. Overlap of OPC (NG2, PDGFRA, and A2B5) and oligodendrocyte lineage cell marker expression (Olig2 and Sox10) in neonatal (top) and adult (bottom) OPCs based on published in vivo lineage tracing experiments (Clarke et al., 2012; Kang, Fukaya, Yang, Rothstein, & Bergles, 2010; Karram et al., 2008; Ligon et al., 2006; Riverset al., 2008; Stallcup & Beasley, 1987). A2B5 data was generated from immunostainings of OPCs isolated with the A2B5 antibody (unpublished data from Franklin Lab). The overlap of OPC marker expression changes during development: adult OPCs show a higher overlap of the OPC marker proteins when compared to neonatal OPCs. Figure from Foerster, Hill, Franklin 2019.*

1.2 Myelin and Myelin Proteins

Myelin is the insulating membrane which ensheathes the axons of the central and peripheral nervous system (Franklin *et al.* 2012). It is highly conserved throughout vertebrate species. In the central nervous system myelin is formed by oligodendrocytes; arboreal cells which wrap axons in specialised projections of their plasma membrane, one oligodendrocyte my wrap up to 60 internodes forming only one internode on any one axon (Chong *et al.* 2012).

Myelin is composed of proteins and fats; Figure4. It is produced in the central nervous system by oligodendrocytes, and in the peripheral nervous system by Schwann Cells. Table 1 outlines the composition of central myelin.

Substance		% of total	Total
Proteins	MBP	22.5	30%
	PLP	30.0	
	LH-20 components	17.5	
	Others	30.0	
Lipids	Cholesterol	27.7	70%
	Cerebroside	22.7	
	Cerebroside Sulfate	3.8	
	Sphingomyelin	7.9	
	Gangliosides	<1.0	
	Others	36.9	

Table 1: The composition of the myelin membrane in vertebrates highlighting the distribution of proteins and fats and their major subtypes. Adapted from Deber and Reynolds Clinical Biochemistry 1991

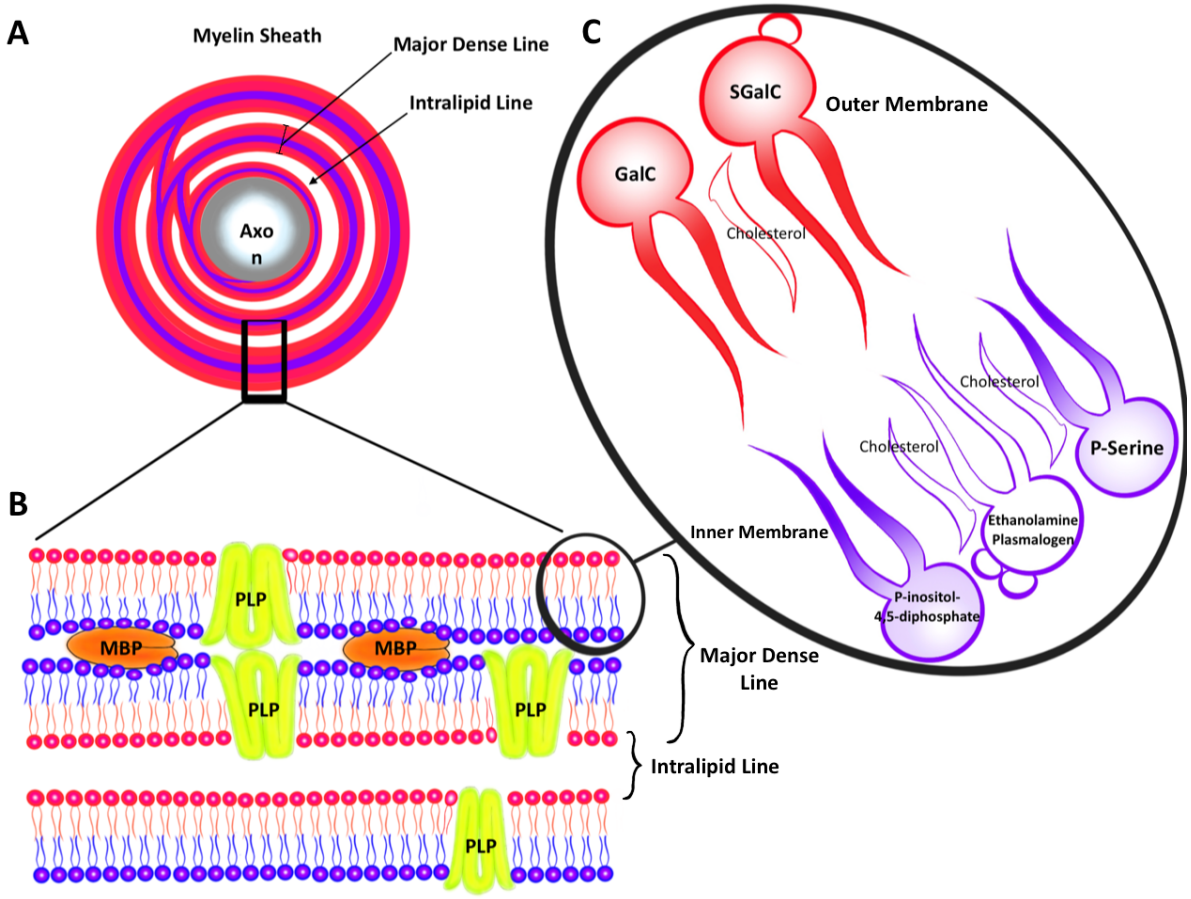

Figure 3: Composition and structure of the Central Myelin Sheath.
*Schematic representation of the main components of the myelin sheath in the CNS. Compact Myelin is formed by the appositional wrapping of the oligodendrocyte plasma membrane projections **A**. The 'Inner Membrane' represents the cytoplasmic side of the plasma membrane, making MBP an 'intracellular' component, and the 'Outer Membrane' is the extra cellular side of the plasma membrane, making the PLP component a transmembrane protein **B**. The plasma membrane comprises specialised components to form the classical phospholipid bilayer with the spiral structure augmented by myelin proteins such as MBP and PLP **C**.* (Aggarwal, Yurlova, and Simons 2011); (Deber and Reynolds 1991); (Laule et al. 2007)

The presence of myelin is highly conserved in vertebrates with myelin first arising in the gnathastome fish (Zalc, Goujet, and Colman 2017). Evidence from the fossil record demonstrates the oculomotor nerve of some paleozoic fish maintains a similar diameter to that of their ancestors, but is increased in length. The inferred corollary of this is that in order to maintain conduction along an increased length at a fixed diameter, conduction speed must have been augmented by the addition of the myelin sheath (Gans and Northcutt 1983).

In the vertebrate, oligodendrocytes develop form the neuroepithelium in the ventral portion of the spinal cord, the same region from which motor neurons arise and is mediated by sonic hedgehog signalling, but temporally separated (Warf, Fok-Seang, and Miller 1991). Although some invertebrate species do demonstrate some glial derived axonal wrapping, (Hartline and Colman 2007) it is only the vertebrate which exhibits myelin as a fully specialised component of the nervous system.

The fossil record has an understandable paucity of evidence regarding the nature of myelinating cell types; however, examination of extant species is more illuminatory in this regard. It is not unreasonable, given their existence in all modern vertebrates, to assume that the nervous systems of extinct species bore similarities in composition to those of their evolutionary progeny, and that they might, therefore have exhibited similar patterns of heterogeneity. Evidence examined by Tomassy and colleagues suggests that the greatest degree of heterogeneity in the myelinating orchestra exists in the upper layers of the cerebral cortex in mice (Tomassy and Fossati, 2017). In the chicken spinal cord molecular heterogeneity of oligodendrocytes has been identified based on the expression of the cell surface peptide T4-O, with T4-O high cells appearing to myelinate earlier in development and targeting larger

diameter fibres (Anderson *et al.* 1999). In addition, lower orders of vertebrate such as the rattle snake have been shown to have less myelin basic protein post translational modification in comparison to bovine MBP (Zhang *et al.* 2012), suggesting that more complex myelin is required for higher levels of function.

The developmental heterogeneity of OPC origin (Dorsal vs Ventral) has been identified in the chick in a similar fashion to that seen in the mouse: Sox10 positive, PDGFRα positive OPCs appear ventrally around E6 and then populate the whole cord (Ono *et al.* 1995). In the forebrain chick OPCs originate in the ventral telencephalon, going on to populate both the ventral and dorsal forebrain (Olivier *et al.* 2001), and both dorsally derived and ventrally derived OPCs have been shown to exist in both the embryonic mid brain (Fu *et al.* 2009) and the hindbrain (Davies and Miller 2001).

Although many of the markers of the oligodendroglial linage are conserved between lower and higher species, the point at which they appear frequently differs; for example, it has been shown that O4, the pre-myelinating marker in mammals, does not appear in the chick until fulminant differentiation has occurred making it a later stage marker in this species than in most mammals (Ono *et al.* 1995; Hall, Giese, and William D Richardson 1996; Bansal and Pfeiffer 1997). The expression of A2B5 appears to label differing subsets of OPC in the rat vs the mouse (Fanarraga, Sommer, and Griffiths 1995).

It is unclear if there is truly an increase the diversity of oligodendrocytes or their progenitors with increasing phylogenetic complexity, the absence of evidence for this diversity in the lower

orders cannot be assumed to be evidence of absence. However, within complex vertebrates there is does appear to be an ever increasing body of evidence.

Modern vertebrate myelin shows a highly organised structure of compacted encircling layers around an axon divided up into nodal structures that facilitate saltatory conduction. There are many proposed models for how the wrapping of the myelin around the axon actually takes place these include the 'carpet crawler model' where the leading edge of the myelinating wrap progresses under the previous layer (Bunge *et al*., 1989), a bi directional ensheathment (Knobler *et al*., 1976,) the liquid croissant model proposed by Sobottka and colleagues (Sobottka *et al.* 2011) and a unidirectional coiling around the internode region (Pedraza *et al*., 2009).

Although the exact formation of the sheath is still hotly debated, a better understanding of the structure of the sheath has been achieved. The layers of membrane which encircle the axon are of a uniform thickness of around 12nm with a characteristic electron dense : electron light appearance by electron microscopy (Hartline 2008). The electron dense, or major dense line is the formed by the compacted cytoplasmic myelin membrane, where as the electron light regions of the outer membranes (Figure 4B). Each internode is approximately 150μm (Aggarwal, Yurlova, and Simons 2011) in length with the node of Ranvier, where sodium channels are concentrated being approximately 1μm.

Myelin is composed largely of fats and proteins. The functional role of these has been best illustrated by mouse mutants. For example, mice which lack the ability to synthesise galactosylceramide and sulfatide die prematurely, with disorganised paranodes (Coetzee *et al.* 1996), however, by and large, changes in lipid composition bring out functional redundancy in

the system and are compensated for by other structural lipids (Aggarwal, Yurlova, and Simons 2011). Conversely, the proteins, which are often membrane spanning or intermembrane, appear to show far less redundancy, with mouse mutant models such as the shiver and jimpy showing significant dysmyelination and functional impairment (Readhead and Hood 2018; Nave *et al.* 1986).

1.3 Myelination and Remyelination

Myelination is a complex sequence of events that we believe to be recapitulated almost exactly in the regenerative process of remyelination (Fancy *et al.,* 2011). The over-all sequence of events can be summarised in seven steps (1) proliferation and migration of oligodendrocyte precursor cells (OPCs) in white matter tracts, (2) recognition of target axons and axon – glia signalling, (3) differentiation of OPCs into oligodendrocytes, (4) membrane outgrowth and axonal wrapping, (5) trafficking of membrane components, (6) myelin compaction, and (7) node formation (Simons and Nave 2016); (Barres and Raff 1999); (Baumann and Pham-Dinh 2001); (Emery 2010); (Simons *et al.* 2012); (Bakhti *et al.* 2013); (Freeman and Rowitch 2013).

In development, OPCs migrate away from the neuroepithelium of the ventricular and subventricular zone of the brain into the developing white matter, in which they proliferate. *In vivo* time-lapse imaging in transgenic zebrafish and mice show that OPCs continuously extend and retract processes as they migrate throughout the CNS (Kirby *et al.,* 2006); (Hughes *et al.,* 2013). It is thought that these processes contribute to self repulsion; a phenomenon that allows OPCs to distribute with a uniform density throughout the CNS. (Czopka *et al.,* 2013); (Hines *et al.,* 2015); (Koudelka *et al.,* 2016); (Mensch *et al.,* 2015). Following distribution throughout the developing parenchyma OPCs will undergo one of two

fates; some will remain in the progenitor state, whilst the others will undergo differentiation to form myelin making oligodendrocytes, any excess cells are later eliminated by apoptosis (Raff *et al.,* 1993); (Barres and Raff 1994); Trapp *et al.,* 1997).

One mechanism that determines the final number of oligodendrocytes is the competition for target-derived growth and survival factors, such as PDGFα, and FGF-2, amongst others (Barres and Raff 1994). During development OPCs are highly proliferative with cell cycle times around 6hours at embryonic day 14 and 24hours at around birth (Calver *et al.,* 1998); (Young *et al.,* 2013), this may be as a result of an excess of mitogenic factors (Noble *et al.,* 1988); (Raff *et al.,* 1988); (Richardson *et al.,* 1988). Overall approximately twice as many OPCs are made as will ultimately survive (Barres *et al*., 1992).

It appears that OPCs 'decide' which axons to myelinate on the basis of a number of factors, however axon diameter appears to be, potentially, the most significant (Lee *et al*., 2012). OPCs cultured in the presence of synthetic axons were able to differentiate and wrap around these synthetic fibres suggesting that oligodendrocytes (unlike Schwann cells) do not require axonal adhesion molecules and growth factors to initiate the formation of myelin (Lee *et al.,* 2012). The diameter size appeared to be critical; nanofibres under 400nm were rarely myelinated. Although larger axons appear to be preferentially myelinated in vivo, axons as small as 200 – 300 nm can be myelinated in some regions of the CNS. It is likely that oligodendrocytes receive specific signals from small diameter axons to initiate myelination. (Umemori *et al.,* 1994).

Once an oligodendrocyte process has engaged with an axon its plasma membrane process undergoes a remodelling (Butt and Berry 2000); (Pedraza *et al.,* 2009); (Sobottka *et al.,* 2011); (Ioannidou *et al.,* 2012) resulting ultimately in the formation of compact myelin. During this remodelling he various membrane components are synthesized and transported from a variety of subcellular location (Simons and Nave 2016). For example, in development MBP is located to the process by transportation of its mRNA within cytoplasmic granules (Colman *et al.,* 1982; Ainger *et al.,* 1993). Subsequently there is location translation of the mRNA in the process (White *et al.,* 2008); (Laursen *et al.,* 2011); (Wake *et al.,* 2011). Myelin compaction is mediated by the progress of the MBP protein from the outside of the sheath to the inside as wrapping occurs (Snaidero *et al.,* 2014). CNP is thought to act as a break to allow compaction to occur distant to the site of translation: mice lacking CNP exhibit more rapid compaction extending to the innermost layers of the sheath whereas transgenic overexpression of CNP results in areas of myelin that lack compaction (Gravel *et al.,* 1996); Snaidero *et al.,* 2014). It can therefore be seen that there must be an equilibrium between MBP expression and CNP in early development in order to achieve orderly compaction. Once MBP is bound to two adjacent cytoplasmic membrane surfaces, it appears to polymerize by lateral interactions with previously deposited MBP monomers, thereby driving membrane closure at the cytoplasmic surfaces of the myelin bilayer (Aggarwal *et al.,* 2013). Myelin wrapping of single axonal segment has been demonstrated (in the zebrafish) to take only a few hours (Czopka *et al.,* 2013).

Once compacted the membrane is relatively stable (Aggarwal *et al.* 2011); myelin membrane components have been shown to have half lives in the order of weeks to month. Cholesterol was shown by Smith and colleagues to have a half life of 7-8months (Smith and Eng 1965),

and MBP a half life of 19-22 days minimum (Sabris, Bone, and Davison 1974). Recent studies using radioactive nitrogen isotopes have demonstrated that myelin proteins, alongside histones, nucleoporins, and laminins are some of the most long-lived proteins in the mouse (Toyama *et al.,* 2013).

Myelination as a developmental process continues well after birth in most species. In humans for example the brain continues to myelinate in to the adolescent years (Giedd and Rapoport 2010), and white matter volume continues to increase in to middle age, a phenomenon which is likely to be largely as a result of on going myelination (Timmler and Simmons, 2019).

Historically the focus of myelin biologists has been on the white matter where myelin is a dominant feature, however in recent years there has been an increased understanding of the role of myelin in grey matter (Timmler and Simmons, 2019). Here the role of myelin is thought to range from metabolic support for fast spiking basket cells (Micheva *et al.,* 2016), to co ordinate spiking, and conduction velocities (Pajevic, Basser, and Fields, 2014); (Ford *et al.*, 2015); (Seidl, Rubel, and Harris, 2010), and to play a role in plasticity and learning (Mckinzie *et al.,* 2014).

Remyelination is a rare example of regeneration within the CNS (Franklin and ffrench-Constant 2008). The myelin sheath facilitates both saltatory conduction (Smith, Blakemore, and McDonald 1979; Felts, Baker, and Smith 1997) and axonal maintenance (Blakemore and Irvine 2008). Remyelination efficiently restores conduction velocity (Smith, Blakemore, and McDonald 1979) and reverses functional deficits (Jeffery and Blakemore 1997; Duncan *et al.* 2009). It is the normal physiological response of the body in both spontaneous disease and

experimental models of demyelination (Smith and Jeffery 2006; Franklin and ffrench-Constant 2017).

Remyelination in the CNS is carried out by the differentiation of the OPC in to mature myelinating Oligodendrocytes. OPCs are a stem cell like cell (Crawford *et al.* 2014) widespread throughout the CNS (5-8% of CNS cells), which are found both in white and grey matter.

Evidence for the role of the OPC in *de novo* and repairing oligodendrogenesis comes from a variety of experimental studies. Transplantation of oligodendrocytes in to demyelinated lesions has been shown to result in no remyelination (Targett *et al.* 1996), and CNS which has previously been denuded of its OPC population by irradiation, has been shown to be unable to remyelinate regions of toxin induced demyelination (Keirstead and Blakemore 1997; Blakemore and Patterson 1973) suggesting that it is not the mature oligodendrocyte, but a progenitor population which is responsible for the formation of new oligodendrocytes (Zawadzka *et al.* 2010). In response to a demyelinating insult local OPCs become activated in response to signals produced by activated astrocytes and microglia at the site of injury. Following activation OPCs migrate towards the site of injury and proliferate (Franklin and ffrench-Constant 2008). OPCs then make contact with the denuded axon and differentiate into mature myelin forming oligodendrocytes (Zawadzka *et al.* 2010). Each newly differentiated oligodendrocyte expresses myelin genes, and produces the myelin sheath, which is wrapped and compacted around multiple surrounded axons (Franklin and Goldman 2015). The myelin sheath is a plasma membrane structure comprising a mixture of proteins and lipids. Proteolipid Protein (PLP), Myelin basic Protein (MBP), Myelin Associated Glycoprotein (MAG), and Myelin Oligodendrocyte Protein (MOG) are the main protein

components of the myelin sheath with Proteolipid Protein being the most abundant (Deber and Reynolds 1991).

Although robust, and usually complete, there are some instances where remyelination fails. These instances are significant because they are characteristic of many diseases of myelin discussed in brief previously, most notable amongst them being the chronic failures typical of chronic progressive multiple sclerosis (Franklin and ffrench-Constant 2017). The underlying cause of this failure has not been fully elucidated however it is likely to be multifactorial and include factors such as ageing (Sim *et al.* 2002).

In order for remyelination to take place OPCs must first be recruited to the lesion site, then proliferate, before finally differentiating as shown in Figure 3. Remyelination is a recapitulation of developmental myelination (Fancy *et al.* 2011), with the only notable difference being that, following injury in the adult brain, remyelinated axons are encircled with a thinner myelin sheath (Blakemore 1974; Franklin *et al.* 2002; Franklin and ffrench-Constant 2008).

In response to injury (Figure B&C), microglia and astrocytes first become activated (Figure D) (Carroll and Jennings 1994; Emery *et al.* 2009), and as a consequence of, amongst other things, PDGF and FGF-2 signalling OPCs are recruited to the lesion site where they undergo proliferation (Figure E&F) (Woodruff *et al.* 2004);(Murtie *et al.* 2005). Following recruitment OPCs enter in to a differentiation phase (Figure G), this is initiated through contact with a denuded axon and a variety of growth factor signals such as IGF-1 amongst others (Hinks and Franklin 1999); (Zhao, Li, and Franklin 2006) this triggers a change in their genetic profile and they begin down regulating the classical OPC genetic markers such as PDGFRα, and being up

regulating genes which are required in the production of myelin such as CNPase and myelin basic protein (MBP). Following differentiation, new oligodendrocytes mature and are largely indistinguishable from the *de novo* cells, save only the formation of thinner sheaths (Figure H)(Blakemore 1974).

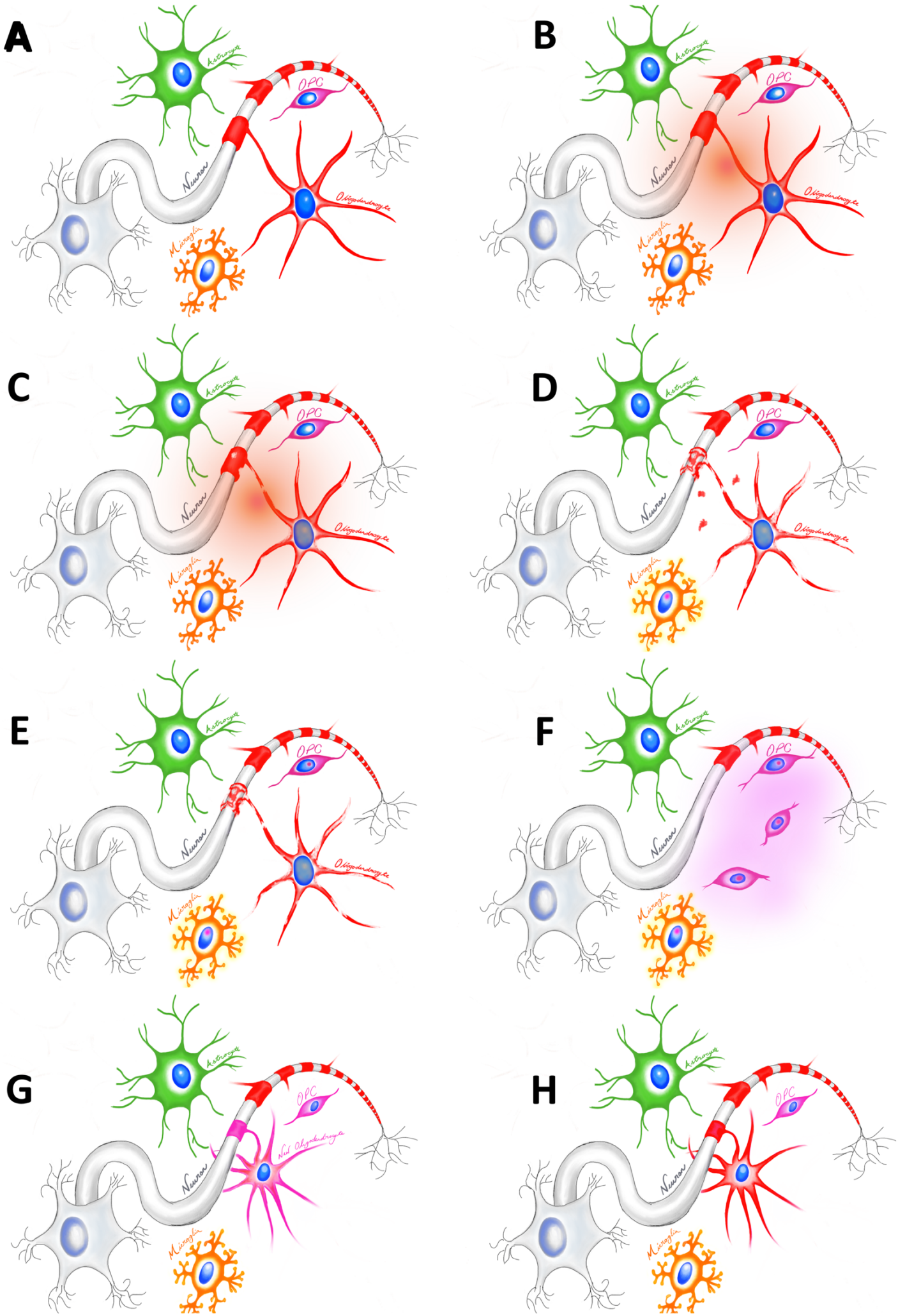
A
Astrocyte
OPC
Neuron
Oligodendrocyte
Microglia
B
Astrocyte
OPC
Neuron
Oligodendrocyte
Microglia
C
Astrocyte
OPC
Neuron
Oligodendrocyte
Microglia
D
Astrocyte
OPC
Neuron
Oligodendrocyte
Microglia
E
Astrocyte
OPC
Neuron
Oligodendrocyte
Microglia
F
Astrocyte
OPC
Neuron
Microglia
G
Astrocyte
OPC
Neuron
Microglia
H
Astrocyte
OPC
Neuron
Microglia

Figure 4: The process of Remyelination following a demyelinating Injury.

A: Normal Appearing White Matter comprising of Oligodendrocytes, Oligodendrocytes Progenitor Cells, Astrocytes, and neuronal axons.

B: Injury to the white matter, this may be primary inflammation, as in MS; or secondary inflammation resulting from ischaemia as seen in stroke, or dysmyelination; or direct injury as seen in many models of demyelination such as cuprizone, lysolecithin, or Ethidium bromide.

C: The inflammation (primary or secondary),or toxin leads to degeneration of the myelin membrane and oligodendrocyte death

D: microglia and astrocytes first become activated(Carroll and Jennings 1994);(Emery et al. 2009) leading to the activation of local OPCs (E).

F: PDGF and FGF-2 signalling lead to OPCs being recruited to the lesion site and proliferating (Woodruff et al. 2004);(Murtie et al. 2005).

G: Following recruitment OPCs enter in to a differentiation phase, this is initiated through contact with a denuded axon and a variety of growth factor signals such as IGF-1 amongst others (Hinks and Franklin 1999) (Zhao, Li, and Franklin 2006) this triggers a change in their genetic profile and they begin down regulating the classical OPC genetic markers such as PDGFRa, and being up regulating genes which are required in the production of myelin such as CNPase and myelin basic protein (MBP).

H: Following differentiation, new oligodendrocytes mature and are largely indistinguishable from the de novo cells, save only the formation of thinner sheaths(Figure H)(Blakemore 1974).

1.4 Diseases of Myelin

Diseases of myelin occur for a number of reasons: they may result from inherent defects in the oligodendrocytes; genetic errors in genes encoding myelin proteins or lysosomal structures, ischemic injury which kills off a region of oligodendrocytes and OPCs, or immune targeting of antigens expressed by oligodendrocytes. These diseases are of considerable significance.

1.4*i* Multiple Sclerosis

Most significant amongst the immune mediated myelin diseases is Multiple Sclerosis (MS) which is the most common neurological condition of young adults in the western world (Compston and Coles 2008). First described by Jean Marie Charcot, a French neurologist, MS is a chronic inflammatory disease of the CNS in which myelin is lost from the axons of neurons (Compston and Coles 2008). In MS oligodendrocytes are targeted by an autoreactive T cell response that results in the denuding of axons (Goverman 2009). The normal physiological response of the body to this insult is to resolve the inflammation and remyelinate the denuded regions. New myelin sheaths are formed by the differentiation of endogenous OPCs in to mature oligodendrocytes. This is usually a robust and complete response, however, in MS the repeated demyelinating insults, and the inherent decline in efficiency of the repair response result in the persistence of denuded axons leading to a chronic accumulation of pathology and loss of function. Failure to remyelinate leads to a block in salutatory conduction (Felts, Baker, and Smith 1997); and in the long term eventually results in axonal degeneration, due to loss of trophic support (Griffiths *et al.* 1998) (Figure 5).

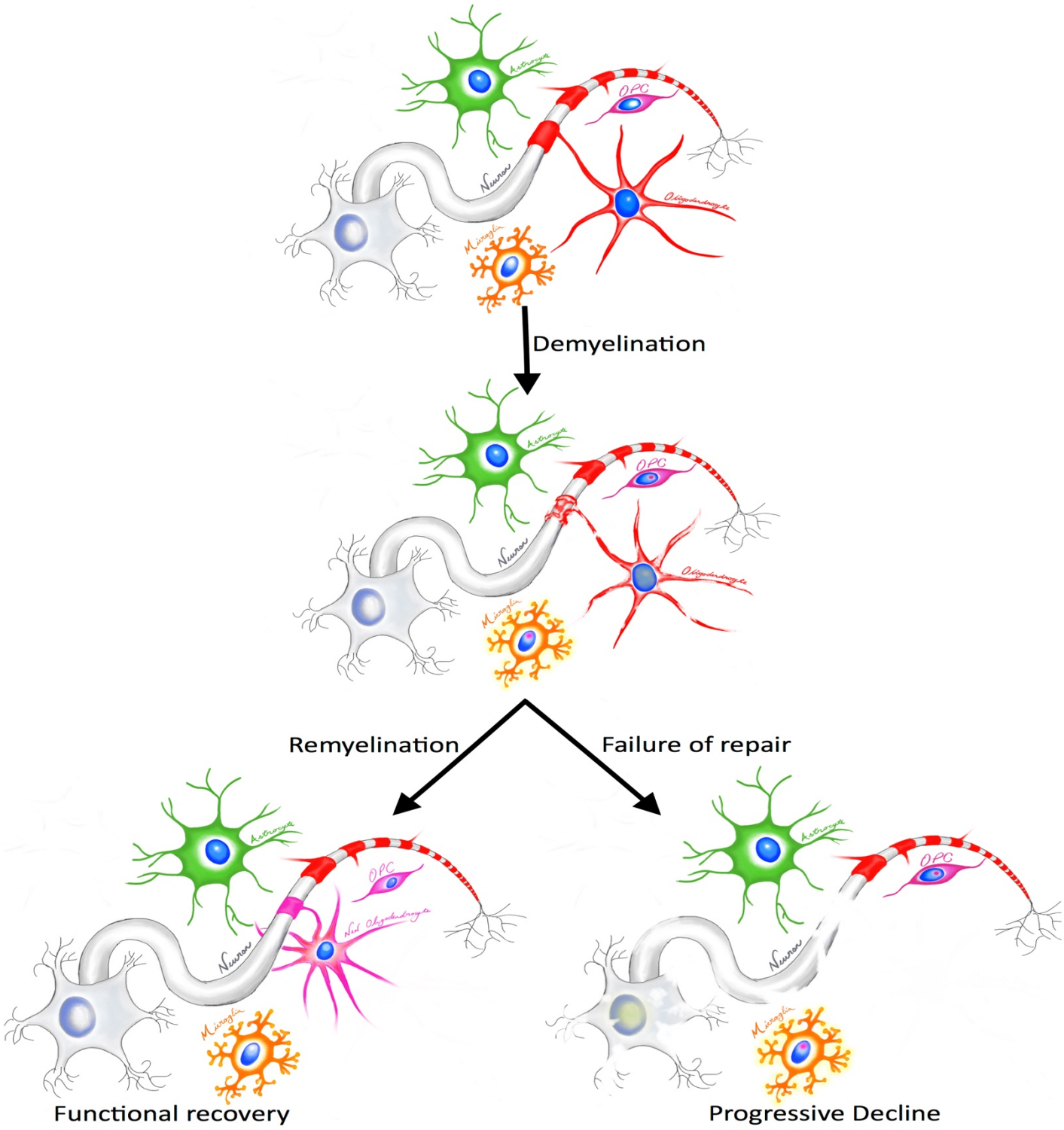

Figure 3: *Repair vs Neuronal loss following demyelination. Following an insult to the myelin sheath, and subsequent demyelination the usual response of the CNS is to undergo spontaneous repair; laying down a new myelination sheath and achieving a functional recovery through the differentiation of OPCs in to Oligodendrocytes. However, it is clear that this scenario fails to occur in certain disease processes, and appears to fail with increasing frequency with age. A key question remains as to what triggers this failure, and how this can be overcome. Based upon a similar diagram in Franklin & ffrench Constant 2008.*

The consequence of repeated bouts of demyelination is the accumulation of neurological deficits, characteristic amongst these are weakness, spasticity, pain fatigue, tremor, and motor or co-ordination difficulties (Compston and Coles 2008). MS affects over 2.5 million worldwide, but shows a distinct geographical and demographical distribution (Compston and Coles 2008). The clinical presentation is categorised in to three main forms; Primary Progressive (PPMS), Secondary Progressive (SPMS) and Relapsing Remitting (RRMS), with RRMS being the most frequently diagnosed (Fisniku *et al.* 2008). Primary progressive is characterised by an onset of clinical symptoms which show continuous deterioration, Relapsing Remitting (RRMS) on the other hand, is characterised by periods of remission of clinical symptoms between clinically active disease episodes. In most patients relapsing remitting MS will progress on to the final categorisation of secondary progressive which is defined as a period of continuous clinical decline which follows a prior period of RRMS (MacDonald *et al.* 2001). A majority of relapsing remitting patients will progress to the secondary progressive form between the ages of 40 and 50. Patients newly diagnosed with MS after this age are only rarely diagnosed with RRMS, and are more commonly diagnosed with primary progressive. This suggests that age plays a significant role in the development of the disorder (Fisniku *et al.* 2008; Compston and Coles 2002; Franklin *et al.* 2002; Ruckh *et al.* 2012).

The aetiology of multiple sclerosis is complex; however, the current consensus is that there are environmental and genetic risk factors, and that these interplay with immune system dysregulation. Multiple sclerosis, despite its worldwide distribution, is most commonly diagnosed in Caucasian populations in the northern hemisphere with 'hot spots' in Scandinavia, Scotland and Sardinia (Simpson *et al.* 2011; Ahlgren, Odén, and Lycke 2014). Diagnoses are more common in women than in men, twin studies have demonstrated a familial

recurrence rate of 20% (Compston and Coles 2008), and various genome wide association studies have identified genetic loci in immune regulatory regions including the Major Histocompatibility Complex (MHC), in particular HLA-DRB1*1501. This is unsurprising given the role the MHC has been demonstrated to play in other diseases of autoimmunity. Equally the distribution of this allele is most common in countries with a high geographical instance of MS (Sawcer, Franklin, and Ban 2014). Additionally infectious agents such as the Epstein Barr virus, amongst others, have been suggested to be triggers potentially via a molecular mimicry mechanism (Serafini *et al.* 2007).

Current treatments for multiple sclerosis centre around control of the inflammatory cascade. These include interferon beta which is thought to stablise the blood brain barrier, modulate T cell function, and up regulate of adenosine production (Airas *et al.* 2007; Stuve *et al.* 1996; Kraus *et al.* 2004), and immunosupressives including corticosteroids which act on the ecoisanoid pathway and mitoxantrone and chemotherapeutic which intecalates in to DNA thus reducing proliferation of immune cells (Fox, E.,J. 2004). Additionally monoclonal antibodies such as alemtuzumab, an antibody against CD52, have been employed in the treatment of relapsing remitting multiple sclerosis (Coles 2012). There are no therapies which target the repair process of multiple sclerosis, however this is an area of significant current investigation. At the time of writing there are 25 clinical trials looking at molecules or therapies which may improve the remyelination and repair of lesions, for a list of currently active clinically trials into remyelination therapies see Appendix 1.

1.*4ii* Leukodystrophies

Distinct from MS are the leukodystrophies; diseases of central white matter that result in dystrophic formation of myelin due to defects in the myelinating cells themselves. These largely result from inherited defects, or spontaneously arsing mutations in genes which code for components of myelin or the myelin:axon interaction (Knaap and Bugiani 2018). They arise at any stage of myelination from prenatal to established myelin and are usually fatal (Aubourg 1993).

Broadly speaking, the leukodystrophies can be grouped in to disorders of myelin (hypomyelinaiting, demyelinating, and myelin vacuolisation), astrocytopathies, leuko-axonopathies, microgliopathies, and leukovasculopathies (Knaap and Bugiani 2018). A variety of recessive and dominant mutations are responsible for these disorders. Unlike multiple sclerosis, where autoimmunity is thought to drive myelin damage and loss, in the leukodystrohies genetic abnormalities result in disordered or dysregulated myelination which is progressive, and unlike MS, does not undergo spontaneous and efficient repair (Köhler, Curiel, and Vanderver 2018).

The first of these disorders to be identified was Pelizeus Merzbacher's Disease (PMD); an X-Linked leukodystrophy resulting from mutations in the gene encoding the myelin protein Proteolipid Protein (PLP). Males who inherit this disorder show a range of dysmyelination ranging from moderate hypomyelination to severe hypomyelination. These children have severe and progressive disability and many will not live beyond their teenage years (Gupta *et al.* 2012).

Treating these diseases is a huge challenge for the biomedical community. In diseases such as MS, where the cell type responsible for repair is intact and normal, research is focused on identifying and overcoming the barriers to successful differentiation of the OPC into the newly myelinating oligodendrocyte. These may be drugs or small molecules that block inhibitory pathways aberrantly activated, or that up regulate one or many of the cascades of cellular process that lead to successful remyelination. These therapies are known collectively as Pro-Remyelination-Therapies and are distinct from the current wave of treatments currently available for diseases such as MS that are only able to target the immune damage which results in the initial demyelination. In contrast, however, such therapies are of little use where the myelinating cell type is inherently defective, such as in PMD. Here a source of unimpaired myelin forming cells is required. In some cases this may require exon skipping technologies such as those used in Duchene Muscular Dystrophy, or in CRISPR techniques to correct the genetic defects. However, transplantation of new cells is widely thought to be one of the most promising potential therapies. This dichotomy can be summarised by the endogenous vs exogenous therapy paradigm shown Figure 6.

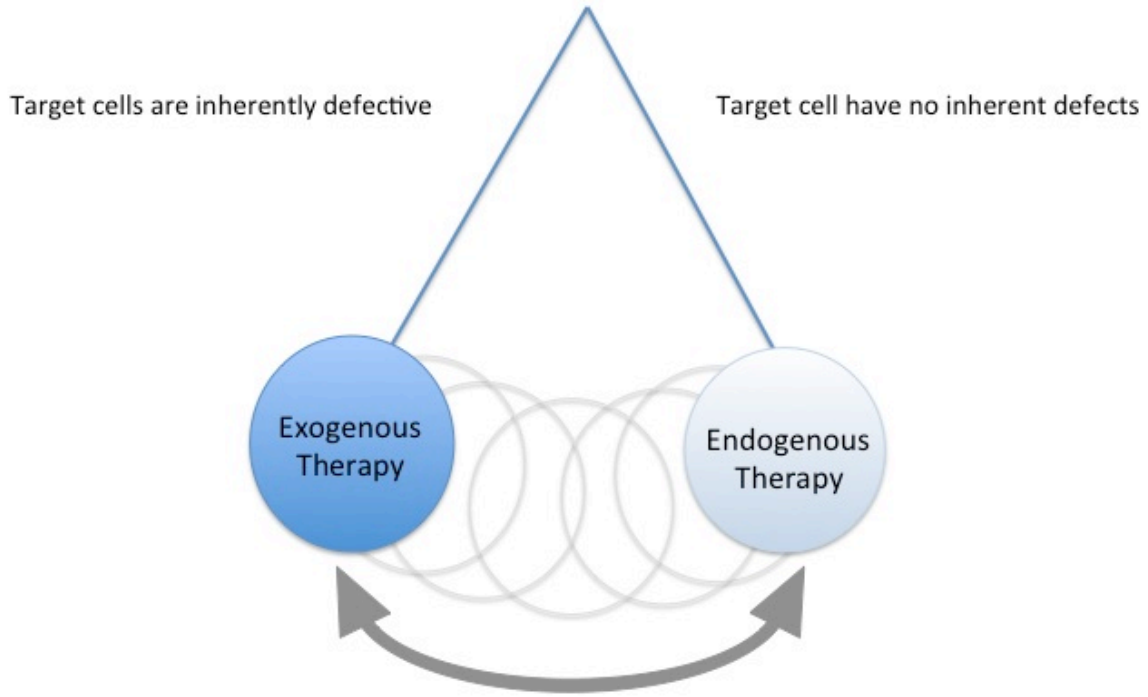

Figure 4: Exogenous vs Endogenous Therapies Exogenous therapies. Endogenous therapies dichotomy. Where there are inherent defects in the target cell population, such as in PMD, where mutations in the PLP gene lead to dysmyelinaton, therapies that replace these cells or correct these defects are required. This is in contrast to diseases where there is no inherent defect in the target cell, such as in MS, where there is an aberrant immune response, where pharmaceuticals targeting cellular pathways can be directed at promoting repair.

1.5 Magnetic Resonance Imaging

Magnetic resonance imaging (MRI) is based on the physics of nuclear magnetic resonance first demonstrated by Purcell and Bloch in 1946 (Purcell 1946; Bloch 1946). MRI exploits the magnetic properties of atomic nuclei to create an imaging modality that can produce three dimensional images of tissue structure that can be applied to clinical diagnostics as well as research questions.

MRI creates contrast between different tissues by exploiting the magnetic properties of atomic nuclei, most commonly the proton in the form of the hydrogen atom. The proton lends itself

to use with this technique because it is abundant in all biological tissues, and because of its inherent magnetic properties; namely the presence of spin. Any atomic nucleus which possesses the property of spin can be exploited in a magnetic resonance experiment. Spin is an inherent property of an atomic nucleus based on an imbalance between the number of protons and neutrons in the nucleus (Levitt, 2001). A nucleus with an even number of protons and neutrons will have no spin, whereas a nucleus with more protons than neutrons (such as hydrogen (^{1}H): one proton no neutrons) or more neutrons than protons (such as carbon-13 (^{13}C): six protons seven neutrons) will have spin.

Spin is expressed in units of Planck's constant, *h*. Planck's constant is the quantum mechanical property that links the amount of energy a photon carries to its electromagnetic wavelength. It has a value of 6.6260×10^{-34} m^2 kg / s or 6.6260×10^{-34} Js. Essentially, it is a measure of energy, and with regard to spin, indicates the amount of angular momentum the nucleus possesses. The property of spin, combined with the property of mass causes these nuclei to have a magnetic moment.

MRI manipulates the spin properties of these protons using magnetic fields. The behaviour of the protons when exposed to a magnetic field, and their subsequent relaxation, or return, to their original or equilibrium state, is known as spin relaxation. Different tissues with different distributions or densities of protons will demonstrate differing spin relaxation behaviour. This provides tissue contrast.

Spin relaxation behaviour is a description of how nuclei behave when exposed to a magnetic field. In any given substance, in the absence of a magnetic field, the spins of adjacent atoms

will be in disarray. If a magnetic field (B_0) is applied the spins will align with the applied magnetic field Figure 7.

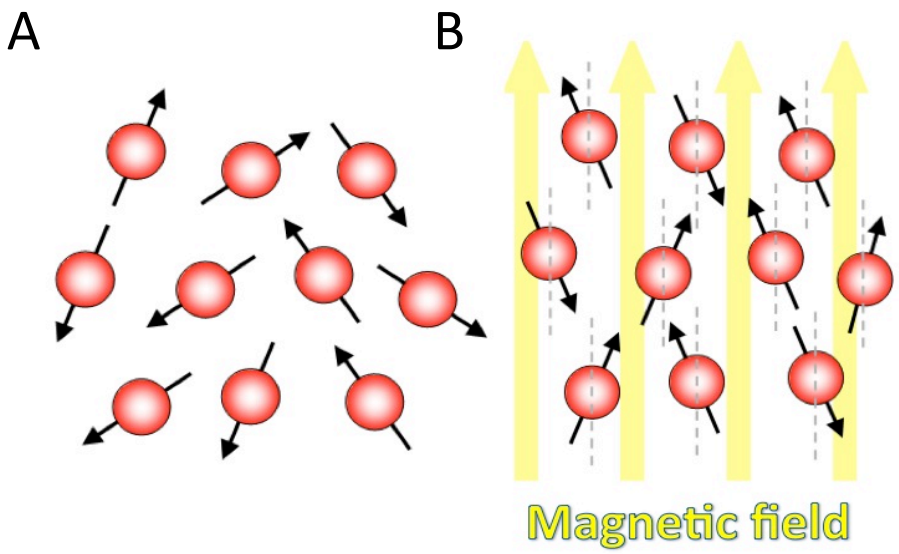

Figure 5: Magnetic Spin.
*Spin is a nuclear property caused by imbalances in sub atomic particles. It causes nuclei to have rotation (like the rotation around the axis of a planet); **A**. Hydrogen nuclei, in the absence of a magnetic field have spins which are in disarray. When a magnetic field is applied the spins of Hydrogen nuclei align; **B**. The total spin is the vector sum of all the spins.*

The combination of spin and a magnetic dipole leads to precession; where the spins don't align exactly with the field but precess about the field axis. The precessional frequency is defined as the Lamor frequency (ω), and is based on the relationship between the strength of the magnetic field, and the gyromagnetic ratio of the nucleus (γ). This is described by the Lamor equation:

$$\omega = \gamma B_0$$

B_0 is the applied magnetic field in Tesla (T). The gyromagnetic ratio represents the ratio of a particles magnetic moment to its angular momentum and is specific to a nucleus.

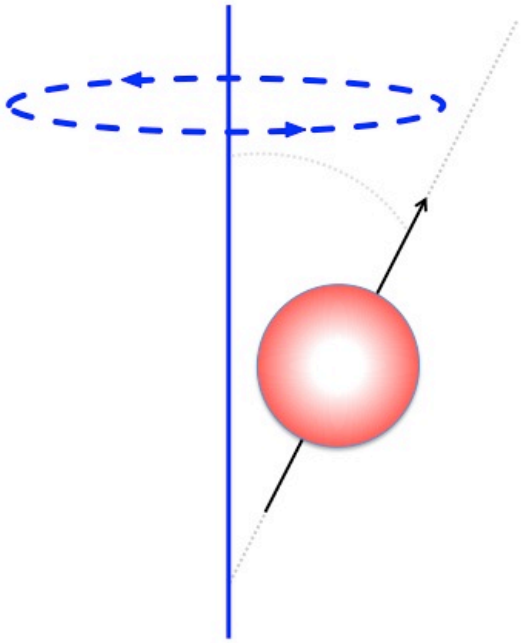

Figure 6: Magnetic Precession.
Precession is the phenomena of off axial rotation (like the rotation of the north or south pole of a planet as it spins around its axis, or the precession of a gyroscope in the earth's gravitational field). Hydrogen nuclei will precess around their axis in aligmnet with a magnetic field when a second magnetic field is applied, perpendicular to and oscillating around a static magnetic field.

Table 2 shows the different spin quantum numbers, gyromagnetic ratios, and relative concentrations in human tissue of a variety of different nuclei. It can be seen from this table that it is a combination of these properties that are required when selecting an element for nuclear magnetic resonance techniques. Protons have a non integer spin (a requirement for detection), a high gyromagnetic ratio (a large magnetic moment), and have both high natural abundance and high concentration in biological tissues.

Element	Number Protons	Number Neutrons	Spin	Gyromagnetic Ratio	Abundance	Concentration (human tissue)
Hydrogen ^{1}H	1	0	½	42.58 (MHz/T)	c.100%	88M
Deuterium ^{2}H	1	1	1	6.53 (MHz/T)	0.015%	13mM
Carbon-13 ^{13}C	6	7	½	10.81 (MHz/T)	1.1%	
Sodium ^{23}Na	11	12	$^{3}/_{2}$	11.27 (MHz/T)	c.100%	80mM
Fluorine ^{19}F	9	10	½	2.627 (MHz/T)	c.100%	4mM
Oxygen ^{17}O	8	9	$^{5}/_{2}$	-5.77 (MHz/T)	0.04%	16mM
Phosphorous ^{31}P	15	16	½	1.131 (MHz/T)	c.100%	75mM

Table 2: *Magnetic properties of a selection of biologically relevant nuclei.*
The subatomic characteristics of the nucleus of an isotope will dictate their magnetic properties. For a nuclei to be useful in MRI they must have a non integer spin. For conventional MRI it is also beneficial for the isotope to be abundant biologically and at reasonably high concentrations in tissue such that it can be detected. Adapted from James, T. L. 1975. Nuclear Magnetic Resonance in Biochemistry. Academic Press, New York.

1.6 Acquisition of the MR image

When a magnetic field is applied (B_o) the ^{1}H spins will either align with, or against the field (Figure 7). Furthermore, they will precess around the B_0 field direction with the z component

of the magnetization aligned with B_0 (lower energy state) or against B_0 (higher energy state). The number of spins in each orientation (with or against the B_0 field) can be estimated from the Boltzman distribution:

$$\frac{N_{high}}{N_{low}} = e^{-\Delta E/kT}$$

N represents the number of nuclei in the low or high energy states (spin parallel or anti parallel), k is a constant, T is temperature in Kelvin and ΔE is the difference in energy between the states. An unequal distribution of spins results in a net magnetization that is aligned with the field.

If a second magnetic field is applied orthogonal to B_0 (B_1), which oscillates around the sample at the same frequency as the Lamor frequency of the nucleus of interest, then for a spin ½ nucleus it will induce transitions between the two allowed energy levels. When B_1 is applied in the form of a radio frequency (RF) pulse (a 90 degree pulse), it flips the net magnetization out of alignment with the B_o field (the z axis) into the xy plane. The spins then dephase (the spins loose synchronicity or coherence) and relax back into alignment with the z axis. This dephasing, characterised by the T_2, or spin-spin relaxation time, is influenced by the properties of the tissue and the presence of other magnetic or paramagnetic compounds. The relaxation back towards the z axis is termed T_1, or spin lattice relaxation.

Rotation of the net magnetization vector in the xy plane induces a current in the receiver coil (RC). This decaying signal (the free induction decay or FID) is converted into a spectrum by Fourier Transformation. As the Lamor frequency of each nucleus is dependent on the strength of the magnetic field the use of magnetic field gradients allows the position in space of each nucleus to be encoded. Using frequency and phase encoding gradients allows the spatial

location of a nucleus to be extracted by using the Fourier transformation in two dimensions. Three-dimensional information is acquired by combining the frequency and phase data in two dimensions with either multiple slices through the sample, or by using a gradient across the sample in the third dimension. An example sequence is shown in Figure 7.

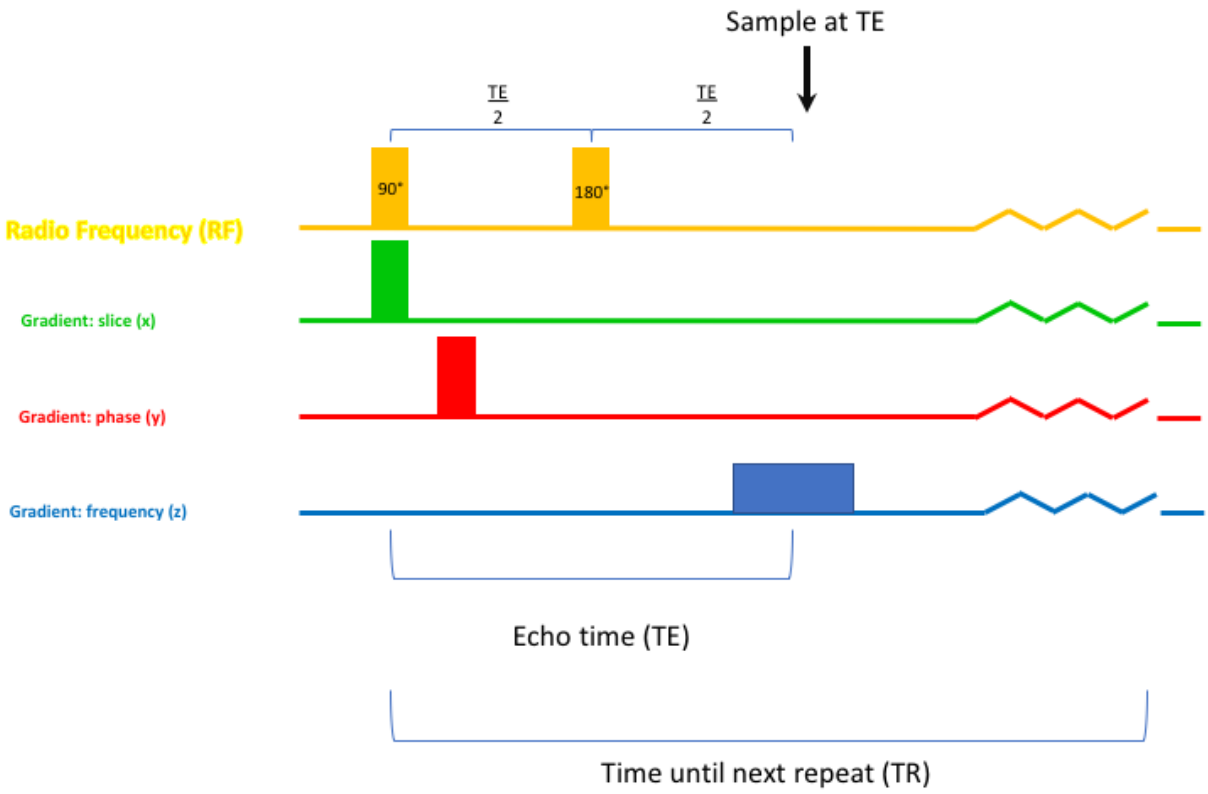

Figure 7: Example of an MRI pulse sequence showing the TE and the TR.
A sequence is made up of three gradient pulses and a radio frequency pulse. The 90° Radio Frequency pulse (yellow) tips the net magnetization in to the plane orthogonal to the static field, and this is refocused using the second 180° Radio Frequency pulse to form the echo. These are timed at TE/2 ie half the echo time). The echo time will be selected on the basis of the tissue being imaged. Signal is collected at intervals separated by the TE.
The three gradients, formed by gradients of a magnetic field, are aligned with the x,y, and z axis in this example, but in reality are aligned relative to the slice selected. They are switched on and off to create a pulse sequence that enables information to be encoded spatially. To collect a full image the sequence is repeated multiple times.

For an object imaged in a standard MRI experiment this means that upon application of the 90° pulse, the net magnetization vector that was previously aligned with the static magnetic field B_0, will move in to the x-y plane. This net magnetization vector will decay due to spin-spin relaxation and the loss of phase coherence owing to magnetic field inhomogeneity. The loss of phase coherence which results from inhomogeneity can be refocused by the use of the second pulse, this time at 180°. This forms the spin echo. Application of a phase-encoding gradient along the *y* axis between the 90° pulse and the 180° pulse results in the phase of the resulting echo varying as a function of the location in space of the nuclear spin relative to that gradient (the y axis). Multiple acquisitions of signal with incremental phase encoding leads to phase modulation of the decay profiles at frequencies which are dependent upon on the position of the spins in the gradient. By applying the Fourier transformation to this phase modulation, a profile of the sample in the *y* axis can be established. Images are usually acquired with T_1 or T_2 weighting, meaning that repetition and echo times are adjusted so that signal intensity is a function of spin lattice or spin spin relaxation.

T_1 or T_2 weighting affects image contrast. By using a combination of different sequences which are differentially T_1 or T_2-weighted, an understanding of the composition and architecture of a tissue can be gained.

The degree to which an image is T_1 or T_2 weighted will depend on the pulse sequence used for image acquisition, notably the timing of the Radio Frequency (RF) pulses and the signal readout. Pulse sequences can have several variable parameters, but two of the most important are the TE (echo time) and the TR (repetition time). The TE is the time between the RF pulse and the readout of the signal from the echo. The TR is the time between the successive applications of

the pulse sequence.

MR images can be produced in vivo with high spatial resolution eg. a 3D voxel size of 0.27nL (Howles *et al.* 2009), or 2D in-plane resolution of < 30nm (Boretius *et al.* 2009), allowing highly detailed whole body images to be produced with anatomical detail.

1.7 T1 weighted imaging

T_1 relaxation time is the longitudinal relaxation, or spin lattice relaxation time, and is a measure of the rate at which the net magnetization returns to the z axis after the RF pulse which flips it into the xy plane (Figure 10). The term lattice refers to the local environment of the nuclei. The T_1 value of a tissue is the time take for 63% of the net magnetization to realign with the z axis (with the B_o magnetic field). To acquire a T_1 weighted image a pulse sequence with a short repetition time TR), and a short echo time (TE) are used. Typical T_1 values for various tissues are given in Table 3.

Tissue Type	T_1 /ms (approx.)	T_2 /ms (approx.)
Liver	812 ± 64	42 ± 3
Skeletal Muscle	1412 ± 13	50 ± 4
Heart	1471 ± 31	47 ± 11
Kidney	1194 ± 27	56 ± 4
Blood	1932 ± 85	275 ± 50
Optic Nerve	1083 ± 39	78 ± 5
Spinal Cord	993 ± 47	78 ± 2
White Matter	1084 ± 45	69 ± 3
Grey Matter	1820 ± 114	99 ±7

Table 3: Values for T_1 and T_2 for different tissues. The typical relaxation rates for biological tissues in milliseconds in a 3Tesla magnet (Stanisz et al. 2005). These values act as a guide around which sequences will be designed depending on the tissue or region of the body being imaged.

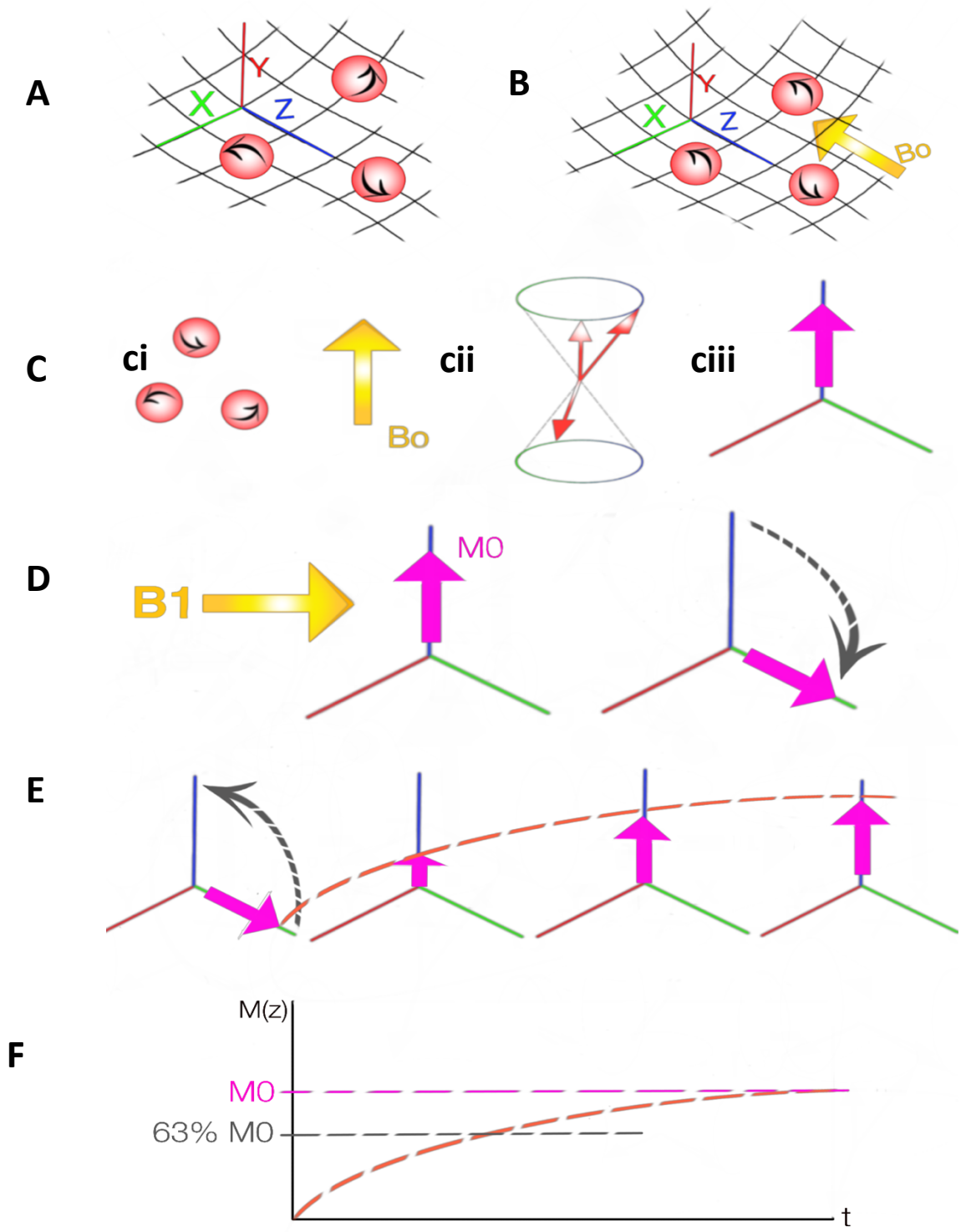

Figure 10: Spin Lattice relaxation.
*Protons exist in an environment made up of other protons and their associated magnetic dipoles, referred to as the lattice. In the absence of an external magnetic field, there is no alignment of the proton spins (**A**). When an external magnetic field is applied, B_0, the protons will align either parallel or anti parallel to the field(**B**), and they precess about this field at the Lamor frequency; (**ci** and **cii**), their net magnetization can be represented as a net magnetization vector (**ciii**) where the magnitude of the net magnetization is M_0. When an RF pulse (B_1) is applied, the net magnetization vector moves from the z axis into the xy plane (**D**). When B_1 is removed (**E**), the magnetization vector relaxes back along the z axis. T_1 relaxation is the time constant for the recovery of the net magnetization along the z axis to 63% of M_0 (**F**)*

1.8 T1 weighted contrast agents

Contrast agents are used to provide greater insight into the architecture or physiology of a given tissue. In MRI, a T_1 contrast agent is one that causes the spins in a tissue to return more rapidly to alignment with the z axis. A more rapid return results in a higher signal, which corresponds to a brighter image, therefore T_1 contrast agents give positive contrast in an MR image. Short TR times result in signal being collected when the nuclei have not fully relaxed back to their equilibrium distribution; they remain partially saturated. T_1 contrast agents cause shortening of the T_1 by increasing the relaxation rate of water molecules in their vicinity, resulting in the loss of the partial saturation and an increase in signal.

T_1 contrast agents most commonly exploit the presence of unpaired electrons, which cause them to be paramagnetic. The resultant large magnetic dipole causes a local oscillating magnetic field which interacts with neighbouring spins to promote spin lattice relaxation. The faster return of the spins back to their equilibrium state increasing the amount of signal that can be captured and therefore creating a greater positive signal.

Substances with a higher number of unpaired electrons have a greater paramagnetic effect. The most commonly used contrast agent is the gadolinium ion (Gd^{3+}) which has seven unpaired electrons. Gadolinium is extremely toxic and therefore it is administered as a tightly bound chelate. Another ion commonly used is Manganese (Mn^{2+}), which has 5 unpaired electrons.

The effect of a paramagnetic ion on surrounding water protons will have three different types of interaction, these interactions bring about a shortening of the T_1. These interactions are known as: 1) inner sphere interactions, 2) outer sphere interactions, and 3) local magnetic field

effects (Lauffer 1987).

Inner sphere interactions result from the binding of a water molecule in the primary co-ordination sphere of the paramagnetic ion and exchange with bulk water. This occurs when water molecules are within 1-2 angstroms (Å), (1 Å is 0.1 nanometers) of the paramagnetic ion.

Outer-sphere interactions occur when the water molecule is within 5 Å of the paramagnetic ion, and involve an interaction between the water molecule and another molecule that is interacting with the paramagnetic ion. These sorts of interactions are more common in chelated forms of the contrast agent, and less common with the free paramagnetic ions which can more easily interact via the inner-sphere mechanism.

The difference in the magnitude of T_1 enhancement between the inner-sphere and the outer-sphere relaxation is proportional to $\frac{1}{r^6}$, where r is the distance between the metal ion and the water proton. The effect of the local magnetic field from paramagnetic ions is the smallest of the three effects in its contribution to T_1 relaxation.

The strength of T_1 enhancement that a compound has on water is linearly dependent on its concentration. As a result of this relationship a value can be calculated for its relaxivity by taking the gradient of the line when R_1 ($\frac{1}{T1}$) is plotted against the contrast agent concentration, which is expressed in mM^{-1} $second^{-1}$.

1.9 T2 weighted imaging

T_2 weighting is obtained by using a long TE and long TR, this is because a long gap between excitations (ie a long TR) minimises T_1 effects by allowing time for all the protons to relax fully. Unlike T_1, which describes the rate of return of the magnetization vector along the z axis. T_2, also known as spin-spin or transverse relaxation, describes the rate at which the net magnetization is lost whilst still in the xy plane (Figure). The T_2 value is the time taken for the signal to decay to 37% of its initial value. This loss results from loss of coherence in the spin isochromats as they precess in the xy plane, resulting in a decrease in the net magnetization.

Tissues with a high macromolecular content, or high concentrations of paramagnetic centres, tend to have shorter water proton T_2 relaxation times, whereas tissues with more free water tend to have longer T_2 values. Tissues where water has a long T_2 are more bright in a T_2-weighted image.

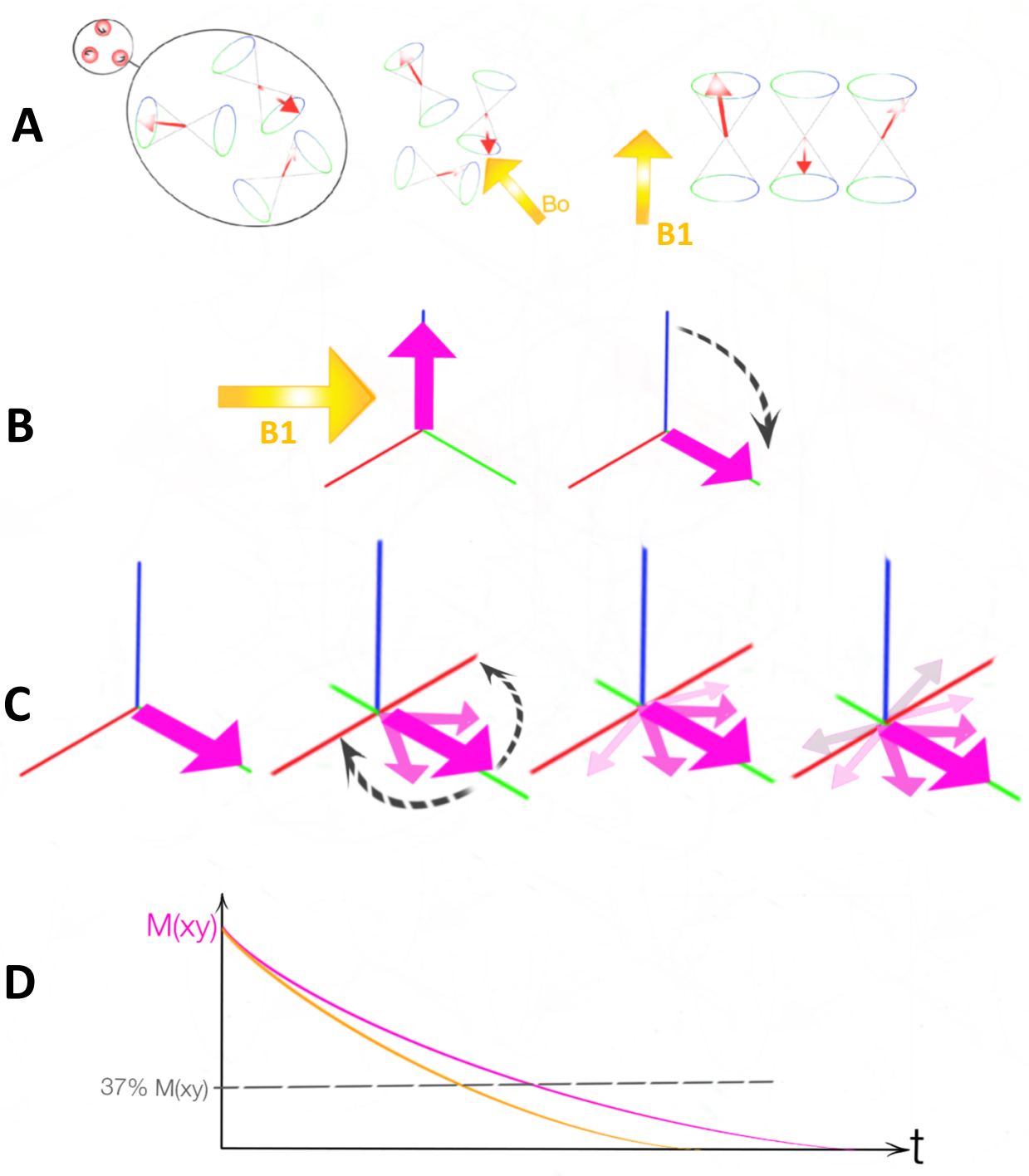

Figure 11: Spin-Spin, or Transverse, T2 relaxation.
*When a magnetic field B_0 is applied across a substance the proton spins align parallel or anti parallel to the applied field and precess about the axis of the field. In the presence of a second magnetic field, B_1, rotating at the Lamor frequency of the nuclei, the spins will precess in phase. When B_1 is applied as a pulse orthogonal to B_0 it moves the net magnetization into the xy plane (**B**). When B_1 is removed, the spins relax back along the z axis and lose phase coherence in the xy plane (**C**). Spin-Spin relaxation describes the energy exchange between neighbouring spins (true T_2) or local magnetic inhomogeneities as they lose phase coherence in the xy plane. The combination of the effects of spin-spin interactions and field inhomogeneities gives a relaxation time called T_2* relaxation.*

1.10 T2 contrast agents

Like T_1 weighting, T_2 effects can be enhanced by using paramagnetic agents. However, unlike T_1 agents, which increase signal intensity in T_1-weighted images, T_2 agents decrease signal by shortening T_2 relaxation times. This leads to hypointensities; darker areas on an image known as negative contrast. Most T_2 contrast agents are based on super-paramagnetic compounds. Like paramagnetic compounds used for T_1 contrast agent, these have unpaired electrons, however, unlike paramagnetic agents, super paramagnetic particles have a net magnetization in the absence of an external magnetic field. Most commonly these compounds exploit iron in the form of superparamagnetic iron oxide nanoparticles.

1.11 NMR

In addition to the production of anatomical images, magnetic resonance can also be exploited to elucidate chemical structures. For example, a proton bound to an oxygen atom (as in water), will have a different magnetic environment to a proton bound to a carbon atom (as in glucose for example). This difference in the strength of the magnetic field around individual protons is due to the shielding effect of surrounding electrons and is known as chemical shift. As a result protons in different chemical environments (in different chemical entities) resonate at slightly different frequencies. The spectra that result are characteristic of different chemical compounds.

1.12 Gene reporters

A reporter gene is one which, when expressed, can be detected to provide a quantifiable signal. They are used to make inferences about the qualitative or quantitative state of another genes expression in a cell or tissue.

A reporter gene construct will most commonly consist of the reporter gene under the control of a cell specific reporter sequence such that one promoter sequence is activated the expression of the reporter gene will be switched on. Once expressed the reporter gene gives off a signal detectable by imaging equipment, an example is depicted in Figure 12. This methodology differs from other mechanisms of gene expression measurement, such as polymerase chain reaction (PCR), western blotting or northern blotting, in a number of key ways. Firstly they allow longitudinal and real time monitoring of gene expression rather than snap shots, and importantly, are minimally invasive.

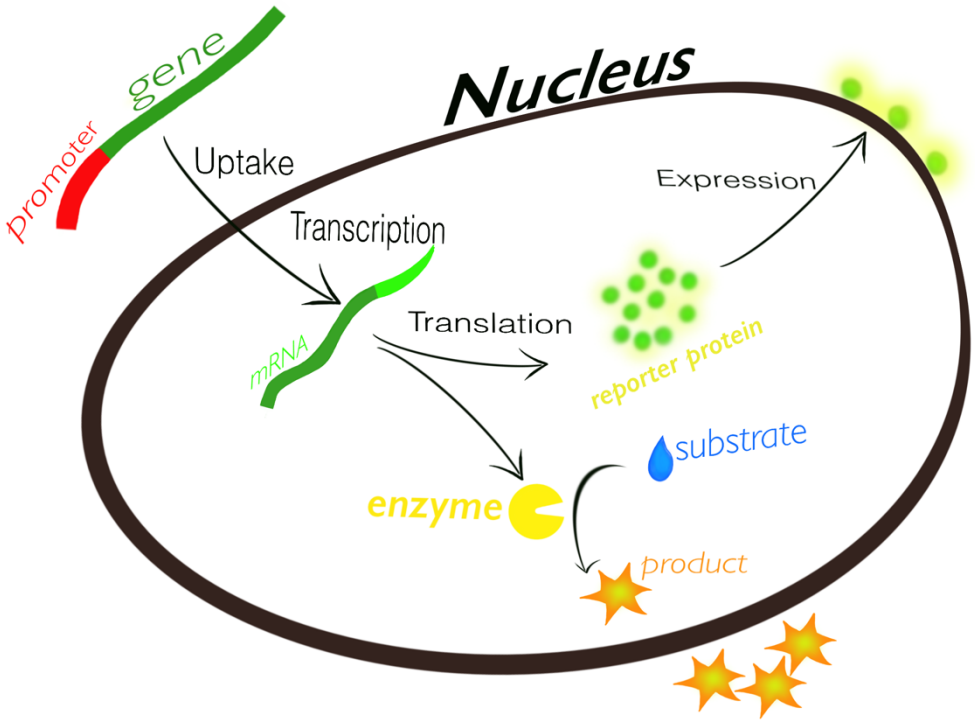

Figure 12: *Example of gene reporter systems, commonly reporter genes encoding detectable proteins (such as GFP), or enzymes which catalyse the production of a detectable product (such as horse radish peroxidase) are used.*

The field of optical gene reporters really began with beta galactosidase and the LacZ operon, and this system has been commonly used to monitor cellular processes ever since. LacZ, remains one of the most widely used and useful of all gene reporters (Price, Turner, and Cepko 1987; Mulder *et al.* 2012; Lyons, Patrick, and Brindle 2013).

New substrates have been developed to convert this system for in vivo use, but numerous technical and practical issues have limited the use of these systems (Debacq-Chainiaux *et al.* 2009; Degenfeld, Wehrman, and Blau 2009). However, with the description of green fluorescent protein (Chalfie *et al.* 1994) in the 1990's this field expanded exponentially. GFP and reporter genes like it offer superior resolution to that achieved by

traditional light microscopy, and enable high levels of temporal resolution (Nakano 2002). However, these methodologies rely on the penetration of light, and therefore are not very applicable to *in vivo* systems where signal attenuates rapidly due to tissue depth. The optical window is the range of wavelengths which will travel through a tissue Figure 13, the optical window for visible light is relatively limited in normal tissue due to minimal light penetration.

Near infra red imaging (NIR) achieves greater tissue penetration as the wave length of this part of the electromagnetic spectrum has greater tissue penetration. This reduces the amount of signal attenuation through tissue however the brightness achievable with these is still far inferior to that of the traditional fluorescent proteins such as GFP (Shu *et al.* 2009).

Tissue clearing techniques aim to overcome the narrow optical window for visible light wavelengths by reducing the signal attenuation due to the presence of opaque tissues. Unlike transparent models such as the zebra fish (Buckley, Goldsmith, and Franklin 2008), these techniques reduce light scattering, and therefore signal loss, by transforming tissue in to a hydrogel-tissue hybrid by removing lipids whilst leaving microstructure and gross anatomy intact. These techniques have achieved far superior resolution of neuroanatomy, in the region of 10s of micrometers (Tomer *et al.* 2014), in comparison to other three dimensional techniques, however, as with all histological techniques they are only applicable to post mortem tissues and so can only answer a limited array of questions.

Bioluminecense; the property of producing visible light by an organism, usually via a redox reaction between luciferin and oxygen and catalysed by a luciferase enzyme, have been

harnessed in imaging through combination with gene reporter systems to achieve expression of detectable light by biological systems (Badr and Tannous 2011).

Bioluminecent imaging (BLI) can be used to probe gene expression (Patrick, Lyons, *et al.* 2014), protein-protein interactions (Pichler *et al.* 2008), protein folding (Suzuki *et al.* 2007) and to trace stem cells (Sacco *et al.* 2008). In the latter study muscle stem cell were traced following transplantation in to the tibialis muscle of a mouse, this study clearly demonstrates the potential for BLI to be used in stem cell fate mapping, however the interrogation of model systems of greater tissue depth than the relatively superficial hind leg of a mouse, may highlight the major limitation of this technique which is signal attenuation though the tissue, common to all optical imaging techniques. Techniques to increase luciferin signal may help to overcome this limitation such as the use of OATP (Patrick, Lyons, *et al.* 2014).

Intravaital microscopy can be used to detect fluorescence proteins and dyes a few hundred micrometres beneath the skin with high resolution in vivo, but at greater depths the sensitivity and resolution are greatly reduced (Weigert, Porat-Shliom, and Amornphimoltham 2013). IVM encompasses a variety of different modalities including one, two and three photon imaging, however currently non of these techniques offer more that 500μm depth penetration into tissues (Masedunskas *et al.* 2014). This tissue penetration may pose few issues when utilising mouse disease models, however, larger species pose greater depth challenges, and there are very clear challenges for translations in to man.

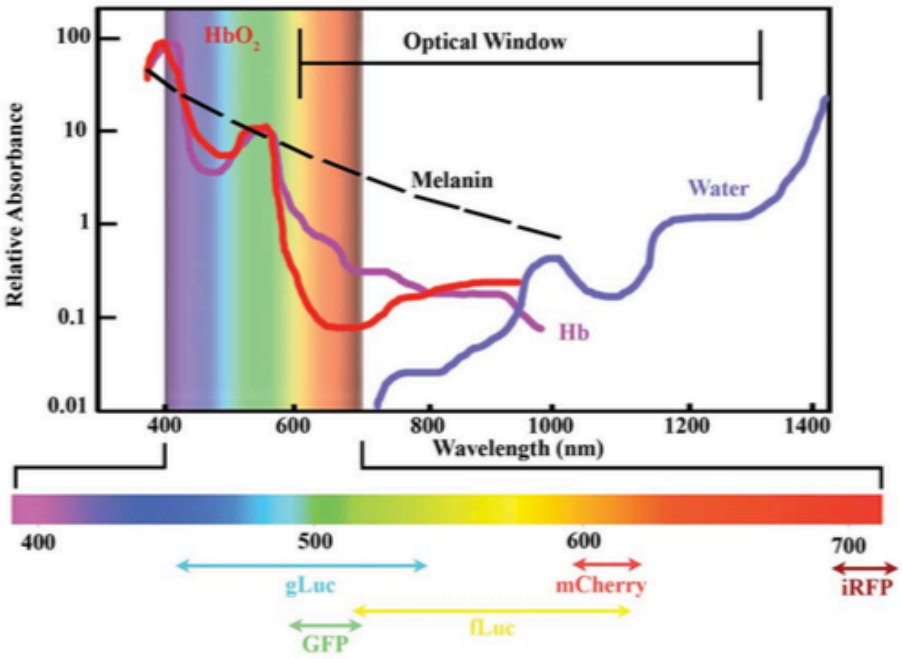

Figure 13: *The Optical Window. The efficiency of light transmission through a biological tissue is reduced by the presence of light absorbing molecules including blood (Heamoglobin (Hb) in its various oxygenation states), pigment etc. Wavelengths towards the red end of the visible spectrum, and in the near infrared region, overlap more with the optical window; the wavelegths where light has its maximal tissue penetration. Light emitting reporters in these ranges will be more effective in biological systems than those whose wavelengths sit outside the optical window. Adapted from Lyons et al 2013.*[666]

1.13 Imaging Remyelination: The Status Quo

1.13*i* Diagnostic Clinical Imaging

Magnetic Resonance Imaging

The diagnosis of MS relies heavily on diagnostic imaging techniques, alongside neurological examination, and a relevant clinical history. MRI is the most commonly performed investigation in the work up of a patient were MS is considered a potential differential diagnosis (Polman *et al.* 2011; Filippi *et al.* 2016)

Diagnostic criteria for MS focus on white matter lesions, their number, location and temporal frequency, however these alone are not unique to MS, with similar lesions appearing in many other disorders, therefore more subtle characteristics such as Dawson fingers, juxta- cortical lesions and short partial and eccentric spinal cord lesions are necessary to support a diagnosis of MS (Toledano, Weinshenker, and Solomon 2015; Chen *et al.* 2016). Additionally tests which are able to help rule out some of the MRI mimics of MS, such as the antibody mediated Neuromyelitis Optica Spectrum Disorders (NMOSDs) or Acute Demyelinating Encephalomyelitis (ADEM) for which Anti auaraporin 4 and anti myelin oligodendrocyte protein antibodies can be detected, are important in making definitive diagnoses (Geraldes *et al.* 2018). A summary of the current diagnostic criteria for MS are given in Table 4.

<table>
<tr><th>Primary criteria:</th><th>Plus two or more of the following:</th></tr>
<tr><td rowspan="3">1 year of disability progression, retrospectively or prospectively determined independent of clinical relapse</td><td>One or more T2-hyperintense lesions characteristic of multiple sclerosis in one or more of the following brain regions: periventricular, cortical or juxta cortical, or infratentorial</td></tr>
<tr><td>Two or more T2-hyperintense lesions in the spinal cord</td></tr>
<tr><td>Presence of CSF-specific oligoclonal bands</td></tr>
<tr><td colspan="2">Unlike the 2010 McDonald criteria, no distinction between symptomatic and asymptomatic MRI lesions is required.</td></tr>
</table>

Table 4: Diagnostic criteria for multiple sclerosis generated by International Panel on the Diagnosis of MS in 2001 with subsequent revisions in 2010 and, most recently in 2017; known as the MacDonald criteria (revised). Figure adapted from Thompson, Banwell, Barkhoff et al. 2017. These criteria are used in the clinical diagnosis of multiple sclerosis and in the differentiation of Multiple Sclerosis from other potential differential diagnosis such as neuromyelitis optica.

White matter lesions are the classical hallmark of MS, although lesions can be found throughout the CNS. Spinal cord imaging poses distinct challenges to imaging in the brain. This is largely as a result of the small cross sectional area of the cord, its proximity to the large vertebral bodies which can cause susceptibility artefacts, alongside interference that the pulsatile flow of CSF can cause to certain sequence types. Its specific imaging modalities and their inherent challenges will not be further examined here.

White matter lesions are typically visualised using T_2 weighted imaging and pre and post contrast T_1 weighted imaging. MS plaques are typically imaged with T_2 weighted sequences. Here lesions are detected as hyperintensities. However the sensitivity for detecting the underlying pathology is poor (Tillema and Pirko 2013). In particular it is challenging to differentiate between the various features associated with MS, and hallmarks of other pathological processes for example remyelination inflammation oedema and axonal loss, all part of the pathology seen in MS can be almost impossible to differentiate from cell infiltration or neoplasia as all these have similar characteristics on T_2 weighted imaging (Group 1993) (Tillema and Pirko 2013). Fast spin echo sequences and fluid attenuation inversion recovery (FLAIR) sequences are the most common sequences to use in T_2 weighted imaging. FLAIR imaging supresses the water signal from CSF thus giving improved tissue contrast, however it can obscure lesions in certain locations, and for this reason FLAIR sequences alone are insufficient to make diagnoses (Stevenson *et al.* 1997).

Contrast agents are rarely used in T_2 weighted imaging, iron oxide nanoparticle-based contrast agents that can give hypointense signal changes on T_2* weighted imaging, but most of these

are experimental and with limited use in human studies (Dousset *et al.* 2006; Pirko *et al.* 2004; Vellinga *et al.* 2008)

In addition to the difficulty in correlating imaging findings with pathology there appears to be a weak correlation between the T_2 lesion load, and clinical disability (Molyneux *et al.* 1998; O'Riordan *et al.* 1998; Zivadinov and Leist 2006). This difficulty may result from the inability to reliably identify a remyelinated lesion (Tillema and Pirko 2013).

T_1 weighted imaging alone offers little specific support for the diagnosis of or identification of MS lesions, however some T_2 hyperintensities are hypointense on T_1 (Uhlenbrock and Sehlen 1989), these T_1 black holes arise as a result of two main disease processes:

1) A majority of T_1 black holes are seen early in lesion formation (Bagnato *et al.* 2003);(Levesque *et al.* 2010) with cellular infiltration in newly forming lesions associated with focal oedema. Lesions of this type often resolve (Brex *et al.* 2002; Losseff *et al.* 2001)

2) Approximately 30% of T_1 'black holes' will persist, becoming a lifelong feature (Ciccarelli *et al.* 1999; van Waesberghe *et al.* 1999). These are thought to represent severe tissue loss with areas of axonal injury or loss (Bitsch *et al.* 2001). Here the degree of hypointensity is thought to be proportional to axonal density (Bitsch *et al.* 2001), with the most hypointense black holes having little in the way of remaining neuronal structures (van Waesberghe *et al.* 1999). The presence of the T_1 black hole is better correlated with clinical disability than the T_2 weighted image.

T_1 post contrast enhancement is considered to be the hallmark of the 'active lesion' as it represents the presence of a permeable blood brain barrier through which the contrast agent

(and therefore inflammatory infiltrates) can pass in to the parenchyma. Gadolinium post contrast enhancement are typically present in the first 4-6 weeks of a lesions lifecycle (Miller *et al.* 1988) . However, the presence of post contrast enhancement does not necessarily indicate an imminent clinical relapse. Thompson and colleagues identified T_1 post contrast enhancement 5-10 times more frequently than clinically observable relapses (Thompson *et al.* 1992). Therefore, despite the fact that post contrast enhancement is the only conventional imaging tool we have that correlates directly to the pathological state of a lesion, its correlation to clinical state is limited.

Diagnostic criteria are clearly focused on the identification of existing pathology and the correct elimination of other differentials. However, monitoring of patients once a diagnosis has been made is of critical importance both in assessing their relative severity of disease, but also in monitoring of response to treatment.

Conventional imaging modalities rely on the characteristics discussed above, however advanced MRI techniques are being developed in order to address the shortfalls in correlation between imaging finds and histopathology. It is simply not possible to reliably identify remyelination with any current conventional MRI techniques (Absinta, Sati, and Reich 2016).

Myelin Water Fraction

Mapping of Myelin water content (the Myelin Water Fraction (MWF)) has been developed as an advanced MRI technique for detecting myelin (MacKay and Laule 2016; Sati *et al.* 2013). This technique relies on different T_2 relaxation times of water in different anatomical environments. It has been shown that protons in water within the myelin membranes have a

short T_2 relaxation time of 10-55ms (usually around 20ms),(McKay et al 1994). By examining the relationship between the short (water T_2 times, and the total water signal a ration of myelin water content can be extrapolated. This myelin water fraction has histopathological correlation with lesion changes and is unaffected by axonal degeneration or inflammatory cell infiltration and oedema (Laule *et al.* 2006)

This methodology it is limited by poor signal to noise ratios and reproducibility between scanners (Alonso-Ortiz, Levesque, and Pike 2014), additionally in order to get adequate brain coverage long sequence acquisition times are required when using sequences such as T_2 prep three dimensional SPIRAL, a gradient echo sequence suitable for whole brain imaging if the MWF (Nguyen *et al.* 2012).

Magnetisation Transfer Ratio

Magnetization Transfer Ratio (MTR) may offer more specific insights in to the demyelination:remyelination relationship (Levesque *et al.* 2010). Magnetisation transfer imaging is a semi quantitative technique which uses traditional magnetic resonance physics but exploits the physiology of the anatomical environments in which the proton (^{1}H nuclei) exist; namely a free 'liquid' pool, in which protons are mobile, and a restricted 'semisolid' where a protons mobility is restricted as a result of its relationships with macromolecules it comprises with or it interacts with.

Transfer, or the exchange, of magnetisation takes place between these two pools, by using an additional radio frequency pulse in the sequence. The bulk of signal in conventional MRIs

comes from the free proton pool because the restricted proton pool has a such a short T_2 relaxation that signal decays prior to sampling making this compartment relatively invisible on conventional sequences. By exploiting the exchange of magnetisation which occurs as result of the specialised pulse sequences Magnetisation Transfer Ratio Imaging gives insight into this previously 'invisible' pool of protons. This is particularly pertinent to remyelination as myelin is a major source of 'semi solid' or restricted protons. Magnetisation Transfer imaging provides access to the restricted protons, which are located in biologically interesting tissue regions. The main factors which influence Magnetisation Transfer Ratio are shown in Table 5:

Factor	CHANGE	Reference
Myelin loss	↓	Schmierer K, Scaravilli F, Altmann DR, *et al.* Magnetization transfer ratio and myelin in postmortem multiple sclerosis brain. Ann Neurol 2004;56:407–15.
Oedema	↓	Rai, Ahuja, Agrawal, Kalra, et al Reversal of Low-Grade Cerebral Edema After Lactulose/Rifaximin Therapy in Patients with Cirrhosis and Minimal Hepatic Encephalopathy. Clinical and Translational Gastroenterology (2015) 6, e111
Low axonal density	↓	Schmierer K, Scaravilli F, Altmann DR, *et al.* Magnetization transfer ratio and myelin in postmortem multiple sclerosis brain. Ann Neurol 2004;56:407–15.
Cell Infiltration	↓	Gareau, Rutt, Karlik and Mitchell. Magnetization Transfer and Multicomponent T_2 Relaxation Measurements With Histopathologic Correlation in an Experimental Model of MS. J. Mag. Res. Im. 2000:11;586-595

Table 5: *Factors which influence MTR relevant to remyelination and demyelination.*

Using MTR white matter lesions show a reduction in transfer in comparison to NAWM, with remyelinated lesions showing an increase in Magnetisation Transfer Ratio relative to lesions (Schmierer, Wheeler-Kingshott, *et al.* 2007). In MS the MTR shows the following relationship (Barkhof *et al.* 2003);(Chen *et al.* 2008);(Schmierer, Wheeler-Kingshott, *et al.* 2007):

Demyelinated>Remyelinated>NAWM>Control healthy white matter of non MS patient

Although very sensitive to myelin Magnetisation Transfer Ratio, is only semi-quantitative, and shows a degree of variability in its quantification between different sequences and scanners (Mallik *et al.* 2014). Magnetisation Transfer Ratio has been shown not to correlate with myelin content in a murine model of of MS; the MOG-EAE model (Fjær *et al.* 2015). Mathematical modelling to extract the quantitative features is possible, and overcomes this issue to a great extent (Levesque *et al.* 2010; Schmierer, Tozer, *et al.* 2007; Cercignani *et al.* 2005), however the degree to which these values can be used as biomarkers is not fully established as oedema in particular can attenuate the reduction in Magnetisation Transfer Ratio following demyelination, and as sequential readings are required on a per lesion basis, this attenuates any increase in Magnetisation Transfer Ratio which might be expected as a result of repair (Ou *et al.* 2009)

Diffusion Tensor Imaging

Diffusion Tensor Imaging is a quantitative technique which measures the motion of water molecules in their different anatomic environments inferring information about microstructural anatomy though changes in this water motion. Similar to Magnetisation Transfer Ratio it relies on the fact that a majority of MRI signal is obtained from protons bound as water, and that water exists in different anatomical environments be that fixed or free. The motion calculated in DTI is not flow, but the Brownian motion of the proton as a particle. Free water will have 100% random motion, however when anatomical structures such as axons or myelin are introduced the degree and direction of this motion will be constrained by the macromolecular structures and their orientation. DTI takes three main measurements; the

fractional anisotropy, the radial diffusivity and the axial diffusivity with the addition of the mean diffusivity which is a global measure of water motion.

1) FA is a fractional measure of the freedom with which water can diffuse or move. An FA of 0 indicates unimpeded motion in all directions. And FA of 1 indicates uniplanar motion, i.e. it is restricted along a single axis. FA is thought to correlate with axonal density and myelination (Gouw *et al.* 2008).

Factor	FA	RD	AD	Reference
Inflammation (usually reported as astrogliosis, or cell infiltration and oedema)	↑	-	↓	(Tu *et al.* 2016; Xie *et al.* 2010) (Wang *et al.* 2011)
Demyelination	↓	↑↑	--	(Song *et al.* 2005) (Song *et al.* 2002)
Loss of axonal density	↓	↓	↓↓	(Song *et al.* 2003) (Winklewski *et al.* 2018)

***Table 6**: Relationships between DTI factors*

2) Radial Diffusivity is the rate of diffusion perpendicular to the main axis, or in the transverse plane. It is thought to reflect the degree of myelination (Song *et al.* 2005).

3) Axial Diffusivity is the rate of diffusion in the longitudinal plane or in plane with the main axis, it has been correlated with axonal integrity (Winklewski *et al.* 2018).

The major limitation of this technique however, is that it relies on accurate tractography and calculation of fibre orientation (Mallik *et al.* 2014), and again is a proxy measure for myelin rather than a direct quantification.

Magnetic Resonance Spectroscopy

Magnetic Resonance Spectroscopy (MRS) works analyses the proton in its chemical environment giving parts per million read out for different metabolites. It is able to detect

active lesions as it will demonstrate peaks in lipid and choline spectra associated with demyelination and the break down of the myelin sheath (Narayana 2005), however it offers little insight into intact myelin (Laule *et al.* 2007), though some suggest that it more accurately represents instability, suggesting that peaks could represent demyelination or remyelination (De Stefano *et al.* 2005; Lin *et al.* 2005). Either way, it is a non specific measure of myelin activity.

Positon Emission Tomography

Positron Emission Tomography, in contrast to all the previously described techniques is a nuclear modality which relies on ionising radiation. A radioactive ligand is piggy backed into the body on a tissue relevant biologically active molecule, this allows tissue metabolism and regional blood flow to be probed on the basis on the rate of uptake and decay of the ionising radiation (Niccolini, Su, and Politis 2015). The most commonly used ligand for brain imaging is ^{18}F-FDG a fluorinated glucose tracer used to investigate tissue metabolism, its main diagnostic role is to aide division of lesions in to active or chronic (Schiepers, Van Hecke, and Vandenberghe 1997). A few myelin specific ligands have been designed (Stankoff *et al.* 2011), however, there is significant research in to developing a wider array of molecules for clinical use (Niccolini, Su, and Politis 2015). ^{11}C PiB, in particular shows promise as an agent capable of differentiating remyelination (Bodini *et al.* 2016), however currently it is challenging to synthesis and has a prohibitively short half life (Sormani and Pardini 2017). Somewhat more common is the PET imaging of microglia which gives insights into microglial activation and inflammation (Takano *et al.* 2013). However, all PET imaging processes are limited by their relative expense and the concerns over imaging chronically ill patients repeatedly with multiple doses of ionising radiation.

1.13*ii* Preclinical Imaging of Remyelination

A majority of clinical imaging technologies have gone through often considerable development in preclinical models, however at the current time none of them are used for routinely evaluating remyelination therapies in clinical models of MS or toxin induced demyelination.

There are a wide range of modalities available for pre clinical evaluation of myelin, these techniques are largely light and electron microscopy techniques, these modalities require post mortem tissue and will not be further examined here. The focus instead will be on longitudinal imaging modalities, with particular emphasis on those which have the potential to be translated in to clinically applicable techniques.

Stem cell transplant therapies are being widely explored for a range of CNS conditions including MS and spinal cord injury (SCI), current molecular imaging to trace these cells falls in to two main categories, physical cell labelling and the use of gene reporters. Current physical strategies include T_2 contrast agents such as USPIOs and SPIO, radionuclide labelling for SPECT or PET, and nanoparticle labelling for fluorescent imaging. Currently available gene reporters include the bioluminescent proteins including firefly luciferase and the fluorescent protein gene reporters discussed previously such as GFP. A range of gene reporter systems for MRI exist, discussed in section 1.14. However, to date, none of these have been used to probe myelin dynamics.

Labelling of endogenous progenitors and the interrogation of their remyelinating potential has been widely studied with a variety of genetic fate mapping techniques, as well as a number of

viral introduced reporter gene systems, these systems rely on optical imaging methodologies which are no clinically translatable and therefore not examined further here.

SPIO

Superparamagnetic iron oxide (SPIO) particles, are composed of multiple magnetite crystals, each particle is 200 nm in diameter. Ultra Small SPIO (USPIO), consist of a single crystal core and have an average particle diameter of 50 nm (Modo, Hoehn, and Bulte 2005). Relaxivity increases with increasing crystal density, and so SPIO – with several magnetite crystals per core and a large magnetic moment – can generate more contrast per mole of iron than USPIO (Wáng and Idée 2017; Modo, Hoehn, and Bulte 2005).

SPIOs are taken up in to the target cells by endocytosis, with particles localising in endosomes, this increases susceptibility effects (Kraitchman and Bulte 2008). Long term the SPIO is broken down by intracellular lysosomes, or alternatively phagocytosed by monocyte lineage cells where they may be degraded in turn. The liberated iron then enters endogenous iron homeostatic pathways and may be stored as hemosiderin or ferritin in tissues (Wáng and Idée 2017).

USPIO and SPIO in myelination/remyelination SPIO particles have been used to label NPCs, OPCs, OECs and mesenchymal cell transplants into damaged CNS without deleterious effects to cellular function (Sandvig *et al.* 2011; Lin *et al.* 2013; All *et al.* 2012; Kobayashi *et al.* 2012; Luo *et al.* 2013; Bottai *et al.* 2010; Amemori *et al.* 2013; Hu *et al.* 2012; Jung *et al.* 2009; Lepore *et al.* 2006; M. E. Cohen *et al.* 2009; Dunning *et al.* 2006; Franklin *et al.* 1999). These cells have been detected by T_2 MRI sequences, and in some studies functional improvements following

transplantation have been recorded in models of spinal cord injury. Oligodendrocyte precursors have also been labelled with SPIOs and successfully transplanted with detection at over one week post transplantation (Bulte *et al.* 1999; Franklin *et al.* 1999), and similarly labelled Schwann cells have been shown to form functional myelin following transplantation (Dunning *et al.* 2006). To date this study, alongside Bulte and colleagues (Bulte *et al.* 1999) recapitulation of this study in the myelin deficient rat, remains the only examples of a myelinating cell type being detected successfully by MRI with confirmed myelin formation. However, like all SPIO studies, functionality is not detectable by MRI and requires histopathological processing. Equally SPIO particles can persist in phagocytic cells following cell death thus impairing their specificity as a cell survival indicator (Kraitchman and Bulte 2008).

PET and SPECT in myelination/remyelination

Preclinical PET and single photon emission computed tomography (SPECT) operate on the same principles as the clinical imaging modalities. Cell identification is feasible in the short term, however imaging for periods long enough to visualise remyelination is limited due to the short half live of the radio ligands available (Scarfe *et al.* 2018).

High Field MRI

High field imaging (using scanners above 3 tesla) may also offer greater insight, (Chmierer *et al*. 2009). However, there are limitations on the availability of these scanners for clinical use and sequences are not directly transferable from lower field strength scanners.

1.14 Reporter Genes for MRI

Gene reporter systems are used to visualize or quantify the expression or activity of genes in biological systems. First developed in 1985, firefly luciferase is still widely used today. The repertoire of gene reporters has since been expanded and includes GFP, and creatinine kinase which can be used in magnetic resonance imaging (de Wet *et al.* 1985). However, despite much work on the development of new MR reporter genes, very few advances have been made with their use (Gilad, McMahon, *et al.* 2007).

The first reporter gene used for MRI was creatine kinase (Koretsky *et al.* 1990) in 1990, since then over 20 other systems have been published. See Appendix 2. However there are many challenges to their development (Gilad, Winnard, *et al.* 2007).

Possibly due to the almost ubiquitous usage of the T_2 sequence in clinical and pre clinical MR work, ferritin, which can be used to provide T_2 weighted contrast enhancement, is one of the most widely used reporters (Genove *et al.* 2005). However, it has many disadvantages, in particular it provides negative contrast (a reduction in signal below background levels), and is not hugely specific due to the presence of other iron containing tissues (blood) in the body.

The development of the Urea Transport Protein reporter system (Schilling *et al.* 2016) has facilitated relatively low resolution (0.93mm x 0.93mm x 3mm), but highly specific imaging of reporter genes in the murine brain providing an imaging modality which does not require a contrast agent using apparent water exchange as a measure for the reporter genes expression. This methodology lends itself well to translation in to the human imaging as it relies on

endogenously generated contrast (water movements), however the relatively low spatial resolution may be too low to allow cell fate mapping, and resolution is likely to decrease in lower field clinical scanners

Few reporter genes have been developed to provide T_1 weighted contrast (Bartelle *et al.* 2013) Koretsky and Silva 2004). T_1 contrast is preferable as it is positive (increased signal relative to background). Until recently the few reporter systems that did exist provided poor resolution and suffered from toxicity issues. However with the development of the OATP reporter gene system now exists which provides excellent spaciotemporal resolution (Patrick, Hammersley, *et al.* 2014).

Based on the current literature, it is clear that there is a predominance of MRI reporter gene systems for use in T2 weighted imaging (Weissleder et al. 1997); (Weissleder et al. 2000); (Moore et al 2001); (Alfke et al 2003), (Cohen et al. 2005); (Genove et al. 2005); (Tannous et al. 2006); (Zurkiya, Chan, and Hu 2008); (Cui et al. 2010); (Niers et al. 2012); (Patrick et al. 2016); (He et al. 2016); (Wu et al. 2018). Cui and colleagues achieved a 3.5 fold decrease in signal using a LacZ:S-Gal plasmid system under a cytomegalovirus promoter (Cui et al. 2010), however this required direct transfection of tumour cells by intra tumoral injection and this system has not yet been replicated in a systemic delivery model. Many of the T2 weighted systems make use of iron or ferritin reporter systems, the most effective of these, reported by Weissleder and colleagues reported a 5.3 fold decrease in signal in vivo (Weissleder et al. 2000). The approach used by Weissleder and colleagues aimed to overcome previous requirements for high levels of over expression of the Transferrin receptor, and for the potential toxicity of high levels of free iron seen in some previous studies. This was achieved

by the use of monocrystalline iron oxide particles coupled to holo-transferrin, and an engineered transferrin receptor over expressed on tumour cells. This would result in the accumulation of non toxic iron oxide particle in the cytosol of cells expressing only the engineered receptor in a tumour cell line. Such particles require systemic intravascular administration, marking their use completely inappropriate for imaging within the CNS. As discussed previously, a T2 contrast enhancement usually result in a reduction in the signal collected and therefore in 'negative' contrast on an image. This can be challenging to identify visually on an image and therefore significant efforts have been made to develop positive contrast modalities applicable to T1 weighted imaging or to more advanced imaging techniques such as Chemical Exchange Saturation Transfer MRI (Meier et al. 2018) or Apparent Water Exchange Rate MRI (Schilling et al. 2017).

Attempts have been made to exploit manganese, an alternative paramagnetic metal to gadolinium which also provides T1 weighted contrast. Manganese contrast has been reported with both exogenously delivered contrast in the form of manganese chloride (Bartelle et al. 2013), and manganese loaded ferritin(Patrick et al. 2016), however both these systems suffer from the toxicity of manganese, and in first instance of significant levels of background contrast as Manganese can be taken up in to neurones due to its similarities to calcium, and the divalent metal transporter over expressed in the study is present on a all CNS cells to some degree (SkjÃ rringe et al. 2015). The later of these studies aims to overcome this background issue by using a T cell immunoglobulin and mucin domain containing protein which is an alternative form of ferritin receptor, coupled with either iron or manganese loaded ferritin for both T1 and T2 weighted imaging, and achieves a significant change in both T1 and T2 signal *in vitro*, however despite loading the manganese in to

apoferritin particles, the toxicity of manganese is still a significant challenge and the *in vitro* T1 imaging could not be recapitulated *in vivo*.

The only system to date which is reported in the literature of t1 weighted contrast agent, already approved for use in humans with acceptable toxicity profiles (as judged by Food and Drug Administration (USA) and National Institute for Clinical Excellence (UK) approval, and widespread clinical usage) is that of the OATP transporter proteins reported by Patrick and colleagues (Patrick et al. 2014). This system, discussed in more detail in the next section uses viral delivery of the transgene to facilitate the cytosolic uptake of the paramagnetic ion gadolinium and aims to overcome many of the issues around toxicity, low resolution and background or endogenous contrast with have contributed to relative obsolescence of many of the other techniques previously reported.

Of the techniques that target more advanced MRI imaging sequences the UDP reporter used by Schilling and colleagues is one of the most exciting developments in the field as it as no toxicity associated with the contrast agent as it makes use of endogenous water movements for imaging using AXR sequences(Schilling et al. 2017). Like the OATP vector it uses a lentiviral system, and like any other viral gene therapy technique there are challenges around the translation of lentiviruses in to clinically applicable tools, however these are likely to surmountable as viral vector technologies improve. Equally as exciting is a Lysine rich protein promoter(Meier et al. 2018) which again uses endogenous contrast and MTR imaging, although not amenable to longitudinal imaging this technique makes use of an adeno-associated viral vector which is potentially less problematic for translation to the clinic due to their increasing use in other forms of gene therapy (Keeler, ElMallah, and Flotte 2017). This

lysine rich protein reporter requires MTR sequences which can be challenging to standardise and do not form part of the standard range of diagnostic sequences therefore it is unlikely that this, or the UDP system will find an application in clinical diagnostics in the near future. They may however be useful tools in refining and standardising these sequences such that they can be transitioned to clinical tools more rapidly.

1.15 Organic Anion Transporter Proteins

The Organic Anion Transporter Proteins (OATP) are a family of transmembranous proteins expressed on the membranes of a wide range of cells throughout the bodies of mammalian species. They serve to transport a range of uncharged organic molecules into the cells cytoplasm including thyroid hormone and oestrogen. Oatp1a1 is the protein isoform expressed on the basolateral membrane of hepatocytes, its expression is highly restricted (Hagenbuch and Meier 2003; Roth, Obaidat, and Hagenbuch 2012).

The restricted expression of Oatp1 has been harnessed by clinical hepatologists as its expression is up regulated in certain forms of hepatic carcinoma. A contrast agent has been designed which is specific to the Oatp1 chanel. Primovist (Bayer) is a gadolinium containing linear chelate (Gd-EOB-DTPA) which is specifically transported by the Oatp1a1 channel (van Montfoort *et al.* 1999). In cases of hepatic carcinoma this results in an accumulation of this contrast agent intracellularly which is visible as contrast enhancement on T_1 weighted MRI.

By expressing this protein ectopically in xenografts the Brindle group have demonstrated that Oatp1a1 can be used as a specific and sensitive gene reporter which provides positive contrast

on MRI. It is also able to enhance uptake of luciferase resulting in a ten fold increase in signal (Patrick, Lyons, *et al.* 2014). The expression of the Oatp1a1 has been linked to a fluorescent reporter gene; mStrawberry, by an E2A sequence facilitating equimolar expression.

Preliminary work by Patrick *et. al*. using recombinant mammalian expression vectors have been used to transfect a variety of cell lines to demonstrate selective and reversible take up of gadolinium contrast agent (Figure 14). Xenografts expressing Oatp1a1 have been shown to result in reversible contrast enhancement specific to administration of Primovist (Bayer) Figure 15; here the expression of Oatp1a1 is under the control of the constitutively active promoter sequence Phosphoglycerokinase (PGK).

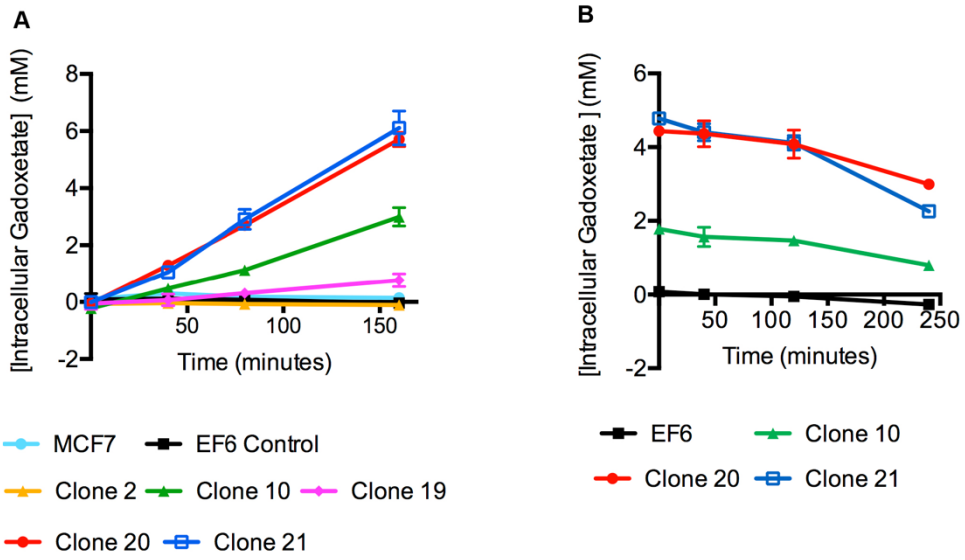

Figure 14: Primovsit Uptake in vitro. Primovist (Gd-EOB-DTPA) uptake and washout in cells transfected to express Oatp1a1. Measurements of uptake (A) and washout (B) in un transfected cells, cells stably transfected with empty vector, and cells stably transfected with an oatp1a1-expressing vector. From Patrick et al (2014).

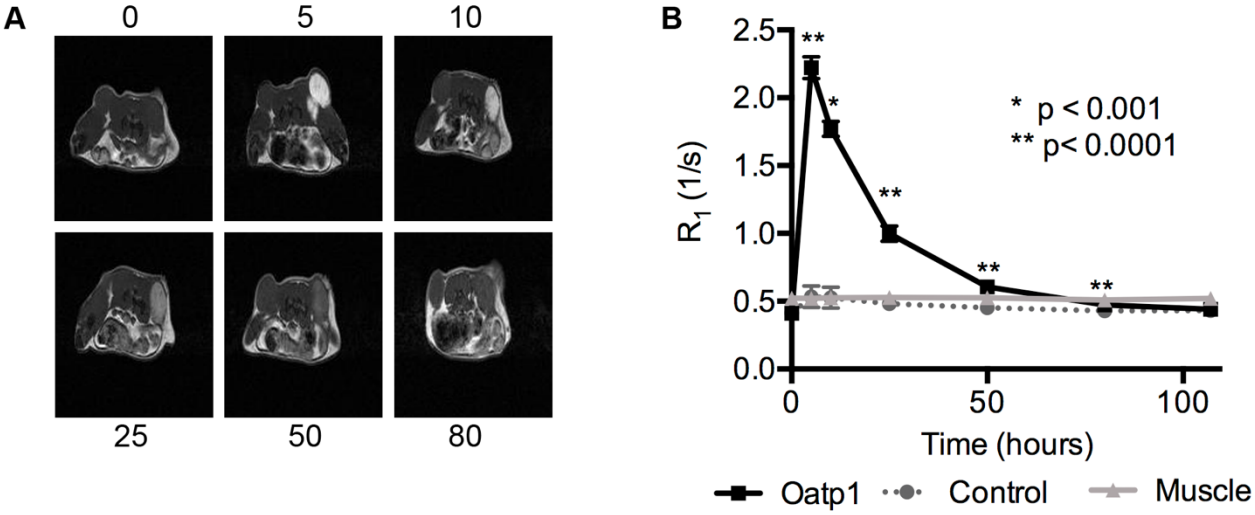

Figure 15: Primovist uptake in vivo. ***A.*** *T_1 images after contrast agent injection. Left are control xenografts, right side xenograft express Oatp1a1.* ***B.*** *R_1 before and following injection of Gd-EOB-DTPA were significantly greater compared to controls. From Patrick et al (2014) PNAS.*

2. Aims

This project aims to develop a novel technique which is able to non invasively, and longitudinally identify the expression of new myelin in an experimental model of demyelination.

The project aims to 1) image differentiation of endogenous OPCs into remyelinating oligodendrocytes *in vivo*, and 2) to image differentiation of transplanted OPCs into remyelinating oligodendrocytes *in vivo.*

This will be achieved by using the novel imaging strategy first developed by the Brindle group: the OATP transporter channel. By controlling the expression of this channel in OPCs and Oligodendrocytes using constitutively active, and lineage specific promoters, cells will take up gadolinium based contrast agents detectable by nuclear resonance imaging techniques. The uptake of the contrast agent will therefore be directly related to the expression of these genes. This project will use the EB-CCP lesion as an experimental model of demyelination and remyelination in which to develop this technique. It will use two different paradigms in its development: The first, looking to achieve OATP expression in endogenous OPCs as they differentiate in to myelinating oligodendrocytes. This methodology might form the foundation of an outcome measure for therapies for diseases such as multiple sclerosis were new therapies are likely to revolve and pharmacological manipulation of the immune and inflammatory cascades. The second, looking to achieve OATP expression in to OPCs differentiating in to oligodendrocytes following transplantation in to demyelinating lesions. This methodology might form the foundation for an outcome measure for new therapies to

treat diseases such as Pelizeus Merszbacher Disease, where new therapies are likely to require cell based therapies.

Specifically this project aims to address the following questions:

1) Can OPCs and Oligodendrocytes be infected by, and express a viral vector carrying the OATP1a1 transporter channel?
2) Can OPCs or Oligodendrocytes expressing OATP take up imaging contrast agents?
3) Can imaging protocols be developed to detect these contrast agent *in vitro* and *in vivo*?
4) Is it possible to detect demyelination and remyelination in the EB-CCP model system?
5) Can outcome measures and techniques for the new methodology be developed to allow validation of the new technique?

In the future it is hoped that full *in vitro* and *in vivo* models can be generated in which oligodendrocyte lineage cells, expressing the OATP channel under the control of a myelin promoter, take up contrast as they differentiate in to the myelinating oligodendrocyte. This contrast agent will be detectable by non invasive imaging and can be used to monitor remyelination. Specifically it can be used as a non invasive outcome measure for assessing the efficacy of new myelin regenerative therapies.

3. Materials and Methods

3.1 Molecular Biology Protocols

3.1i Restriction Enzyme Digestion

To confirm the structure of the plasmids inherited from Dr. P.S. Patrick, restriction enzyme digestions were performed. Over ice, 1µL of restriction enzyme was added to 1µg of DNA 2µL of the appropriate buffer (CutSmart, New England Biolabs (NEB) B7204S) and dH_2O up to a volume of 20µL, the solution was then incubated at 37°C for one hour. Digestion products were then mixed with 5µL loading dye (New England Biolabs B7024S) and run on a 1% agarose gel electrophoresis for 35 minutes at 110 volts with a DNA Ladder (New England Biolabs N3232S). A list of restriction enzymes is given in Appendix 5.

3.1ii Vector Construction

Five plasmids were inherited from Dr. P.S. Patrick; a three vector lentivirus packaging system containing pRev, V-VSG, and pMDL, and two pBOBI lentiviral transfer plasmids; one expressing OATP under the PGK promoter and one under an MBP promoter. Restriction enzyme digestions confirmed that the inherited packaging and PGK plasmids matched existing maps; however, the MBP vector did not, and not did it appear to work in initial trial infections. Therefore, the MBP fragment was sequenced and synthesised using PCR. The fragment was ligated in to the vector using 40 ng of cut vector and a 1:3 molar ratio of vector to insert, 0.5µL of T4 DNA ligase, 1µL of ligase buffer, and Milli Q water to make a final volume of 20µL. Prior to ligation the vector was dephosphorylated using Antarctic phosphatase (NEB) together with the supplied buffer in order to prevent re-circularisation of the plasmid in the absence of the insert. Following the dephosphorylation step, the phosphatase was inactivated by incubation

at 65°C for 15 minutes. Ligations were incubated at room temperature for 1 hour, before being used to transform competent bacteria (New England Biolabs: C2987I).

3.1iii Bacterial Transformation and Plasmid Purification

In order to obtain concentrated pure plasmid competent bacteria (New England Biolabs 5-Alpha: C29871) were transformed and expanded before protein extraction. 50µL of competent *E.coli* were thawed on ice for 10 minutes. 50ng of plasmid DNA was added to the solution which was mixed by flicking the tube 5 times before being incubated on ice for 30 minutes. The bacteria were then heat shocked for 30 seconds and then returned to ice and incubated for a further five minutes. 950 µL of SOC media (NEB: B9020S) was added at room temperature and then incubated at 37°C and 250 rotations per minute(rpm) for 60 minutes. Serial dilutions of the competent bacterial solution were added to pre warmed selective *LB Agarose Plates* and incubated overnight at 37°C to allow colony expansion.

Single colonies were then selected and added to 5ml of selective *LB Broth* in a 15mL loosely capped falcon tube, and incubated at 37°C, 250 rpm for 6 hours to form starter cultures, these were then expanded seeding 1mL in to 100mL of pre warmed selective *LB Broth* in 250mL conical flasks and incubated overnight.

Bacterial pellets were harvested from the expanded cultures by centrifugation at 6000g for 20 minutes at 4°C, supernatant was carefully removed prior to protein extraction or freeze storage at -80°C.

Protein extraction was performed using Qiagen Mini, Midi, or Maxi QIAprep (QIAGEN: 10023) kits according to manufacturers guidelines.

3.1iv Lentivirus Production

Plasmids for production of the lentivirus were inherited from Dr. P.S. Patrick via the Verma lab, Stalk Institute, California. HEK293T Cells were plated on 15cm dishes (Sigma CLS430599) in *Mixed Glia Media* to achieve a confluence of 80% on day one of transfection. 22.5ug of pBOBI vector, 14.7μg pMDL plasmid, 8μg VSV-G plasmid and 5.7μg pRev plasmid were added to 600μL OptiMEM (Lifetech 31985062) in one tube. In a second tube 80μL of lipofectamine 2000 (Invitrogen 11668-019) was added to 600μL OptiMEM. Tubes were incubated for 5 minutes at room temperature. The second mix was then pipetted in to the first and allowed to incubate at room temperature for 30minutes. The transfection solution was then added to 13ml of pre equilibrated OptiMEM and added to the cells. 12 hours later 5mL of *nOPC media* (serum free) was added. 48 hours after vectors were added supernatant is collected and fresh *nOPC media* was added.

Virus for use in vitro was concentrated using Millipore Centricon Plus-70 filters (Merck Millipore, UFC710008), and aliquots frozen at -80°C. Virus for use in *in vivo* experiments was concentrated using ultracentrifugation.

3.1v Virus Concentration

Virus for use *in vitro* was concentrated using Millipore Centricon Plus-70 filters (Merck Millipore, UFC710008)according to the manafacturers instructions, and aliquots frozen at -80°C.

Virus for use in *in vivo* experiments was concentrated using ultracentrifugation. Supernatant was collected and filtered through a 0.45µm syringe filter (Millipore) to remove debris. A 20% sucrose cusion was pipetted in to the bottom of a 30mL conical ultracentrifugation tube (Beckmann Coulter) beneath the filtrate. The filtrate was centrifuged at 24 000 rpm in for 2 hours at 4°C, using a swinging bucket rotor (SW28, Beckmann). This process was repeated removing supernatant and adding fresh filtrate multiple times to concentrate the virus. After the final centrifugation, the supernatant was removed, and the conical tubes left to dry in a sterile environment. Pellets were then re-suspended in PBS, and vortexed gently every 20 minutes for 2 hours. The virus was then aliquoted and stored at – 80°C.

3.1vi Viral Tire Quantification

Viral titres were calculated by infecting HEK cells using a limiting dilution series. HEK293T cells were infected at 70% confluence in OptiMEM media using a 10 fold serial dilution of the stock virus, 72 hours following infection cells were detached from the plates using trypsin and stained with DAPI for flow cytometry. The percentage of mStrawberry fluorescing cells was calculated and the number of viral particles per ml calculated using the equation:

$$\frac{\%\ \text{mStraw+} \times \text{total number of cells at time of infection} \times \text{dilution factor} \times 1000}{\text{volume of virus used to infect in } \mu\text{L}}$$

3.2 *In Vitro* Cell Culture Protocols

3.2i Media Recipes

HALF See appendix 3i

SATO See appendix 3ii

Modified MWB See appendix 3iii

nOPC Media See appendix 3iv

CSC Media See appendix 3v

MG Media See appendix 3vi

LB Broth See appendix 3vii

Selective Bacterial LB Agar See appendix 3viii

MACS Dissociation Solution See appendix 3ix

Mixed Glia Dissociation Solution See appendix 3x

CryoProtectant Solution See appendix 3xi

3.2ii Cell Culture

HEK293T cells and OPCs were seeded at densities according to Table 7. HEK293T Cells were cultured in *Mixed Glia Media*, nOPCs were cultured in serum free defined media; *nOPC Media*, see appendix 8.3. Cells were incubated at 37°C and 5% CO_2.

	Surface Area (cm^2)	OPC	HEK
24 well plate (/well)	2	10,000	n/a
T25	25	200,000	n/a
T75	75	500,000	500,000
150mm dish	152	n/a	1,000,000

Table 7: Cell densities for plating of HEK and nOPCs

3.2iii HEK293T Cell Freezing

Cells were grown to approximately 80% confluence, trypsinised, resuspended in *Mixed Glia Media*, and pelleted by centrifugation at 3000g for 5 minutes. The supernatant was removed and the pellet was resuspended in freezing medium (80% growth medium, 10% Fetal Bovine Serum (FBS) and 10% DMSO), and transferred to 2mL Cryovials (Corning). The vials were then placed in a cell-freezing container (Mr Frosty, Nalgene), before being stored at -80°C.

3.2iv HEK Cell Thawing

Frozen Cryovials of HEK cells stored at -80°C were heated to 37°C in a water bath, until no ice remained. The content of the vial was then diluted 1 in 10 using growth *Mixed Glia Media*, and centrifuged at 300g for 5 minutes, to form a cell pellet. The supernatant was removed and the cells were resuspended in an appropriate volume of *Mixed Glia Media* and transferred to a cell culture flask

3.2v Trypsin Dissociation of HEK Cells

HEK cells were grown to 70 to 80% confluence, washed with PBS (Gibco), trypsinised (0.5% trypsin, Invitrogen in DMEM(Gibco)), and mechanically agitated until they were separated from the surface of the flask. Cells were then diluted in *Mixed Glia Media* to neutralise the trypsin, before being diluted further to an appropriate concentration for plating.

3.2vi Papain Dissociation of nOPCs

To dissociate OPCs from plasticware a milder dissociation protocol was required than that used for HEK cells (Trypsinisation - see above). Media was removed from flasks and washed with pre warmed PBS (Gibco), and *Mixed Glia Dissociation Solution* Activated by warming to 37°C for 15 minutes. 3ml of *Mixed Glia Dissociation Solution* were added per T75 flask and incubated

for 3 minutes at 37°C. Flasks were agitated by tapping the side of the flask five times, flasks were checked to ensure cells were fully detached, agitated or incubated further as necessary. Dissociation Solution was inactivated by the addition of 6ml of *Mixed Glia Media* and the solution collected in to 15mL Falcon tubes. Flasks were washed with a further 6mL *Mixed Glia Media* which was added to the Falcon tube, and the solution was centrifuged at 250g for 8 minutes. Cells were resupended in *nOPC Media* with 4μg/mL Insulin and 30ng/mL of FGF and PDGF added and incubated for 30-60minutes before being diluted as appropriate.

3.2vii Cell Counting

HEK cells were washed with PBS, trypsinised until separated from the surface of the flask, and resuspended in PBS. 100μL of the cell suspension was put into a cuvette, and made up to 10 mL using cell counting diluent (1 in 100 dilution). The cuvette was placed inside a Z2 Particle counter (Beckmann Coulter), and the number of cells per mL estimated. Alternatively, and always with OPCs diluted cell suspensions were counted using Trypan Blue in a manual haemocytometer and cells per ml calculated based upon the average of four counts

3.2viii nOPC isolation – MACS

Neonatal OPCs were isolated from wild-type Sprague Dawley rat pups at post natal day 0-7. Pups were sacrificed according to Schedule 1 methods of humane killing, using a lethal dose of pentobarbitol 0.7mL/kg (Animalcare, 01452) intra-peritoneally, followed by decapitation.

Following euthanasia, the whole brain was dissected out and the brain placed immediately in *HALF* on ice. The meninges and olfactory bulbs were removed and the dissected brains were

chopped using a scalpel. The *HALF* containing the tissue was placed into a 15mL falcon tube and spun for 1 minute at 100g (Eppindorff 5810 R). The *HALF* was aspirated, and the pelleted brain tissue re-suspended in activated filtered *Dissociation Solution*, added in equal volume to the volume of the pelleted tissue. The brains were then placed on a 55 RPM orbital shaker at 35˚ C for 30 minutes (Thermo Fisher; SHKA4000), and incubated for 30 minutes.

The tissue was then centrifuged at 300g for 5 minutes, the supernatant was removed, and the homogenate was resuspended in *HALF* containing 2mM sodium pyruvate, and 2% B27 (Thermo Fisher; 17504-001).

Using a 5mL pipette, the dissected brains were gently titurated 10 times. Using fire polished pipettes of decreasing diameter, the homogenate was further titurated until appearing as a single cell suspension. The cell suspension was then passed through 70µM filter (Corning; 352350) to remove any remaining clumps of cells.

To remove myelin debris from the suspension, 1 part 90% Percoll (GE; 17-0891-01), diluted in 10 x PBS was added to 3 parts cell suspension. The cell suspension was then spun at 800g for 20 minutes, the pellet re-suspended in *Modified MWB*, and a cell count performed.

The cells were pelleted at 300g for 5 minutes and re suspended in in 500µL *Modified MWB* and 2.5µL A2B5 antibody (Millipore; MAB312) per $1x10^7$ cells. After a 30 minute incubation on a gentle rocker at 4˚C, 5 times the volume of the cell suspension of *Modified MWB* was added, and the cell suspension was spun at 300g for 5 minutes. The pelleted cells were then resuspended in 80µL *Modified MWB* and 20µL MACS beads (Miltenyi; 130-047-302).

After a 30-minute incubation on a gentle rocker at 4°C, the cell suspension was centrifuged at 300g for 5 minutes and re-suspended in 1mL *MWB*. An MS column (Miltenyi; 130-042-201) was placed in a MiniMACS Separator (Miltenyi; 130-042-102), and washed 3 times with 500µL *MWB*, waiting each time for the liquid to pass completely through the column. The cell suspension (max $5x10^8$ cells) was placed in the column, 1mL of *MWB* was added to the column, the column was removed from the stand to remove the magnetic field, and the plunger depressed. The positive fraction suspended in *OPC* media and counted and the volume adjusted for plating according to densities shown in Table 7.

3.2ix nOPC isolation – Mixed Glia

Neonate OPCs were isolated from wild-type Sprague-Dawley rat pups at post natal day 0-3. Pups were sacrificed according to Schedule 1 methods of humane killing, using a lethal dose of pentobarbital 0.7ml/kg (Animalcare, 01452) intra-peritoneally followed by decapitation.

Following euthanasia, the whole brain was dissected out and the brain placed immediately in *HALF* on ice. The meninges and olfactory bulbs were removed and the dissected brains were chopped using a scalpel. The *HALF* containing the tissue was placed into a 15mL falcon tube and spun for 1 minute at 100g (Eppindorff 5810 R). The *HALF* was aspirated, and the pelleted brain tissue was re-suspended in 2mL of activated filtered *Mixed Glia Dissociation Solution*. The brains were then placed on a 55 rpm orbital shaker at 35°C for 60 minutes (Thermo Fisher; SHKA4000).

The tissue is then homogenized through a P1000 filter pipette. An equal volume of *Mixed Glia Media* is added to stop the papain, the solution is pelleted at 300g for 5 minutes and resuspended in fresh pre equilibrated *Mixed Glia Media*.

The brain homogenate is distributed between T75 flasks 1 - 1.5 brains per flask. Media is changed on alternate days and the mixed culture is maintained for ten days before mechanical dissociation and fractionation known as 'Shake Off'.

On the day of Shake Off, flasks are sealed and secured on the orbital shaker at 37°C for 1 hour. Media is aspirated after 1hour and fresh pre equilibrated media added. The flasks are returned to the shaker at 37°C for 16 to 20 hours. The supernatant is then placed in to an untreated 10cm petri dish for microglia depletion. The dish is incubated at 37°C and 5% CO_2 for 30 minutes. The supernatant is removed, a cell count performed, and cells pelleted by centrifugation at 300g for 5 minutes. The pellet is resuspended in *nOPC media* and diluted as appropriate for plating at densities as per Table 7.

3.2x Maintenance and Differentiation of nOPCs

Cells isolated by MACS or by mixed glia shake off (MGSO) were plated as follows for use in *in vitro* studies and in preparation for transplantation studies.

Glass 96 well plates (In Vitro Scientific; P96-1.5H-N), 13mm cover slips (VWR 631-1578) or T75 flasks (Greiner BIO One 658175) were coated with 200μL of PDL in 40mL dH_2O (Sigma; P6407) and incubated at 37°C for 1 hour. Plates were washed twice with dH_2O. Isolated OPCs were plated at a densities as per table F. For proliferation media was changed on alternate days

with *OPC* media supplemented with 30ng/mL bFGF (Peprotech; 100-18b) and 30ng/mL PDGF (Peprotech; 100-13a). To differentiate the cells, media was aspirated off the cells, and replaced with OPC media supplemented with 40ng/mL Triiodo-L-Thyronine (Sigma, T2877). The cells were kept in an incubator at 37°C and 5% CO_2.

3.2xi Cerebellar Slice Culture

P10 Sprague Dawley neonatal rats were euthanized by intra peritoneal injection of pentobarbital (0.7mL/kg). The brain was dissected out and sagittal section 300μm thick of the cerebellum were taken using a microtome. Sections were incubated in *HALF* on ice before being individually separated and placed onto MilliCell 0.4μM membranes (Merck Millipore PICMOR50) in a six well plate in pre equilibrated *CSC Media*. Slices were incubated at 37°C 5%CO_2, and media changed every second day for ten days prior to demyelination in 25mg/mL Lysolecithin (Sigma L1381). Lysolethocin was applied directly to the slices and incubated overnight before being washed twice in PBS and then being returned to normal *CSC Media*.

For slices infected with lentivirus work was carried out in a CL2 tissue culture hood. 1μL/1000μL media of concentrated virus was added to media and incubated for 8 hours before being washed three times in PBS and then return to normal *CSC Media*.

Slices were then fixed at the appropriate time point and frozen in *Cryoprotectant Solution* at -80°C until staining.

3.2xii Cell Viability Assay

nOPCs were obtained by MACs sorting and expanded by proliferation on 15cm PDL coated dishes. Following five days of proliferation cells were infected with lentivirus carrying the Oatp1a1 gene under the PGK promoter. Some nOPCs were left uninfected as a negative control. 1μL of concentrated virus was added to *nOPC Media* without antibiotics and cells were incubated for 8 hours before media was aspirated and the cells were washed with PBS and fresh, pre equilibrated, media added. 48 hours following infection, Primovist was added to all cells at a final concentration in media of 5mM. Cells were incubated for five hours in the gadolinium containing media. Media was aspirated and cells washed 3x with, pre warmed, sterile PBS.

Cells were incubated in Trypan Blue (Sigma T8154) and cell counts performed accounting for total number of cells, dead cells (Trypan Blue positive), and alive cells. 5 samples were taken from each condition and counts were expressed from an average of four counts per sample.

3.2xiii Cell Fixation

Cover slips and glass 96 well plates with nOPC and oligodendrocyte cultures, or HEK293T cultures were fixed in 4% PFA in PBS for 10 minutes at room temperature. PFA was aspirated and samples were washed in PBS three times, 10 minutes per was. Cover slips and plates were stored fully immersed in PBS, sealed with Parafilm and protected from light at 4°C until staining.

3.2xiv Cerebellar Slice Culture Fixation

CSCs were removed from the Millicell insert using a paintbrush and were fixed in 4% PFA in PBS for 60 minutes minutes at room temperature. PFA was aspirated and samples were washed in PBS with 0.05% three times, 10 minutes per wash. Slices were stored at -80°C in *Cryoprotection Solution* protected from light.

3.3 In Vivo Procedures

3.3i Animal Husbandry

Sprague Dawley (SD) rats were bred in the Innes Building and Mira Building Animal Facility; University Biological Services at the University of Cambridge. Adult Sprague Dawley rats were also purchased from Harlan Laboratories and housed at the Biological Resource Unit, Cambridge Institute, Cancer Research UK. All animals were fed a standard diet and were kept on 12 hour light;dark cycles. All procedures were performed in accordance with the regulations of the Animals in Scientific Procedures Act 2016, and the requirements of the Home Office of the United Kingdom.

3.3ii Caudal Cerebellar Peduncle Focal Demyelination

12 week old SD rats were anaesthetised by inhalation of 1.5-3.5% isoflurane in oxygen, once anaesthetised animals received preoperative multimodal analgesia with buprenorphine 0.02-0.05mg/kg by subcutaneous injection, and local anaesthetic in to the external auditory canal (EMLA), they also received subcutaneous fluids with 1mL of warmed compound sodium lactate,

Animals were prepared for surgery by the removal of hair from the dorsal aspect of the skull from the level of the dorsal orbit to the neck, including removal of hair from the aboral aspect of the pina, and the skin prepared aseptically.

Animals were placed in a sterotaxic frame (Stoetling) such that the skull was secured in the horizontal position, and surgical drapes and anaesthetic monitoring applied. A midline skin incision was performed over the caudal 2/3 of the skull and the subcutaneous tissues and periosteum removed such that the skull and its sutures could be visualised. Co ordinates were taken with respect to the suture landmarks 'bregma' and 'lamda' (Figure 16) and craniotomies made uni- or bi-laterally through the skull at the location directly dorsal to the CCP. Using a 10μL Hamilton micro injection syringe with bevelled tip, 4μL of 0.01% Ethidium Bromide was injected slowly over 4 minutes. The needle was left in situ for a further 4minutes to reduce backflow in to the needle. The craniotomy site(s) were sealed with bone wax (Ethicon W31G), and a three layer closure of the soft tissues using soluble suture material in a simple interrupted or cruciate suture pattern was performed. Animals were recovered in a temperature controlled recovery chamber. Post operative analgesia was provided by means of oral transmucosal buprenorphine dissolved in Hartman's jelly and post operative assessments were carried out daily for three days following surgery. Particular attention was paid to the development of neurological signs including head tilt or ataxia.

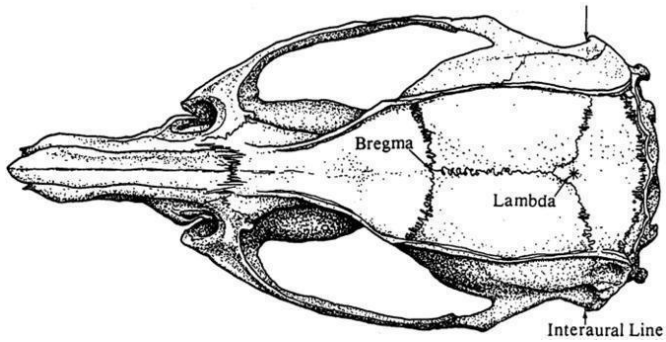

Bregma minus lambda:	<8	8 - 8.2	8.2 - 8.5	8.6 - 9.0	9.0 - 9.4	9.5 - 10.0	10.0 -10.5
Rostro-caudal (λ-CCP)	2.1	2.2	2.2	2.2	2.3	2.4	2.5
DV (λ-CCP)	7.2 (7.1)	7.2	7.2	7.2	7.3	7.4	8.4
Lat (λ±CCP)	2.5	2.5	2.5	2.5	2.6	2.65	2.9

Figure 16: Co ordinates used to identify the caudal cerebellar peduncle in the rat. Co ordinates for bregma and lamda are identified. The skull is checked to be flat and straight (a leniency of +/- 0.2). The location of the craniotomy site is calculated rostrocaudally and laterally relative to lambda, and dorsoventrally relative the flat of the skull at lambda.

3.3iii Perfusion Fixation

For the harvesting of tissue for analysis animals underwent perfusion fixation. Animals were anaesthetised by inhalation using 5% isoflurane in oxygen, following the onset of deep anaesthesia animals were injected with pentobarbital 0.7mL/kg intraperitoneally. Once all reflexes were lost a midline incision was made just caudal to the xyphisternum, the diaphragm insides and the rib cage opened by incising bilaterally along the costochondral junction. The heart was exposed and stabilised using forceps and a 22 gauge butterfly catheter inserted in to the left ventricle. Paraformaldehyde 4% in phosphate buffered saline was pumped in to the left ventricle at a rate of 22 rpm, immediately following the onset of trans radial perfusion with the fixative, the right atrium was opened to facilitate open drainage of blood and fluid. 1mL/g body weight of paraformaldehyde fixative was used, and following the onset of rigidity, tissues were collected for further procession.

3.3iv Cell Transplantation

12 week old Sprague Dawley rats underwent EB-CCP bilateral lesions 3-5 days prior to intended transplantation, an example timeline is given in Table 8.

Mixed glia cultures were set up 15 days prior to intended date of transplantation. OPCs were isolated from the mixed glia culture and plated in proliferation conditions for 24 hours prior to being infected with high titre virus (10^6-10^8). Virus was added to fresh pre equilibrated *OPC Media* with 2μg/ml Polybrene (Sigma) and incubated for 8 hours. Following this, media was changed, and fresh media with 30ng/mL growth factors (PDGF and FGF, Peprotech), and Insulin 4μg/ml (Gibco) added. Media was changed after a further 24 hours, again with the addition of 30ng/ml growth factors, and OPCs were maintained for a total of 48 hours following infection, before being dissociated by Papain Dissociation (see previous).

The cell suspension was resuspended in *HALF Media* and concentrated by serial centrifugation at 450g for 5 minutes. A variety of cell suspension concentrations were used, but most commonly 100,000 cells per 1μL. Cells were transported on ice prior to transplantation in to the site of prior demyelination.

Rats were anaesthetised and prepared as per EB-CCP protocol, cell suspensions were loaded in to 10uL Hamilton syringes, and injected in to the site of the prior lesion 3-5 days post lesion (dpl). Animals were recovered. 1μL of cells were retained for immunohisotchemistry.

Days	Cell Culture	Surgeries
1	Mixed Glia Set Up	
2		
3		
4		
5		
6		
7		
8		
9		
10	Shake Off	Surgery 1 (for 5dpl transplants)
11	Recovery	
12	Infection	Surgery 1 (for 3dpl transplants)
13	Recovery	
14	Recovery	
15	Dissociation and Transplantation	Second Surgery

Table 8: Example Timeline of Transplantation surgeries

3.3v Intracranial injection of Virus

12 week old Sprague Dawley rats underwent EB-CCP bilateral lesions 5-7 days prior to intracraninal injection.

High titre virus (10^6-10^8), was kept on dry ice prior to injection. 5μL was delivered unilaterally in to the site of previous demyelination 5-7 dpl. PBS was delivered contralatrally. Animals were recovered.

3.4 Tissue Staining Immunostaining

3.4i *In Vitro* Cell Culture Immunostaining

Cells were fixed in 4% PFA (Thermo Fisher; 10131580) for 10 minutes at room temperature. The cells were then washed twice in PBS (Thermo Fisher; BP3994) and then blocked in PBS with 0.1% Triton X-100 (Sigma; T8787) and 5% Donkey Serum (Sigma; D9663) for 30 minutes at room temperature. Primary antibodies diluted appropriately (Appendix 8.4) in PBS with 0.01% Triton X-100 (0.1% for intracellular markers) and 5% Donkey Serum were then added to each well and cells were stained overnight at 4°C. Cells were then washed twice for 10 minutes in PBS with 0.1% Triton X-100. Cells were then incubated or two hours in fluorescent secondary antibodies diluted appropriately (Appendix 4) in PBS with 0.1% Triton X-100 and 5% Donkey Serum. Cells were again washed twice for 10 minutes in PBS with. Following this cells were incubated with Hoechst 33342 (Thermo Fisher; H1399) diluted 1:10000 in PBS for 10 minutes. Cells were stored in PBS at 4°C.

3.4ii Organotypic Slice Culture

Slices were lifted from the membrane using a fine paint brush and immersed in 0.05% Triton in PBS in a 48 well plate. Slices were transferred from well to well for each step of the staining. They were equilibrated to room temperature. Slices were blocked in PBS with 5% serum, 0.5% Triton.

Slices were incubated in primary antibody (Appendix 4) overnight at 4°C, and then washed twice in 0.05% Triton in PBS for ten minutes per wash. Slices were then incubated in secondary immunofluorescent antibodies (Appendix 4) in a 0.05% Triton PBS solution for two hours at room temperature. Slices were then washed once in PBS before a 10 minute incubation in

Hoechst 33342 (Thermo Fisher; H1399) diluted 1:10000 in PBS. Cells were than transferred to dH_2O, and then mounted using Fluromount-G (eBioscience 00495802) on Polysine glass slides (VWR 6310107) and 22mm square cover slips (VWR 6310124).

3.4iii Haematoxolin and Eosin, Luxol Fast Blue Staining of Paraffin Embedded Tissue Sections.

Tissue was transferred from 4% PFA to 70% Ethanol. Tissue was processed for sectioning my paraffin embedding and subsequent staining by the core facilities at Cancer Research UK, Cambridge Institute. Sections were stained with Luxol Fast Blue overlaid by Haematoxolin and Eosin.

3.5 *Ex Vivo* and Post Mortem MRI Imaging

3.5i Cell Pellet Assay

nOPCs were obtained by MACs sorting and expanded by proliferation on 15cm PDL coated dishes. Following five days of proliferation cells were infected with lentivirus carrying the Oatp1a1 gene under the PGK promoter. Some nOPCs were left uninfected as a negative control. As a positive control HEK Cells (A gift from Dr. H Pohl, originally from Sigma 85120602) were simultaneously infected with the same lentivirus. 1μL of concentrated virus was added to serum free media and cells were incubated for 8 hours before media was aspirated and the cells were washed and fresh media replaced. 48 hours following infection, Gadolinium chelate (Pimovist, Bayer 3212461) was added to all cells at a final concentration in media of 0.5mM.

Cells were incubated for five hours in the gadolinium containing media. Media was aspirated and cells washed three times with pre warmed sterile PBS. Cells were dissociated from the

plates and pelleted and then fixed in suspension using 4% PFA for ten minutes. Following fixation cells were washed counted and resuspended in an appropriate volume of PBS.

A 4% agarose solution was made using low melt agar (Invitrogen 16520), using a modified 96 well plate the cell suspension was added to agar to achieve a 2% agar suspension with wells containing 5 or 10 million cells. The plates were rapidly cooled to allow the agar to set without the cells settling to the bottom of the wells. A standard curve of gadolinium concentrations was pipetted around the cell pellets, Figure 17.

The plate was imaged using an inversion recovery sequence at 7T (Oxford Instruments, UK) equipped with actively shielded gradients (Magnex) interfaced to a VNMRS (Varian Inc, Palo Alto, CA, USA) imaging console. A quadrature volume coil (Rapid Biomedical, Germany, diameter 72 mm) was used in transmit/receive mode. A 1 mm imaging slice was selected through a modified 96 well plate. Experiments were performed with the help and support of Dr Tiago Rodrigues and Dr Alan Wright.

A

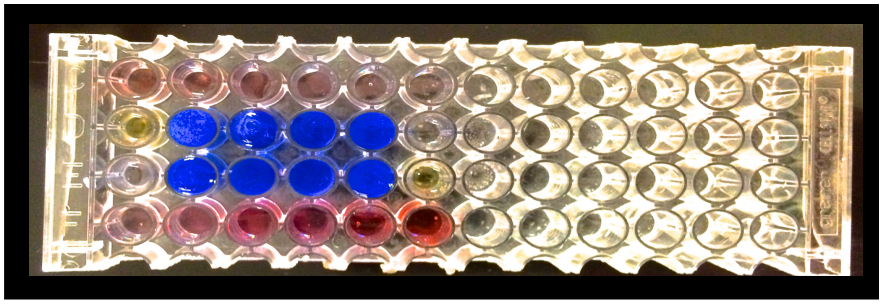

B

Gd 1e-3	Gd 1e-4	Gd 1e-5	Gd 1e-6	Gd 1e-7	Gd 1e-8
Fomblin	Sample	sample	Sample	sample	water
water	sample	Sample	Sample	Sample	Fomblin
Gd 5e-8	Gd 5e-7	Gd 5e-6	Gd 5e-5	Gd 5e-4	Gd 5e-3

*Figure 17: Modified 96 well plate layout used for MRI. **A** Photograph of layout with false colouring. **B** stylised map, concentrations of gadolinium in moles.*

3.5ii Ex vivo MRI of whole cerebllae

Ex Vivo MR Images were acquired in a 9.4T horizontal magnet fitted with active shield gradients and interfaced to a VNMRS (Varian IN. Palo Alto, CA, USA) imaging console. Following fixation in 4% PFA with and without gadoxetate in the perfusion and storage solution, tissue was suspended in fomblin (Sigma 317962) and packed in to a 50mL falcon tube (Corning 430828) and held in place by packing fomblin soaked cotton wool or gauze around the fixed brain.

T_1 and T_2 values were calculated from the MR data by Dr Alan Wright using Matlab software (Mathworks, Cambridge, UK). MR images were acquired with the help of Joseph Guy and Dr. Alan Wright.

3.5iii Cell Transplant Titration using ex vivo MRI

Ex vivo MRI was developed as a potential validation technique to assess post mortem brains which had received cell transplantations. In order to assess what the lower resolution of the

number of cells detectable by *ex vivo* MRI was titrations were performed where OPCs expressing OATP under the PGK promoter, previously incubated in Primovist, were injected in to cerebellae.

Cells were incubated in Primovist for five hours and then dissociated and prepared as per the transplantation protocol. Tissue was obtained from adult rats, and cells injected. Volumes and cell concentrations were varied, see Results. Brain tissue was either pre or post fixed in 4% PFA, and wherever possible, cerebellae were taken from rats sacrificed by Schedule 1 for the acquisition of other tissues to ensure that the principles of the ***3R***s were observed.

3.5iv *Ex Vivo* MRI of whole cerebllae transplanted with OATP expressing cells

Cerebellae were fixed for 24 hours at room temperature in 4% PFA. *Ex Vivo* MR images were acquired in a 9.4T horizontal magnet fitted with active shield gradients and interfaced to a VNMRS (Varian IN. Palo Alto, CA, USA) imaging console. Following fixation in 4% PFA tissue was suspended in Fomblin (Sigma 317962) and packed in to a 50mL falcon tube (Corning 430828) and held in place by packing Fomblin soaked cotton wool or gauze around the fixed brain.

T_1 and T_2 values were calculated from the MR data by Dr Alan Wright using Matlab software (Mathworks, Cambridge, UK). MR images were acquired with the help of Joseph Guy.

3.6 *In vivo* MRI studies

Control animals, both lesioned and unlesioned, and animals receiving transplantation and intracranial virus underwent in vivo imaging. Prior to scanning some rats received intravenous contrast agent or intravenous contrast agent and mannitol. Imaging was performed under anaesthesia in 2% - 4% isoflurane in oxygen. Body temperature was maintained using a controllable flow of warm air at 37°C, and was monitored using a rectal probe. Breathing rate was monitored using a pressure sensitive pad. Imaging was carried out in a 7T horizontal system (Agilent) and VnmrJ software. T_1- weighted spin-echo images, T_1 maps were acquired using a single slice inversion recovery Fast Low Angle SHOT (FLASH) pulse sequences. In vivo imaging was performed with Dr Alan Wright.

3.7 Nuclear Magnetic Resonance Assays

NMR was explored as a potential method for validating gadolinium uptake experiments. Samples were transferred with minimal additional liquids and transferred to NMR tubes. D_2O was added in fixed volumes in to the NMR tubes using a 12 french urinary catheter. Samples were capped and placed in the appropriate coils. NMR imaging and analysis was carried out by Dr Alan Wright.

3.8 ICP Mass Spectrometry

Gadolinium containing samples and controls were weight matched and sealed in 2mL Cryovials (Corning). Samples were shipped on dry ice to Dr. Simonetta Geninatti-Crich

Department of Molecular Biotechnology and Health Sciences, University of Torino, Italy.

3.9 Statistical Analysis

All statistical analysis was performed in GraphPad Prism (GraphPad Software, Inc.). For data derived from the quantification of immunohistochemical staining, comparisons between two groups were performed with Wilcoxon's non parametric Rank Test. For all statistical tests, differences were considered significant at $p<0.05$. Animal work was performed on a pilot study basis therefore power calculations were not performed, they will however, inform future studies where power calculations will be used.

4. Results

The results presented in this thesis will be subdivided in to 4 sections:

Results 4.1 Oligodendrocyte Progenitor Cells are able to express OATP without detriment and can take up gadolinium contrast agent

Results 4.2: Oligodendrocyte Progenitors Cells are able to express Organic Anion Transporter Protein under the MBP Promoter

Results 4.3: The Ethidium Bromide Caudal Cerebellar Peduncle model of demyelination can be characterised by Magnetic Resonance Imaging *ex vivo* and *in vivo*

Results 4.4: Results 4: Rats receiving transplanted OPCs expressing OATP under the MBP promoter can take up gadolinium in vivo.

4.1 - Results 1: Oligodendrocyte Progenitors Cells are able to express Organic Anion Transporter Protein without detriment and can take up a gadolinium contrast agent

4.1*i* Introduction

OPCs arise from distinct anatomical regions during development migrating throughout the CNS to populate it the maturing brain, some of these OPCs differentiate in to the myelinating oligodendrocyte, and some remain resident in the mature brain as tissue resident stem like cells (Pringle *et al.* 1992; Crawford, Chambers, and Franklin 2013).

It is recognised that OPCs in the neonatal rodent brain behave differently to those of the adult rodents (Wren, Wolswijk, and Noble 1992; Shi, Marinovich, and Barres 1998), and for this reason isolation of adult OPCs has been very challenging. In contrast, neonatal OPCs have been isolated by enzymatic digestion of perinatal rodent cerebral cortex, followed by co culture and fractionation (The Mixed Glia Culture [MGC], (McCarthy and de Vellis 1980). More recently, cell sorting has been used to isolate OPCs more directly from tissue using targeted antibodies to positively select a population of OPCs. These techniques have included magnetic cell sorting (MACS) (Cizkova *et al.* 2009), immunopanning (Barres *et al.* 1992; Wren, Wolswijk, and Noble 1992), and Fluorecent Antibody Cell Sorting (FACS) (Sim et al. 2011). Given that spinal cord MRI imaging is very challenging, a cranial demyelinating lesion is necessary, and as the rat EB-CCP lesion is a major toxin model in the rat used and developed in the Franklin lab, I elected to work with rat OPCs in a rat model of demyelination rather than a mouse model. The corollary of this is that the OPC isolation techniques available where somewhat reduced as antibodies raised in rat are inappropriate (as are many

antibodies for use in FACS), and processing via FACS or immunopanning introduces elements of stress, such as multiple protease incubations or shear stress, which can affect proliferation and differentiation potential. Thus a choice between MACS and MGC needed to be made.

As the goal of my work was, ultimately, to transplant OPCs in to demyelinated lesions, criteria for successful isolations were defined as 1) high repeatable yields of OPCs per gram tissue, and 2) high percentage differentiation. I therefore elected to first establish which of these techniques, MACS or MGC gave me the most optimal cell yield, and to establish if OPCs derived from either technique where more amenable to infection with a viral vector.

For MACS isolation a magnetic associated antibody against a cell surface antigen is used. Commonly available antibodies relevant to the OPC lineage, include PDGFRa, NG2, and A2B5. The PDGFRa antibody is raised in rats, and therefore inappropriate for use against rat tissues, and NG2 has been reported to be expressed in other cells of the CNS including microglia and endothelial cells (Yokoyama *et al.* 2006). Therefore, MACS isolation using A2B5 was selected. This is a protocol previously used by others (Wren, Wolswijk, and Noble 1992; Shi, Marinovich, and Barres 1998; Barres *et al.* 1992), and by other members of the laboratory (Segel *et al.* unpublished data, Neumann *et al.* unpublished data).

Lentiviruses have previously been shown to successfully infect OPCs endogenously and exogenously (Zhao *et al.* 2003), additionally they allow labelling of progeny cells and therefore are more appropriate for transplantation studies than other potential viral vector systems such as adenoviruses where the viral genome does not integrate fully in to the host cells, and therefore does not result in progeny cells being labelled (Zhao *et al.* 2003). A

lentiviral vector for the OATP1 protein has previously been constructed under the PGK promoter therefore initially this viral system will be used and validated (Patrick, Hammersley, *et al.* 2014).

4.1*ii* Experimental Strategy

A lentiviral vector for OATP using a PGK promoter, inherited from P. Stephen Patrick of the Brindle group, was sequenced and free virus obtained and used as the basis for viral experiments.

OPCs derived by MACs and MGC were isolated and maintained in proliferation and differentiation conditions. Yields and rates of differentiation were assessed in naïve cells and in cells infected with a lentiviral vector. MACs isolation was selected for some experiments where purity and proliferative ability were important, whereas MGC isolation was used when differentiation capacity was important, or where very large synchronous cell yields were required.

4.1*iii* Results

4.1iiia OPCs can be isolated and differentiated by both mixed glial dissociation and magnetic antibody sorting techniques.

OPCs were isolated using both the mixed glia and MACS techniques and were plated at a density of 20,000 cells per cover slip. Cells were cultured in *nOPC media*, see Methods, in either proliferation, or differentiation conditions for up to 7 days before fixation and staining. Figure 18: shows an example of cells isolated by MACs which were morphologically indistinguishable from those isolated by MG dissociation.

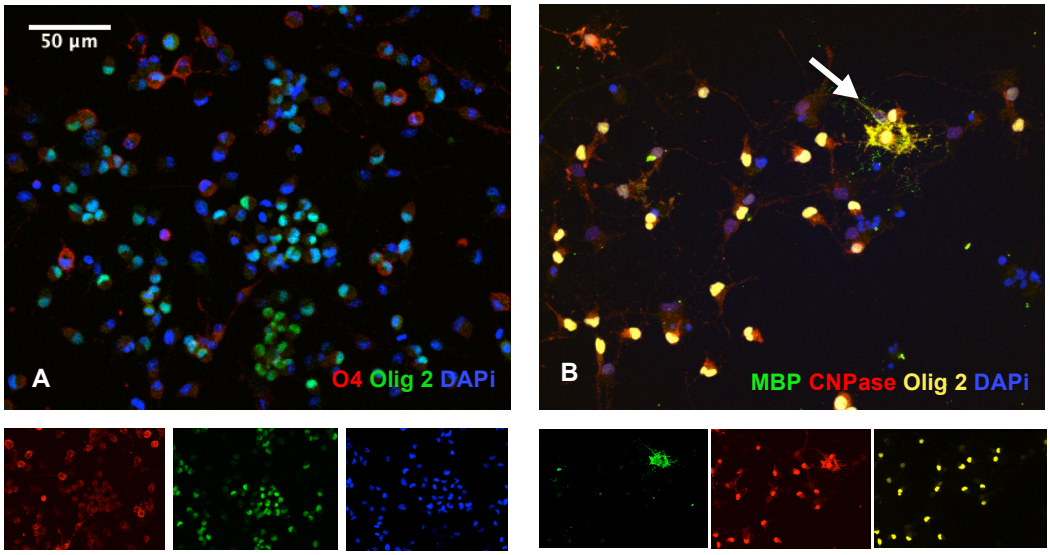

Figure 18: Oligodendrocyte Progenitor Cells (A), and differentiated oligodendrocytes (B) isolated by MACS and cultured in nOPC media, stained with O4, Olig2, CNPase, and MBP. MACS and MGC isolated cells are morphologically identical.

Cells were further isolated for calculation of yields from both isolation techniques. MACS isolation yielded by far the greatest number of OPCs per neonatal brain used, with a mean yield of 1.47 x 10^6 cells, whereas MGC yielded far fewer 1.12 x 10^6 cells (n of 5) (Figure 19).

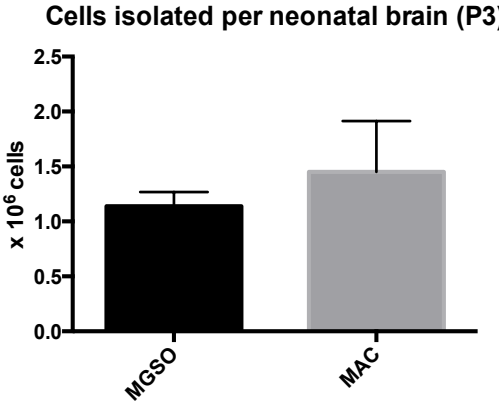

Figure 19: Mean yields from MGC vs MACS from neonatal rat brains at p3. Cells were isolated from p3 rat pups and cell counts to calculate yield carried out. MAC isolation gave higher average yields, but failure of the technique (and therefore 0 yield) was more common. n of 6 per technique

However there was considerably greater variation in the yields achieved with MACs, which showed a variance (F value) of 35.92 (p=0.0043). Counts were performed using automated haemocytometers.

Following isolation and counting, cells were cultured in differentiation media for 5 days before fixation and staining. Cover slips were stained with antibody combinations against OPCs; A2B5 and Olig 2, and Astrocytes; GFAP. At 5 days in differentiation media the percentage of cells still expressing Olig2 lineage markers were calculated; Figure 20.

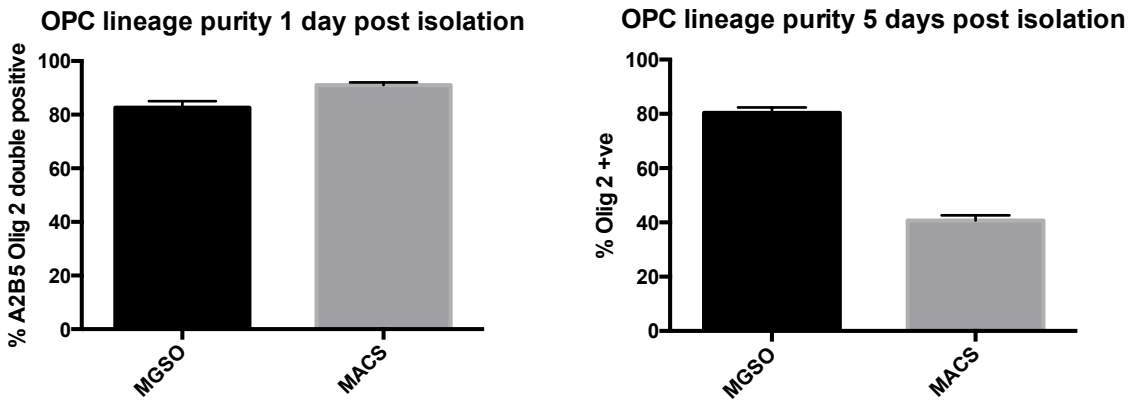

Figure 20: Purity assay of Oligodendrocyte lineage cells at 5 days post culture. Cells were isolated by Mixed Glia Shake Off, or by Magnetic Antibody Cell Sorting. Cells were fixed and stained at 1 and 5 days following isolation. A2B5 is a marker of the progenitor cell state, Olig2 marks the full lineage. Three biological replicates per isolation technique

Cells isolated via MGC retained greater purity than those isolated by MACS with 82% purity at isolation (A2B5 Olig2 double positive) dropping to 80% at day three, with a majority of the contaminents being microglia. In MACS 91.4% of cells isolated were A2B5 double positive on day one, droping to 39% at day five, with a majority of the cells which were Olig2 negative being GFAP positive, or Olig2 negative and MBP positive, and where presumed to be dead.

4.1iiib OPCs can be infected by a lentiviral vector, and express the OATP channel under the PGK promoter

A third generation lentiviral vector system was obtained from Dr P.S. Patrick formerly of the Brindle Laboratory. The vector was confirmed by multiple restriction enzyme digestions Figure 21, a map of which is shown in figure 5. A table of expected products is shown in Appendix 5.

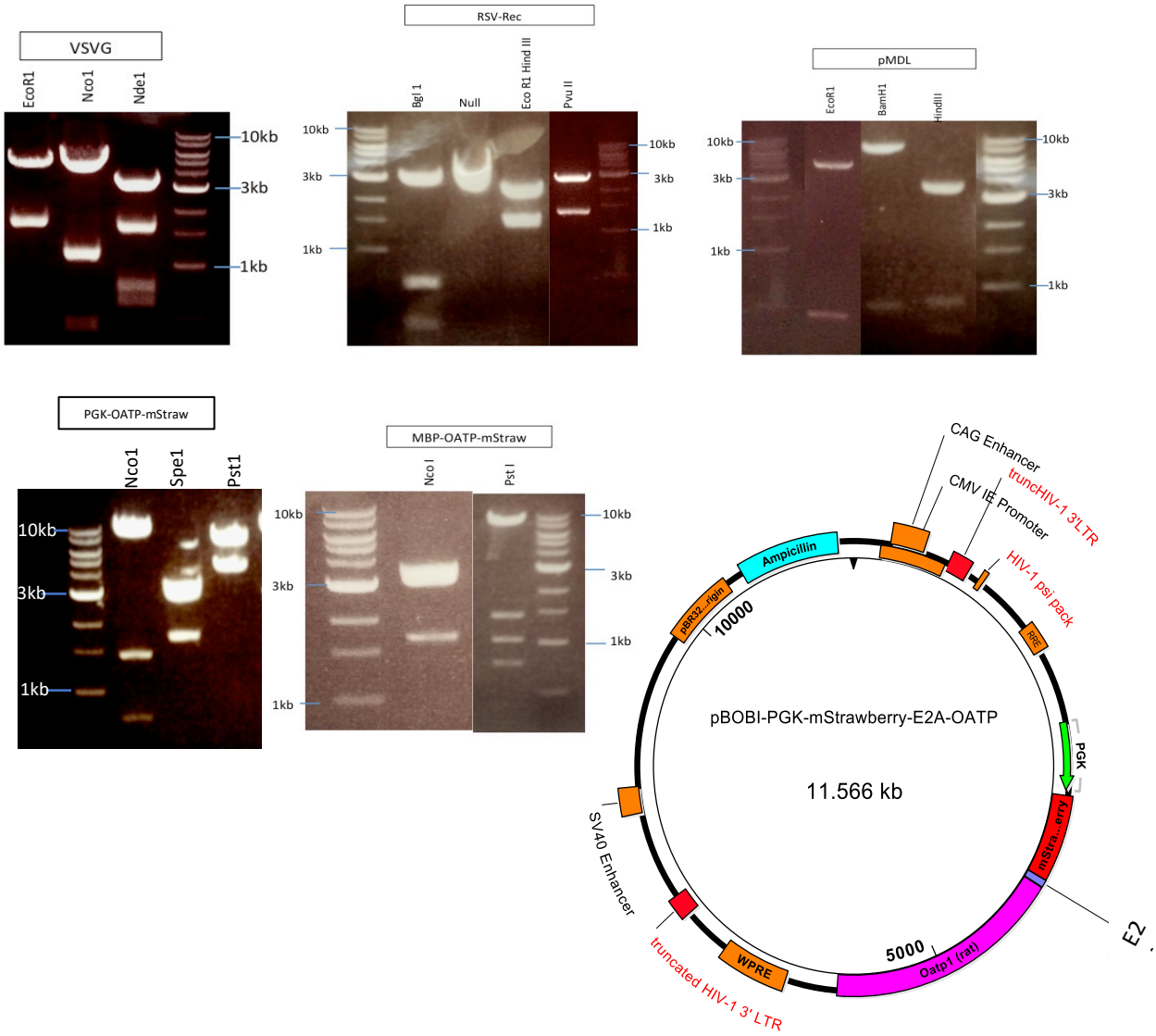

Figure 21: Restriction Enzyme digestion confirmation of the lentiviral vector system. Restriction digests were carried out to confirm the vector maps were accurate. The vectors were also sent for sequencing.

Virus was manufactured using HEK293T cells and serial dilution was performed to ascertain the optimal concentration of viral particles for use in oligodendrocytes. This was performed a new for each batch of virus.

Cultures were infected with 10μL of concentrated virus (titres of 10^4-10^6), and were cultured for up to 5 days before fixation and staining. OPCs were stained with Olig 2 and anti RFP antibody against mStrawberry. OPCs were found to express mStrawberry from 48 hours in culture. As mStrawberry expression was equimolar linked to the expression of OATP via the including of the E2A sequence, RFP staining was taken to be equivalent to OATP expression.

OPCs expressing OATP were then compared to control which had been infected with a sham virus; the PBOBi contrast with only the mStrawberry and PGK promoter. They were dissociated from flasks and incubated with Trypan blue, at 5 days post infection, to assess if OATP affected cell survival. There was no significant difference in cell survival between the OATP expressing group and the sham group.

OATP expressing and control cells were further cultured in differentiation conditions and the number of cells which differentiated in to Olig2 MBP double positive cells were compared. There was no difference between the levels of differentiation (Figure 22).

Figure 22: (Overleaf) OPCs can express OATP under the PGK promoter. nOPCs isolated by MACs can be infected with lentiviral vectors and express the OATP channel under a PGK promoter (A). Expression peaks around 48 hours post infection and remains stable for at least 5 days (B) around 80% of cells in culture become infected (C), OPCs are able to differentiate and express myelin basic protein whist expressing OATP (D) and the levels of differentiation do not significantly differ between OATP infected cells and those infected with a sham virus (E). Viability, as measured by cell exclusion of Trypan Blue, does not differ significantly between OATP infected, sham virus infected, or naïve, uninfected cells. Three biological replicates with representative microscopy images.

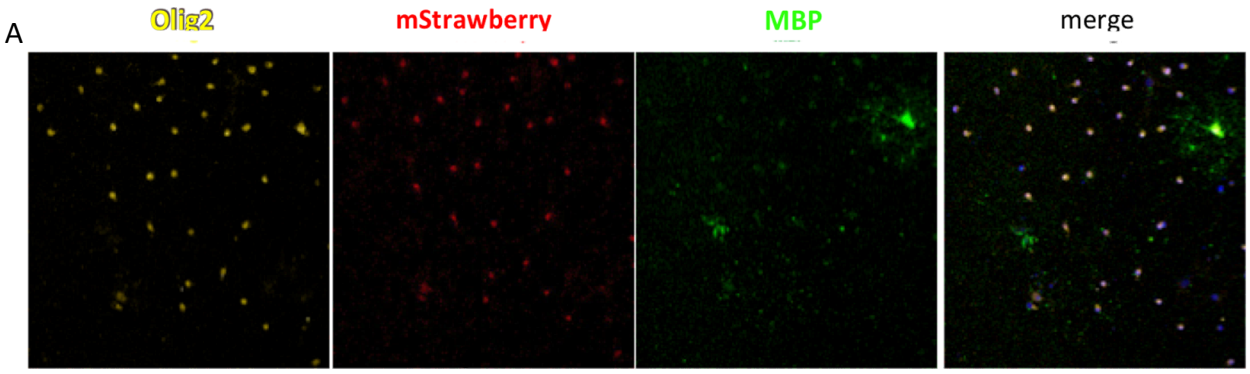
A
Olig2
mStrawberry
MBP
merge

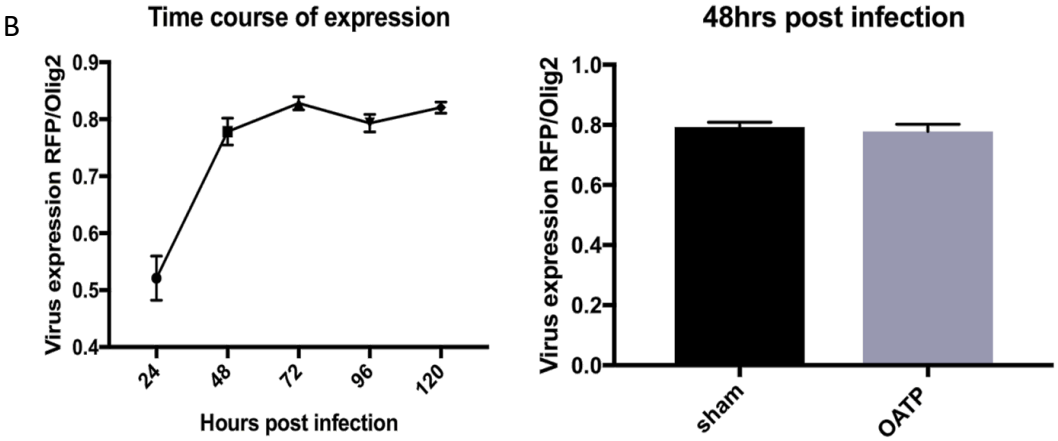
B
Time course of expression
Virus expression RFP/Olig2
0.9
0.8
0.7
0.6
0.5
0.4
24
48
72
96
120
Hours post infection
48hrs post infection
Virus expression RFP/Olig2
1.0
0.8
0.6
0.4
0.2
0.0
sham
OATP

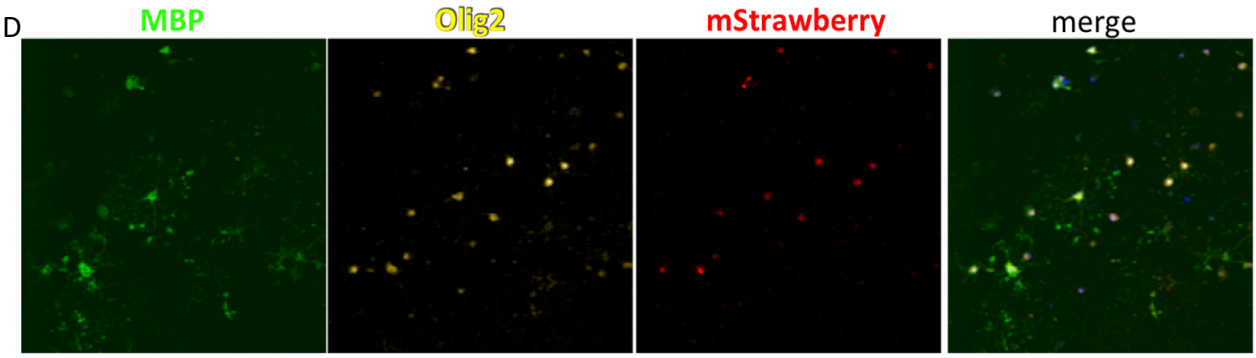
D
MBP
Olig2
mStrawberry
merge

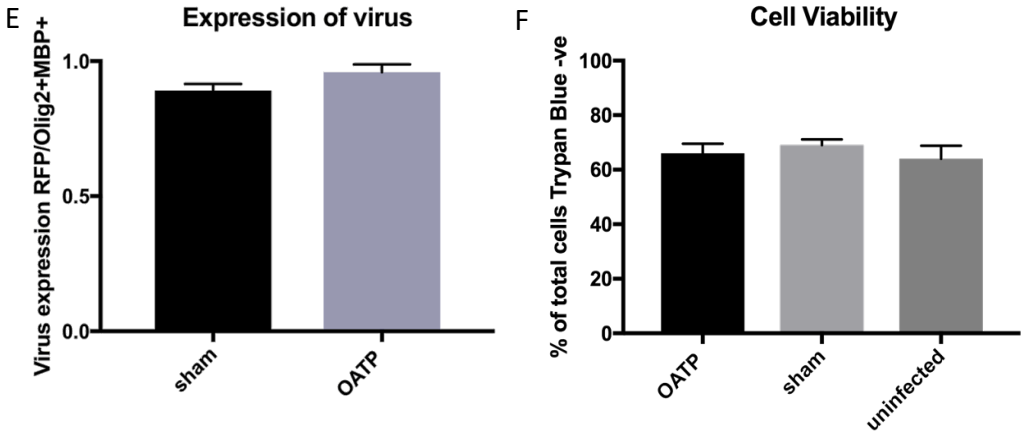
E
Expression of virus
Virus expression RFP/Olig2+MBP+
1.0
0.5
0.0
sham
OATP
F
Cell Viability
% of total cells Trypan Blue -ve
100
80
60
40
20
0
OATP
sham
uninfected

4.1*iii*c OPCs expressing OATP under the PGK promoter can take up gadolinium contrast agent

Cultured OPCs were incubated in 15cm dishes with media containing 0.05mmol Primovist, a gadolinium containing substrate for the OATP channel, for 5 hours, before being washed three times in PBS, and suspended in low melting point agarose in a modified 96 well plate. The agarose phantoms where rapidly chilled over ice and surface bubbles removed. Controls containing OPCs with sham virus, also incubated in Primovist, and HEK cells expressing OATP, and naïve HEK cells were similarly suspended in the modified 96 well plate. HEK cells were used as a positive and negative control as they have previously been shown by Patrick and colleagues, to be successfully infected, and be capable of functional expression (Patrick, Hammersley, et al. 2014).

The agarose phantoms were placed in the magnet of a 7 tesla horizontal bore MRI machine and T_1 weighted images, and T_1 maps were obtained. The rate of T_1 shortening was used to calculate the concentration of gadolinium contained within each phantom, Figure 23.

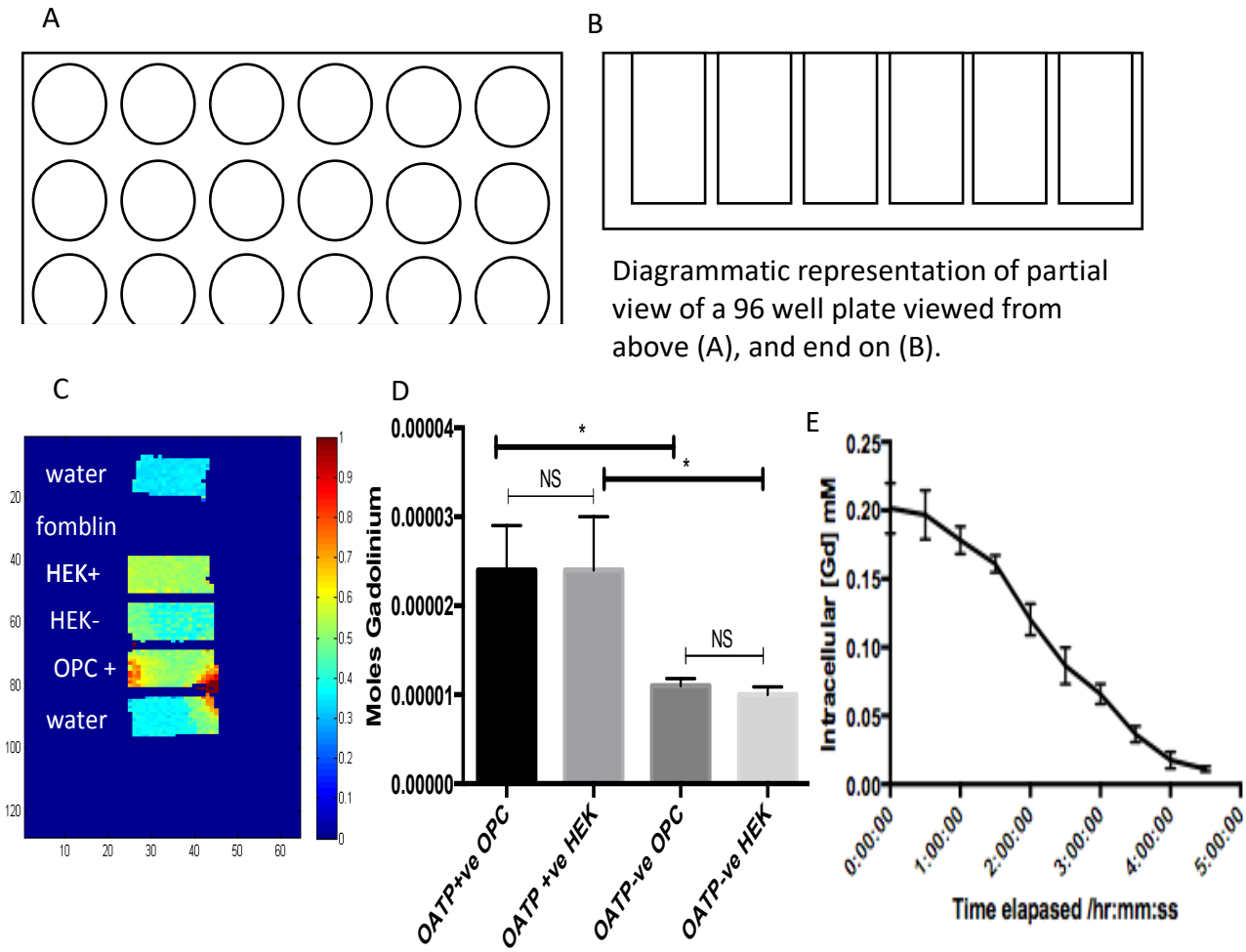

*Figure 23: OPCs expressing OATP under PGK promoter is functional and takes up contrast reversibly. Cells suspended in agarose in 96 well plates as described in Methods 3.5i and imaged using T_1 weighted imaging, a transverse image through the wells (orientated as in panel B) shows a heat map representation of the whole well, the scale bar is in R1; the T1 rates (1/T1). Fomblin which is 'invisible' on MRI due to an absence of protons is a negative control. It can be seen that HEK+ and OPC+ (cells expressing OATP) have much high rates of T1 than HEK- (control cells infected with sham virus) or water. There appears to be some spillage of cells from the agarose in to the water well likely due to a pipetting error. (**D**)shows a quantification of the amount of gadolinium in the cells based on the R1 values at time zero from three biological replicates, samples analysed with nonparametric Wilcoxan Rank Test. (**E**) Samples show reversible uptake with signal decaying over the five hours following removal of gadolinium from the media, each time point is a separate triplicate experiment with removal of Gd media at time point 0, and suspension in agarose according to the time point (eg 2 hours after removal), cells were maintained in un supplemented media during the intervening period.*

4.1*iv* Discussion

The data in this chapter show that OPCs can be isolated and cultured, and that they can be infected with lentiviral vectors without any obvious detriment to their function. Although MACS isolations produced a higher mean yield of cells, these yields were highly variable, and the isolation protocol had a far higher absolute failure rate in my hands. This is likely to be largely as a result of handling speed and accuracy as others in the group appear to achieve more consistent yields (mean 1.8 x 10^6-2 x 10^6 cells B. Neumann unpublished data). However, given the higher purity and the more robust differentiation, MGC appear to be the better choice for transplantation at a latter stage, therefore this isolation technique will be pursued for the remaining experiments.

The use the MGC may have additional benefits in that it retains the heterogeneity of the OPC population. By selecting on the early stage OPC marker, A2B5 in the MACS isolation, a potentially homogenous population whose behaviour and physiology may not be entirely representative of OPCs in general, may be selected. The question of heterogeneity is a vast and complex one requiring considerable investigation, and is beyond the scope of the work presented here. Therefore no further exploration will be attempted at this stage; however, it is a questions that may become increasingly pertinent at future stages of the project.

Methods of assessing survival and differentiation are not fully standardised. Most commonly Ki67 staining, an indicator of cellular division, is used as a marker for proliferating cells, equally EdU staining; a thymidine analogue, can be used as it incorporates in to DNA and can be detected by light microscopy. TUNEL staining can also be used as a measure for

apoptosis. Trypan blue exclusion, on the other hand, is a measure of cell membrane permeability, with negative staining cells having an intact, non porous membrane, dead or dying cells having a permeable membrane which therefore take up the stain. This is a far more general, and less mechanistic measure of cell viability, but, whilst crude, given that there was no significant difference between cell populations, it seems unnecessary at this stage to confirm the myriad of cell proliferation and apoptotic measures agree. Again, given the somewhat promiscuous nature of the OATP channel this may become increasingly relevant as the project progresses.

The agarose phantoms demonstrate that the expression of OATP by OPCs is functional, and that OPCs are capable of taking up gadolinium reversibly. As Primovist is a negatively charged compound it is unlikely, though not impossible, to be adhering to the surface of the cells even after three washes. The OPC:sham virus control, showed no greater T_1 contrast, than the HEK293T cells unexposed to gadolinium, therefore this 'three wash' protocol seems adequate at removing gadolinium from the surface.

4.2 Results 2: Oligodendrocyte Progenitors Cells are able to express Organic Anion Transporter Protein under the MBP Promoter

4.2*i* Introduction

Having demonstrated that a lentiviral OATP vector could be used to achieve OATP expression in OPCs, I next wanted to control expression of the channel under a differentiation-stage linked promoter. OPCs express a range of different markers (Figure 24), as they differentiate from the progenitor state, into a mature myelinating oligodendrocyte.

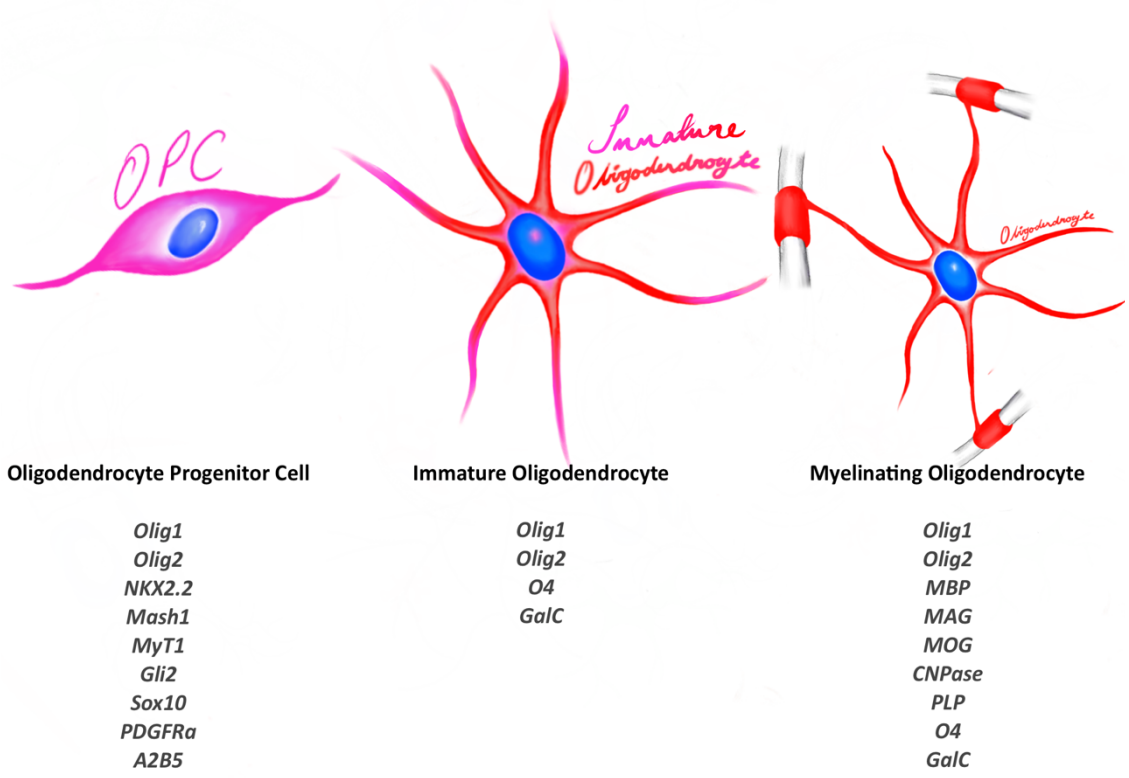

Figure 24: OPC, immature oligodendrocyte, and myelinating oligodendrocyte markers. Markers change as the OPC differentiates towards the myelinating mature phenotype. In the OPC these markers include; transcription factors such as Olig1,and 2, Sox10, Nkx2.2, Mash1,MyT1, and Gli2, and cell surface antigens such as A2B5 and PDGFRa. The Pre myelinating and immature Oligodendrocyte is characterised by expression of the transcription factors Olig1 and 2, and early myelin proteins O4 and GalC. The mature Oligodendrocyte retains these transcription factors, with the addition of the full myelin protein orchestra. Adapted from Miron et al 2011 and Levine et al 2001. Cells are not to scale.

Transcription factor promoters have been widely used in the creation of transgenic mouse lines (Richardson et al. 2011); (Dimou et al. 2008); (Kessaris et al. 2005); (Rivers et al. 2008); however, given the aim of imaging new myelin formation it seemed prudent to use a myelin associated promoter sequence in order to ensure that contrast enhancement was as closely related to myelin production as possible. For this reason, a choice between the major myelin associated gene promoter sequences; MBP, PLP, MAG, MOG, GalC, CNPase and O4 needed to be made. As can be seen in Figure 24, O4 and GalC are expressed in the immature and pre myelinating oligodendrocyte (Miron, Kuhlmann, and Antel 2011), and therefore do not exclusively label the mature myelinating oligodendrocyte. Of the latter stage myelin genes, PLP is also expressed by Schwann Cells, albeit at very low levels (Puckett *et al.* 1987), as are MBP (Gow *et al.* 1992), MAG (Quarles 2007) and CNPase (Sprinkle 1989). MOG, alone is restricted to the oligodendrocyte; however, as it makes up only 0.05% of the myelin sheath (Jaquet *et al.* 1999), it is unlikely to result in adequate expression of an OATP transporter to achieve detection. The promoter sequence for MAG is 2.2kb, and has been successfully used in the oligodendroglial linage in an adenoviral vector (Jonquieres *et al.* 2016); however, it has not been reported in a lentiviral system. Similarly, a 1kb CNPase promoter sequence has been used in a transgenic mouse line (Miyamoto *et al.* 2018); however, there are currently no reports of its use in lentiviruses.

Conversely the MBP promoter has been widely used in both adenoviral and lentiviral vectors. Its promoter sequence contains a number of different regions which, when activated by a different pattern of transcription factors, direct expression in either the oligodendroglial lineage, or Schwann cell lineage, meaning an oligodendrocyte specific promoter sequence can be selected (Taveggia et al. 2004); (Gow, Friedrich, and Lazzarini 1992). The PLP promoter

appears to have been widely studied (Yoshida and Macklin 2005; Hamdan et al. 2015), and PLP accounts for around 50% of the total protein content of myelin (Baumann and Pham-Dinh 2001). The human promoter sequence is commercially available via Addgene (Berndt, Kim, and Hudson 2001), it has however, been reported to be expressed outside the oligodendroglial lineage (Guo et al. 2009; Michalski et al. 2011).

MBP, which has been widely reported in multiple vectors including lentiviruses (McIver *et al.* 2005) (Li et al. 2010; Jonquieres et al. 2013), and whose promoter sequence is commercially available (mouse) via AddGene, has been shown to lead to more consistent expression in a range of oligodendroglial lineage cells (Miyao *et al.* 1997). A sequence was obtained from Dr. Chao Zhao, and Dr. P.S. Stephen Patrick for which I am very grateful. The sequence of the promoter used is homologous to that which is commercially available via adgene which was first published by Wei and colleagues. The sequence of the MBP promoter from mouse, rat, and human has been shown to be highly conserved across sepcies especially in the core promoter region (Wei, Miskimins, and Miskimins, 2003). This sequence retains both the Nkx2.2 and Sox 10 binding elements as well as core regulatory elements that facilitate CNS expression.

4.2*ii* Experimental Strategy

My aim was to recapitulate the experiments undertaken with the PGK promoter. Therefore I constructed a transfer plasmid containing the MBP promoter fragment inherited from Dr. P.S.Patrick. Free virus was manufactured and used to establish if the expression of OATP could be controlled under the MBP promoter. Assessing contrast uptake in cell pellets of OPCs was

challenging due to the numbers of OPCs required per well, therefore a cerebellar slice culture (CSC) was used to assess contrast uptake. CSCs are a well established *ex vivo* model for remyelination and are thought to offer a more complete representation of the *in vivo* response (Zhang *et al*. 2011). The uptake of gadoxetate was assessed by three different methods: MRI imaging, NMR Spectroscopy, and Inductively Coupled Plasma Mass Spectrometry (ICP-MS). Developing a reliable protocol to quantify gadolinium uptake by a non MRI methodology is of great importance as it will be necessary to have a secondary technique to asses *in vivo* samples.

4.2*iii* Results

4.2iiia OATP can be expressed under the control of the MBP promoter

An MBP promoter transfer vector was constructed by replacing the PGK promoter in the original vector with the MBP promoter obtained from Dr S.P. Patrick. A map of the synthesised

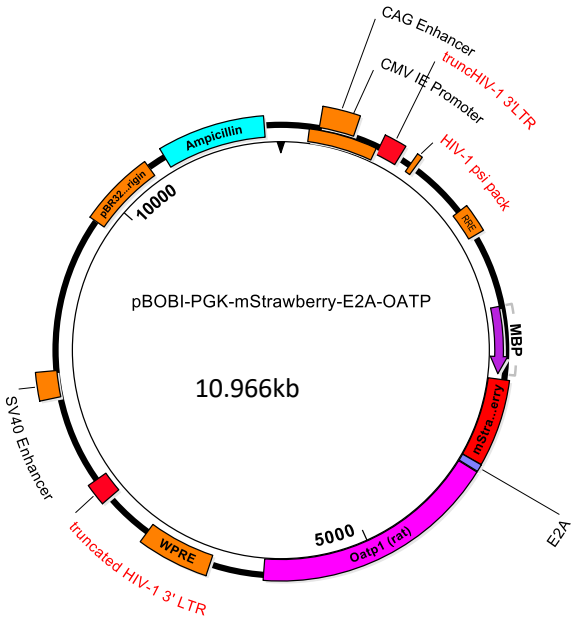

Figure 25: Map of the MBP promoter transfer plasmid constructed containing a 600 base pair sequence specific to oligodendrocyte MBP expression.

vector is shown in Figure 25, and the sequence of the MBP promoter sequence used is detailed in Appendix 7.

OPCS were isolated by MACs and plated a density of 20,00 cells per well in a 96 well plate, they were cultured in OPC media in proliferation conditions for 24 hours, before being infected with MBP:OATP lentivirus. OPCs plated at this density have a tendency to differentiate in to astrocytes as well as oligodendrocytes in culture depending on their seeding density. Cells were cultured for up to 10 days in differentiation conditions before being fixed and stained for mStrawberry, MBP, Olig2, and GFAP Figure 26. No GFAP positive cells were mStrawberry positive showing that expression is restricted to the oligodendrocyte lineage, and no Olig2 positive MBP negative cells were mStrawberry positive either showing that expression is restricted to the stage of differentiation where MBP is being expressed.

A

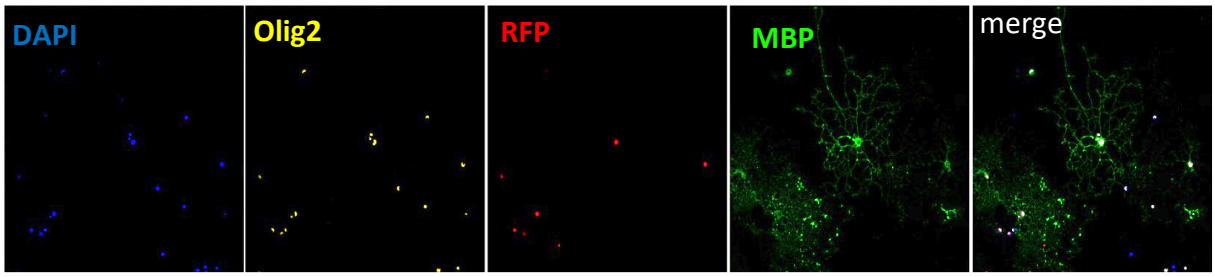

B

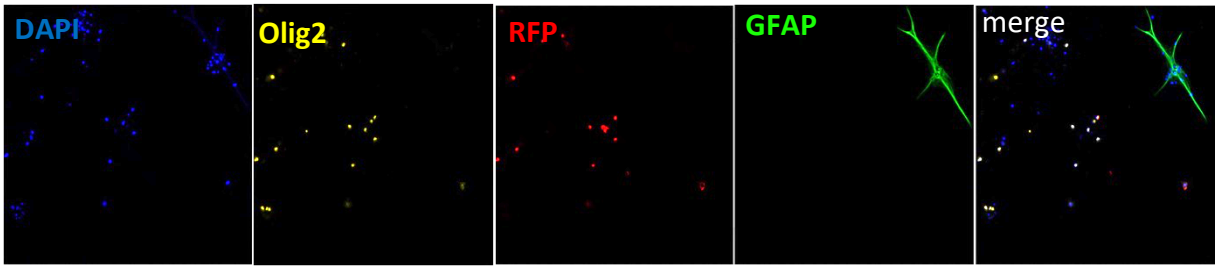

C

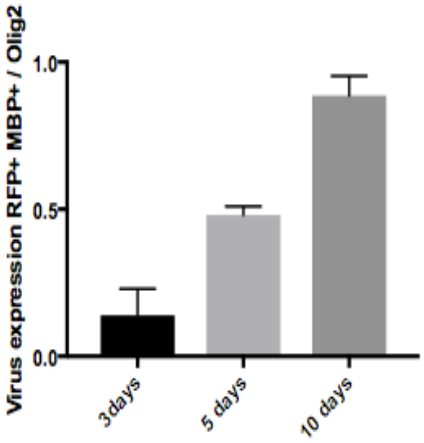

Figure 26: OATP expression is restricted under the MBP Promoter
OATP expression is restricted to cells expressing MBP (A). By 10 days post culture up to 81% of Olig2 expressing cells differentiated in to MBP positive cells and also co expressed RFP(C). No GFAP expressing cells co expressed RFP (B), and no pre myelinating Oligodendrocyte lineage cells (those expressing Olig2 but not MBP) expressed RFP. There were rare MBP+ Olig2+RFP- cells. A GFAP positive, RFP negative astrocyte (white triangle) can be seen (B), and several MBP+Olig2+RFP+ Oligodendrocytes can be seen (white arrow head) (A). MBP and RFP expression increased over 10 days in differentiation conditions (C). OATP is expressed at equimolar levels to RFP. Quantification was performed using Fiji (Image J) on three biological replicates per time point.

OPCs and oligodendrocytes expressing OATP under the PGK promoter had previously been cultured in vitro and phantom experiments performed using cells suspended in agarose for MRI. However, this technique required 1 x 10^7 cells per well, meaning very large numbers of neonatal rat pups were required for a single well in these experiments. In the spirit of the three Rs,(*Reduce* animal use, *Refine* experiments requiring animals, *Replace* animals with alternatives where possible), and to reduce the likelihood of handling errors, an attempt at refining the experimental design was made, and cerebellar slice cultures were used instead.

Slice cultures were prepared from p10 rat pups, cultured for seven days in *Cerebellar Slice Culture Media* before being demyelinated using 0.5mg/ml lysolecethin as described by (Birgbauer, Rao, and Webb 2004), and then infected with the MBP:OATP lentivirus. Slices were stained for Neurofilament (NHF), CNPase, and mStrawberry. CNPase mStrawberry double positive cells were counted in the CSC at three and five days post infection Figure 27.

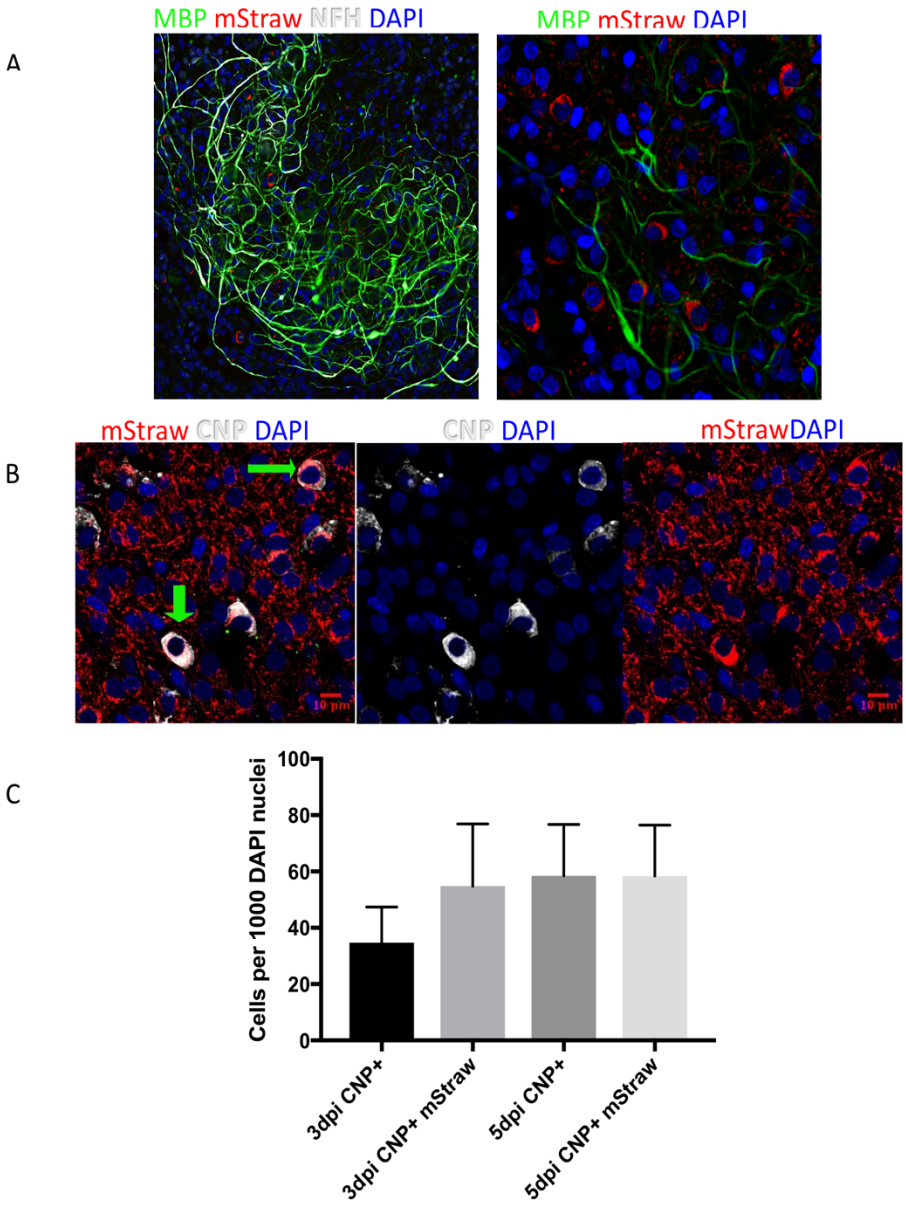

*Figure 27: OATP was expressed by cells co expressing CNPase a marker of later stage oligodendrocyte differentiation. No mStrawberry staining was found in cells staining for GFAP , IBa1 or NFH. (**A**) 40x image of cerebellar slice culture showing MBP staining of axons, however co localisation of MBP with mStrawberry is challenging, therefore and alternative stain for late oligodendroglial lineage was used; CNP in (**B**), a representative image at 100x. Quantification was performed in Fiji (ImageJ) on three biological repeats.*

4.2iiib Oligodendrocytes in CSCs expressing OATP can take up Gadolinium contrast agents detectable by Inductively Coupled Plasma Mass Spectrometry.

CSCs were then incubated in 0.5mM Primovist in modified CSC media overnight, they were washed in PBS, before fixation in 4% PFA for 1hour. Slices were then analysed for their Gd content by one of three methods: T_1 weighted MRI, 10 slices/well (Figure 28), NMR spectroscopy 5 slices/vial (figure 29), or ICP-MS 3 slices/sample (Figure 30). T_1 imaging was carried out in 0.2ml PCR tubes in a 7 tesla horizontal bore magnet, NMR was carried out, both with the help of Dr Alan Wright, and ICP MS was carried out with the help of Dr Andre Neves, by Dr. Simonetta Geninatti-Crich, Department of Molecular Biotechnology and Health Sciences, University of Torino, Italy.

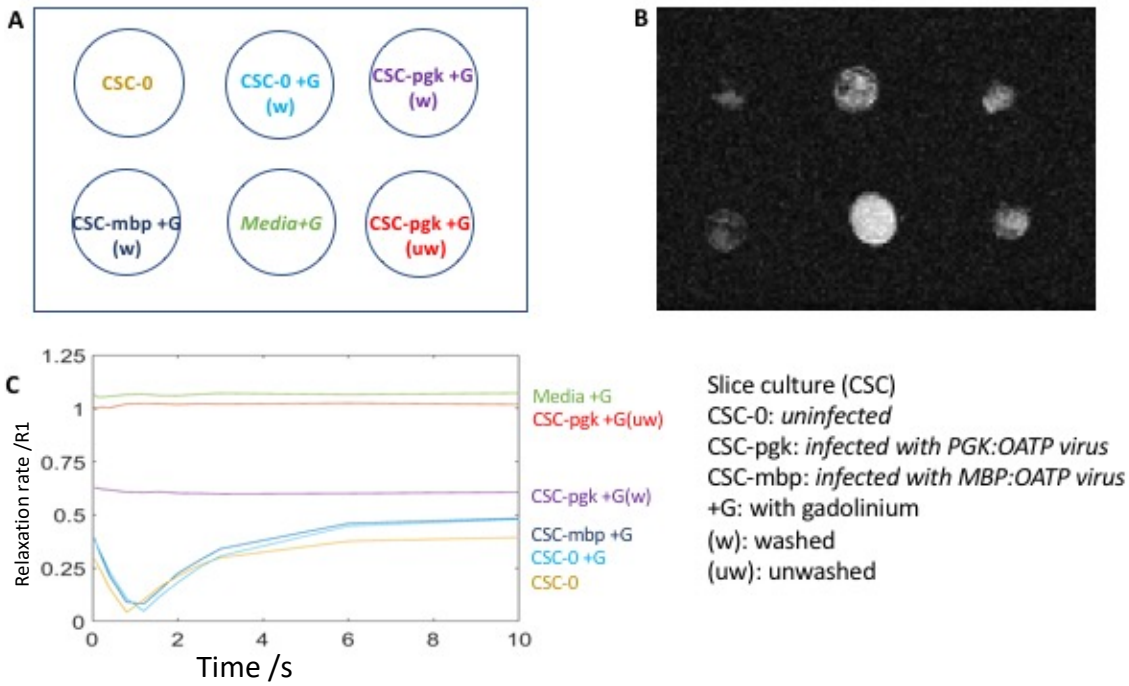

Figure 28: CSC expressing OATP analysed using MRI.
*CSCs expressing OATP were incubated in Primovist and imaged by MRI **A** and **B**, A shows a diagrammatic map of the lay out of the wells in a 96well plate, shows a representative cross section (viewed from above) of the T1 weighted image from the MRI. **C** shows that there is no gadolinium in negative control CSC-0 and CSC-0+G, or in the MBP expressing slice incubated with gadolinium (GSC-mbp +G), the positive controls show so much gadolinium that shortening is too rapid to calculate the quantity. Slices expressing PGK also show a similar, though slighltly slower rate of shortening still too rapid to calculate the gadolinium content. This may have resulted from incomplete washing, or excessive incubation There are a number of reasons this experiment may have failed.*
Abbreviations: CSC: Slice culture, CSC-0: uninfected, CSC-pgk: infected with PGK:OATP virus, CSC-mbp: infected with MBP:OATP virus, +G: with gadolinium, (w): washed, (uw): unwashed

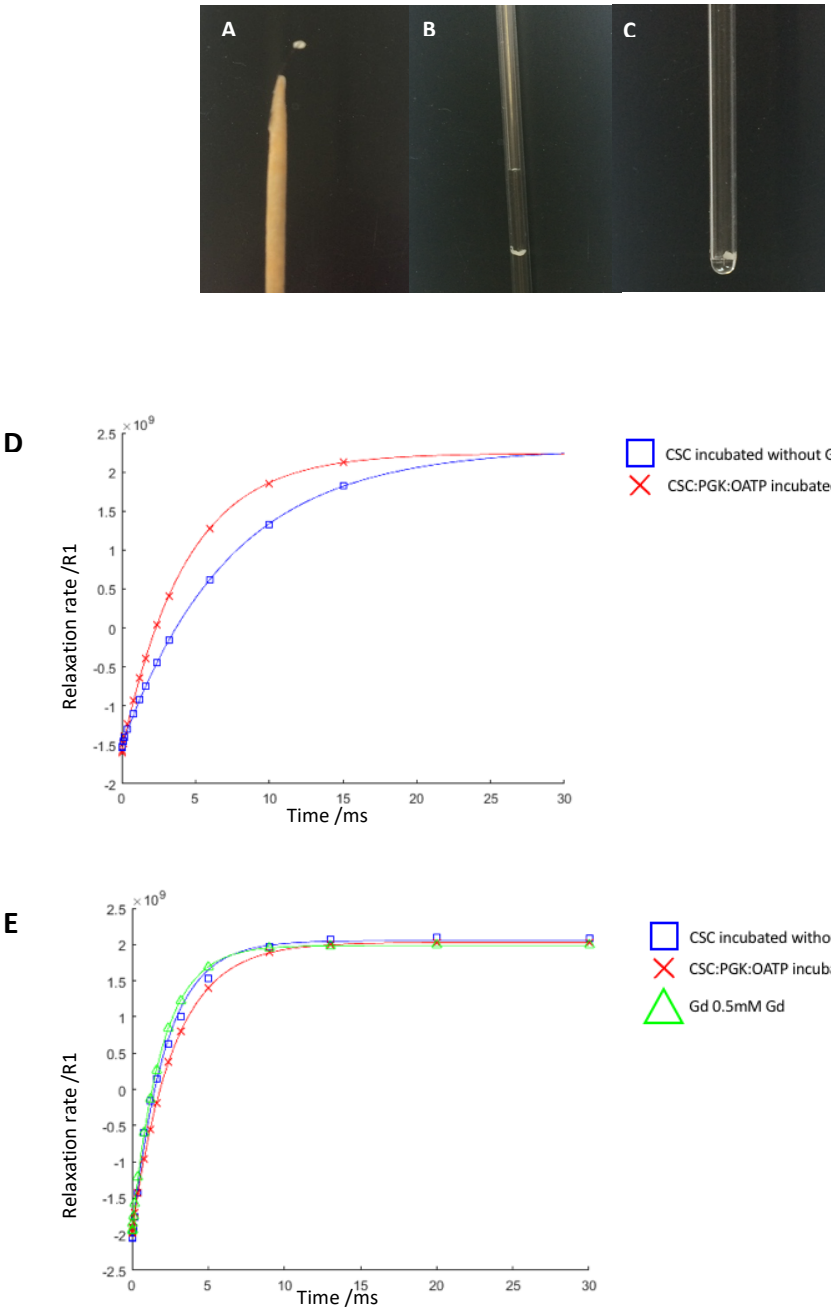

Figure 29: *NMR T_1 rates for cerebellar slice cultures. Panel **A-C**: 5 slices were lifted from the Millicert insert membranes using modified probe (**A**) and were placed in the bottom of a 3mm diameter NMR tube (**B**), before being immersed in deuterated water which was added using a 12 Fr urinary catheter, one slice is shown above **A-C**. **D;** The first iteration of this experiment was promising and showed a difference in T_1 between rates for CSC incubated with Gd and without Gd, however repeats of this with positive control (0.5mM Gd) showed no significant difference (**E**). Experiments performed with Dr A. Wright, ^{1}H-NMR spectra were recorded at 400.13 MHz on a Bruker (Karlsruhe, Germany) Avance III console with a 9.4T vertical wide bore magnet from Oxford Instruments (Oxford, UK), equipped with a 10mm Bruker broadband probe. Analysis was performed in MatLab*.

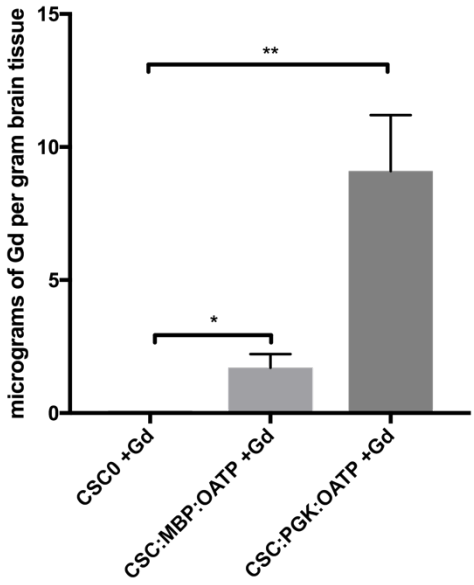

Figure 30: Cerebellar slice cultures expressing no OATP channel (CSC0), expressing OATP under the PGK(CSC:PGK:OATP) or MBP promoter (CSC:MBP:OATP) were incubated with 0.5mM Gd for five hours before being washed, fixed, and then analysed by ICP Mass Spectrometry. There was a significant difference in the amount of Gd detected between both the CSC:MBP:OATP and negative control (p=0.0115), and CSC:PGK:OATP and negative control (p= 0.0045). Three biological replicates, analysed by Wilcoxon Rank Test.

4.2iv Discussion

The data presented here demonstrate that expression of OATP can be restricted by controlling expression under the MBP promoter and that CSCs expressing OATP in this fashion can take up gadoxetate. Gadoxetate uptake was challenging to detect using MRI probably due to the small size of the CSCs, which are 1mm x 2mm x 300μm. However, it may also be that samples were incompletely washed and therefore contained so much signal that they caused shim artefacts. Shim artefacts occur when the T_1 shortening is so fast that it is not detected by the sequence. Therefore, further work on the protocol and the sequences will be required. ICP proved a sensitive method for detecting Gadolinium in CSCs unpaired parametric t tests demonstrated that the uptake of Gadolinium was significantly greater than the detectable

levels of Gd in the OATP null CSCs(CSC0). The OATP null CSCs which were incubated in gadolinium and washed according to the same protocol as the OATP expressing CSCs showed low, but detectable levels of Gd (0.00398 – 0.02311 μg/g), suggesting that the three wash protocol is sufficient, but the degree of variation suggests that it has the potential to be a confounding factor, and therefore future iterations of the protocol may require additional washing steps. NMR spectroscopy also proved a difficult and unreliable method for detection of gadolinium. Multiple protocols using a variety of different volumes of deuterated water, numbers of CSC slices, diameters and thicknesses of tube were attempted all with hugely variable and inconsistent results, an example of data from two of these experiments is included here. Refinement of this protocol does not appear to hold sufficient promise of utility and therefore NMR spectroscopy will not be taken forward as a validation technique, or as an experimental outcome measure for assessing gadolinium levels in samples or tissues.

The development of the CSC model for infection of endogenous OPCs with the MBP:OATP lentivirus has the potential to be further used as an *ex vivo* model system. By refining this model, and using it as the foundation to develop a CSC transplant model: where exogenously infected OPCs are seeded on to a CSC, a complete *ex vivo* model system could be developed to model the *in vivo* system I hope to establish. Alongside sequence development for MRI the exogenous/endogenous OPC:OATP system could be more thoroughly characterised, and modulators of remyelination trialled in this model prior to use *in vivo*. It is hoped that developing this system more completely will be part of the future work of this project.

4.3 Results 3: The Ethidium Bromide Caudal Cerebellar Peduncle model of demyelination can be characterised by Magnetic Resonance Imaging *ex vivo* and *in vivo*

4.3*i* Introduction

In order to establish a model in which demyelination can be identified, and remyelination can be monitored, both by MRI, surgical protocols, imaging protocols, and image sequences needed to be established. The MRI characteristics of the EB-CCP have not been previously reported. The model has, however, been thoroughly characterised by more conventional modalities.

The EB-CCP lesion was chosen because it has been demonstrated to be a highly stereotyped lesion with a predictable and reproducible pathophysiology. As brain imaging at high resolutions can be challenging *in vivo*, the larger rodent species, the rat, seemed more appropriate than a mouse model. Models of demyelination and remyelination can be broadly split in to two groups: The first; models which recapitulate pathological mechanisms of injury such as Experimental Autoimmune Encephalomyelitis (EAE) which models some aspects of the immune component of immune mediated damage to central myelin. Secondly the toxin models which do not model any aspect of disease injury mechanisms, but instead provide a platform on which repair processes can be studied (Blakemore and Franklin 2008; Franklin and ffrench-Constant 2017). This latter group offer the opportunity to elucidate true mechanisms of repair, but are not intended to recapitulate human diseases, or answer questions about their aetiopathogenesis. As this study does not aim to elucidate mechanisms of pathology the former category of model is not necessary, leaving the toxin models.

Toxin models are divided in to the focal and the general or systemic toxins. Cuprizone, the only systemic toxin for inducing demyelination, results in loss of myelin in the corpus callosum, internal capsule, anterior commissure and the cerebellar peduncles. However, the results are somewhat variable, and only the corpus callosum is generally used for analysis. This model is most commonly used in the mouse, though can be carried out in the rat (Adamo *et al.* 2006), but has been shown to lead axonal damage, and equivocal evidence of de and remyelination in corpus callosum, party due to the predominance of smaller diameter axons in this region (Stidworthy *et al.* 2003). The model requires feeding of dietary cuprizone (Carlton 1967), a copper chelator, for around 8 weeks, with demyelination becoming apparent 2-3 weeks after induction (Blakemore 1972). The model gives variable degree of demyelination with a sporadic pattern of remyelination across the various lesion sites(Blakemore 1974), and therefore does not offer an ideal paradigm in which to develop a new method of evaluating or monitoring new myelin formation. It may however lend itself well to confirming the utility of the model once fully developed.

The focal toxins models have the advantage of a localised and predictable lesion whose size and location can be controlled by the user. The most common focal toxins in use are Lysolethocein and Ethidium Bromide; however, Anti-Galactocerebroside antibodies, endotoxin, and 6-Aminonicotinomide have also been used (Blakemore and Franklin 2008). Lysolecithin is a membrane dissolving agent usually injected in to the spinal cord where it will make a lesion up to 8mm long, but of <0.5mm in diameter. It disrupts the myelin membranes preferentially sparing the cell membranes of most other cell types and may spare some mature oligodendrocytes and some progenitors (Arnett *et al.* 2004). Ethidium bromide is an

intercalating DNA toxin, and when injected in to a white matter tract, will kill off all glia present whilst preserving axons. The CCP lesion is around 0.6mm^2 in cross section, and are remyelinated largely by oligodendrocytes (Woodruff and Franklin 1999). In the spinal cord however they have been shown to remyelinate with a higher proportion of Schwann cells (Franklin and Blakemore 1993).

Spinal cord imaging is very challenging in MRI of rodents due to the significant movements of the thoracic region and the very small size. Therefore, a cranial lesion offered the best chance of reliable imaging. The larger rodent species; the rat, offered additional size advantages as well. Both EB and Lysolecithin can be injected in to both the corpus callosum and the cerebellar peduncles. As the CCP contains larger diameter fibres, confirming remyelination by electron microscopy is more reliable, therefore, lesioning this region has advantages for the development of a new methodology. Equally, the slightly longer time course for remyelination seen in the EB lesion also offers more flexibility when trying to develop new techniques and protocols. Therefore, the rat EB-CCP lesion was felt to be the most appropriate model system upon which to base the study.

Ex vivo MRI can offer microscopic level imaging in three dimensions giving resolution in the tens of micrometers (Dashevsky *et al.* 2015). A major concern in the development of this imaging modality is that the small size of the lesion will prove a challenge to image *in vivo*. Therefore developing an alternative outcome measure that can detect Gadolinium and the lesion is important. There are no antibodies for gadolinium, so histological techniques will only partially address the question. Microscopic *ex vivo* MRI therefore, offers a method of

addressing both arms of the question simultaneously. The addition of gadolinium to perfusion protocols has been shown to increase tissue resolution significantly (Johnson, *et al.* 2002).

Currently the imaging of demyelination and remyelination models using MRI appears to have been restricted to the Cuprizone and EAE models (Nathoo, Yong, and Dunn 2014; Song *et al.* 2005). Spinal cord imaging of lysolecithin lesions has been reported (Dunning *et al.* 2006; McCreary *et al.* 2009), LPS in the rat brain has been reported by Deloire-Grassin and colleagues (Deloire-Grassin *et al.* 2000), and lysolecitiin in the centrum semiovale has been reported in primates (Dousset *et al.* 1995), however the MRI character of lysolecithin lesion in the peduncles, or EB lesion anywhere in the brain has not been reported.

4.3*ii* Experimental Strategy

In order to develop an *in vivo* imaging methodology, outcome measures and validation techniques for the final process needed to be established. As no prior reports of the MRI character of the EB-CCP lesion existed in the literature it needed to be characterised and matched to histology. *Ex vivo* imaging techniques were developed to ensure a post mortem method for imaging tissue was in place, and these images were mapped against the histology to ensure that similar patterns of damage and repair were detectable by MRI. *In vivo* images of the lesions were then obtained. This work was done in conjunction with Joseph Guy (*ex vivo* and *in vivo*), and Dr Alan Wright (*in vivo*).

4.3*iii* Results

4.3*iii*a The EB-CCP shows characteristic demyelination followed by remyelination over four weeks which corresponds to conventional histology

Rats who had previously undergone a unilateral EB-CCP lesion were perfused with either 4% PFA or 4% PFA with 1.0mM gadolinium contrast agent, and tissue collected for imaging or histology. Haematoxylin & Eosin staining, overlaid with Luxol Fast Blue (myelin) staining was performed with the core facilities at CRUK on tissue fixed with only PFA.

Ex vivo MRI techniques were developed for imaging the whole cerebellum of tissue fixed with both gadolinium and without. First, reliable *ex vivo* MRI sequences were developed. Figure 31 shows an example of an early sequence, and an improved sequence. It was of particular importance to ensure that air pockets were removed when submerging samples in fomblin as air artefacts caused significant disruption to the image, the fourth ventricle in particular was challenging to clear of air pockets, it was found that overnight submergence in fomblin packed with cotton wool soaked in fomblin in a 50mL falcon, before then re packing with additional pre packed fomblin worked best.

Following this, based on reports by Johnson and colleagues (Johnson, *et al.* 2002), gadoxetate perfusion was attempted to help improved tissue contrast. Figure 32 shows an MRI of 21dpl lesions perfused with or without gadolinium. Both cerebellae were suspended in fomblin and scanned simultaneously using the same sequence (Figure 32). Once reliable high resolution images could be obtained a time course of the lesion was established to characterise its appearance corresponding to the expected histopathology (Figure 33).

A

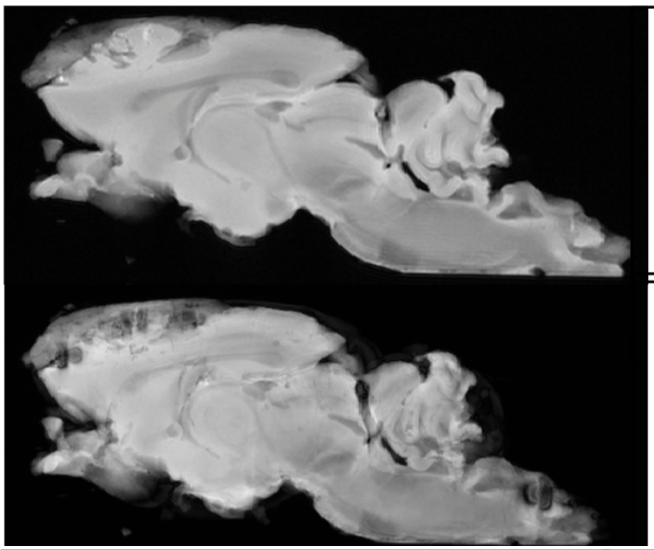

T_2
Sequence type: 2D fsems
Coil: Millipede 40 mm volume coil
Resolution: 80µm in plane, 1200 µm slices (400µm gaps)
TR 1000 ms, ETL = 4, kzero =2, ESP = 9.54 ms, Effective TE = 19.07 ms
Receive Bandwidth 208333 Hz
RF pulses: SGLgauss 800 µs for both 90° and 180°
*64 averages * 10 acquisitions*

*T_2**
Sequence type: 3D ge
coil: Millipede 40 mm volume coil
Resolution: 80µm inplane (sagittal), 1600µm thick slices
TR= 75 ms, TE=10 ms, Flip Angle = 12°
Receive bandwidth = 25,000 Hz
Slab fraction= 140%
*32 averages * 6 acquisitions*

B

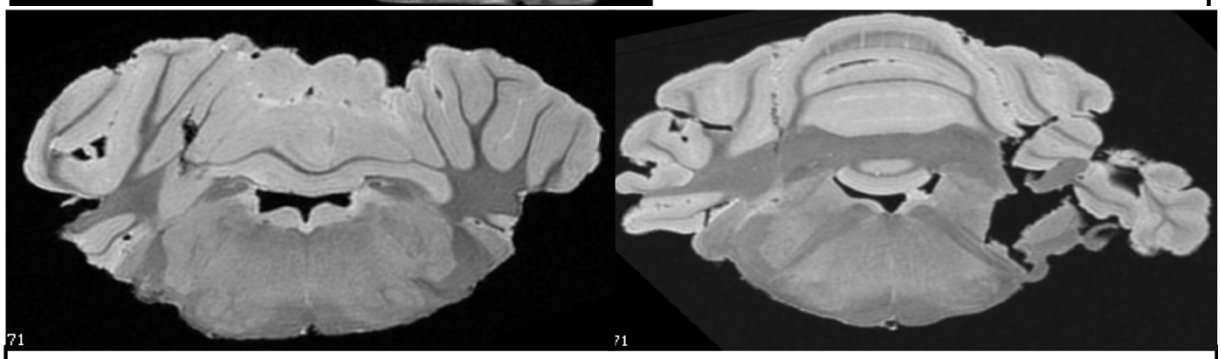

Matrix: 350 x x150 x x 240
FOV: 28 12 19.2 mm
3DGE: TE = 10ms TR = 50ms Slab fraction = 1.4 Flip Angle 12 degrees
Receiver bandwidth = 30488Hz
Averages = 8
Aqucisition Time = 4h0m
Aqucisitions = 15
Total time = 60 hours

C

Scan	A	B	C	D	
Isotropic Resolution	0.08	0.05	0.04	0.03	mm
Voxel size	512	125	64	27	Picoliters
Scan Time	36	18	42	34	hours
Relative Resolution	1	4.096	8	18.96296296	

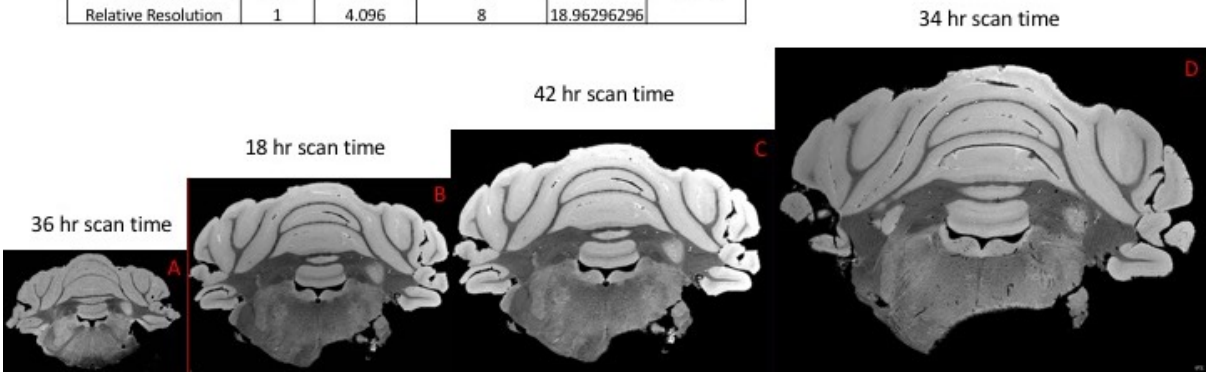

*Figure 31: Example images of ex vivo MRI of cerebellae used in the development of the ex vivo imaging methodology. **A** shows early attempts using both T2 and T2* sequences, with **B** showing the more refined sequences and improved image quality. **C** shows the sequence development and the improvement in resolution. Imaging was performed in the 9.4T horizonal magnet. Studies performed with J.Guy.*

A

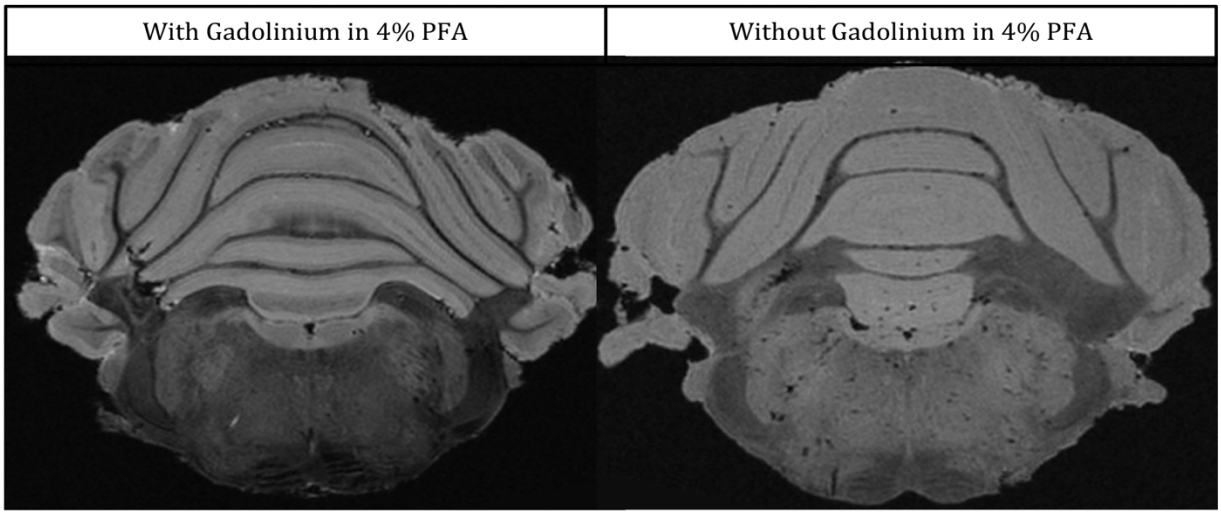

TR: 22.44
TE :11.24
Flip F+Angle 10'
Matrix: 512x144x200
FOV: 32x9.0x12.12.5
Resolution: 62.5uM isotropic
Gain: 36db
Receiver Bandwidth: 27174
RF Excitation Pulse: 200.us width SGLGauss
Slab fraction: 1.4

B

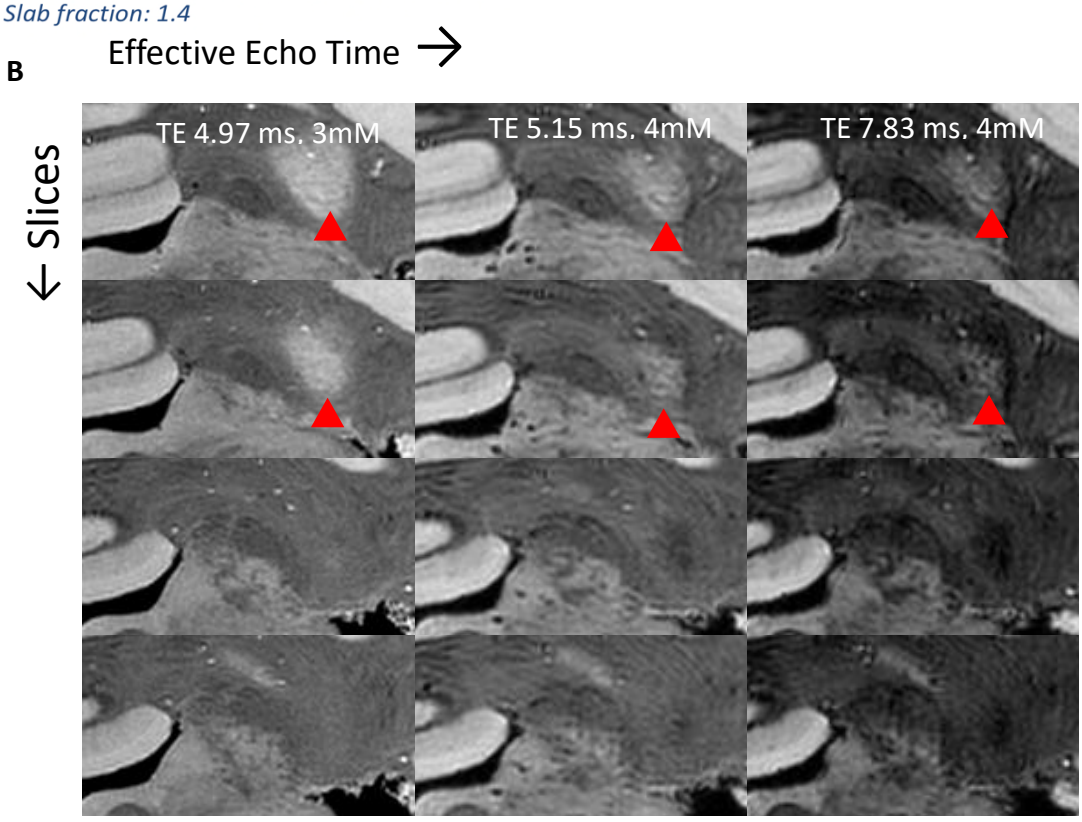

Figure 32: *Comparison of Gadolinium PFA Perfusion and standard perfusion both with post perfusion storage in PFA(**A**), a transverse image through the cerebellum. **B;** development of the sequence by varying TE times (shown along the top), and slice position (along the vertical axis). Imaging was performed in the 9.4 T horizontal bore magnet. A single brain was used for the development of these sequences*

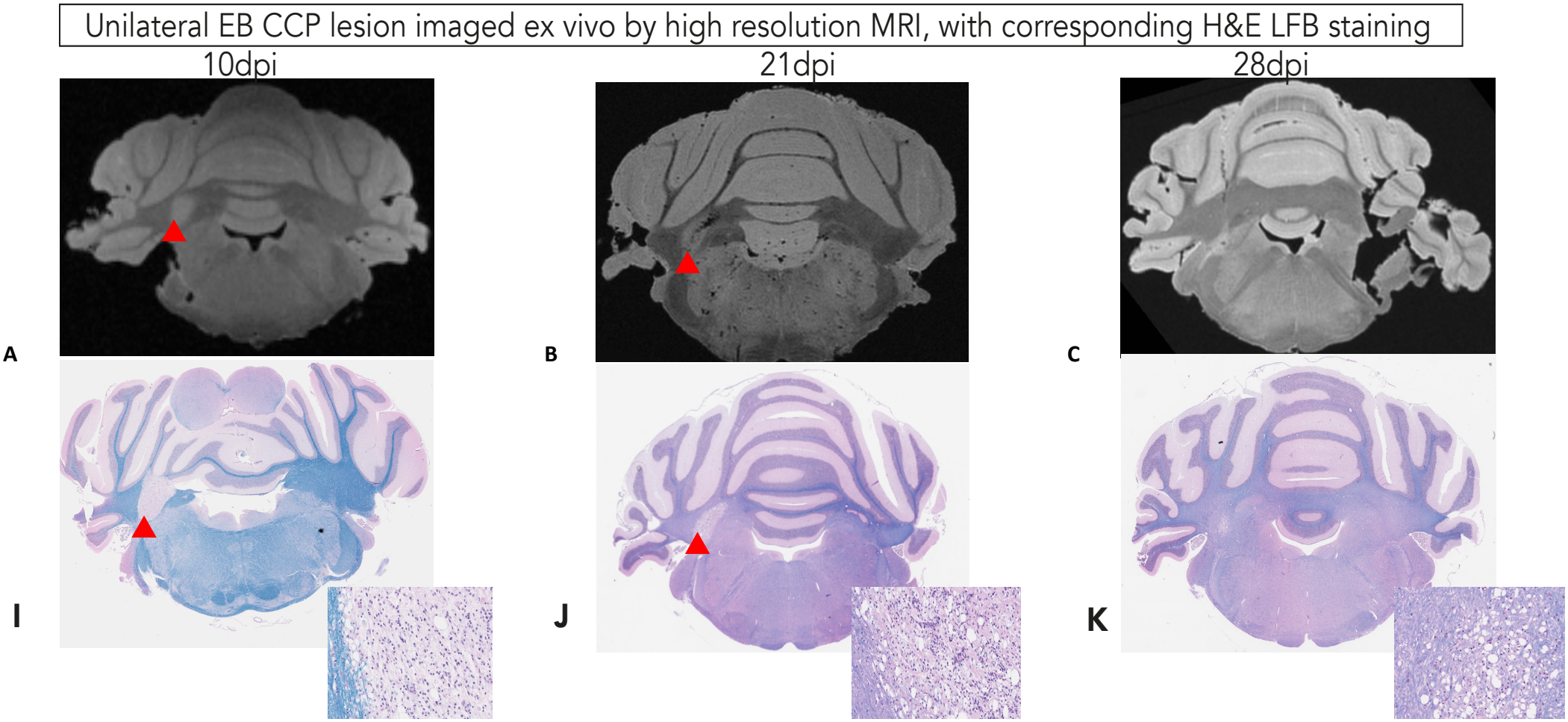

Figure 33: *Histological:MRI time course to characterise the lesion. Panels A-C show a time course from 10dpl to 28dpl with the lesion highlighted by the red triangle. Panels I-K show the corresponding histology with the region of the lesion expanded to show detail, the lesion is highlighted with the red triangle. The expansion is from the region of the boarder of the lesion and normal surrounding tissue. MRI performed in the 9.4T horizontal magnet using the same sequence as shown in Fig.31B.*

Having established that the CCP lesion could be easily identified and characterised using MRI *in vivo* images were obtained. Rats were imaged in a 7T horizontal magnet with active warming and temperature and heart rate monitoring. Images were obtained at 3, 5, or 7 days post unilateral CCP lesion, before being sacrificed and histopathology performed to confirm the location of the lesion. Figure 4 show the *in vivo* imaging of the lesion.

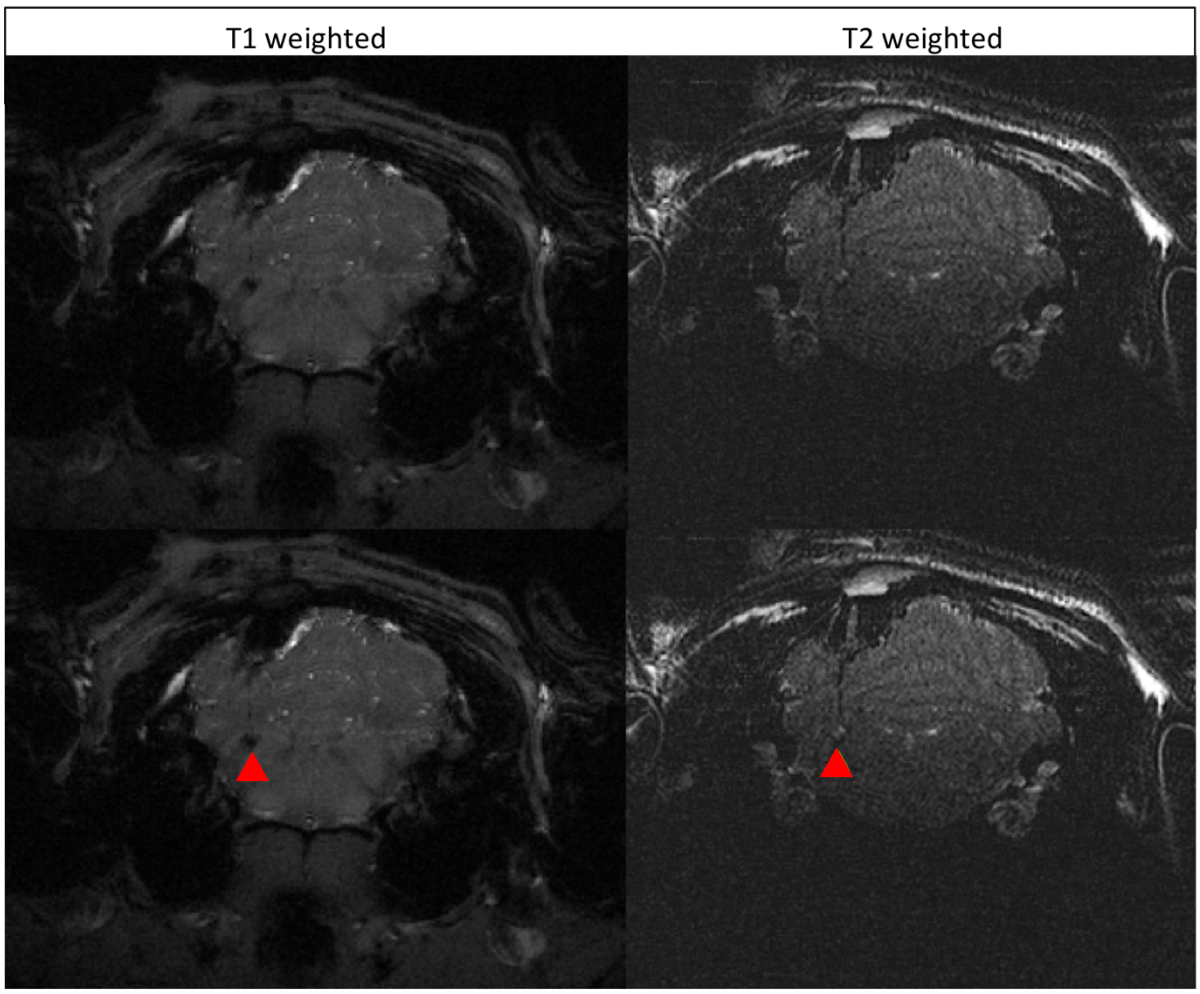

Figure 34: *In vivo image of the CCP lesion. 10 days post lesion imaged with T_1 and T_2 weighted sequences, shown unlabelled, (top panel) and labelled (bottom panel). T_1 image was acquired using a gradient echo sequence, T_2 image was acquired with a Fast Spin Echo Sequence: TR of 1.8ms, effective echo time of 40ms, 16 averages, 15 slices 1mm thick and matrix of 256 x 256, geometry 4cm x 4cm. Lesion highlighted in the second slice (bottom panels) with a red triangle. Experiment was repeated three times with similar results in all animals, representative images from one animal presented.*

4.3*iv* Discussion

The data shown here highlight the challenge of imaging such a small lesion *in vivo*. The image is easily and reliably detected by *ex vivo* imaging, which correlates well the histology, but the *in vivo* lesions are small and only visible in 1-2 slices. Some of these challenges could be overcome by making larger lesions with high concentration of EB, or larger volumes; however, this is likely to increase the number of adverse events in an already severe lesion model.

Current *in vivo* imaging has all been performed using a surface RF coil, volume coils or phased array coils offer improved signal at depth. Attempts to make a coil with greater CNR and SNR were made by Joe Guy, with some success; however, the coil was too fragile for repeated use. Commercially available alternatives do not appear readily available for use with Varian imaging systems. It may, therefore, become necessary to revive the development of specialised coils if greater resolution is to be achieved.

Alternatively relocating the lesion to the corpus callosum (CC) may offer improved signal given its proximity to the coil. Although the CC has many draw backs in terms of analysis of remyelination, it may be necessary in the development phase to use the site as part of the proof of principle strategy in method development.

Developing these methods has highlighted the technical challenges in tissue processing that whole brain imaging can cause, in particular, the degree of fixation required to obtain good MRI images is significantly greater than that for good immunohistochemistry or histology meaning that brains can not be dual processed. Additionally, extraction and manipulation of the cerebellum in to the fomblin and the removal of air pockets can result in damage the

surface architecture of the tissue. This does not pose significant problems at this stage, however it may become more relevant as cell transplantations are attempted.

Overall these data show that *ex vivo* MRI is an important tool in the development of this imaging modality, and that it can provide high resolution images, comparable to histological processing. Images in the region of 60-70μm isotropic are obtainable by ex vivo MRI which is far superior to the current in vivo resolution of 125μm isotropic. This technique is not intended as a final outcome measure; therefore, it may not be necessary to finesse the techniques at this stage. There is, however, significant scope for refinement in the methodologies. In particular, co-registration of histology to the MRI imaging to ensure exact correspondence may be necessary for validating transplantation techniques. This has proven a significant challenge in the field, with most groups using computational methods to overcome the 3D:2D, and resolution mismatches. However, the use of 3D printing of bespoke cutting cradles may allow co registration far more simply and with absolute accuracy (Guy *et al.* 2016).

4.4 Results 4: Rats receiving transplanted OPCs expressing OATP under the MBP promoter can take up gadolinium *in vivo*.

4.4*i* Introduction

In vitro, and organotypic slice culture work detailed previously showed that OPCs were capable of expressing OATP and taking up gadolinium detectable by various techniques. The aim of this thesis was to develop an *in vivo* imaging modality, capable of detecting contrast uptake by OPCS/oligodendrocyte lineage cells as they differentiated in to myelin forming cells, where the uptake of gadolinium could be correlated with the expression of the myelin protein MBP.

In order to do this, an *in vivo* strategy was devised. Figure 35 details the timeline for the protocol and highlights variables which required establishing.

Based on the literature the following parameters were determined:

-Cell number

-Infection day

-Transplant day

-Gadolinium contrast infusion protocol

-Protocol for allowing contrast to cross the blood brain barrier (BBB)

Cell transplantation in to the CNS is well established in rodents, previously studies have transplanted cell at concentrations ranging from 10,000/µl, total number 40,000 cells, in to the spinal cord (Chari *et al.* 2006) to 100,000 cells/µl, total number 100,000, in to the spinal cord (Brüstle *et al.* 1999), and 50,000cells/µl, total number 100,000 cells in to the cerebellum (Mendonça *et al.* 2014), to 900,000 total number in to the lateral ventricle (Brüstle *et al.* 1999).

The standard EB-CCP lesion is made with 4 µl of EB in saline, however volumes up to 6µL have been used without causing significant secondary damage (Woodruff and Franklin 1999). Therefore 500,000 cells in 5µl was chosen as the starting point for cell transplantations.

Day zero of the experiment was the day of lesioning, prior to this cells and virus will be prepared. Selecting the day on which to transplant cells or deliver intralesional virus may dictate the success of the engraftment or the number of cells infected. Woodruff and Franklin showed that OPC density was at its highest at 7 days post lesion in the lysolecithin model (Woodruff *et al.* 2004), and at around 5 days in the EB model (Sim *et al.* 2002) (Fancy, Zhao, and Franklin 2004) with MBP expression peaking at around 30 days, with cells beginning to migrate in to the lesion from 3 days (Sim *et al.* 2002). Based on this an initial protocol of transplanting cells in to the lesion at 3 days, before the endogenous cells begin to dominate the area was chosen. Intralesional virus will be injected at 7days post lesion when the greatest number of endogenous OPCs are present in the lesion in order to maximise the number of cells infected.

The study upon which this work is based, that of Patrick and colleagues, showed that at five hours after an injection of gadolinium contrast agent T_1 shortening of an OATP expressing xenograft was detectable, and was maximal between 5 and 10 hours depending on the cell line of the xenograft, and declines thereafter (SP Patrick Thesis, 2013) (Patrick *et al.* 2014). Therefore, a five hour contrast to imaging time lag was selected. Similarly doses of gadolinium were based on this prior study and manufacturers guidelines.

The use of an agent to facilitate the crossing of gadolinium in to the xenograft was not relevant in these studies performed by Patrick and colleagues (Patrick *et al.* 2014*)*. In this work, however, the BBB poses a potential block to the passage of contrast agent into the extracellular fluid around the lesion. In the early phase of the lesion the blood brain barrier is likely to be impaired, given that EB is an intercalating DNA toxin, it will kill of cells whose cell bodies are in the region of injection; in a white matter tract this includes the glia (including astrocytes, whose podocytic processes form the parenchymal boarder of the BBB), and the endothelial cells and pericytes of the vasculature (which contribute to the vascular wall of the BBB). However, as the lesion remyelinates, the BBB will repair as well. The contrast enhancement characteristic of acute lesions in MS is as a result of a similarly 'leaky' BBB, and the resolution of these lesions, and their transition into non contrast enhancing, is equally characteristic of their repair. It is likely, therefore, that a methodological paradox may occur: As the BBB becomes increasingly impervious to contrast, expression of MBP is likely to increase. Therefore the lesion will be expressing the most OATP at the point at which the least contrast agent is available in the extra cellular fluid to be transported in to the cytoplasm. Consequently, methods for opening the BBB may be required. Most commonly used is the delivery of the synthetic sacchride mannitol (Cosolo *et al.* 1989), (Rapoport 2000), which opens the BBB via an osmotic disruption of the tight junctions (Rapoport 2000). The exact protocol to be used in conjunction with the contrast agent will need to be established; however, initially contrast will be delivered immediately following mannitol infusion as Cosolo and colleagues showed reversal of the osmotic opening within five minutes of infusion (Cosolo *et al.* 1989).

4.4ii Experimental Strategy

The intention was to begin translating the *in vitro* work into live animals. A protocol was drawn up in which rats would receive bilateral EB-CCP lesions, receive either intracranial virus to infect endogenous OPCs, or receive a cell transplant of exogenously infected OPCs. Following transplant/intracranial virus injection, they were to undergo serial imaging by MRI with the aim of detecting gadolinium contrast uptake by the cells. However, early attempts failed, and therefore trouble shooting was required. A majority of this chapter details the process by which trouble shooting and validation was carried out.

4.4iii Results

Based upon the work in Chapter 4.3, *in vitro* imaging was attempted. Rats underwent bilateral EB-CCP lesions, and then received exogenously infected OPCs expressing OATP under the PGK promoter or intracranial virus. Imaging was carried out with contrast agent administered with or without mannitol 5 hours prior to imaging. Figure 35 shows an example of the lesion imaged following viral injection and transplantation, despite multiple repeats there is no evidence of contrast enhancement. Therefore, the processes were broken down in to its components and attempts to optimise each step were taken.

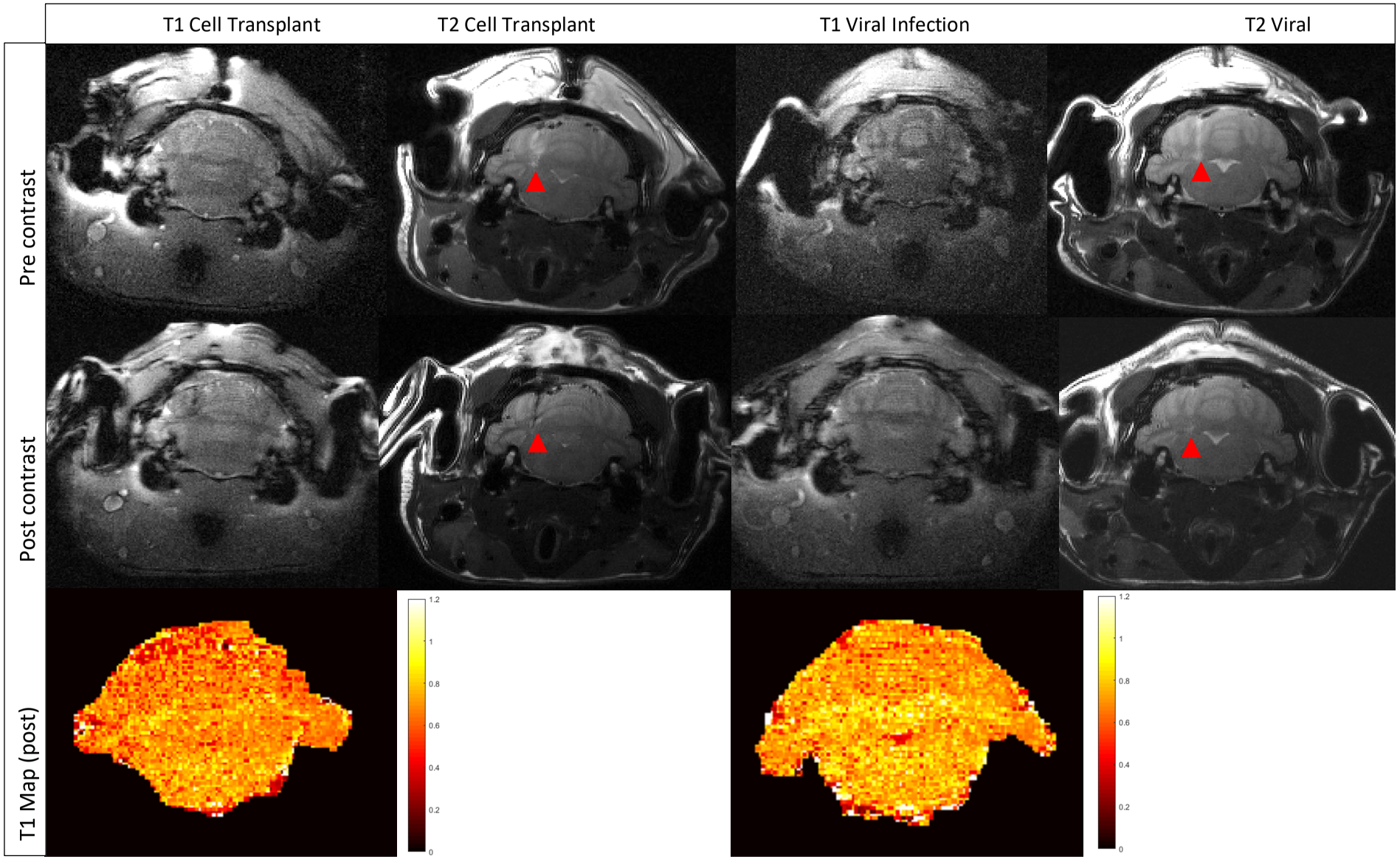

Figure 35: in vivo imaging of OPC transplants and viral infection of endogenous OPC.
See Description over leaf

Figure 35 (continued from overleaf): in vivo imaging of OPC transplants and viral infection of endogenous OPC. In vivo imaging following transplantation of OATP expressing cells, and intracranial (intralesional) infusion of PGK:MBP:OATP virus. Animals were imaged at 3 days post lesion (Pre) with no contrast administration, and then 21 days post lesion (Post with contrast administration 5 hours prior to imaging). T1 maps were acquired using IR FLASH sequences with TR 2.98seconds, TE 1.46 ms, Trelax 12ms, Flip Angle 10 degrees, 32 averages, 1 slice of 1mm thick and matrix of 256 x 256, geometry: 4cm x 4cm. T2 weighted images were acquired using a Fast Spin Echo Sequence with TR of 1.8ms, effective echo time of 40ms, 16 averages, 15 slices 1mm thick and matrix of 256 x 256, geometry 4cm x 4cm. Lesions are highlighted with red triangles where they can be confidently identified. Representative image from one animal, experiment performed in three animals with similar results.

In order to establish if cells expressing OATP could be detected at all, the *ex vivo* MRI of tissue was returned to. Cells were injected into, fixed cerebllae before being imaged, and the protocol refined from there. Figure 36 shows a cerebellum in transverse section in to which fixed HEK cells expressing OATP under the PGK promoter were injected. HEK cells were chosen for this as they are easier to manipulate and can be grown in large numbers far more rapidly than OPCs. As these experiments were largely trouble shooting and protocol optimisation, it seemed prudent to use a rapidly growing cell type which could withstand significant handling, rather than the OPC which requires significant numbers of animals to be sacrificed in order to isolate, and requires very gentle handling.

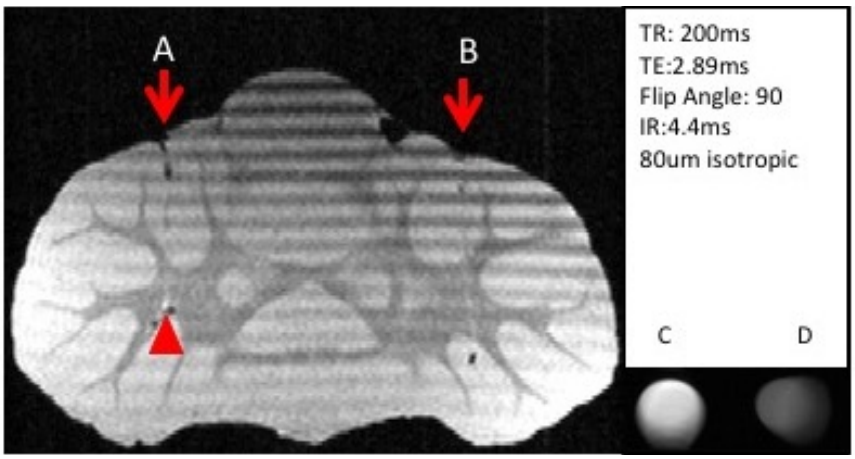

Figure 36: Ex vivo MRI of fixed HEK cells injected in to post mortem tissue. HEK cells expressing OATP (A) and infected with sham virus (B) were incubated in Primovist, before being fixed, washed and then injected in to a pre fixed cerebellum. The cerebellum was then imaged, ex vivo, as previously described. The syringes containing remaining cells were simultaneously imaged (C-expressing OATP, and D infected with sham virus, and therefore not expressing OATP) as a control. The injection tracts can be seen in both A and B, and contrast enhancing cells can be seen (red triangle, below the A injection tract. Distal to the B injection tract a hypo intensity can also be seen, this is likely to be the non expressing cells which do not contrast enhance.

Cells imaged in the syringes (C and D) in Figure 36 clearly show T_1 shortening consistent with containing gadolinium. A small region marked by the arrow head may be some of these transplanted cells. Further refinements were made to the injection technique and image sequences. Under these refined protocols Figure 7 was generated using fixed cells and fixed tissue as in Figure 36.

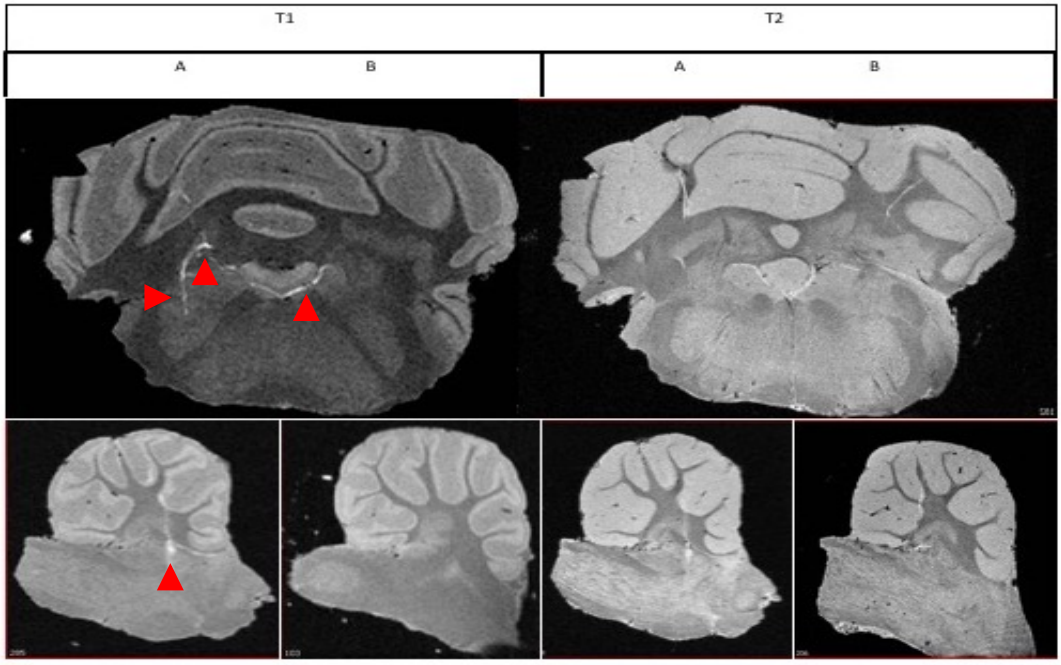

Figure 37: Ex vivo MRI of transplanted cells with improved technique and image sequences. Fixed HEK cells expressing OATP(A), and sham infected cells (B) injected in to fixed tissue. The 'lightening bolt' distribution can be seen on the T_1 sequences. The top panel shows the cerebellum in transverse section, the bottom panels show the corresponding right and left sagittal images with the slice positioned over the injection site (A), and the anatomical equivalent on the contralateral side of the cerebellum. The T2 panels show the cells are isontense to the tissue as would be expected. Red arrouw heads highlight the contrast enhancing cells on the T1 sequence images. T_2 images were acquired using the following parameters: TE 11.94ms, TR 60ms Flip Angle 15 degrees 70us gauss, 8 acquisitions, 1 average per acquisition T_1 images were acquired using the following parameters: TE 3.82ms, TR 11.0ms, Flip Angle 90 degrees, 70us gauss 32 acquisitions, 4 averages per acquisition.

As can be seen in the image T_1, shortening is detectable in a linear 'lightning bolt' pattern. This does not well represent the *in vivo* transplantation where it would be expected that, following initial injection, cells stayed localised to the injection site. Therefore, fixed HEK cells were injected in to un fixed tissue and then post fixed (Figure 38).

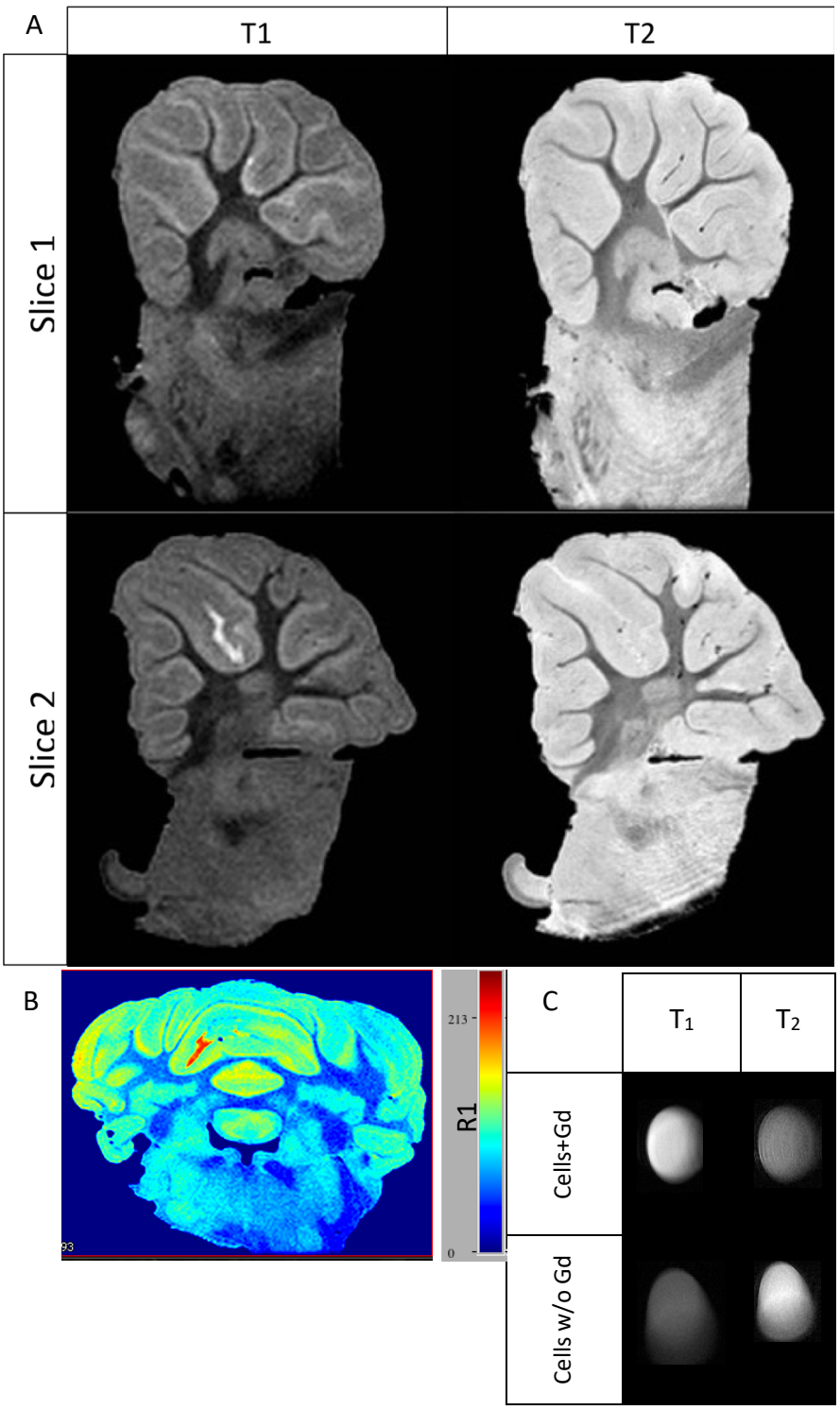

T_1 Sequence:
TE 3.82ms
TR 11.0ms
Flip Angle 90 70us gauss
32 Acquisitions,
4 Av per acquisition
14mins 27sec/acquisition
7hr 43 mins total

T_2 Sequence
TE 11.94ms
TR 60ms
Flip Angle 15 70us gauss
8 Acquisitions,
1 av per acquisition
44mins 21sec per acquisition
5hr 55mins total

Figure 38: Ex vivo MRI of un fixed cells in to un fixed tissue. Following injection of cells, the tissue was post fixed before being imaged by MRI using T1 and T2 weighted sequences (A), representative sagittal images shown. A heat map with the R1 values (1/T1 in seconds^{-1}) was made from a transverse section through the cerebellum. It can be seen that the 'hot spot' coloured red on the R1 corresponds to the anatomical location of the contrast enhancing cells in the T1 image (slice 2). The syringes used to inject the cells (with some remnants left in them) were imaged simultaneously to act as a control. N of 1.

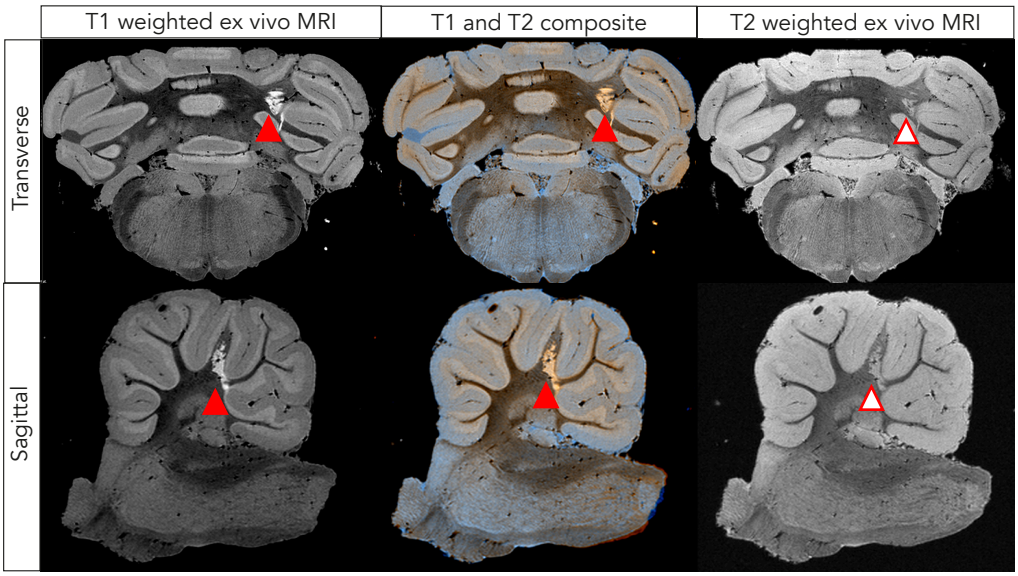

Figure 39: *OPCs expressing OATP under the PGK promoter in post mortem tissue, imaged by ex vivo MRI. Sequence as described previously. A composite image (centre) comprising two false colour images which have been overlaid where yellow is T1 signal, and blue for T_2 . This image shows that the red triangle area on the T1 image to the right (where the lesion is hyper intense and therefore bright), when flase coloured appears yellow, this region overlaps with an iso intense T2 region (red and white triangle), the overlaying of the T1 hyperintense in yellow, and T2 isointense(no colour) highlights the colocalisation of the transplant. The upper images represent transverse images through the cerebellum whereas the bottom panels represent sagittal images where the slice in line with the injection tract has been selected. N of 1.*

The method used in Figure 38 re capitulated the *in vivo* transplantation, and showed T_1 shortening in the region of cell injection showing cells could be detected. Therefore the protocol was repeated using OPCs expressing OATP under the PGK promoter (Figure 39). Having demonstrated that cells could be detected in post mortem tissue a titration of cell number was performed to establish to lower limit of detection (Figure 40).

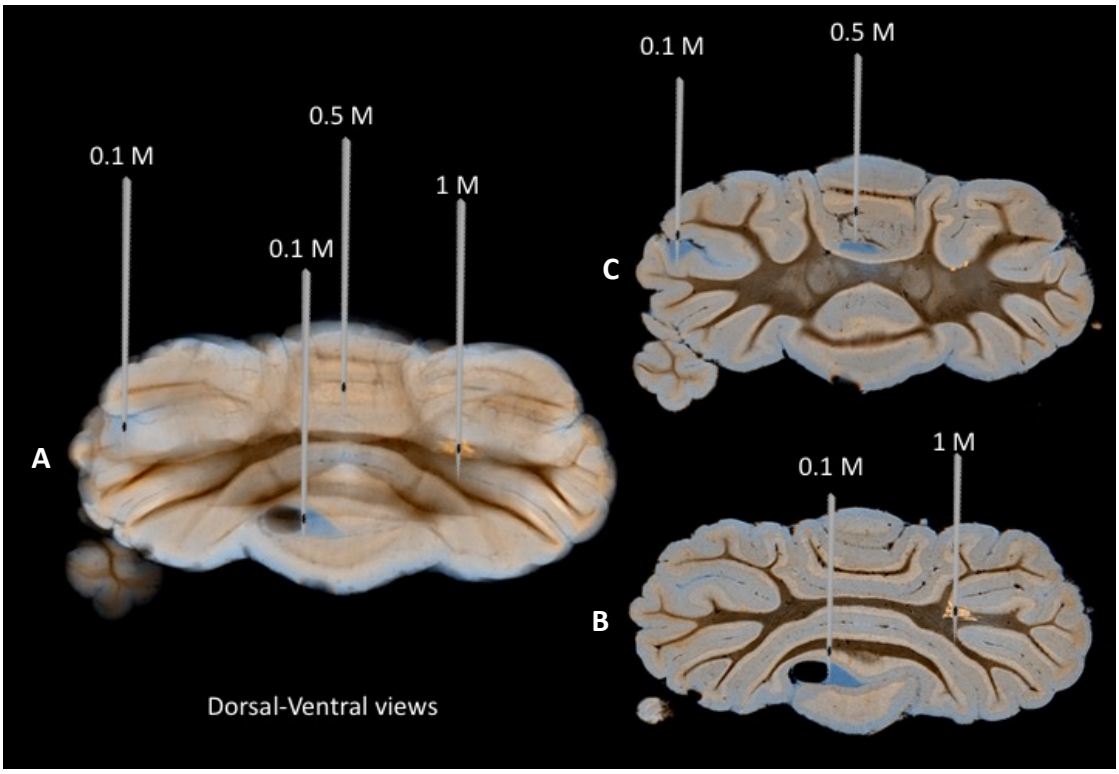

Figure 40: Titration of cell numbers injected in to post mortem tissue and imaged by ex vivo imaging showing false colour composite images. The minimum number of detectable cells was 1million in 5uL. Image A shows a dorsoventral view on to the cerebellum highlighting the locations of the injection sites through which cells were injected in to the un fixed tissue. B and C show coronal sections in which the transplanted cells can be identified. As in Figure 39, false colour images have been used to show co localisation of T1 and T2 signals. Cells containing Gd are expected to be hyper intense on T1 and iso intense on T2. Hyper intense signal on T2 would be expected from water. Therefore areas corresponding to transplants which appear blue on the composite are highlighting the transplant medium, but not the cells, and areas corresponding to transplants which appear yellow are highlighting detectable T1 contrast enhancement associated with Gd containing cells. From these data it can be seen that the smallest detectable number of cells in 5uL of media is 1 million cells. N of 1.

Following the cell titration a single repeat of the *in vivo* protocol was attempted. Three rats underwent a bilateral EB-CCP surgery, one received OPCs expressing OATP under the MBP promoter five days post lesion, on one side, and un infected cells on the other, the second received a single transplantation of OPCs expressing OATP under the PGK promoter, incubated prior to transplantation in gadoxetate, and sacrificed by perfusion fixation under terminal anaesthesia, this was used as a positive control, and the third animal received a single injection of transplant media (vehicle) with no cells, this was used as a negative control, and was perfusion fixed under terminal anaesthesia following intracranial injection of vehicle. The first rat which had received OPCs expressing OATP under the MBP promoter received an injection of mannitol, followed by an infusion of gadolinium, and were then perfusion fixed 5 hours following administration of contrast agent. Tissue was then sent for analysis by ICP-MS, Figure 41.

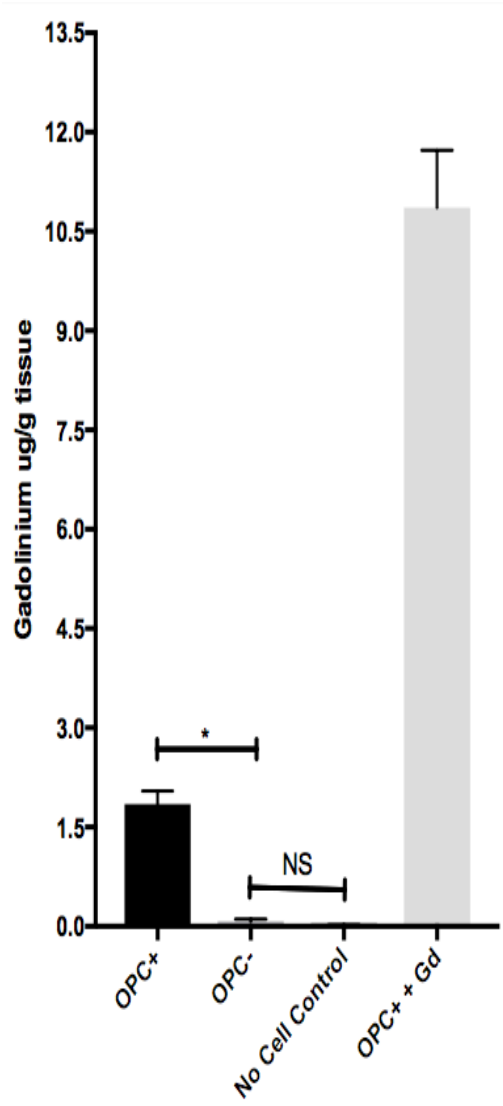

Figure 41: Gadolinium concentration in post mortem tissue analysed by ICP MS following transplantation and contrast agent delivery. Three rats underwent bilateral CCP lesions. One (the 'experimental animal') received a transplant of OPC expressing cells under the MBP promoter (OPC+) on one side and uninfected OPCs in to the contralateral lesion (OPC-). The second animal received a transplant of OPCs expressing OATP under the PGK promoter which had been incubated in Gd containing media directly prior to transplantation, this transplant was performed directly before being sacrificed by perfusion fixation (OPC+ + Gd), this was a positive control. A third animal received Gd free transplant media only as a negative control. The experimental animal received Gd and Mannitol co injection three weeks after the transplant and was sacrificed 6 hours post injection. Following sacrifice tissue sent for analysis by ICP-MS. These data show that OPC+ (cells expressing OATP under the MBP promoter) were able to take up detectable levels of Gd following intravascular injection with Gd: Mannitol. Groups were analysed with Wilcoxon Rank Test. Error bars represent technical repeat values provided by the ICP-MS facility

4.4*iv* Discussion

Figure 35 shows that *in vivo* imaging of transplanted, exogenously infected cells, and of endogenously infected cells did not work. This could be for many reasons including cells not surviving, insufficient cells becoming infected, imaging at a time point when expression was suboptimal, failure of contrast agent to reach cells, insufficient contrast agent, or inappropriate imaging sequences being used; any one, or any combination of these may have been at play.

In order to establish which element of the protocol needed adjustment a table of possible problems and ways to detect them was constructed; Table. The data in the remainder of this chapter details attempts to address some of these areas. The remaining areas will be addressed in future work.

Potential bottleneck / Failure point	Reasoning	Method for troubleshooting
Cells not expressing prior to transplantation	Cells unsuccessfully infected transplanted will not express OATP	• Check cultures for fluorescence using light microscope prior to detachment and pelleting > *refinement: calculate the number of cells expressing prior to detachment and pelleting, and how many are lost in the dissociation and resuspension protocol* • Check cells for expression by retaining a sample from the Hamilton, fixing and staining this sample for Olig2 and mStrawberry
Cells dying following transplantation	Transplantation in to an inhospitable environment (too much myelin debris in the lesion etc.) may increase cell death following transplantation Transplantation technique may cause pressure necrosis if too large a volume is used or excessive shear stress if inappropriate technique or cell concentrations are used	• Design a qPCR for the OATP gene and run a genotype style tissue characterisation on tissue post transplantation or intralesional virus injection • Carry out tissue clearing (Tomer *et al.* 2014) and stain sections for cell cycle markers eg BrdU/Ki67, and co staining of a cell tracker
Cells failing to differentiate	If cells are transplanted or infected at an in hospitable stage in the pathophysiology of the demyelinating lesion this may alter their propensity to differentiate	• Carry out tissue clearing (Tomer *et al.* 2014) and stain sections for markers of differentiation and create a time course to establish when differentiation and MBP expression is maximal > *refinement: optimise imaging sequences and protocol based on this timeline*
Cells dispersing or being 'off target'	Cells may be transplanted off target if stereotactic surgeries are not carried out correctly Cells may migrate throughout the CNS following transplantation reducing their density in the target region Virus may distribute throughout the CNS resulting in either inadequate focal infection or in widespread low level infection and expression	• Carry out tissue clearing and stain sections for mStrawberry, to identify dispersal of transplanted cells or the spread of infectivity in 3D. Other transplantation studies have not identified this as a cause for failure [references] • Use tissue clearing to refine surgical protocols to ensure cells or virus are being delivered to the optimal location, this may not be in to the centre of the lesion • Develop histological and MRI co registration using 3D printed cutting cradles to validate imaging and ensure MRI corresponds precisely with histology (Guy *et al.* 2016)
Viral titre too low to infect endogenous cells	*In vitro* infections have used polybrene to improve infectivity, however polybrene is not suitable for use *in vivo*. Very high titres may be required to achieve adequate tissue expression (Schilling *et al.* 2016).	• Refine virus manufacture to improve titres • Perform *in vivo* titration of virus to establish necessary titre level, confirm with conventional IHC
Too few endogenous progenitors infected	Even at high titres, numbers of progenitors infected locally may be too low to detect	• Make an adenovirus for systemic delivery to allow whole brain progenitor targeting (Chan *et al.* 2017). This may offer a positive control against which the focal infection with lentivirus can be compared.

Infection causes masking inflammatory response	Unpublished observations by the Brindle group has found that OATP can cause significant inflammatory respone up to 14 days following infection, this may affect cell survival, differentiation or proliferation, it may result in overlaying of inflammatory signals on MRI imaging obscuring contrast enhancement. It may also potentiate opening of the BBB facilitating contrast uptake further in to the lesions repairing state	• IHC characterisation of the lesion (post transplantation/infection) to establish if the lesion behaves differently to those previously characterised in the literature. OATP is a relatively promiscuous transporter capable of carrying various hormones including thyroid hormone, this may result in different behaviours of cells expressing OATP *in vivo*, than were seen in defined media *in vitro*.
Gadolinium not crossing the BBB	Gadolinium contrast agents are used in conventional diagnostic imaging in their 'vascular' or acute post vascular phase – when they are in the blood, or having exited the vasculature through leaky blood vessels in to the parenchyma. In this study we are taking advantage of OATP to sequester gadolinium in to the cytoplasm long after vascular clearance has occurred. If gadoxetate can not cross out of the blood vessels in to the parenchyma it will not be available in the ECF to be sequestered by OATP.	• Mannitol can be used to open the blood brain barrier > *refinement: develop a protocol which optimises time of mannitol administration to gadolinium infusion to achieve maximal uptake. This may require use of a Oligodendroglial cell line such as CG4* (Chari *et al.* 2006) *to ensure large numbers of robust cells being transplanted, this will necessitate immunosuppression and may therefore fundamentally alter the character of the lesion model.*
Gadolinium delivered too late or too early relative to imaging time point	Work by SP Patrick showed that peak T1 shortening was xenograft dependant and that it was between 5 and ten hours. Current protocols have been carried out at 5 hours post contrast, this may be too early.	• Carry out imaging time course once the full protocol is in place > *refinement: tissue from multiple time points can be analysed by ICP-MS in order to most accurately define the time points to be used*
OATP not active	OATP has been demonstrated to be active in xenografts (Patrick *et al.* 2014), and in cell pellets and endogenously infect cells *in vitro*, however nothing in the literature confirms its expression in transplanted cells, though there is no logical reason for it to loose function in this paradigm.	• Develop the Cerebellar Slice Culture model to include a transplantation on to the organotypic slices • Repeat the ICP-MS of tissue infected and transplanted having been exposed to contrast *in vivo*, as in Figure 41.
Imaging sequence not detecting Gadolinium	Shim artefacts, inadequate resolution, inappropriate slice placement may all impede detection of T1 shortening	• Once a pipeline can be reliably established to get rats to the point of undergoing serial imaging studies, sequence development and coil development can take place.

Table 9: Trouble shooting process for in vivo imaging method development

In order optimise the *ex vivo* transplant model various methods of tissue processing were attempted. The first was to inject HEK cells, expressing OATP under the PGK promoter, and then fixed in 4% PFA, in to fixed cerebellar tissue. As Figure 7 shows, this resulted in fissure formation and the cells distributing linearly rather than staying in at the injection site, and in Figure 36, cells probably leaking back up the injection tract. In Figure 36, only a small region of T1 enhancement is visible. This may, in part, be due to the inappropriate sequence used (the linear artefact probably resulting from the inversion pulse being too close at 4.4ms), and as noted above, cells coming out of the injection site and being washed away by the processing. Figure 38 and Figure 39 show refinements of this protocol, both in terms of the imaging sequences, and in the tissue processing. In Figure 38, fixed cells were injected in to unfixed tissue, left to rest for 10 minutes and then fixed. The fixation of cells appeared to cause significant clumping and blocking of needles, making the concentration of cells by serial centrifugation very difficult. Figure 39 shows unfixed OPCs expressing OATP under the PGK promoter injected in to unfixed tissue, left to stand, the injection site sealed with a small amount of tissue glue, and then fixed, this appears to be the optimal technique.

Before returning to *in vivo* imaging a titration of cell number was performed, as shown in Figure 40. This along with the other *ex vivo* imaging confirms that cells expressing OATP, containing gadolinium, in tissue can be detected by MRI. However, the lower threshold for this detection was 1 million cells. This number is significantly higher than the number usually transplanted in most studies.

In vivo imaging was attempted using both transplanted cells, and endogenously infected cells, as mentioned above, neither were detectable by MRI.

A major challenge of refining this protocol was that post mortem imaging required significant fixation in PFA, and probably as a result, the use of the anti RFP antibody to detect the mStrawberry fluorescence failed, detection without the antibody in cryosectioned samples variably showed a few expressing cells; however, samples bleached rapidly. A reliable method for confirming the survival of the cells post transplant has therefore not yet been found. Prior to transplant, cells were examined under light microscopy to check mStrawberry expression. However, it remains unclear how many of these cells survived transplantation. In order to refine the transplantation protocol in the future an adjustment to the protocol will be required, and an additional experiment will be carried out prior to the next iteration. Of the former, a fluorescent cell tracker will be used; cells will be incubated in it prior to transplantation, and samples kept back for appropriate staining at each step of the protocol, including retaining a sample from the needle following transplantation to confirm the cells transplanted were, in fact, expressing. With regard to the latter, before any further *in vivo* imaging is attempted, a tissue clearing protocol will be carried out in order to identify, quantify and locate transplanted cells. This experiment will be repeated with brain tissue which received intracranially injected virus.

In order to address the question of whether gadolinium contrast agent was penetrating the BBB and thus able to be taken up by the transplanted cells post mortem tissue from an *in vivo* protocol was examined by ICP-MS. This 'n of 1' experiment, which shows that OPCs expressing OATP under the MBP promoter can take up gadoxetate *in vivo*, is far from unequivocal

confirmation that the technique works. It is however a significant step forwards in that direction.

5. Discussion

As new therapies are being developed for diseases of myelin, in particular the development of therapies which look to enhance (re)myelination there becomes a more urgent need for outcome measures to assess these therapies. Currently there are no non-invasive techniques for assessing, specifically, the production of new myelin. Although *in vitro*, this may not be a rate limiting factor, when it comes to translating new molecules or techniques in to *in vivo* models and therapies, it certainly limits the certainty with which we can pronounce a technique to be truly effective in enhancing remyelination.

This project looks to address this issue by developing a technique which harnesses concepts previously developed in the field of cancer biology, and applies them to the study of myelin. By using a technique; MRI, widely used in clinical imaging, and a contrast agent already in wide spread use in the National Health Service, and approved by the FDA, I intend to develop a method which can be applied to both the preclinical and the clinical investigation of myelinopathy treatments. The ultimate aim is to develop a tool and protocol in which exogenously infected transplanted, and endogenously infected, progenitor cells in a demyelinated lesion can be imaged by MRI, longitudinally and non invasively, and that over time, a change in T_1 weighted imaging can be correlated with contrast uptake and therefore with remyelination.

The non-invasive nature of this technique may also allow us to reduce the number of animals used in screening of molecules as serial imaging could replace the sacrifice of multiple animals at longitudinal time points. This also has the advantage of potentially allowing the translation to use in clinics; allowing patients to under go serial imaging to assess their response to a

treatment, potentially opening up the possibility for personalised medicine if and when a raft of pro remyelination techniques become available.

The methodology may also have applications in assessing the treatment of transplantation therapies now being developed for diseases such as MS and PMD. PMD in particular, can be such a debilitating disease, that any intervention which provides clinical improvement may be of benefit. However, given the potential concerns over safety and oncogenicity of stem cell transplants, it is vital that we have evidence to support their functional use, and that we understand if such transplants are truly forming new myelin, or if it is other, paracellular effects, which are causing any clinical improvements seen. Work by Ruckh and colleagues using the heterochronic parabiosis model demonstrated the rejuvenating capacity of young cells entering a lesion in an old mouse leading to a degree of 'rescue', in these studies migratory monocytes were implicated (Ruckh *et al.* 2012), and this, and a raft of studies like it has fuelled renewed interest in the potential of cell therapies for a variety of diseases and age related declines (Rebo *et al.* 2016). However, direct evidence of the contribution of the cell itself, as opposed to its secretome or other paracellular effects is still lacking. Indeed Wagers and colleagues demonstrated further that it was likely to be humoral factors, and not the cell itself which contributed to the rescue (Loffredo *et al.* 2013). For an understanding of a cells role in these putative therapies, cell tracking, lineage, and fate mapping is required, and whilst this is well established in mouse models for the study of development, few techniques exist for integrating function in disease models.

There have been many challenges in developing this technique, not least the inherent challenges of generating primary cell cultures of oligodendrogilal cells. Although the

components of the model were established across both laboratories, their combination was entirely novel, and required adaptation of already complex methodologies. The data generated so far provides a starting point for translation of this method to *in vivo* models, However, refinement of many of the *in vitro* techniques is still required.

A lot of effort has been put in to the *ex vivo* techniques, for which I am very grateful to my colleague Joseph Guy for his support and assistance. In particular, the development of sequences which achieve high resolution, and suitable coils for this work has allowed us to generate a knowledge base which we hope we can apply to validating the method as it develops.

At the outset of this project it was hoped that a fully established *in vivo* imaging protocol would be in place, as a result stepwise characterisation was traded off against progress towards that final goal. In hindsight, this may have been an inappropriate trade off, with a thorough understanding of the biology and behaviour of OATP expressing progenitor cells *in vitro*, in CSCs, and *in vivo*, remaining patchy and incomplete. However, broad proof of principle progress has been made towards the end goal of an *in vivo* imaging modality.

The data presented here demonstrates that progenitor cells can be infected by lentiviral vectors leading to the functional expression of the OATP channel and that cells can reversibly take up gadoxetate. The refinement of the agarose phantom experiments provided a reliable and repeatable model system in which to assess cells by MRI. It was found that achieving uniform distribution of cells in the agarose, and removing air bubbles, was of significant importance in obtaining representative results, the use of a cut down 96 well plate was

significant in the streamlining of the method as it allowed the uniform arrangement of standards and samples which would be rapidly cooled on ice and mixed simultaneously. Previous studies have used eppindorfs but handling multiple samples and standards simultaneously led to uneven setting of the agarose which made slice selection and sequence optimization difficult. Having established a reliable and repeatable protocol for this technique it can be used in the future development and refinement of the method.

The premise of this model is that OATP expression can be directly correlated to MBP expression by differentiated progenitors, and that, to as great an extent as any imaging modality can, this can be interpreted as evidence of remyelination. Pre-requisite therefore, are two key elements; that OATP expression can be restricted to progenitors and controlled under the MBP promoter, and that these progenitors contribute to the repair of a demyelinated lesion. The latter point has been widely studied by others in the field, and a general consensus exits that remyelination is carried out by the differentiation of oligodendrocyte progenitors in to myelinating oligodendrocytes. Direct evidence that progenitors expressing OATP under the MBP promoter, contribute to the repair of demyelination in the context of *this* lesion paradigm, is however, still to be established. On the former point, chapter 4.2 attempts to demonstrate that expression can be restricted to MBP expressing cells, confirming in the process, that GFAP positive cells, and the axonal region of neurones do not express OATP. Direct evidence that OATP is not expressed by endogenous microgila has not been shown, but there is no reason to expect that it would be.

The restriction of OATP expression by the use of the MBP promoter offers two distinct advantages, the first being cell selectivity: no other cell in the CNS expresses MBP aside from

the myelinating oligodendrocyte, the second being: phenotypic restriction: only mature oligodendrocytes, not the full lineage will express OATP. The questions to which this methodology is intended to apply are therefore restricted to those around MBP expression. However, once established, there is no reason why OATP, under tissue or phenotypic expression restriction, could not be applied to a wide range of other questions. For example, tracing the distribution of bone marrow derived haematopoetic or mesenchymal stem cell transplants now being widely trialled in the treatment of myelinopathies See Appendix 1.

Currently, the proposed rational for the use of haemtopoetic stem cells is the replacement of a patients autoreactive immune system with a new non-autoreactive immune system by ablating their bone marrow, and then infusing an autologous transplant isolated from the patient, pre ablation, at an early stage of haematopoietic differentiation, prior to T cell selection (Atkins *et al.* 2016). The rational for mesenchymal stem cell therapies, However, is, their potential immunomodulatory effect whereby they supress the proliferation and differentiation of the resident B and T cells (Yamout *et al.* 2010), clinical improvement in these patients was not correlated with radiological improvements therefore evidence of the fate and function of transplanted cells is very important (Akiyama *et al.* 2002). By controlling OATP expression under a promoters associated with this immunosuppressive phenotype such as the promoters for MHC-II expression (Masternak and Reith 2002), associated with the antigen presenting phenotype, atypical to MSCs but seen in these transplantation studies (Chan *et al.* 2006), or the production of certain elements of the secretome (Zappia 2005) may offer insights in to their function, fate, and utility.

When developing this method it was of great importance to have a clear characterisation of the EB-CCP lesion, and its appearance and behaviour when imaged by MRI. Its cellular characteristics are well documented, and the mechanistic insights it use has provided, have contributed significantly to the field of remyelination biology in the years since its first publication. Chapter 4 aims to document the MRI characteristics of the lesion, and in so doing has optimised the *ex vivo* imaging modality providing levels of tissue resolution comparable to those available with conventional histology. This technique has the potential to be used for the validation of the method as it is developed, in particular its use for examining post mortem tissue alongside conventional histology and ICP-MS, can be used to detect the presence of gadolinium. This will be key in overcoming some of the challenges discussed in Chapter 4.

The data presented in the final results chapter, Chapter 4.4, offer little progress towards the final methodology. However, in spite of this, its generation has occupied a significant portion of the project time thus far. Instead, However, it represents the process of trouble shooting the initial failure of the *in vivo* imaging. As is discussed in the next chapter, this is the area of the project which still requires the most work. Table 2 in Chapter 4.4 currently summarises the main potential reasons for this failure, all of which will need to be addressed. The biggest challenge in this trouble shooting process has been the lack of established positive and negative controls. Therefore, these need to be developed for each step of the protocol and validated against other techniques if a reliable methodology is to be generated. For example, without definitive evidence that mannitol is opening the blood brain barrier, the time, degree and anatomical distribution of this opening, and the free passage of gadolinium out of the vasculature and in to the ECF in the region of the lesion, any continued failure of contrast enhancement cannot be attributed to any one aspect of the protocol, but could be as a result

of failure of gadolinium entry, uptake, OATP expression, or, of contrast detection. This is one aspect of complex protocol which needs to be optimised, but every element will require similar optimisation and validation.

Once fully established this method will hopefully provide evidence for the differentiation of progenitors in to myelinating oligodendrocytes non invasively over a time course. However, in order to achieve this, significant improvements in the technique, in the quality of the characterisation carried out thus far, and in the validation of the protocol are still required.

6. Future Plans

6.1 Review of previous work plan

The scheme below summarises the planned work flow I established at the start of my PhD:

	6 months	12 months	18 months	24 months	30 months	36 months
Generation of viral vectors						
Validation of viral vectors						
Imaging endogenous OPCs						
Imaging transplanted OPCs						
Thesis write up						

***Table 10**: Initial PhD work timeline*

It is clear from the work presented in this thesis, that this plan was over ambitious. In order to fully address the questions inherent in this project and fully establish and validate the method being developed, considerably more work is required.

The main reason for the failure to achieve these previously established goals was the lack of reliable techniques with which to validate results, foremost among these was detection of gadolinium without MRI. Multiple methodologies were attempted in order to address this, the use of NMR and in vitro MRI are detailed in previous chapters. However, in addition I also attempted to make a positive control cell line which could be infected and transplanted intracranially and would take up significant amounts of contrast agent in order to refine the in vivo imaging protocols. No data is presented here as no useful data of any sort was generated from this attempt. The strategy attempted was to use C6 glioma cells as I hoped that, as these secrete a large amount of VEGF (Plate *et al.* 1993), that they would grow relatively slowly, and cause a leaky blood brain barrier (BBB) (Shivers, Edmonds, and Del Maestro 1984) therefore facilitating the passage of contrast agent in to the extracellular space. The hope being that cell

transplant numbers could be titrated down to establish the lowest detectable number of cells in vivo. However no protocol was established by which the C6 cells could be infected with the lentivirus. The challenge remains, and therefore, going forward, attempts at addressing this challenge, either with a new protocol, or with an alternative cell line will need to be considered.

The use of ICP-MS proved to be a sensitive and reliable method by which to detect gadolinium in samples and as such can be used to refine the protocols established earlier in the project. In particular, ensuring that gadolinium is not adhering to the surface of cells or samples in in vitro experiments. However, it does not offer a solution to the second challenge of establishing the cellular limits of resolution.

Achieving high resolution is a combination of adequate tissue contrast, appropriate coils, and suitable imaging sequences. These have been refined significantly since the commencement of the project. However, without positive controls for the *in vivo* model it is not possible to assess if there are truly optimised yet.

6.2 Future work plan

It is clear that the original aims of the project are still far from fruition. In order to progress this project, developments will be made on the foundations of the work detailed here, and additionally new innovations will be attempted in order to overcome some of the hurdles encountered.

The main challenges remaining can broadly be split in to four categories:

A) Refining answers to questions already addressed

B) Developing validation techniques for the methodology

C) Developing the ex vivo model (cerebellar slice culture) to be a full recapitulation of the Endogenous:Exogenous paradigm

D) Developing and refining the in vivo model to make it robust and suitable for translation

Once this has been completed its hoped that the model system can be ultimately validated by perturbing remyelination using known enhancers and inhibitors of remyelination, thus demonstrating its utility as an outcome measure in the development of new therapies and in basic research.

6.2i Refining answers to questions already addressed (A)

Chapter 4.1 aimed to address the fundamental characterisation of progenitors expressing OATP under a constitutively active promoter; PGK. This promoter was chosen by the Brindle group as they found that a weak promoter was optimal in the cell lines they used. This principle was carried forward in to the work presented here. The development of the overarching methodology may not require full or intimate characterisation, however, in the long term it would be beneficial.

Initially a more complete characterisation would include comprehensive immunohistochemical analysis. Ki 67 is a nuclear antigen associated with the cell cycle and proliferation, it is present during all phase of the cell cycle apart from quiescence (G0), counts can be used to more accurately assess the rates of proliferation in cells (Scholzen and Gerdes 2000). Assessing Ki67 counts before and over a time course following infection will provide

insights into any lag in proliferation in infected vs control, and any over all effect on progenitor proliferation rates. EdU and BrdU are synthetic DNA bases which incorporate in to S phase of the cell cycle. Both incorporate instead of thymidine and is analysed using a click reaction whereas BrdU is usually analysed using an anti-BrdU antibody (Salic and Mitchison 2008), both elucidate the number of cells entering S phase and, when examined in conjunction with EdU (or BrdU) give a more comprehensive insight in to the mitotic behaviours of cells. Propidium iodide (PI) by contrast is a viability stain which intercalates in to DNA when cell membranes are non viable. PI was not used as a measure of viability in this study as it fluoresces in the red spectrum, and would therefore be indistinguishable from cells expressing the OATP:mStrawberry construct. Trypan blue exclusion was carrier out instead, however a new transfer vector could be constructed linking the mStrawberry:E2A: fluorophore to a different gene such as GFP. PI can be used in flow cytometry and therefore larger and more reliable counts could be performed. Use of TUNEL staining, which detects DNA fragmentation; a marker of apoptosis, will be required as part of the histological analysis of post mortem tissue following transplantation when assessing the viability of cells transplanted and the effect of viral infection.

Migration assays, using transwells, may be of use in characterising the in vitro effects of OATP expression, however, they will be most important in assessing the functional capacity of cells following transplantation. As *in vivo* imaging has thus far been unsuccessful, a full exploration of the functionality of transplanted or endogenously infected cells has not been carried out. In order to do this, a two pronged approach will be taken. The first is to retain samples from the transplantation and assess them in vitro through migration, proliferation and differentiation assays. The second is to assess the post transplant/infection tissue by

immunohistochemistry, and importantly electron microscopy. In the first instance this will be done by TUNEL staining, mStrawberry, Olig2, and MBP or CNPase expression to assess cell survival in cryosectioned samples. To fully characterise the anatomical extent of the infection, and the level of cellular migration tissue clearing and light sheet microscopy with 3D reconstruction (Tomer *et al.* 2014) will be used with staining against the mStrawberry fluorophore. Functionality will also be expressed by looking at the MBP:Neurofilament ratios in CSC in infected vs controls as an intermediate step(La Fuente *et al.* 2015).

Initially these should be carried out under the PGK promoter, however, other constitutively active promoters suck as *Akt* could also be attempted (Flores *et al.* 2008).

Once a more comprehensive characterisation of cells expressing OATP under a constitutively active promoter has been carried out, the selective expression under the MBP promoter can be revisited. IHC staining in cells cultured in vitro, and in CSC show no premature expression, and no expression in GFAP positive astrocytes, although expression in microglia, though unlikely have not been ruled out, this can be carried out both in co culture and in CSCs.

Chapter 4.3 has attempted to characterise EB-CCP lesion by *ex vivo* and *in vivo* MRI. This has been largely with the intention of using the *ex vivo* MRI as an outcome or validation technique in the development of the in vivo protocol. Ideally this would be refined by using co registration of histology to MRI, which has been shown to have up to 100% matching, using 3D printed cutting cradles made bespoke for each brain (Guy *et al.* 2016).

6.2ii Developing validation techniques (B)

The mainstay of validation techniques, and positive controls developed so far have relied on the use of gadolinium standards measured by MRI, of the ex vivo high resolution MRI imaging of post mortem tissue, and the use of ICP-MS as a non magnetic method for measuring and detecting Gadolinium. Validation techniques differ from other methods used in the development of the protocol in that they are intended to be used regularly as controls or outcome measures for steps within the protocol itself, rather than just as a means by which to improve and develop the methodology.

There are three main points in the proposed protocol which I believe will require the development of specific validation methods. The first is confirming the expression of OATP in cells following their transplantation, or following endogenous infection by delivery of virus. The second is the assessment of the functionality of cells which have been transplanted or infected endogenously, this is discussed briefly in the section above as it also ties in to confirming the effect of OATP on the physiology of the cells. The third is the validation of contrast agent reaching the ECF following IV administration during in vivo imaging.

The first of these is the confirmation of expression of OATP in transplanted or endogenously infected cells. This is of paramount importance in the development of the in vivo protocol, particularly prior to successful in vivo MRI detection of contrast uptake by MBP:OATP expressing cells, as it will help identify points of failure in the protocol. Even once established it will be a vital checkpoint in confirming the gadolinium detection can be correlated with OATP expression and has not accumulated in tissue for any other reasons. I intend to use two approaches to tackle this, the first is to develop a qPCR to detect and quantify the level of OATP

expression in the brain following transplant or endogenous infection. This can be used in conjunction with a time course to establish peak OATP expression in vivo, and confirm expression in post mortem tissue. Tissue clearing techniques, as discussed above can also be applied during the development of the protocol to confirm expression, and importantly, to confirm location of cells. This is significant, when combined with co registration of MRI imaging as incorrect slice selection may yield false negative results. By developing a clearer understanding of where expressing cells migrate to (or not), better slice selection based on anatomical markers can be made, and if necessary sequences run where slice intervals overlap to ensure maximum information is gathered and positive signal not lost between slices.

The second of these, confirming functionality of transplanted and endogenously infected cells in vivo will require some of the techniques discussed above with regard to assessment of proliferation, migration, and cell death. Additionally it is important that their capacity for myelination is assessed, this will be carried out by EM. Identification of transplanted cells will by co labelling them SPIO particles (Franklin *et al.* 1999), Schwann cells carrying SPIO have been shown to form compact myelin following transplantation (Dunning *et al.* 2006). Confirmation of true function is challenging as conduction speeds would need to be assessed, however the EB-CCP lesion, does not show significant clinical impairment and conduction speeds can't be calculated for white matter tracts in the cerebellum. Full electrophysiological characterisation of OATP expressing oligodendrocytes may be beyond the scope of this project.

Validation or confirmation that gadolinium has reached the ECF following intravenous infusion, is somewhat more challenging. Opening of the blood brain barrier can be informally confirmed by increased urination (due to osmotic diuresis) in rats studied, and histologically by the

confirmation of the entry of dyes such as Evans blue in to the parenchyma. Electron microscopy changes, including the loss of tight junctions and morphological changes to endothelia cells have been described but are variably correlated with Evans blue staining, perhaps as this technique is prone to processing artefacts associated with drying which may mimic the changes associated with BBB opening (Cosolo *et al.* 1989; Rapoport 2000). A combination of histology and acute post mortem ICP-MS may be necessary if a clear confirmation of gadoxetate delivery is to be achieved.

6.2iii Developing the cerebellar slice culture model (C)

Additionally the model only recapitulates the infection of endogenous OPCs, not those transplanted in to a region of demyelination. Attempts to seed nOPCs on to CSCs were made, however all the seeded cells died (data not shown). Bin and colleagues have demonstrated that it is possible to seed cells on to organotypic slice cultures in shiverer mice (Bin *et al.* 2012), therefore work needs to be done in order to achieve this. Alterations to the protocol might include: using younger tissue, Bin and colleagues used p0 pups, whereas, based on work by Guzman and colleagues and Birgbauer and colleagues p9-p10 were used (La Fuente *et al.* 2015; Birgbauer, Rao, and Webb 2004), equally, thinner sections of 200µm (*cf.* 300µm) may improve survival, and transitioning towards a serum free media may also be required following 7-9 days recovery in vitro.

6.2iv Developing and refining the in vivo model (D)

This has been discussed briefly in Chapter 4 where it is clearly shown that there remain a number of challenges still to be overcome in order for the *in vivo* imaging technique to work.

The general approach to developing this system will be to ensure that all component parts are fully functioning before then combining them in sequence to bring together the full protocol. Even with all the individual components in place, the timescales for the protocol, and between each step, are likely to have a big impact on the success, therefore an iterative approach will be used. This iterative approach was attempted during the curse of the work presented here, but was, in hindsight, premature, as the component parts had not been fully validated. A summary of steps that require optimisation is detailed in Chapter 4.4, but they will be discussed in detail below, some have been discussed previously in this Chapter.

Cell Failure

As discussed in Chapter 4.4 and to some extent above, failure of transplanted or endogenously infected OPCs by be a potential underlying cause for the failure of the *in vivo* imaging to detect contrast agent uptake. Cell failure may result from a failure of engraftment and cell death, a failure of transplanted cells to express OATP under the constitutively active promoter, or a failure to differentiate and therefore to express OATP under the MBP promoter, or from significant levels of cell death following endogenous infection. Substantial characterisation of OATP expression in cell lines, and the data presented here has found no evidence of increased cell death or any effect on proliferation or differentiation. As discussed above, more thorough characterisation will be part of the ongoing development of the model, at each transplantation cells will be retained and kept in culture to confirm their viability and expression. By generating a qPCR against OATP a quantitative assessment of the level of expression can be made, this will allow the time point of peak expression following endogenous infection to be targeted, and will give an indication of the level of cell survival following transplantation. This

information can be used in conjunction with tissue IHC straining for markers of proliferation to give a full understanding of the OATP expressing cells behaviour.

Cell death may be influenced by a number of technical factors including transplantation medium, technique needle type, and rate and volume of transplant.

Cells may appear to fail if they are injected off target of migrate significantly. It has been shown in a number of models that transplanted progenitors and CG4 lines are able to migrate widely throughout the CNS (Franklin, Bayley, and Blakemore 1996; Franklin and Blakemore 1997; Vignais *et al.* 1993 ; Van Evercooren *et al.* 1996), therefore selecting time points at which cells are expressing, but also relatively focal around the lesion will maximise the signal available to be collected. Alternatively increased numbers of cells could be transplanted to increase the number that remain in the lesion. In conjunction with staining for other cell lines such astrocytes and microglia, and for cell cycle and viability markers surgical techniques can be refined. By using tissue clearing techniques such as CLARITY (Tomer *et al.* 2014), mStrawberry positive cells can be traced throughout the brain giving an indication of the specificity of transplantation, the degree of migration, and spread of focal infection away from the injection site. By combining antemortem MRI, with 3D printed cutting cradles it may even be possible co register the images to allow direct comparisons. This has been carried out using conventional staining (Guy *et al.* 2016), but the principles should be possible to apply to the cutting of a hydrogel converted brain. The MRI of a cleared brain, is however, unlikely to be of much use as the loss of fats will alter signals significantly, therefore comparisons will always have to be ante mortem MRI:post-mortem IHC. Ideally a system which allows antemortem MRI, post mortem MRI, and post mortem IHC could be developed, however this may be

beyond the scope of this project. With respect to optimising the I vivo imaging protocol CLARTITY will also allow accurate determination of maximal MBP expression which will be vital for the determination of time points for imaging.

Gadolinium and the BBB

As has been discussed at length above achieving passage of gadolinium across the BBB such that it is available in the ECF as a substrate for the OATP channel requires a number of factors to work in synchrony: The BBB must be permeable; there must be enough contrast agent delivered at the correct time relative to imaging that it can be taken up in to the cytosol, this has to be long enough after injection that enough has been take up, but not so long that the reversible nature of the channel has not removed a majority of the contrast; and finally the sequence needs appropriate parameters to detect the shortening: too much gadolinium may result in such short T1 readings, a standard sampling time point may not detect it causing a shim artefact. In order to optimise these systems a combination of Evans –Blue staining to characterise the BBB permeability, ICP-MS to quantify the amount of gadoxetate present, and time course analysis to calculate the peak signal post contrast injection, will be required.

In addition, the generation of a positive control may be necessary. As previously discussed an attempt at a C6 control cell line was made, but was abandoned early as it showed little promise, however, using a tumour model during development, in order to establish sequences, and timings may be very beneficial. CG4 cells are an oligodenroglial immortalised cell line which can be transplanted in to lesions in the rodent CNS (Louis *et al.* 1992; Franklin, Bayley, and Blakemore 1996; Franklin and Blakemore 1997; Chari *et al.* 2006). CG4 have the potential to form astrocytes, as well as oligodendrocytes in vivo (Franklin, Bayley, and Blakemore 1996),

however their expression of MBP can be enhanced by the administration of erythropoietin *in vitro* (Cervellini *et al.* 2013; Gyetvai *et al.* 2017), which may be particularly useful is OATP expression needs to be upregulated.

Time points

Key to the development of the in vivo imaging protocol will be establishment of correct time points. Work by S. Patrick and colleagues showed that peak signal could be collected from xenografts between 5 and 10 hours post contrast injection. In the work shown here 5 hours was chosen, however as discussed above a time curve will be required to ensure maximal signal can be collected. A time line based on the current understanding of the behaviour of OATP expressing cells and the EB-CCP lesion is laid out in Figure 42.

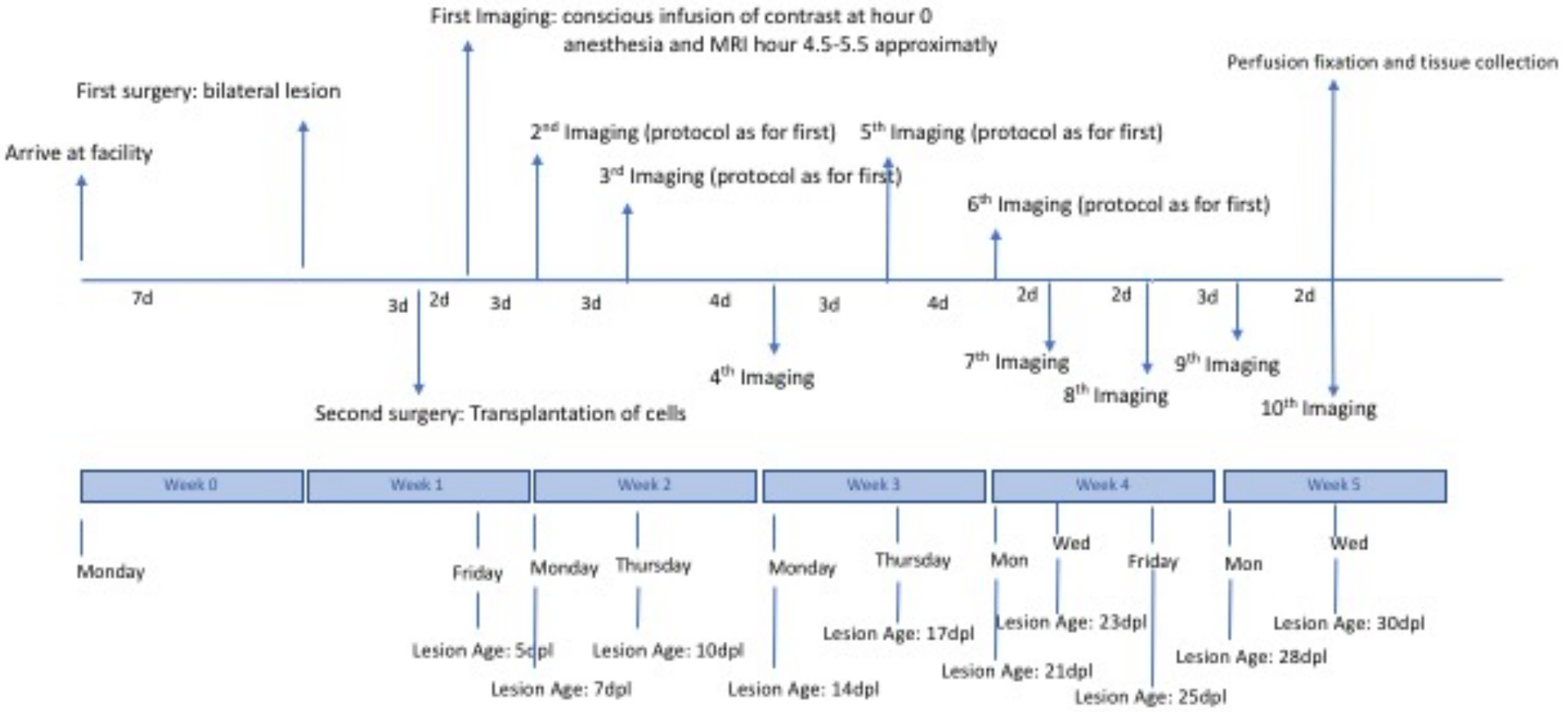

Figure 42: Example of the expected imaging timeline for in vivo studies

6.3 Maximising the potential for translation of the technique

In the short term, the development of this technique is one of *proof-of-principle*. The aim of detecting differentiating progenitor cells using a T1 weighted MRI technique has not been reported elsewhere and has the potential to be applied to many basic science questions, and in drug development. However, in the long term it may also be refined for use in man as an outcome measure for personalised medicine; it may allow differentiation of the resolution of an active lesion, from that of a truly repairing lesion in a far more rapid fashion than current methodologies permit. This may allow patients to be switched from a treatment that is not working for them, or see evidence of efficacy far more rapidly. At this stage, this is a distant goal, however, by making small adjustments to the current techniques employed, the method can be made increasingly translatable. The first of these is to alter virus delivery to use an adenoviral vector rather than a lentiviral vector, and the second is to look at the safety of the contrast agent.

6.3i Developing an AAV for systemic viral delivery

The direct injection of lentiviral vectors into lesions is valuable for establishing proof-of-principle, however it clearly has limitations in terms of its translational value where there would 1) be a degree of morbidity associated with delivery, and 2) would mean that only a very limited number of the many lesions with the MS brain lesions could be assessed. It is therefore necessary to explore ways in which OATP could be more widely distributed through the brain. Additionally intracranial injection, carries with it inherent risks such as bleeding, infection, and the risks associated with any anaesthesia, all of which are better avoided, particularly infection

which can lead to pyrexia which can cause Uhrthoff's phenomena which is associated with a worsening of neurological symptoms (Frohman *et al.* 2013). A minimally invasive alternative to the intralesional injection of virus would be the recently developed neurotropic adeno associated viral vector which can be delivered systemically. As AAVs are single stranded DNA viruses that are non-integrating and non-replicating, they are an attractive vector for gene therapy (Bennett *et al.* 2016). There are multiple strains of AAV, each that have viral capsid proteins that can efficiently target specific cell-types with the recently developed AAV-PHPeB is able to readily infect the CNS (Chan *et al.* 2017).

Systemic AAV administration would allow for large-scale gene transfer across the CNS. However, most systemically administered AAVs inefficiently cross the blood brain barrier and very high titres of AAVs are required. To overcome these limitations of AAV vectors, AAV particles have been generated with randomly modified capsid protein sequences that cross the blood brain barrier and target the cells of the CNS with high specificity (Chan *et al.* 2017). As the AAV is highly specific for the CNS, it is possible to efficiently target the CNS with viral titers one thousand times lower than previously reported. In particular an AAV that express GFP under the MBP promoter, has been shown to be able to label up to 70% of oligodendrocytes across the CNS (Chan *et al.* 2017).

Using this new vector I would be able to develop both a focal and systemic model in tandem, preliminary work by colleagues in the Franklin group has shown show that ≥70% of CNS progenitors in the rodent brain are infected with this AAV 21 days-post intravenous infusion.

6.3ii Improving safety of Gadolinium chelators

Primovist is Gadolinium containing MRI contrast agent manafactored by Bayer for use in imaging of hepatic carcinomas. Hepatic carcinomas show upregulation of OATP channels, but can appear relatively homogenous on standard imaging, contrast studies however, are more elucidatory as Primovist accumulates in the neoplasia making its assessment and response to treatment far easier to monitor. However Gadolinium is an inherently toxic element, and its use in pharmaceutical agents is only made possible by its chelation. Chelators can be unstable, and the central ion can drop out of the chemical encasement becoming free in the body. Accumulation of gadolinium has been seen in post mortem samples in the basal ganglia, and elsewhere in the brain (Kanda *et al.* 2015). There are, therefore clear safety concerns around its use. Although no adverse effects have been reported due to its accumulation in the CNS, and there is no evidence of acute neurotoxicity reported (Olchowy *et al.* 2017), however its use is known to be associated with nephrogenic systemic fibrosis (Rogosnitzky and Branch 2016). The propensity of Gd3+ to drop out of a chelator varied with the chelator chosen. Linear ionic chelators, such as are used in Primovist, are thought to be most prone to this, whereas the macrocyclic chelators, such as those found in ProHance (Bracco Diagnostics) have lower dissociation constants, and are therefore less likely to undergo transmetalation. If, however, evidence does arise to suggest that accumulation is detrimental efforts may need to be made to alter the chemistry of the OATP channel such that macrocyclic chelators can be transported by it.

The methodology being developed here, and the techniques used in its development, are applicable questions over the safety of long term accumulation of Gd3+ in glial cells, and may

therefore go some way to elucidating the safety profile of gadolinium as a long term imaging agent.

6.4 Use of the final imaging protocol

Once developed and fully functional, it's is hoped that the methodology whose early development is detailed here will be capable of non invasively identifying the expression of MBP, that this will be correlated to remyelination, and that serial imaging will possible to monitor the repair process longitudinally. In order to fully validate the technique as a tool for use in remyelination biology it will be used as outcome measure in the assessment of known modulators of remyelination whose effects are well characterized by histology. Up regulators of remyelination including Retinoid X-Receptor Gamma agonists such as 9-cis-retinoic acid and or Bexarotene (Huang *et al.* 2011; Huang *et al.* 2010), and antimuscarinics like Clemastine (Deshmukh *et al.* 2013; Mei *et al.* 2014), and down regulators of the remyelination response, such as using aged rodents in the model (Sim *et al.* 2002). I would expect that the histologically demonstrated enhancement or retardation of remyelination should be mirrored by a post contrast onset of T1 shortening in the region of the lesion location. By testing the method in treated vs control in the against the EB-CCP lesion we hope to demonstrate its utility in drug development and as a non invasive measure of remyelination.

6.5 Future work flow

This chapter hopes to lay out a plan of the experimental work and development that will be required in order to progress towards the final goal of generating an in vivo tool for imaging

remyelination. Below is a proposed work flow which lays out the remaining work over a three year period. It is hoped that by then end of this period the tool will be functional and validated.

Based upon the challenges identified in this chapter a hierarchy of priorities can be identified; the most pressing issue is to unequivocally confirm that gadolinium contrast agent is able to cross the blood brain barrier at an appropriate time point and in sufficient quantities , or that the blood brain barrier can be manipulated (for example with mannitol) such that it can be opened at an appropriate time point. Once this has been established , ways of increasing the amount of signal captured can be worked on. These might include increasing the number of cells transplanted, increasing the amount of gadolinium administered, using a more dorsal lesion closer to surface coils to reduce signal loss, using a model with greater area for remyelination like the *shiverer* mouse, or changing technical aspects such as MRI coils or sequences. Table 11 below summarises potential remaining challenges and their solutions, and Table 12 lays these out in terms of their relative priority.

	6months	12months	18months	24months	30months	36months
A: refinements of current work						
B: validation of OATP expression in vivo						
B: validation of transplanted cells / endogenously infected cells viability						
B: Validation of BBB opening, and Gd crossing in to the ECF						
C: Generating the cell transplant model in cerebellar slice cultures						
D: Refinement of In vivo imaging						
Generation of AAV						
Perturbation of CSC model and in vivo model using modifiers of remyelination						

Table 11: Proposed work flow diagram detailing the work remaining on the project in order to bring it to fruition.

A **Refining answers to questions already addressed**		**B** **Developing validation techniques for steps in the protocol**		**C** **Developing the organotypic slice culture model**		**D** **Refining the *in vivo* imaging method and protocol**	
Question	*Answer*	*Question*	*Answer*	*Question*	*Answer*	*Question*	*Answer*
1. Does OATP expression affect OPC/Oligodendrocyte proliferation, differentiation, migration, or survival	Ki67 EdU TuNEL Migration Assays Propidium Iodide	1. Validation of OATP expression in vivo	qPCR for OATP gene- 'genotype' tissue following transplant/infection in vivo transplants and infection followed by tissue clearing + time course viral titration for in vivo infection followed by tissue clearing and conventional sectioning for markers of inflammation	1. Can oligodendrocyte progenitors be transplanted in the CSC, engraft, and remyelinate	Develop organotypic technique for transplant. IHC time course gadolinium incubation MRI of slices ICP-MS of slices	1. Can cells expressing OATP be see by in vivo imaging	Correct number of cells imaged at the right time point, with the right contrast agent protocol, with the optimal imaging protocol
2. Does the MBP promoter restrict expression	Co cultures to rule out aberrant/off target expression Extended time course and quantification of OATP:MBP	2. Validation of transplanted cell viability	Retain samples for immediate fixation and staining following transplantation Retain samples for culture – demonstrate they remain viable in			2. Can the model be perturbated with modulators of remyelination in order to demonstrate real utility as a non invasive outcome measure	Once established and functional, manipulate the lesion using molecules like bexatrotene or clemastine.

	expression and in vitro and CSC		culture by staining a time course				
3. Can OATP:virus infect OPCs	Improve virus manufacture and concentration to achieve high viral titres to refine all in vitro and in vivo protocols	3. Validation of in vivo contrast administration	*Develop a technique which can be carried out during each experiment to confirm that Gd has crossed the BBB – for example always have a sentinel animal with an intracranial xenograft. Always sacrifice one animal at the imaging time point and send for ICPMS for gadolinium detection*				
4. Can the EB-CCP lesion be characterised by MRI	Develop co registration of histology and MRI using 3d printed cutting cradles						

Table 12: Summary table of major outstanding questions and their potential solutions

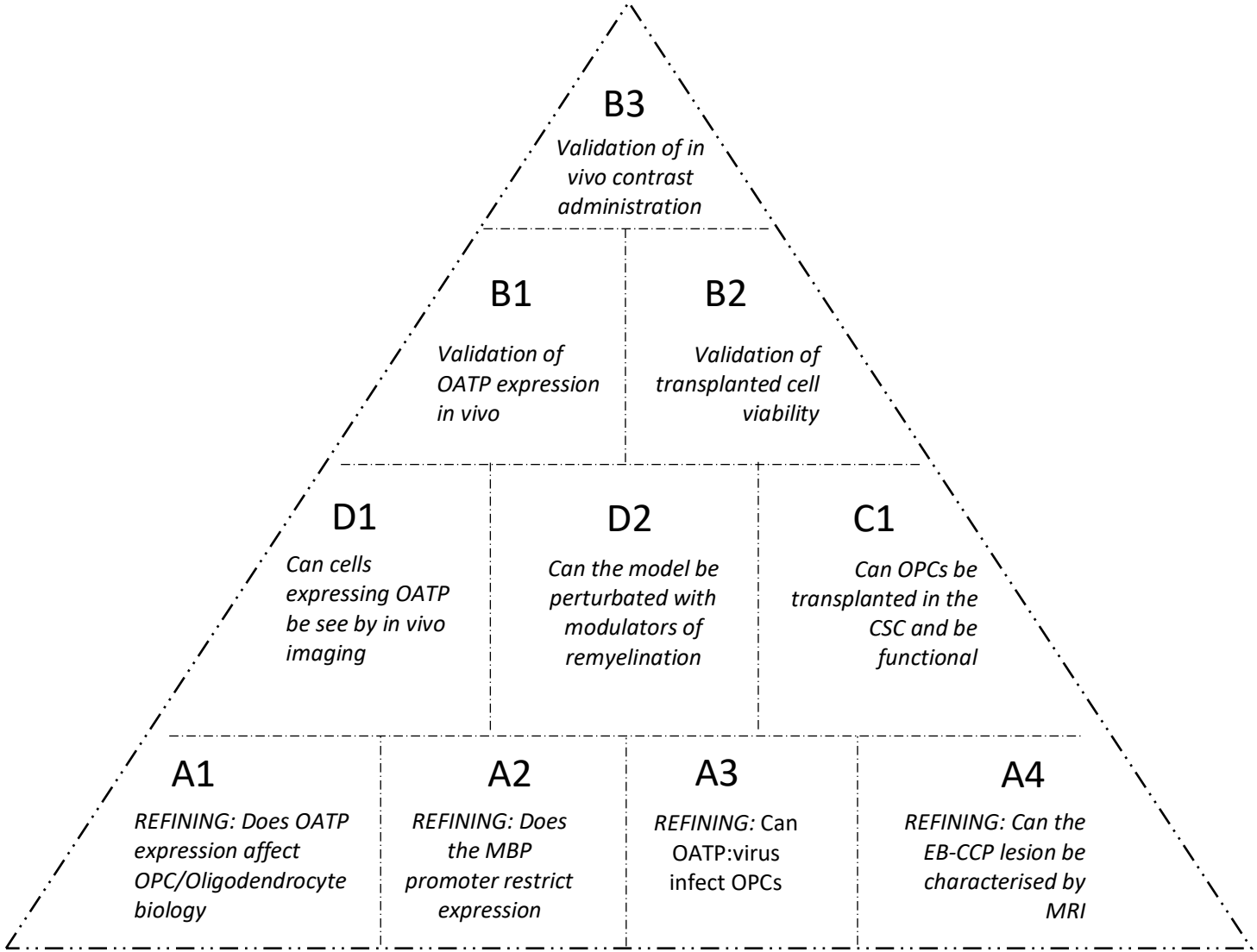

Table 13: Hierarchy of Challenges to be Addressed. Based upon the work in this thesis and on the assessment of chapter 6 in particular, it is apparent that establishing if gadolinium can cross the BBB is the most important next step in developing this work. This is followed by developing the appropriate validation techniques. Following this it is likely that full in vivo imaging experiments can be attempted, with tier 3 and 4 questions being addressed simultaneously to in vivo imaging.

7. Conclusions

This thesis forms the basis for the development of a completely new technique for the assessment and study of progenitor cells in vivo. However, the methodology has the potential to be applied to any system in biology. By using cell line specific promotor sequences Oatp expression can be restricted even where viral infection cannot be, and allows expression to be linked to functional states. Although modelled here in regenerative neurobiology, any cellular state which is sustained enough to be longitudinally imaged could be traced.

There is significant work still to do in order to fully develop and most importantly, to validate this technique, however if progress continues to be made in this vein, it is hoped that this could represent direct, *in vivo*, evidence for differentiation of progenitors; specifically the formation of new myelin, and be a valuable tool for the drug development and clinical trials community alike.

References

Absinta, Martina, Pascal Sati, and Daniel S Reich. 2016. “Advanced MRI and Staging of Multiple Sclerosis Lesions.” *Nature Publishing Group* 12 (6). Nature Publishing Group: 358–68. doi:10.1038/nrneurol.2016.59.

Adamo, A M, P M Paez, O E Escobar Cabrera, M Wolfson, P G Franco, J M Pasquini, and E F Soto. 2006. “Remyelination After Cuprizone-Induced Demyelination in the Rat Is Stimulated by Apotransferrin..” *Experimental Neurology* 198 (2): 519–29. doi:10.1016/j.expneurol.2005.12.027.

Aggarwal, Shweta, Larisa Yurlova, and Mikael Simons. 2011. “Central Nervous System Myelin:Structure, Synthesis and Assembly.” *Trends in Cell Biology* 21 (10). Elsevier Ltd: 585–93. doi:10.1016/j.tcb.2011.06.004.

Aggarwal S, Snaidero N, Paehler G, Frey S, Sanchez P, Zweckstetter M, Janshoff A, Schneider A, Weil MT, Schaap IA, Goerlich D, Simons M. 2013. “Myelin membrane assembly is driven by a phase transition of myelin basic proteins into a cohesive protein meshwork”. *PLoS Biology* 11(6)doi: 10.1371/journal.pbio.1001577

Aguirre, Adan, Jeff L Dupree, J M Mangin, and Vittorio Gallo. 2007. “A Functional Role for EGFR Signaling in Myelination and Remyelination..” *Nature Neuroscience* 10 (8). Nature Publishing Group: 990–1002. doi:10.1038/nn1938.

Ahlgren, Cecilia, Anders Odén, and Jan Lycke. 2014. “High Nationwide Incidence of Multiple Sclerosis in Sweden.” Edited by Jerson Laks. *PLoS ONE* 9 (9): e108599–6. doi:10.1371/journal.pone.0108599.

Ahn, Byeong-Cheol, Natesh Parashurama, Manish Patel, Keren Ziv, Srabani Bhaumik, Shahriar Shah Yaghoubi, Ramasamy Paulmurugan, and Sanjiv Sam Gambhir. 2014. “Noninvasive Reporter Gene Imaging of Human Oct4 (Pluripotency) Dynamics During the Differentiation of Embryonic Stem Cells in Living Subjects.” *Molecular Imaging and Biology* 16 (6): 865–76. doi:10.1148/radiology.213.3.r99dc14866.

Ainger K, Avossa D, Morgan F, Hill SJ, Barry C, Barbarese E, Carson JH. 1993. “Transport and localization of exogenous myelin basic protein mRNA microinjected into oligodendrocytes.” *Journal of Cell Biology* 123: 431–441.

Airas, L, J Niemela, G Yegutkin, and S Jalkanen. 2007. “Mechanism of Action of IFN-Beta in the Treatment of Multiple Sclerosis: a Special Reference to CD73 and Adenosine.” *Annals of the New York Academy of Sciences* 1110 (1): 641–48. doi:10.1196/annals.1423.067

Akiyama, Yukinori, Christine Radtke, Osamu Honmou, and Jeffery D Kocsis. 2002. “Remyelination of the Spinal Cord Following Intravenous Delivery of Bone Marrow Cells..” *Glia* 39 (3): 229–36. doi:10.1002/glia.10102.

Alfke, Stöppler, Nocken, Heverhagen, Kleb, Czubayko, Jochen Klose (2003) "In Vitro MR Imaging of Regulated Gene Expression" ***Radiology*** 228;2 doi.org/10.1148/radiol.2282012006

All, Angelo H, Faith A Bazley, Siddharth Gupta, Nikta Pashai, Charles Hu, Amir Pourmorteza, and Candace Kerr. 2012. "Human Embryonic Stem Cell-Derived Oligodendrocyte Progenitors Aid in Functional Recovery of Sensory Pathways Following Contusive Spinal Cord Injury.." *PLoS ONE* 7 (10). Public Library of Science: e47645. doi:10.1371/journal.pone.0047645.

Allaman, Igor, Mireille Bélanger, and Pierre J Magistretti. 2011. "Astrocyte-Neuron Metabolic Relationships: for Better and for Worse.." *Trends in Neurosciences* 34 (2): 76–87. doi:10.1016/j.tins.2010.12.001.

Alonso-Ortiz, Eva, Ives R Levesque, and G Bruce Pike. 2014. "MRI-Based Myelin Water Imaging: a Technical Review." *Magnetic Resonance in Medicine* 73 (1): 70–81. doi:10.1016/S0301-0082(98)00083-5.

Amemori, Takashi, Nataliya Romanyuk, Pavla Jendelova, Vit Herynek, Karolina Turnovcova, Pavel Prochazka, Miroslava Kapcalova, Graham Cocks, Jack Price, and Eva Sykova. 2013. "Human Conditionally Immortalized Neural Stem Cells Improve Locomotor Function After Spinal Cord Injury in the Rat.." *Stem Cell Research & Therapy* 4 (3). BioMed Central: 68. doi:10.1186/scrt219.

Anderson, Emma S, Carl Bjartmar, Gunilla Westermark, and Claes Hildebrand. 1999. "Molecular Heterogeneity of Oligodendrocytes in Chicken White Matter." *Glia* 27 (1). Wiley-Blackwell: 15–21. doi:10.1002/(SICI)1098-1136(199907)27:1<15::AID-GLIA2>3.0.CO;2-I.

Arnett, Heather A, Stephen P J Fancy, John A Alberta, Chao Zhao, Sheila R Plant, Sovann Kaing, Cedric S Raine, D., H Rowitch, Robin J M Franklin, and Charles D Stiles. 2004. "bHLH Transcription Factor Olig1 Is Required to Repair Demyelinated Lesions in the CNS.." *Science* 306 (5704): 2111–15. doi:10.1126/science.1103709.

Atkins, H L, M Bowman, D Allan, G Anstee, D L Arnold, A Bar-Or, I Bence-Bruckler, et al. 2016. "Immunoablation and Autologous Haemopoietic Stem-Cell Transplantation for Aggressive Multiple Sclerosis: a Multicentre Single-Group Phase 2 Trial." *The Lancet* 388 (10044). Elsevier Ltd: 576–85. doi:10.1016/S0140-6736(16)30169-6.

Aubourg, P. 1993. "The Leukodystrophies: a Window to Myelin.." *Nature Genetics* 5 (2). Nature Publishing Group: 105–6. doi:10.1038/ng1093-105.

Badr, Christian E, and Bakhos A Tannous. 2011. "Bioluminescence Imaging: Progress and Applications." *Trends in Biotechnology* 29 (12). Elsevier Ltd: 624–33. doi:10.1016/j.tibtech.2011.06.010.

Bagnato, Francesca, Neal Jeffries, Nancy D Richert, Roger D Stone, Joan M Ohayon, Henry F McFarland, and Joseph A Frank. 2003. “Evolution of T1 Black Holes in Patients with Multiple Sclerosis Imaged Monthly for 4 Years..” *Brain* 126 (Pt 8): 1782–89. doi:10.1093/brain/awg182.

Bakhti M, Aggarwal S, Simons M. 2013. “Myelin architecture: Zippering membranes tightly together”. Cellular and Molecular Life Sciences 71: 1265–1277. doi: 10.1007/s00018-013-1492-0

Bansal, Rashmi, and S E Pfeiffer. 1997. “FGF-2 Converts Mature Oligodendrocytes to a Novel Phenotype.” *Journal of Neuroscience Research* 50 (2): 215–28. doi:10.1002/(sici)1097-4547(19971015)50:2<215::aid-jnr10>3.3.co;2-8.

Barkhof, Frederik, Wolfgang Brück, Corline J A De Groot, Elisabeth Bergers, Sandra Hulshof, Jeroen Geurts, Chris H Polman, and Paul van der Valk. 2003. “Remyelinated Lesions in Multiple Sclerosis: Magnetic Resonance Image Appearance..” *Archives of Neurology* 60 (8). American Medical Association: 1073–81. doi:10.1001/archneur.60.8.1073

Barres, B A, I K Hart, H S Coles, J F Burne, J T Voyvodic, W D Richardson, and M C Raff. 1992. “Cell Death and Control of Cell Survival in the Oligodendrocyte Lineage..” *Cell* 70 (1): 31–46.

Barres BA, Raff MC. 1994. “Control of oligodendrocyte number in the developing rat optic nerve.” *Neuron* 12:935–42.

Barres BA, Raff MC. 1999. “Axonal control of oligodendrocyte development”. *Journal of Cell Biology* 147: 1123–1128.

Bartelle, Benjamin B, Kamila U Szulc, Giselle A Suero-Abreu, Joe J Rodriguez, and Daniel H Turnbull. 2013. “Divalent Metal Transporter, DMT1: a Novel MRI Reporter Protein..” *Magnetic Resonance in Medicine* 70 (3). Wiley-Blackwell: 842–50. doi:10.1002/mrm.24509.

Baumann, N, and D Pham-Dinh. 2001. “Biology of Oligodendrocyte and Myelin in the Mammalian Central Nervous System..” *Physiological Reviews* 81 (2): 871–927. doi:10.1152/physrev.2001.81.2.871.

Bennett, Jean, Jennifer Wellman, Kathleen A Marshall, Sarah McCague, Manzar Ashtari, Julie DiStefano-Pappas, Okan U Elci, et al. 2016. “Safety and Durability of Effect of Contralateral-Eye Administration of AAV2 Gene Therapy in Patients with Childhood-Onset Blindness Caused by RPE65 Mutations: a Follow-on Phase 1 Trial..” *Lancet (London, England)* 388 (10045): 661–72. doi:10.1016/S0140-6736(16)30371-3.

Berndt, J A, J G Kim, and L D Hudson. 2001. “Identification of Cis-Regulatory Elementins the Myelin Proteolipid Protein (PLP)Gene*,” June, 1–8.

Bin, Jenea M, Soo Yuen Leong, Sarah-Jane Bull, Jack P Antel, and Timothy E Kennedy. 2012. "Oligodendrocyte Precursor Cell Transplantation Into Organotypic Cerebellar Shiverer Slices: a Model to Study Myelination and Myelin Maintenance." Edited by Martin Stangel. *PLoS ONE* 7 (7). Public Library of Science: e41237–38. doi:10.1371/journal.pone.0041237.

Birgbauer, Eric, Tadimeti S Rao, and Michael Webb. 2004a. "Lysolecithin Induces Demyelination in Vitro in a Cerebellar Slice Culture System." *Journal of Neuroscience Research* 78 (2): 157–66. doi:10.1002/jnr.20248.

Birgbauer, Eric, Tadimeti S Rao, and Michael Webb. 2004b. "Lysolecithin Induces Demyelination in Vitro in a Cerebellar Slice Culture System." *Journal of Neuroscience Research* 78 (2): 157–66. doi:10.1002/jnr.20248.

Bitsch, Andreas, Tanja Kuhlmann, Christine Stadelmann, Hans Lassmann, Claudia Lucchinetti, and Wolfgang Brück. 2001. "A Longitudinal MRI Study of Histopathologically Defined Hypointense Multiple Sclerosis Lesions." *Annals of Neurology* 49 (6). Wiley-Blackwell: 793–96. doi:10.1002/ana.1053.

Blakemore, W F. 1972. "Observations on Oligodendrocyte Degeneration, the Resolution of Status Spongiosus and Remyelination in Cuprizone Intoxication in Mice.." *Journal of Neurocytology* 1 (4): 413–26.

Blakemore, W F. 1974. "Pattern of Remyelnation in the CNS." *Nature* 249 (June): 1–2.

Blakemore, W F, and K-A Irvine. 2008. "Endogenous or Exogenous Oligodendrocytes for Remyelination." *Journal of the Neurological Sciences* 265 (1-2): 43–46. doi:10.1016/j.jns.2007.08.004.

Blakemore, W F, and R C Patterson. 1973. "Suppression of Remyelination in the CNS by X-Irradiation," July, 1–9.

Blakemore, W F, and R J M Franklin. 2008. "Remyelination in Experimental Models of Toxin-Induced Demyelination.." *Current Topics in Microbiology and Immunology* 318: 193–212.

Bloch F. 1946. "Nuclear induction." *Physics Review* 1946;70:460–474.

Bodini, Benedetta, Mattia Veronese, Daniel García-Lorenzo, Marco Battaglini, Emilie Poirion, Audrey Chardain, Leorah Freeman, et al. 2016. "Dynamic Imaging of Individual Remyelination Profiles in Multiple Sclerosis.." *Annals of Neurology* 79 (5). Wiley-Blackwell: 726–38. doi:10.1002/ana.24620.

Boretius, Susann, Lars Kasper, Roland Tammer, Thomas Michaelis, and Jens Frahm. 2009. "MRI of Cellular Layers in Mouse Brain in Vivo." *NeuroImage* 47 (4). Elsevier Inc.: 1252–60. doi:10.1016/j.neuroimage.2009.05.095.

Bottai, Daniele, Daniela Cigognini, Laura Madaschi, Raffaella Adami, Emanuela Nicora, Mauro Menarini, Anna Maria Di Giulio, and Alfredo Gorio. 2010. “Embryonic Stem Cells Promote Motor Recovery and Affect Inflammatory Cell Infiltration in Spinal Cord Injured Mice..” *Experimental Neurology* 223 (2): 452–63. doi:10.1016/j.expneurol.2010.01.010.

Brex, P A, O Ciccarelli, J I O'Riodan, M Sailer, A J Thompson, and D.,H., Miller. 2002. “Longitudinal MR Imaging and Clinical Studies of Cohorts Presenting with Clinically Isolated Syndromes Suggestive of Multiple Sclerosis. ,” January, 1–7.

Brüstle, O, K N Jones, R D Learish, K Karram, K Choudhary, O D Wiestler, I D Duncan, and R D McKay. 1999. “Embryonic Stem Cell-Derived Glial Precursors: a Source of Myelinating Transplants..” *Science* 285 (5428): 754–56.

Buckley, C E, P Goldsmith, and R J M Franklin. 2008. “Zebrafish Myelination: a Transparent Model for Remyelination?.” *Disease Models and Mechanisms* 1 (4-5): 221–28. doi:10.1242/dmm.001248.

Bulte, J W M, S C Zhang, P van Gelderen, V Herynek, E K Jordan, I D Duncan, and J A Frank. 1999. “Neurotransplantation of Magnetically Labeled Oligodendrocyte Progenitors: Magnetic Resonance Tracking of Cell Migration and Myelination.” *Proceedings of the National Academy of Sciences* 96 (26). National Academy of Sciences: 15256–61. doi:10.1073/pnas.96.26.15256.

Butt AM, Berry M. 2000. “Oligodendrocytes and the control of myelination in vivo: New insights from the rat anterior medullary velum.” *Journal of Neuroscience Research* 59: 477–488.

Cai, Jun, Yingchuan Qi, Xuemei Hu, Min Tan, Zijing Liu, Jianshe Zhang, Qun Li, Maike Sander, and Mengsheng Qiu. 2005. “Generation of Oligodendrocyte Precursor Cells From Mouse Dorsal Spinal Cord Independent of Nkx6 Regulation and Shh Signaling.” *Neuron* 45 (1): 41–53. doi:10.1016/j.neuron.2004.12.028.

Calver AR, Hall AC, Yu WP, Walsh FS, Heath JK, Betsholtz C, Richardson WD. 1998. “Oligodendrocyte population dynamics and the role of PDGF in vivo”. *Neuron* 20:869–82.

Carlton, William W. 1967. “Studies on the Induction of Hydrocephalus and Spongy Degeneration by Cuprizone Feeding and Attempts to Antidote the Toxicity.” *Life Sciences* 6 (1): 11–19. doi:10.1016/0024-3205(67)90356-6.

Carroll, W M, and A R Jennings. 1994. “Early Recruitment of Oligodendrocyte Precursors in CNS Demyelination.” *Brain*, May, 1–16.

Cassoli, Juliana Silva, Paul C Guest, Berend Malchow, Andrea Schmitt, Peter Falkai, and Daniel Martins-de-Souza. 2015. “Disturbed Macro-Connectivity in Schizophrenia Linked to Oligodendrocyte Dysfunction: From Structural Findings to Molecules.” *Nature Publishing Group*, September. Nature Publishing Group, 1–10. doi:10.1038/npjschz.2015.34.

Cercignani, Mara, Mark R Symms, Klaus Schmierer, Philip A Boulby, Daniel J Tozer, Maria Ron, Paul S Tofts, and Gareth J Barker. 2005. “Three-Dimensional Quantitative Magnetisation Transfer Imaging of the Human Brain.” *NeuroImage* 27 (2): 436–41. doi:10.1016/j.neuroimage.2005.04.031.

Cervellini, Ilaria, Alexander Annenkov, Thomas Brenton, Yuti Chernajovsky, Pietro Ghezzi, and Manuela Mengozzi. 2013. “Erythropoietin (EPO) Increases Myelin Gene Expression in CG4 Oligodendrocyte Cells Through the Classical EPO Receptor..” *Molecular Medicine* 19 (August): 223–29. doi:10.2119/molmed.2013.00013.

Chalfie, M, Y Tu, G Euskirchen, W W Ward, and D C Prashert. 1994. “Green Fluorescent Protein as a Marker for Gene Expression.” *Science* 263 (February): 1–5.

Chan, Jennifer L, Katherine C Tang, Anoop P Patel, Larissa M Bonilla, Nicola Pierobon, Nicholas M Ponzio, and Pranela Rameshwar. 2006. “Antigen-Presenting Property of Mesenchymal Stem Cells Occurs During a Narrow Window at Low Levels of Interferon-Gamma..” *Blood* 107 (12): 4817–24. doi:10.1182/blood-2006-01-0057.

Chan, Ken Y, Min J Jang, Bryan B Yoo, Alon Greenbaum, Namita Ravi, Wei-Li Wu, Luis Sánchez-Guardado, et al. 2017. “Engineered AAVs for Efficient Noninvasive Gene Delivery to the Central and Peripheral Nervous Systems.” *Nature Neuroscience* 20 (8): 1172–79. doi:10.1038/nn.4107.

Chari, Divya M, Jennifer M Gilson, Robin J M Franklin, and William F Blakemore. 2006. “Oligodendrocyte Progenitor Cell (OPC) Transplantation Is Unlikely to Offer a Means of Preventing X-Irradiation Induced Damage in the CNS.” *Experimental Neurology* 198 (1): 145–53. doi:10.1016/j.expneurol.2005.11.023.

Chen, J J, F Carletti, V Young, D Mckean, and G Quaghebeur. 2016. “MRI Differential Diagnosis of Suspected Multiple Sclerosis.” *Clinical Radiology* 71 (9). The Royal College of Radiologists: 815–27. doi:10.1016/j.crad.2016.05.010.

Chen, Jacqueline T, D Louis Collins, Harold L Atkins, Mark S Freedman, Douglas L Arnold, the Canadian MS/BMT Study Group. 2008. “Magnetization Transfer Ratio Evolution with Demyelination and Remyelination in Multiple Sclerosis Lesions.” *Annals of Neurology* 63 (2): 254–62. doi:10.1212/WNL.51.4.1150.

Chmierer K, Parkes HG, So PW. 2009. “Direct visualization of remyelination in multiple sclerosis using T2-weighted high-field MRI.” *Neurology*. 72(5):472.

Chong, S Y C, S S Rosenberg, Stephen P J Fancy, Chao Zhao, Y A Shen, A T Hahn, A W McGee, et al. 2012. “Neurite Outgrowth Inhibitor Nogo-a Establishes Spatial Segregation and Extent of Oligodendrocyte Myelination.” *Proceedings of the National Academy of Sciences* 109 (4): 1299–1304. doi:10.1073/pnas.1113540109/-/DCSupplemental/pnas.201113540SI.pdf.

Chung, Won-Suk, Laura E Clarke, Gordon X Wang, Benjamin K Stafford, Alexander Sher, Chandrani Chakraborty, Julia Joung, et al. 2013. “Astrocytes Mediate Synapse Elimination Through MEGF10 and MERTK Pathways.” *Nature* 504 (7480): 394–400. doi:10.1016/j.neuron.2009.09.021.

Ciccarelli, Olga, Elisabetta Giugni, Andrea Paolillo, Caterina Mainero, Claudio Gasperini, Stefano Bastianello, and Carlo Pozzilli. 1999. “Magnetic Resonance Outcome of New Enhancing Lesions in Patients with Relapsing-Remitting Multiple Sclerosis.” *European Journal of Neurology* 6 (4). Wiley/Blackwell (10.1111): 455–59. doi:10.1046/j.1468-1331.1999.640455.x.

Cizkova, D, M Cizek, M Nagyova, L Slovinska, I Novotna, S Jergova, J Radonak, J Hlucilova, and I Vanicky. 2009. “Enrichment of Rat Oligodendrocyte Progenitor Cells by Magnetic Cell Sorting.” *Journal of Neuroscience Methods* 184 (1): 88–94. doi:10.1016/j.jneumeth.2009.07.030.

Coetzee, T, N Fujita, J Dupree, R Shi, A Blight, K Suzuki, and B Popko. 1996. “Myelination in the Absence of Galactocerebroside and Sulfatide: Normal Structure with Abnormal Function and Regional Instability..” *Cell* 86 (2): 209–19.

Cohen, Batya, Hagit Dafni, Gila Meir, Alon Harmelin, and Michal Neeman. 2005. “Ferritin as an Endogenous MRI Reporter for Noninvasive Imaging of Gene Expression in C6 Glioma Tumors.” ***Neoplasia*** 7 (2): 109–17. doi:10.1593/neo.04436.

Cohen, Mikhal E, Naser Muja, Nina Fainstein, Jeff W M Bulte, and Tamir Ben-Hur. 2009. “Conserved Fate and Function of Ferumoxides-Labeled Neural Precursor Cells in Vitro and in Vivo.” *Journal of Neuroscience Research* 18: NA–NA. doi:10.1002/jnr.22277.

Coles, Alasdair J. 2012. “Alemtuzumab Therapy for Multiple Sclerosis.” *Neurotherapeutics* 10 (1): 29–33. doi:10.1007/s13311-012-0159-0.

Colman DR, Kreibich G, Frey AB, Sabatini DD. 1982. “Synthesis and incorporation of myelin polypeptides into CNS myelin”. *Journal of Cell Biology* 95: 598–608.

Compston, Alastair, and Alasdair Coles. 2002. “Multiple Sclerosis.” *The Lancet* 359 (9313): 1221–31. doi:10.1016/S0140-6736(02)08220-X.

Compston, Alastair, and Alasdair Coles. 2008. “Multiple Sclerosis.” *The Lancet* 372 (9648). Elsevier Ltd: 1502–17. doi:10.1016/S0140-6736(08)61620-7.

Cosolo, W C, P Martinello, W J Louis, and N Christophidis. 1989. “Blood-Brain Barrier Disruption Using Mannitol: Time Course and Electron Microscopy Studies..” *The American Journal of Physiology* 256 (2 Pt 2): R443–47. doi:10.1152/ajpregu.1989.256.2.R443.

Crawford, A H, C Chambers, and R J M Franklin. 2013. “Remyelination: the True Regeneration of the Central Nervous System.” *Journal of Comparative Pathology* 149 (2-3): 242–54. doi:10.1016/j.jcpa.2013.05.004.

Crawford, A H, J H Stockley, R B Tripathi, W D Richardson, and R J M Franklin. 2014. "Experimental Neurology." *Experimental Neurology* 260 (C). Elsevier Inc.: 50–55. doi:10.1016/j.expneurol.2014.04.027.

Cui, Weina, Li Liu, Vikram D Kodibagkar, and Ralph P Mason. 2010. "S-Gal®, a Novel 1H MRI Reporter for B-Galactosidase." *Magnetic Resonance in Medicine* 64 (1). Wiley-Blackwell: 65–71. doi:10.1002/mrm.22400.

Czopka T, ffrench-Constant C, Lyons DA. 2013. "Individual oligodendrocytes have only a few hours in which to generate new myelin sheaths in vivo." *Development* 25:599–609.

Dashevsky, Brittany Z, Timothy D'Alfonso, Elizabeth J Sutton, Ashley Giambrone, Eric Aronowitz, Elizabeth A Morris, Krishna Juluru, and Douglas J Ballon. 2015. "The Potential of High Resolution Magnetic Resonance Microscopy in the Pathologic Analysis of Resected Breast and Lymph Tissue." *Scientific Reports*, November. Nature Publishing Group, 1–8. doi:10.1038/srep17435.

Davies, Jeannette E, and Robert H Miller. 2001. "Local Sonic Hedgehog Signaling Regulates Oligodendrocyte Precursor Appearance in Multiple Ventricular Zone Domains in the Chick Metencephalon." *Developmental Biology* 233 (2): 513–25. doi:10.1006/dbio.2001.0224.

De Stefano, Nicola, Maria L Bartolozzi, Leonello Guidi, Maria L Stromillo, and Antonio Federico. 2005. "Magnetic Resonance Spectroscopy as a Measure of Brain Damage in Multiple Sclerosis." *Journal of the Neurological Sciences* 233 (1-2): 203–8. doi:10.1016/j.jns.2005.03.018.

de Wet, J R, K V Wood, D R Helinski, and M DeLuca. 1985. "Cloning of Firefly Luciferase cDNA and the Expression of Active Luciferase in Escherichia Coli.." *Proceedings of the National Academy of Sciences* 82 (23): 7870–73. doi:10.1073/pnas.82.23.7870.

Debacq-Chainiaux, Florence, Jorge D Erusalimsky, Judith Campisi, and Olivier Toussaint. 2009. "Protocols to Detect Senescence-Associated Beta-Galactosidase (SA- Gal) Activity, a Biomarkerof Senescent Cells in Culture and in Vivo." *Nature Protocols* 4 (12). Nature Publishing Group: 1798–1806. doi:10.1038/nprot.2009.191.

Deber, C M, and S J Reynolds. 1991. "Central Nervous System Myelin: Structure, Function, and Pathology.." *Clinical Biochemistry* 24 (2): 113–34.

Degenfeld, Georges, Tom S Wehrman, and Helen M Blau. 2009. "Imaging B-Galactosidase Activity in Vivo Using Sequential Reporter-Enzyme Luminescence." In *Methods in Molecular Biology*, 574:249–59. Methods in Molecular Biology. Totowa, NJ: Humana Press. doi:10.1007/978-1-60327-321-3_20.

Deloire-Grassin, M S, B Brochet, B Quesson, C Delalande, V Dousset, P Canioni, and K G Petry. 2000. "In Vivo Evaluation of Remyelination in Rat Brain by Magnetization Transfer Imaging.." *Journal of the Neurological Sciences* 178 (1): 10–16.

Deshmukh, Vishal A, Virginie Tardif, Costas A Lyssiotis, Chelsea C Green, Bilal Kerman, Hyung Joon Kim, Krishnan Padmanabhan, et al. 2013. “A Regenerative Approach to the Treatment of Multiple Sclerosis.” *Nature* 502 (7471). Nature Publishing Group: 327–32. doi:10.1038/nature12647.

Dimou, L, C Simon, F Kirchhoff, H Takebayashi, and M Gotz. 2008. “Progeny of Olig2-Expressing Progenitors in the Gray and White Matter of the Adult Mouse Cerebral Cortex.” *Journal of Neuroscience* 28 (41): 10434–42. doi:10.1523/JNEUROSCI.2831-08.2008.

Dousset, V, B Brochet, A Vital, C Gross, A Benazzouz, A Boullerne, A M Bidabe, A M Gin, and J M Caille. 1995. “Lysolecithin-Induced Demyelination in Primates: Preliminary in Vivo Study with MR and Magnetization Transfer..” *American Journal of Neuroradiology* 16 (2): 225–31.

Dousset, V, B Brochet, M S A Deloire, L Lagoarde, B Barroso, J M Caille, and K G Petry. 2006. “MR Imaging of Relapsing Multiple Sclerosis Patients Using Ultra-Small-Particle Iron Oxide and Compared with Gadolinium..” *American Journal of Neuroradiology* 27 (5): 1000–1005.

Duncan, I D, A Brower, Y Kondo, J F Curlee, and R D Schultz. 2009. “Extensive Remyelination of the CNS Leads to Functional Recovery..” *Proceedings of the National Academy of Sciences of the United States of America* 106 (16): 6832–36. doi:10.1073/pnas.0812500106.

Dunning, Mark D, M I Kettunen, Charles ffrench-Constant, Robin J M Franklin, and K M Brindle. 2006. “Magnetic Resonance Imaging of Functional Schwann Cell Transplants Labelled with Magnetic Microspheres..” *NeuroImage* 31 (1): 172–80. doi:10.1016/j.neuroimage.2005.11.050.

Emery, B.,, D., Agalliu, J., D Cahoy, T., A Watkins, J., C Dugas, S., B Mulinyawe, A., Ibrahim, Keith L Ligon, D., H Rowitch, and B., A Barres. 2009. “Myelin Gene Regulatory Factor Is a Critical Transcriptional Regulator Required for CNS Myelination..” *Cell* 138 (1): 172–85. doi:10.1016/j.cell.2009.04.031.

Fanarraga, M L, I Sommer, and I R Griffiths. 1995. “O-2A Progenitors of the Mouse Optic Nerve Exhibit a Developmental Pattern of Antigen Expression Different From the Rat..” *Glia* 15 (2). Wiley-Blackwell: 95–104. doi:10.1002/glia.440150202.

Fancy, Stephen P J, Chao Zhao, and Robin J M Franklin. 2004. “Increased Expression of Nkx2.2 and Olig2 Identifies Reactive Oligodendrocyte Progenitor Cells Responding to Demyelination in the Adult CNS.” *Molecular and Cellular Neuroscience* 27 (3): 247–54. doi:10.1016/j.mcn.2004.06.015.

Fancy, Stephen P J, Emily P Harrington, Tracy J Yuen, John C Silbereis, Chao Zhao, Sergio E Baranzini, Charlotte C Bruce, et al. 2011. “Axin2 as Regulatory and Therapeutic Target in Newborn Brain Injury and Remyelination.” *Nature Publishing Group* 14 (8). Nature Publishing Group: 1009–16. doi:10.1038/nn.2855.

Felts, P A, T A Baker, and Kenneth J Smith. 1997. “Conduction in Segmentally Demyelinated Mammalian Central Axons.” *The Journal of Neuroscience*, September, 7267–77.

Filippi, Massimo, Maria A Rocca, Olga Ciccarelli, Nicola De Stefano, Nikos Evangelou, Ludwig Kappos, Alex Rovira, et al. 2016. “MRI Criteria for the Diagnosis of Multiple Sclerosis: MAGNIMS Consensus Guidelines.” *The Lancet Neurology* 15 (3): 292–303. doi:10.1016/S1474-4422(15)00393-2.

Fisniku, L K, P A Brex, D R Altmann, K A Miszkiel, C E Benton, R Lanyon, A J Thompson, and D H Miller. 2008. “Disability and T2 MRI Lesions: a 20-Year Follow-Up of Patients with Relapse Onset of Multiple Sclerosis.” *Brain* 131 (3): 808–17. doi:10.1093/brain/awm329.

Fjær, Sveinung, Lars Bø, Kjell-Morten Myhr, Øivind Torkildsen, and Stig Wergeland. 2015. “Magnetization Transfer Ratio Does Not Correlate to Myelin Content in the Brain in the MOG-EAE Mouse Model.” *Neurochemistry International* 83-84 (C). The Authors: 28–40. doi:10.1016/j.neuint.2015.02.006.

Flores, A I, S P Narayanan, E N Morse, H E Shick, X Yin, G Kidd, R L Avila, D A Kirschner, and W B Macklin. 2008. “Constitutively Active Akt Induces Enhanced Myelination in the CNS.” *Journal of Neuroscience* 28 (28): 7174–83. doi:10.1523/JNEUROSCI.0150-08.2008.

Foerster, Sarah, Myfanwy F E Hill, and Robin J M Franklin. 2019. “Diversity in the Oligodendrocyte Lineage: Plasticity or Heterogeneity?.” Glia 25 (18). John Wiley & Sons, Ltd: 2411–19. doi:10.1002/glia.23607.

Fogarty, M. 2005. “A Subset of Oligodendrocytes Generated From Radial Glia in the Dorsal Spinal Cord.” *Development* 132 (8): 1951–59. doi:10.1242/dev.01777.

Ford, M. C., Alexandrova, O., Cossell, L., Stange-Marten, A., Sinclair, J., Kopp-Scheinpflug, C. Pecka,M., Grothe, B. (2015). Tuning of Ranvier node and internode properties in myelinated axons to adjust action potential timing. *Nature Communications*, 6, 8073.

Fox EJ. 2004. “Mechanism of action of mitoxantrone.” *Neurology.* 2004 Dec 28;63

Franklin, R J M, and W F Blakemore. 1993. “Requirements for Schwann Cell Migration Within Cns Environments: a Viewpoint.” *International Journal of Developmental Neuroscience* 11 (5): 641–49. doi:10.1016/0736-5748(93)90052-f.

Franklin, R J, and W F Blakemore. 1997. “Transplanting Oligodendrocyte Progenitors Into the Adult CNS..” *Journal of Anatomy* 190 (Pt 1) (Pt 1). Wiley-Blackwell: 23–33. doi:10.1046/j.1469-7580.1997.19010023.x.

Franklin, R J, K L Blaschuk, M C Bearchell, L L Prestoz, A Setzu, K M Brindle, and C ffrench-Constant. 1999. “Magnetic Resonance Imaging of Transplanted Oligodendrocyte Precursors in the Rat Brain..” *Neuroreport* 10 (18): 3961–65.

Franklin, Robin J M. 2002. “Why Does Remyelination Fail in Multiple Sclerosis?.” *Nature Reviews Neuroscience* 3 (9): 705–14. doi:10.1002/(SICI)1097-4547(19991015)58:2<207::AID-JNR1>3.0.CO;2-1.

Franklin, Robin J M, and Charles ffrench-Constant. 2008. “Remyelination in the CNS: From Biology to Therapy.” *Nature Reviews Neuroscience* 9 (11): 839–55. doi:10.1038/nrn2480.

Franklin, Robin J M, and Charles ffrench-Constant. 2017. “Regenerating CNS Myelin — From Mechanisms to Experimental Medicines.” *Nature Reviews Neuroscience* 18 (12): 753–69. doi:10.1038/nrn.2017.136.

Franklin, Robin J M, and Steven A Goldman. 2015. “Glia Disease and Repair—Remyelination.” *Cold Spring Harbor Perspectives in Biology* 7 (7): a020594. doi:10.1101/cshperspect.a020594.

Franklin, Robin J M, Charles ffrench-Constant, Julia M Edgar, and Kenneth J Smith. 2012. “Neuroprotection and Repair in Multiple Sclerosis.” *Nature Publishing Group* 8 (11). Nature Publishing Group: 624–34. doi:10.1038/nrneurol.2012.200.

Franklin, Robin J M, Susan A Bayley, and William F Blakemore. 1996a. “Transplanted CG4 Cells (an Oligodendrocyte Progenitor Cell Line) Survive, Migrate, and Contribute to Repair of Areas of Demyelination in X-Irradiated and Damaged Spinal Cord but Not in Normal Spinal Cord.” *Experimental Neurology* 137 (2): 263–76. doi:10.1006/exnr.1996.0025.

Franklin, Robin J M, Susan A Bayley, and William F Blakemore. 1996b. “Transplanted CG4 Cells (an Oligodendrocyte Progenitor Cell Line) Survive, Migrate, and Contribute to Repair of Areas of Demyelination in X-Irradiated and Damaged Spinal Cord but Not in Normal Spinal Cord.” *Experimental Neurology* 137 (2): 263–76. doi:10.1006/exnr.1996.0025.

Frohman, Teresa C, Scott L Davis, Shin Beh, Benjamin M Greenberg, Gina Remington, and Elliot M Frohman. 2013. “Uhthoff's Phenomena in MS—Clinical Features and Pathophysiology.” *Nature Publishing Group* 9 (9). Nature Publishing Group: 535–40. doi:10.1038/nrneurol.2013.98.

Fu, H, J Cai, H Clevers, E Fast, S Gray, R Greenberg, M K Jain, et al. 2009. “A Genome-Wide Screen for Spatially Restricted Expression Patterns Identifies Transcription Factors That Regulate Glial Development.” *Journal of Neuroscience* 29 (36): 11399–408. doi:10.1523/JNEUROSCI.0160-09.2009.

Gans, Carl, and R Glenn Northcutt. 1983. “Neural Crest and the Origin of Vertebrates: a New Head.” *Science* 220 (4594). American Association for the Advancement of Science: 268–73. doi:10.1126/science.220.4594.268.

Genove, Guillem, Ulrike DeMarco, Hongyan Xu, William F Goins, and Eric T Ahrens. 2005. “A New Transgene Reporter for in Vivo Magnetic Resonance Imaging.” *Nature Medicine* 11 (43): 450–54. doi:10.1038/nm1208.

Gensert, J M, and J E Goldman. 1997. “Endogenous Progenitors Remyelinate Demyelinated Axons in the Adult CNS,” July, 1–7.

Geraldes, Ruth, Olga Ciccarelli, Frederik Barkhof, Nicola De Stefano, Christian Enzinger, Massimo Filippi, Monika Hofer, et al. 2018. “The Current Role of MRI in Differentiating Multiple Sclerosis From Its Imaging Mimics.” *Nature Publishing Group* 14 (4). Nature Publishing Group: 199–213. doi:10.1038/nrneurol.2018.14.

Giedd, J. N., and Rapoport, J. L. 2010. “Structural MRI of paediatric brain development: What have we learned and where are we going?” *Neuron*, 67, 728–734. doi: 10.1016/j.neuron.2010.08.040

Gilad, Assaf A, Michael T McMahon, Piotr Walczak, Paul T Winnard, Venu Raman, Hanneke W M van Laarhoven, Cynthia M Skoglund, Jeff W M Bulte, and Peter C M van Zijl. 2007. “Artificial Reporter Gene Providing MRI Contrast Based on Proton Exchange.” *Nature Biotechnology* 25 (2): 217–19. doi:10.1038/nbt1277.

Gilad, Assaf A, Paul T Winnard, Peter C M van Zijl, and Jeff W M Bulte. 2007. “Developing MR Reporter Genes: Promises and Pitfalls.” *NMR in Biomedicine* 20 (3): 275–90. doi:10.1002/nbm.1134.

Ginhoux, Florent. 2013. “Origin and Differentiation of Microglia,” April, 1–14. doi:10.3389/fncel.2013.00045/abstract.

Gouw, A A, A Seewann, H Vrenken, W M van der Flier, J M Rozemuller, F Barkhof, P Scheltens, and J J G Geurts. 2008. “Heterogeneity of White Matter Hyperintensities in Alzheimer's Disease: Post-Mortem Quantitative MRI and Neuropathology.” *Brain* 131 (12): 3286–98. doi:10.1093/brain/awn265.

Goverman, Joan. 2009. “Autoimmune T Cell Responses in the Central Nervous System..” *Nature Reviews. Immunology* 9 (6): 393–407. doi:10.1038/nri2550.

Gow, A, V L Friedrich, and R A Lazzarini. 1992. “Myelin Basic Protein Gene Contains Separate Enhancers for Oligodendrocyte and Schwann Cell Expression..” *The Journal of Cell Biology* 119 (3). The Rockefeller University Press: 605–16.

Gow, Alexander, L Victor, V Friedrich, and R A Lazzarini. 1992. “Myelin Basic Protein Gene Contains Separate Enhancers for Oligodendrocyte and Schwann Cell Expression.” *The Journal of Cell Biology* 119 (November): 605–16.

Gravel M, Peterson J, Yong VW, Kottis V, Trapp B, Braun PE. 1996. “Overexpression of 2’,3’ cyclic nucleotide 3’ phosphodiesterase in transgenic mice alters oligodendrocyte development and produces aberrant myelination.” *Molecular and Cellular Neuroscience* 7: 453–466.

Griffiths, Ian, Matthias Klugmann, Thomas Anderson, Donald Yool, Christine Thomson, Markus H Schwab, Armin Schneider, et al. 1998. “Axonal Swellings and Degeneration in Mice Lacking the Major Proteolipid of Myelin .” *Science* 280 (June): 1–5.

Group, The IFNB Multiple Sclerosis Study. 1993. “Interferon Beta-1b Is Effective in Relapsing-Remitting Multiple Sclerosis: I. Clinical Results of a Multicenter, Randomized, Double-Blind, Placebo-Controlled Trial.” *Neurology* 43 (4). Wolters Kluwer Health, Inc. on behalf of the American Academy of Neurology: 655–55. doi:10.1212/WNL.43.4.655.

Groves, A K, Susan C Barnett, R J M Franklin, A J Crang, M Mayer, W F Blakemore, and C Noble. 1993. “Repair of Demyalinated Lesions by Transplantation of Purfied O-2A Progenitor Cells” 362 (April): 453–55.

Guo, F, J Ma, E McCauley, P Bannerman, and D Pleasure. 2009. “Early Postnatal Proteolipid Promoter-Expressing Progenitors Produce Multilineage Cells in Vivo.” *Journal of Neuroscience* 29 (22): 7256–70. doi:10.1523/JNEUROSCI.5653-08.2009.

Gupta, N, R G Henry, J Strober, S M Kang, D A Lim, M Bucci, E Caverzasi, et al. 2012. “Neural Stem Cell Engraftment and Myelination in the Human Brain.” *Science Translational Medicine* 4 (155): 155ra137–37. doi:10.1126/scitranslmed.3004373.

Guy, Joseph R, Pascal Sati, Emily Leibovitch, Steven Jacobson, Afonso C Silva, and Daniel S Reich. 2016. “Custom Fit 3D-Printed Brain Holders for Comparison of Histology with MRI in Marmosets.” *Journal of Neuroscience Methods* 257 (January): 55–63. doi:10.1016/j.jneumeth.2015.09.002.

Gyetvai, Georgina, Trisha Hughes, Florence Wedmore, Cieron Roe, Lamia Heikal, Pietro Ghezzi, and Manuela Mengozzi. 2017. “Erythropoietin Increases Myelination in Oligodendrocytes: Gene Expression Profiling Reveals Early Induction of Genes Involved in Lipid Transport and Metabolism.” *Frontiers in Immunology* 8 (October): 1905–12. doi:10.3389/fimmu.2017.01394.

Hagenbuch, B, and P J Meier. 2003. “The Superfamily of Organic Anion Transporting Polypeptides..” *Biochimica Et Biophysica Acta* 1609 (1): 1–18.

Hall, Anita, Neill A Giese, and William D Richardson. 1996. “Spinal Cord Oligodendrocytes Develop From Ventrally Derived Progenitor Cells That Express PDGF Alpha-Receptors,” November, 1–10.

Hamdan, Hamdan, Neriman T Kockara, Lee Ann Jolly, Shirley Haun, and Patricia A Wight. 2015. “Control of Human PLP1Expression Through Transcriptional Regulatory Elements and Alternatively Spliced Exons in Intron 1.” *ASN Neuro* 7 (1): 175909141556991–12. doi:10.1177/1759091415569910.

Hamilton, Nicola B, and David Attwell. 2010. “Do Astrocytes Really Exocytoseneurotransmitters?.” *Nature Reviews Neuroscience* 11 (4). Nature Publishing Group: 227–38. doi:10.1038/nrn2803.

Hartline, D K, and D R Colman. 2007. “Rapid Conduction and the Evolution of Giant Axons and Myelinated Fibers.” *Current Biology* 17 (1): R29–R35. doi:10.1016/j.cub.2006.11.042.

Hartline, Daniel K. 2008. “What Is Myelin?.” *Neuron Glia Biology* 4 (2). Cambridge University Press: 153–63. doi:10.1017/S1740925X09990263.

He, Xiaoya, Jinhua Cai, Hao Li, Bo Liu, Yong Qin, Yi Zhong, Longlun Wang, and Yifan Liao. 2016. “In Vivo Magnetic Resonance Imaging of Xenografted Tumors Using FTH1 Reporter Gene Expression Controlled by a Tet-on Switch..” ***Oncotarget*** 7 (48). Impact Journals: 78591–604. doi:10.18632/oncotarget.12519.

Hess MW, Kirschning E, Pfaller K, Debbage PL, Hohenberg H, Klima G. 1998. “5000-year-old myelin: Uniquely intact in molecular configuration and fine structure.” *Current Biol*ogy 8: R512–R513.

Hines JH, Ravanelli AM, Schwindt R, Scott EK, Appel B. 2015. “Neuronal activity biases axon selection for myelination in vivo.” *Nature Neuroscience* 18:683–9. doi: 10.1038/nn.3992.

Hinks, G L, and R J M Franklin. 1999. “Distinctive Patterns of PDGF-a, FGF-2, IGF-I, and TGF-B1 Gene Expression During Remyelination of Experimentally-Induced Spinal Cord Demyelination.” *Molecular and Cellular Neuroscience* 14 (2): 153–68. doi:10.1006/mcne.1999.0771.

Howles, Gabriel P, Ketan B Ghaghada, Yi Qi, Srinivasan Mukundan Jr., and G Allan Johnson. 2009. “High-Resolution Magnetic Resonance Angiography in the Mouse Using a Nanoparticle Blood-Pool Contrast Agent.” *Magnetic Resonance in Medicine* 62 (6): 1447–56. doi:10.1002/mrm.22154.

Hu, Sheng-Li, Pei-Gang Lu, Li-Jun Zhang, Fei Li, Zhi Chen, Nan Wu, Hui Meng, Jiang-Kai Lin, and Hua Feng. 2012. “In Vivo Magnetic Resonance Imaging Tracking of SPIO-Labeled Human Umbilical Cord Mesenchymal Stem Cells.” *Journal of Cellular Biochemistry* 113 (3): 1005–12. doi:10.1634/stemcells.2008-0456.

Huang, Jeffrey K, Andrew A Jarjour, Brahim Nait Oumesmar, Christophe Kerninon, Anna Williams, Wojciech Krezel, Hiroyuki Kagechika, et al. 2010. “Retinoid X Receptor Gamma Signaling Accelerates CNS Remyelination.” *Nature Publishing Group* 14 (1). Nature Publishing Group: 45–53. doi:10.1038/nn.2702.

Huang, Jeffrey K, Stephen P J Fancy, Chao Zhao, D., H Rowitch, Charles ffrench-Constant, and Robin J M Franklin. 2011. “Myelin Regeneration in Multiple Sclerosis: Targeting Endogenous Stem Cells.” *Neurotherapeutics* 8 (4): 650–58. doi:10.1007/s13311-011-0065-x.

Hughes EG, Kang SH, Fukaya M, Bergles DE. 2013. “Oligodendrocyte progenitors balance growth with self-repulsion to achieve homeostasis in the adult brain.” *Nature Neuroscience* 16: 668–676. doi: 10.1038/nn.3390

Ioannidou K, Anderson KI, Strachan D, Edgar JM, Barnett SC. 2012. “Time-lapse imaging of the dynamics of CNS glial-axonal interactions in vitro and ex vivo.” PLoS ONE 7: e30775. doi: 10.1371/journal.pone.0030775

Jaquet, V, G Pfend, M Tosic, and J M Matthieu. 1999. “Analysis of *Cis* Acting Sequences From the MOG Promoter.” *Journal of Neurochemistry*, February, 1–9.

Jeffery, N D, A J Crang, M T O'Leary, S J Hodge, and W F Blakemore. 1999. “Behavioural Consequences of Oligodendrocyte Progenitor Cell Transplantation Into Experimental Demyelinating Lesions in the Rat Spinal Cord..” *The European Journal of Neuroscience* 11 (5): 1508–14.

Jeffery, N D, and W F Blakemore. 1997. “Locomotor Deficits Induced by Experimental Spinal Cord Demyelination Are Abolished by Spontaneous Remyelination.” *Brain* 120 (February): 1–11.

Johnson, G Allan, Gary P Cofer, Boma Fubara, Sally L Gewalt, Laurence W Hedlund, and Robert R Maronpot. 2002a. “Magnetic Resonance Histology for Morphologic Phenotyping.” *Journal of Magnetic Resonance Imaging* 16 (4). Wiley-Blackwell: 423–29. doi:10.1002/jmri.10175.

Johnson, G Allan, Gary P Cofer, Boma Fubara, Sally L Gewalt, Laurence W Hedlund, and Robert R Maronpot. 2002b. “Magnetic Resonance Histology for Morphologic Phenotyping.” *Journal of Magnetic Resonance Imaging* 16 (4): 423–29. doi:10.1002/jmri.10175.

Jonquieres, von, Georg, Dominik Fröhlich, Claudia B Klugmann, Xin Wen, Anne E Harasta, Roshini Ramkumar, Ziggy H T Spencer, Gary D Housley, and Matthias Klugmann. 2016. “Recombinant Human Myelin-Associated Glycoprotein Promoter Drives Selective AAV-Mediated Transgene Expression in Oligodendrocytes.” *Frontiers in Molecular Neuroscience* 9 (February). Frontiers: 2136–14. doi:10.3389/fnmol.2016.00013.

Jonquieres, von, Georg, Nadine Mersmann, Claudia Bettina Klugmann, Anne Editha Harasta, Beat Lutz, Orla Teahan, Gary David Housley, Dominik Fröhlich, Eva-Maria Krämer-Albers, and Matthias Klugmann. 2013. "Glial Promoter Selectivity Following AAV-Delivery to the Immature Brain." Edited by Jianming Qiu. *PLoS ONE* 8 (6). Public Library of Science: e65646–11. doi:10.1371/journal.pone.0065646.

Jung, Dong-In, Jeongim Ha, Byeong-Teck Kang, Ju-Won Kim, Fu-Shi Quan, Jong-Hwan Lee, Eung-Je Woo, and Hee-Myung Park. 2009. "Journal of the Neurological Sciences." *Journal of the Neurological Sciences* 285 (1-2). Elsevier B.V.: 67–77. doi:10.1016/j.jns.2009.05.027.

Kanda, Tomonori, Hiroshi Oba, Keiko Toyoda, Kazuhiro Kitajima, and Shigeru Furui. 2015. "Brain Gadolinium Deposition After Administration of Gadolinium-Based Contrast Agents." *Japanese Journal of Radiology* 34 (1). Springer Japan: 3–9. doi:10.1007/s11604-015-0503-5.

Katsuhiko Ono, Rashmi Bansal, Jennifer Payne, Urs Rutishauser, and Robert H Miller. 1995. "Early Development and Dispersal of Oligodendrocyte Precursors in the Embryonic Chick Spinal Cord," April, 1–12.

Keeler, A M, M K ElMallah, and T R Flotte. 2017. "Gene Therapy 2017: Progress and Future Directions." *Clinical and Translational Science* 10 (4): 242–48. doi:10.1001/jamaophthalmol.2013.7630.

Keirstead, H S, and W F Blakemore. 1997. "Identification of Post-Mitotic Oligodendrocytes Incapable of Remyelination Within the Demyelinated Adult Spinal Cord.." *Journal of Neuropathology & Experimental Neurology* 56 (11): 1191–1201.

Kessaris, Nicoletta, Matthew Fogarty, Palma Iannarelli, Matthew Grist, Michael Wegner, and William D Richardson. 2005. "Competing Waves of Oligodendrocytes in the Forebrain and Postnatal Elimination of an Embryonic Lineage." *Nature Neuroscience* 9 (2): 173–79. doi:10.1038/nn1620.

Kirby BB, Takada N, Latimer AJ, Shin J, Carney TJ, Kelsh RN, Appel B. 2006. "In vivo time-lapse imaging shows dynamic oligodendrocyte progenitor behaviour during zebrafish development." *Nature Neuroscience* 9: 1506–1511.

Koudelka S, Voas MG, Almeida RG, Baraban M, Soetaert J, Meyer MP, Talbot WS, Lyons DA. 2016. "Individual Neuronal Subtypes Exhibit Diversity in CNS Myelination Mediated by Synaptic Vesicle Release." *Current Biology* 26:1447– 55.

Knaap, Marjo S, and Marianna Bugiani. 2018. "Leukodystrophies: a Proposed Classification System Based on Pathological Changes and Pathogenetic Mechanisms." *Acta Neuropathologica* 134 (3). Springer Berlin Heidelberg: 351–82. doi:10.1007/s00401-017-1739-1.

Knobler RL, Stempak JG, Laurencin M. 1976. ”Nonuniformity of the oligodendroglial ensheathment of axons during myelination in the developing rat central nervous system. A serial section electron microscopical study.” *Journal of Ultrastructural Research* 55(3):417–432.

Kobayashi, Yoshiomi, Yohei Okada, Go Itakura, Hiroki Iwai, Soraya Nishimura, Akimasa Yasuda, Satoshi Nori, et al. 2012. “Pre-Evaluated Safe Human iPSC-Derived Neural Stem Cells Promote Functional Recovery After Spinal Cord Injury in Common Marmoset Without Tumorigenicity.” Edited by Kenji Hashimoto. *PLoS ONE* 7 (12): e52787. doi:10.1371/journal.pone.0052787.g007.

Koretsky, A P, M J Brosnan, L H Chen, J D Chen, and T Van Dyke. 1990. “NMR Detection of Creatine Kinase Expressed in Liver of Transgenic Mice: Determination of Free ADP Levels..” *Proceedings of the National Academy of Sciences* 87 (8). National Academy of Sciences: 3112–16.

Koretsky, Alan P, and Afonso C Silva. 2004. “Manganese-Enhanced Magnetic Resonance Imaging (MEMRI).” *NMR in Biomedicine* 17 (8): 527–31. doi:10.1148/radiology.144.2.6283594.

Köhler, Wolfgang, Julian Curiel, and Adeline Vanderver. 2018. “Adulthood Leukodystrophies.” *Nature Publishing Group* 14 (2). Nature Publishing Group: 94–105. doi:10.1038/nrneurol.2017.175.

Kraitchman, Dara L, and Jeff W M Bulte. 2008. “Imaging of Stem Cells Using MRI.” *Basic Research in Cardiology* 103 (2): 105–13. doi:10.1007/s00395-008-0704-5.

Kraus, Jörg, Anne K Ling, Stefan Hamm, Kay Voigt, Patrick Oschmann, and Britta Engelhardt. 2004. “Interferon-B Stabilizes Barrier Characteristics of Brain Endothelial Cells in Vitro.” *Annals of Neurology* 56 (2): 192–205. doi:10.1002/ana.20161.

Kreutzberg, G W. 1996. “Microglia: a Sensor for Pathological Events in the CNS..” *Trends in Neurosciences* 19 (8): 312–18.

La Fuente, De, Alerie Guzman, Oihana Errea, Peter van Wijngaarden, Ginez A Gonzalez, Christophe Kerninon, Andrew A Jarjour, Hilary J Lewis, et al. 2015. “Vitamin D Receptor-Retinoid X Receptor Heterodimer Signaling Regulates Oligodendrocyte Progenitor Cell Differentiation..” *The Journal of Cell Biology* 211 (5). Rockefeller University Press: 975–85. doi:10.1083/jcb.201505119.

Lauffer, Randall B. 1987. “Paramagnetic Metal Complexes as Water Proton Relaxation Agents for NMR Imaging: Theory and Design.” *Chemical Reviews* 87 (5): 901–27. doi:10.1021/cr00081a003.

Laule, C, E Leung, D K B Lis, A L Traboulsee, D W Paty, A L MacKay, and G R W Moore. 2006. "Myelin Water Imaging in Multiple Sclerosis: Quantitative Correlations with Histopathology.." *Multiple Sclerosis (Houndmills, Basingstoke, England)* 12 (6): 747–53. doi:10.1177/1352458506070928.

Laule, C, I M Vavasour, S H Kolind, D K B Li, T L Traboulsee, G R W Moore, and A L MacKay. 2007. "Magnetic Resonance Imaging of Myelin.." *Neurotherapeutics* 4 (3): 460–84. doi:10.1016/j.nurt.2007.05.004.

Laursen LS, Chan CW, Ffrench-Constant C. 2011. "Translation of myelin basic protein mRNA in oligodendrocytes is regulated by integrin activation and hnRNP-K." *Journal of Cell Biology* 192: 797–811. doi: 10.1083/jcb.201007014

Lee S, Leach MK, Redmond SA, Chong SY, Mellon SH, Tuck SJ, Feng ZQ, Corey JM, Chan JR. 2012. "A culture system to study oligodendrocyte myelination processes using engineered nanofibers." *Nature Methods* 9: 917–922. doi: 10.1038/nmeth.2105

Lepore, A C, P Walczak, M S Rao, I Fischer, and J W M Bulte. 2006. "MR Imaging of Lineage-Restricted Neural Precursors Following Transplantation Into the Adult Spinal Cord." *Experimental Neurology* 201 (1): 49–59. doi:10.1016/j.expneurol.2006.03.032.

Levesque, Ives R, Paul S Giacomini, Sridar Narayanan, Luciana T Ribeiro, John G Sled, Doug L Arnold, and G Bruce Pike. 2010. "Quantitative Magnetization Transfer and Myelin Water Imaging of the Evolution of Acute Multiple Sclerosis Lesions." *Magnetic Resonance in Medicine* 63 (3): 633–40. doi:10.1002/mrm.22244.

Levitt M. Spin dynamics: basics of nuclear magnetic resonance. New York: John Wiley & Sons; 2001.

Li, Mingjie, Nada Husic, Ying Lin, Heather Christensen, Ibrahim Malik, Sally McIver, Christine M LaPash Daniels, et al. 2010. "Optimal Promoter Usage for Lentiviral Vector-Mediated Transduction of Cultured Central Nervous System Cells." *Journal of Neuroscience Methods* 189 (1): 56–64. doi:10.1016/j.jneumeth.2010.03.019.

Lin, Alexander, Brian D Ross, Kent Harris, and Willis Wong. 2005. "Efficacy of Proton Magnetic Resonance Spectroscopy in Neurological Diagnosis and Neurotherapeutic Decision Making.." *NeuroRx : the Journal of the American Society for Experimental NeuroTherapeutics* 2 (2). Springer-Verlag: 197–214. doi:10.1602/neurorx.2.2.197.

Lin, Wen-Ping, Xuan-Wei Chen, Li-Qun Zhang, Chao-Yang Wu, Zi-Da Huang, and Jian-Hua Lin. 2013. "Effect of Neuroglobin Genetically Modified Bone Marrow Mesenchymal Stem Cells Transplantation on Spinal Cord Injury in Rabbits." Edited by Pranela Rameshwar. *PLoS ONE* 8 (5): e63444. doi:10.1371/journal.pone.0063444.g009.

Loffredo, Francesco S, Matthew L Steinhauser, Steven M Jay, Joseph Gannon, James R Pancoast, Pratyusha Yalamanchi, Manisha Sinha, et al. 2013. “Growth Differentiation Factor 11 Is a Circulating Factor That Reverses Age-Related Cardiac Hypertrophy.” *Cell* 153 (4): 828–39. doi:10.1016/j.cell.2013.04.015.

Losseff, N A, D H Miller, D Kidd, and A J Thompson. 2001. “The Predictive Value of Gadolinium Enhancement for Long Term Disability in Relapsing-Remitting Multiple Sclerosis--Preliminary Results..” *Multiple Sclerosis (Houndmills, Basingstoke, England)* 7 (1): 23–25. doi:10.1177/135245850100700105.

Louis, J C, E Magal, D Muir, M Manthorpe, and S Varon. 1992. “CG-4, a New Bipotential Glial Cell Line From Rat Brain, Is Capable of Differentiating in Vitro Into Either Mature Oligodendrocytes or Type-2 Astrocytes..” *Journal of Neuroscience Research* 31 (1). Wiley-Blackwell: 193–204. doi:10.1002/jnr.490310125.

Luo, Yun, Yu Zou, Linhui Yang, Jia Liu, Sujuan Liu, Jin Liu, Xinfu Zhou, Wensheng Zhang, and Tinghua Wang. 2013. “Neuroscience Letters.” *Neuroscience Letters* 549 (August). Elsevier Ireland Ltd: 103–8. doi:10.1016/j.neulet.2013.06.005.

Lyons, S K, P S Patrick, and K M Brindle. 2013. “Imaging Mouse Cancer Models in Vivo Using Reporter Transgenes.” *Cold Spring Harbor Protocols* 2013 (8): pdb.top069864–64. doi:10.1101/pdb.top069864.

MacDonald, W I, A Compston, G Edan, D Goodkin, H-P Hartung, Fred D Lublin, H F McFarland, et al. 2001. “Recommended Diagnostic Criteria for Multiple Sclerosis: Guidelines From the International Panel on the Diagnosis of Multiple Sclerosis.” *Annals of Neurology* 50 (June): 121–27.

MacKay, A L, and C Laule. 2016. “Magnetic Resonance of Myelin Water: an in Vivo Marker for Myelin.” Edited by Bernard Zalc. *Brain Plasticity* 2 (1): 71–91. doi:10.3233/BPL-160033.

MacKay A, Whittall K, Adler J, 1994. “In vivo visualization of myelin water in brain by magnetic resonance.” Magn Reson Med 1994;31:673–7.

Mallik, S, R S Samson, C A M Wheeler-Kingshott, and D H Miller. 2014. “Imaging Outcomes for Trials of Remyelination in Multiple Sclerosis.” *Journal of Neurology, Neurosurgery & Psychiatry* 85 (12): 1396–1404. doi:10.1136/jnnp-2014-307650.

McKenzie, I.A., Ohayon, D., Li, H., Paes de Faria, J., Emery, B., Tohyama, K. and Richardson, W.D. 2014. “Motor skill learning requires active central myelination.” *Science* 346, 318-322.

Masedunskas, Andrius, Oleg Milberg, Natalie Porat-Shliom, Monika Sramkova, Tim Wigand, Panomwat Amornphimoltham, and Roberto Weigert. 2014. “Intravital Microscopy.” *BioArchitecture* 2 (5): 143–57. doi:10.1073/pnas.1209397109.

Masternak, Krzysztof, and Walter Reith. 2002. “Promoter-Specific Functions of CIITA and the MHC Class II Enhanceosome in Transcriptional Activation..” *The EMBO Journal* 21 (6). EMBO Press: 1379–88. doi:10.1093/emboj/21.6.1379.

McCarthy, K D, and J de Vellis. 1980. “Preparation of Separate Astroglial and Oligodendroglial Cell Cultures From Rat Cerebral Tissue..” *The Journal of Cell Biology* 85 (3). The Rockefeller University Press: 890–902.

McCreary, Cheryl R, Thorarin A Bjarnason, Viktor Skihar, J Ross Mitchell, V Wee Yong, and Jeff F Dunn. 2009. “Multiexponential T2 and Magnetization Transfer MRI of Demyelination and Remyelination in Murine Spinal Cord.” *NeuroImage* 45 (4): 1173–82. doi:10.1016/j.neuroimage.2008.12.071.

McIver, Sally R, Chul-Sang Lee, Jin-Moo Lee, Steven H Green, Mark S Sands, B Joy Snider, and Mark P Goldberg. 2005. “Lentiviral Transduction of Murine Oligodendrocytes in Vivo.” *Journal of Neuroscience Research* 82 (3): 397–403. doi:10.1002/jnr.20626.

McKenzie, Ian A, David Ohayon, Huiliang Li, Joana Paes de Faria, B., Emery, Koujiro Tohyama, and William D Richardson. 2014. “Motor Skill Learning Requires Active Central Myelination..” *Science* 346 (6207). American Association for the Advancement of Science: 318–22. doi:10.1126/science.1254960.

McMurran, Christopher E, Clare A Jones, Denise C Fitzgerald, and Robin J M Franklin. 2016. “CNS Remyelination and the Innate Immune System.” *Frontiers in Cell and Developmental Biology* 4 (e66308): 1142. doi:10.1016/j.neurobiolaging.2005.06.008.

Mei, Feng, Stephen P J Fancy, Yun-An A Shen, Jianqin Niu, Chao Zhao, Bryan Presley, Edna Miao, et al. 2014. “Micropillar Arrays as a High-Throughput Screening Platform for Therapeutics in Multiple Sclerosis.” *Nature Medicine* 20 (8). Nature Publishing Group: 954–60. doi:10.1038/nm.3618.

Meier, Shelby, Assaf A Gilad, J Anthony Brandon, Chenghao Qian, Erhe Gao, Jose F Abisambra, and Moriel Vandsburger. 2018. “Non-Invasive Detection of Adeno-Associated Viral Gene Transfer Using a Genetically Encoded CEST-MRI Reporter Gene in the Murine Heart..” ***Scientific Reports*** 8 (1). Nature Publishing Group: 4638. doi:10.1038/s41598-018-22993-4.

Mendonça, Liliana S, Clévio Nóbrega, Hirokazu Hirai, Brian K Kaspar, and Luís Pereira de Almeida. 2014. “Transplantation of Cerebellar Neural Stem Cells Improves Motor Coordination and Neuropathology in Machado-Joseph Disease Mice.” *Brain* 138 (2): 320–35. doi:10.1093/brain/awu352.

Mensch S, Baraban M, Almeida R, Czopka T, Ausborn J, El Manira A, Lyons DA. 2015. “Synaptic vesicle release regulates myelin sheath number of individual oligodendrocytes in vivo.” *Nat Neuroscience* 18:628–30.

Michalski, John-Paul, Carrie Anderson, Ariane Beauvais, Yves De Repentigny, and Rashmi Kothary. 2011. “The Proteolipid Protein Promoter Drives Expression Outside of the Oligodendrocyte Lineage During Embryonic and Early Postnatal Development.” Edited by Michelle L Block. *PLoS ONE* 6 (5). Public Library of Science: e19772–13. doi:10.1371/journal.pone.0019772.

Micheva, K. D., Wolman, D., Mensh, B. D., Pax, E., Buchanan, J., Smith, S. J., & Bock, D. D. (2016). A large fraction of neocortical myelin ensheathes axons of local inhibitory neurons. eLife, 5, e15784.

Miller, D H, P Rudge, G JOHNSON, B E Kendall, D G MacManus, I F Moseley, D BARNES, and W I McDonald. 1988. “Serial Gadolinium Enhanced Magnetic Resonance Imaging in Multiple Sclerosis..” *Brain* 111 (Pt 4) (August): 927–39.

Miron, Veronique E, Tanja Kuhlmann, and Jack P Antel. 2011. “Cells of the Oligodendroglial Lineage, Myelination, and Remyelination.” *BBA - Molecular Basis of Disease* 1812 (2). Elsevier B.V.: 184–93. doi:10.1016/j.bbadis.2010.09.010.

Miyamoto, Yuki, Tomohiro Torii, Akito Tanoue, Masahiro Yamamoto, and Junji Yamauchi. 2018. “The Promoter Region of 46-kDa CNPase Is Sufficient for Its Expression in Corpus Callosum.” *Molecular Genetics and Metabolism Reports* 15 (June). Elsevier: 78–79. doi:10.1016/j.ymgmr.2018.03.003.

Miyao, Yasuyoshi, Keiji Shimizu, Masakazu Tamura, Hiromi Akita, Kouji Ikeda, Eiichiro Mabuchi, Haruhiko Kishima, Toru Hayakawa, and Kazuhiro Ikenaka. 1997. “Usefulness of a Mouse Myelin Basic Protein Promoter for Gene Therapy of Malignant Glioma: Myelin Basic Protein Promoter Is Strongly Active in Human Malignant Glioma Cells.” *Japanese Journal of Cancer Research* 88 (7). Wiley/Blackwell (10.1111): 678–86. doi:10.1111/j.1349-7006.1997.tb00436.x.

Modo, Michel, Mathias Hoehn, and Jeff W M Bulte. 2005. “Cellular MR Imaging..” *Molecular Imaging* 4 (3): 143–64.

Molyneux, P D, M Filippi, F Barkhof, C Gasperini, T Yousry, L Lruyen, H M Lai, M A Rocca, I F Moseley, and D H Miller. 1998. “Correlations Between Monthly Enhanced MRI Lesion Rate and Changes in T2 Lesion Volume in Multiple Sclerosis.” *Annals of Neurology* 43 (3). Wiley-Blackwell: 332–39. doi:10.1002/ana.410430311.

Mulder, Willem J M, Michael T McMahon, Klaas Nicolay, Moriel H Vandsburger, Marina Radoul, Batya Cohen, and Michal Neeman. 2012. “MRI Reporter Genes: Applications for Imaging of Cell Survival, Proliferation, Migration and Differentiation.” *NMR in Biomedicine* 26 (7): 872–84. doi:10.1529/biophysj.107.116145.

Murtie, Joshua C, Yong-Xing Zhou, Tuan Q Le, Adam C Vana, and Regina C Armstrong. 2005. "PDGF and FGF2 Pathways Regulate Distinct Oligodendrocyte Lineage Responses in Experimental Demyelination with Spontaneous Remyelination." *Neurobiology of Disease* 19 (1-2): 171–82. doi:10.1016/j.nbd.2004.12.006.

Nakano, Akihiko. 2002. "Spinning-Disk Confocal Microscopy -- a Cutting-Edge Tool for Imaging of Membrane Traffic.." *Cell Structure and Function* 27 (5): 349–55.

Nakatani, H, E Martin, H Hassani, A Clavairoly, C L Maire, A Viadieu, C Kerninon, et al. 2013. "Ascl1/Mash1 Promotes Brain Oligodendrogenesis During Myelination and Remyelination." *Journal of Neuroscience* 33 (23): 9752–68. doi:10.1523/JNEUROSCI.0805-13.2013.

Narayana, Ponnada A. 2005. "Magnetic Resonance Spectroscopy in the Monitoring of Multiple Sclerosis." *Journal of Neuroimaging* 15 (suppl 1): 46S–57S. doi:10.1212/01.WNL.0000072264.75989.B8.

Nathoo, Nabeela, V Wee Yong, and Jeff F Dunn. 2014. "Understanding Disease Processes in Multiple Sclerosis Through Magnetic Resonance Imaging Studies in Animal Models." *Ynicl* 4 (C). Elsevier Inc.: 743–56. doi:10.1016/j.nicl.2014.04.011.

Nave, K A, C Lai, F E Bloom, and R J Milner. 1986. "Jimpy Mutant Mouse: a 74-Base Deletion in the mRNA for Myelin Proteolipid Protein and Evidence for a Primary Defect in RNA Splicing." *Proceedings of the National Academy of Sciences* 83 (23). National Academy of Sciences: 9264–68. doi:10.1073/pnas.83.23.9264.

Nave, Klaus-Armin. 2010. "Perspectives." *Nature Reviews Neuroscience* 11 (4). Nature Publishing Group: 275–83. doi:10.1038/nrn2797.

Nguyen, Thanh D, Cynthia Wisnieff, Mitchell A Cooper, Dushyant Kumar, Ashish Raj, Pascal Spincemaille, Yi Wang, Tim Vartanian, and Susan A Gauthier. 2012. "T2prep Three-Dimensional Spiral Imaging with Efficient Whole Brain Coverage for Myelin Water Quantification at 1.5 Tesla." *Magnetic Resonance in Medicine* 67 (3): 614–21. doi:10.1002/mrm.24128.

Niccolini, Flavia, Paul Su, and Marios Politis. 2015. "PET in Multiple Sclerosis.." *Clinical Nuclear Medicine* 40 (1): e46–e52. doi:10.1097/RLU.0000000000000359.

Niers, Johanna M, John W Chen, Grant Lewandrowski, Mariam Kerami, Elisabeth Garanger, Greg Wojtkiewicz, Peter Waterman, Edmund Keliher, Ralph Weissleder, and Bakhos A Tannous. 2012. "Single Reporter for Targeted Multimodal in Vivo Imaging." *Journal of the American Chemical Society* 134 (11): 5149–56. doi:10.1021/ja209868g.

Noble M, Murray K, Stroobant P, Waterfield MD, Riddle P. 1988. "Platelet derived growth factor promotes division and motility and inhibits premature differentiation of the oligodendrocyte/type-2 astrocyte progenitor cell." *Nature* 333:560–2.

Olchowy, Cyprian, Kamil Cebulski, Mateusz Łasecki, Radosław Chaber, Anna Olchowy, Krzysztof Kałwak, and Urszula Zaleska-Dorobisz. 2017. "The Presence of the Gadolinium-Based Contrast Agent Depositions in the Brain and Symptoms of Gadolinium Neurotoxicity - a Systematic Review." Edited by Subhra Mohapatra. *PLoS ONE* 12 (2). Public Library of Science: e0171704–14. doi:10.1371/journal.pone.0171704.

Olivier, C, I Cobos, E M Perez Villegas, N Spassky, B Zalc, S Martinez, and J L Thomas. 2001. "Monofocal Origin of Telencephalic Oligodendrocytes in the Anterior Entopeduncular Area of the Chick Embryo.." *Development* 128 (10): 1757–69.

ORiordan, J I, A J Thompson, D P Kingsley, D G MacManus, B E Kendall, P Rudge, W I McDonald, and D H Miller. 1998. "The Prognostic Value of Brain MRI in Clinically Isolated Syndromes of the CNS. a 10-Year Follow-Up.." *Brain* 121 (Pt 3) (March): 495–503.

Ou, Xiawei, Shu-Wei Sun, Hsiao-Fang Liang, Sheng-Kwei Song, and Daniel F Gochberg. 2009. "Quantitative Magnetization Transfer Measured Pool-Size Ratio Reflects Optic Nerve Myelin Content in Ex Vivo Mice." *Magnetic Resonance in Medicine* 61 (2): 364–71. doi:10.1212/WNL.56.3.304.

Pajevic, S., Basser, P. J., & Fields, R. D. 2014. "Role of myelin plasticity in oscillations and synchrony of neuronal activity." *Neuroscience*, 276, 135–147.

Patrick, P S, J Hammersley, L Loizou, M I Kettunen, T B Rodrigues, D-E Hu, S-S Tee, et al. 2014. "Dual-Modality Gene Reporter for in Vivo Imaging.." *Proceedings of the National Academy of Sciences of the United States of America* 111 (1): 415–20. doi:10.1073/pnas.1319000111.

Patrick, P S, S K Lyons, T B Rodrigues, and K M Brindle. 2014. "Oatp1 Enhances Bioluminescence by Acting as a Plasma Membrane Transporter for D-Luciferin." *Molecular Imaging and Biology* 16 (5): 626–34. doi:10.1007/s11307-014-0741-4.

Pedraza L, Huang JK, Colman D. 2009. "Disposition of axonal caspr with respect to glial cell membranes: Implications for the process of myelination." *Journal of Neuroscience Research* 87:3480–3491.

Pérez-Cerdá, Fernando, María Victoria Sánchez-Gómez, and Carlos Matute. 2015. "Pío Del Río Hortega and the Discovery of the Oligodendrocytes." *Frontiers in Neuroanatomy* 9 (July). doi:10.3389/fnana.2015.00092.

Pichler, A, J L Prior, G D Luker, and D Piwnica-Worms. 2008. "Generation of a Highly Inducible Gal4." *Proceedings of the National Academy of Sciences* 105 (41): 1–6.

Pirko, I., A Johnson, B Ciric, J Gamez, S I Macura, L R Pease, and M Rodriguez. 2004. "In Vivo Magnetic Resonance Imaging of Immune Cells in the Central Nervous System with Superparamagnetic Antibodies.." *FASEB Journal : Federation of American Societies for Experimental Biology* 18 (1): 179–82. doi:10.1096/fj.02-1124fje.

Plate, K H, G Breier, B Millauer, A Ullrich, and W Risau. 1993. “Up-Regulation of Vascular Endothelial Growth Factor and Its Cognate Receptors in a Rat Glioma Model of Tumor Angiogenesis..” *Cancer Research* 53 (23): 5822–27.

Polman, Chris H, Stephen C Reingold, Brenda Banwell, Michel Clanet, Jeffrey A Cohen, Massimo Filippi, Kazuo Fujihara, et al. 2011. “Diagnostic Criteria for Multiple Sclerosis: 2010 Revisions to the McDonald Criteria.” *Annals of Neurology* 69 (2): 292–302. doi:10.1002/ana.21464.

Price, J, D Turner, and C Cepko. 1987. “Lineage Analysis in the Vertebrate Nervous System by Retrovirus-Mediated Gene Transfer..” *Proceedings of the National Academy of Sciences* 84 (1). National Academy of Sciences: 156–60.

Pringle, N P, H S Mudhar, E J Collarini, and W D Richardson. 1992. “PDGF Receptors in the Rat CNS: During Late Neurogenesis, PDGF Alpha-Receptor Expression Appears to Be Restricted to Glial Cells of the Oligodendrocyte Lineage..” *Development* 115 (2): 535–51.

Puckett, C, L Hundson, K Ono, V Friedrich, J Benecke, M Dubois Dalcq, and R A Lazzarini. 1987. “Myelin-Specific Proteolipid Protein Is Expressed in Myelinating Schwann Cells but Is Not Incorporated Into Myelin Sheaths.” *Journal of Neuroscience Research* 18 (4). Wiley-Blackwell: 511–18. doi:10.1002/jnr.490180402.

Purcell EM, Torrey HC, Pound RV. 1946. “Resonance absorption by nuclear magnetic moments in a solid.” Physics Review 1946;69:37–38.39.

Quarles, Richard H. 2007. “Myelin-Associated Glycoprotein (MAG): Past, Present and Beyond..” *Journal of Neurochemistry* 100 (6): 1431–48. doi:10.1111/j.1471-4159.2006.04319.x.

Raff MC, Barres BA, Burne JF, Coles HS, Ishizaki Y, Jacobson MD. 1993. Programmed cell death and the control of cell survival: Lessons from the nervous system. Science 262: 695–700.

Raff M.,C., Lillien L.,E, Richardson W.,D., Burne J.,F., Noble M.,D. 1988. Platelet derived growth factor from astrocytes drives the clock that times oligodendrocyte development in culture.” *Nature* 333:562–5.

Rapoport, S I. 2000. “Osmotic Opening of the Blood-Brain Barrier: Principles, Mechanism, and Therapeutic Applications..” *Cellular and Molecular Neurobiology* 20 (2): 217–30.

Readhead, Carol, and Leroy Hood. 2018. “The Dysmyelinating Mouse Mutations Shiverer (*Shi*) And Myelin Deficient (*Shi*^{Mld})..” *Behaviour Genetics* 20 (2): 213–34.

Rebo, Justin, Melod Mehdipour, Ranveer Gathwala, Keith Causey, Yan Liu, Michael J Conboy, and Irina M Conboy. 2016. “A Single Heterochronic Blood Exchange Reveals Rapid Inhibition of Multiple Tissues by Old Blood.” *Nature Communications* 7 (November). Nature Publishing Group: 1–11. doi:10.1038/ncomms13363.

Richardson WD, Pringle N, Mosley MJ, Westermark B, Dubois-Dalcq M. 1988. “A role for platelet-derived growth factor in normal gliogenesis in the central nervous system.” *Cell* 53:309–19.

Richardson, William D, Kaylene M Young, Richa B Tripathi, and Ian McKenzie. 2011. “NG2-Glia as Multipotent Neural Stem Cells: Fact or Fantasy?.” *Neuron* 70 (4). Elsevier Inc.: 661–73. doi:10.1016/j.neuron.2011.05.013.

Rivers, Leanne E, Kaylene M Young, Matteo Rizzi, Françoise Jamen, Konstantina Psachoulia, Anna Wade, Nicoletta Kessaris, and William D Richardson. 2008. “PDGFRA/NG2 Glia Generate Myelinating Oligodendrocytes and Piriform Projection Neurons in Adult Mice.” *Nature Neuroscience* 11 (12): 1392–1401. doi:10.1038/nn.2220.

Rogosnitzky, Moshe, and Stacy Branch. 2016. “Gadolinium-Based Contrast Agent Toxicity: a Review of Known and Proposed Mechanisms.” *BioMetals* 29 (3). Springer Netherlands: 365–76. doi:10.1007/s10534-016-9931-7.

Roth, Megan, Amanda Obaidat, and Bruno Hagenbuch. 2012. “OATPs, OATs and OCTs: the Organic Anion and Cation Transporters of the SLCO and SLC22A Gene Superfamilies.” *British Journal of Pharmacology* 165 (5): 1260–87. doi:10.1111/j.1476-5381.2011.01724.x.

Rowitch, D., H, and Arnold R Kriegstein. 2010. “Developmental Genetics of Vertebrate Glial–Cell Specification.” *Nature* 468 (7321): 214–22. doi:10.1038/nature09611.

Ruckh, Julia M, Jing-Wei Zhao, Jennifer L Shadrach, Peter van Wijngaarden, Tata Nageswara Rao, Amy J Wagers, and Robin J M Franklin. 2012. “Rejuvenation of Regeneration in the Aging Central Nervous System..” *Cell Stem Cell* 10 (1): 96–103. doi:10.1016/j.stem.2011.11.019.

Sabri MI., Bone, AH., and Davison AN. 1974. “Turnover of Myelin and Other Structural Proteins in the Developing Rat Brain” *Journal of Biochemistry:* 142 499-507

Sacco, Alessandra, Regis Doyonnas, Peggy Kraft, Stefan Vitorovic, and Helen M Blau. 2008. “Self-Renewal and Expansion of Single Transplanted Muscle Stem Cells.” *Nature* 456 (7221): 502–6. doi:10.1038/nature07384.

Salic, Adrian, and Timothy J Mitchison. 2008. “A Chemical Method for Fast and Sensitive Detection of DNA Synthesis in Vivo..” *Proceedings of the National Academy of Sciences of the United States of America* 105 (7). National Academy of Sciences: 2415–20. doi:10.1073/pnas.0712168105.

Sandvig, Ioanna, Marte Thuen, Linh Hoang, Øystein Olsen, Thomas CP Sardella, Christian Brekken, Kåre E Tvedt, et al. 2011. “In Vivo MRI of Olfactory Ensheathing Cell Grafts and Regenerating Axons in Transplant Mediated Repair of the Adult Rat Optic Nerve.” *NMR in Biomedicine* 25 (4): 620–31. doi:10.1002/nbm.1778.

Sati, Pascal, Peter van Gelderen, Afonso C Silva, Daniel S Reich, Hellmut Merkle, Jacco A de Zwart, and Jeff H Duyn. 2013. “Micro-Compartment Specific T2∗ Relaxation in the Brain.” *NeuroImage* 77 (C). Elsevier B.V.: 268–78. doi:10.1016/j.neuroimage.2013.03.005.

Sawcer, Stephen, Robin J M Franklin, and Maria Ban. 2014. “Multiple Sclerosis Genetics..” *The Lancet Neurology* 13 (7): 700–709. doi:10.1016/S1474-4422(14)70041-9.

Scarfe, Lauren, Nathalie Brillant, J Dinesh Kumar, Noura Ali, Ahmed Alrumayh, Mohammed Amali, Stephane Barbellion, et al. 2018. “Preclinical Imaging Methods for Assessing the Safety Andefficacy of Regenerative Medicine Therapies.” *Npj Regenerative Medicine* 2017 (OCT). Springer US: 1–12. doi:10.1038/s41536-017-0029-9.

Schiepers, C, P Van Hecke, and R Vandenberghe. 1997. “Positron Emission Tomography, Magnetic Resonance Imaging, and Proton NMR Spectroscopy of White Matter in MS.” *Multiple Sclerosis* 3 (July): 1–10.

Schilling, Franz, Susana Ros, D-E Hu, Paula D'Santos, Sarah McGuire, Richard Mair, Alan J Wright, et al. 2016. “MRI Measurements of Reporter-Mediated Increases in Transmembrane Water Exchange Enable Detection of a Gene Reporter.” *Nature Publishing Group* 35 (1): 75–80. doi:10.1002/mrm.24395.

Schilling, Franz, Susana Ros, D-E Hu, Paula D'Santos, Sarah McGuire, Richard Mair, Alan J Wright, et al. 2017. “MRI Measurements of Reporter-Mediated Increases in Transmembrane Water Exchange Enable Detection of a Gene Reporter..” *Nature Biotechnology* 35 (1). Nature Publishing Group: 75–80. doi:10.1038/nbt.3714.

Schmierer, Klaus, Claudia A M Wheeler-Kingshott, Phil A Boulby, Francesco Scaravilli, Daniel R Altmann, Gareth J Barker, Paul S Tofts, and David H Miller. 2007. “Is the Magnetization Transfer Ratio a Marker for Myelin in Multiple Sclerosis?.” *NeuroImage* 35 (2). Elsevier Inc.: 467–77. doi:10.1016/j.neuroimage.2006.12.010.

Schmierer, Klaus, Daniel J Tozer, Francesco Scaravilli, Daniel R Altmann, Gareth J Barker, Paul S Tofts, and David H Miller. 2007. “Quantitative Magnetization Transfer Imaging in Postmortem Multiple Sclerosis Brain.” *Journal of Magnetic Resonance Imaging* 26 (1): 41–51. doi:10.1002/jmri.20984.

Scholzen, T, and J Gerdes. 2000. “The Ki-67 Protein: From the Known and the Unknown..” *Journal of Cellular Physiology* 182 (3). Wiley-Blackwell: 311–22. doi:10.1002/(SICI)1097-4652(200003)182:3<311::AID-JCP1>3.0.CO;2-9.

Seidl, A. H., Rubel, E. W., & Harris, D.M. 2010. “Mechanisms for adjusting interaural time differences to achieve binaural coincidence detection.” *The Journal of Neuroscience,* 30, 70–80. doi: 10.1523/JNEUROSCI.3464-09.2010.

Serafini, Barbara, Barbara Rosicarelli, Diego Franciotta, Roberta Magliozzi, Richard Reynolds, Paola Cinque, Laura Andreoni, et al. 2007. “Dysregulated Epstein-Barr Virus Infection in the Multiple Sclerosis Brain.” *The Journal of Experimental Medicine* 204 (12): 2899–2912. doi:10.1111/j.1600-0404.1996.tb07055.x.

Shi, J, A Marinovich, and B A Barres. 1998. “Purification and Characterization of Adult Oligodendrocyte Precursor Cells From the Rat Optic Nerve..” *Journal of Neuroscience* 18 (12): 4627–36.

Shivers, R R, C L Edmonds, and R F Del Maestro. 1984. “Microvascular Permeability in Induced Astrocytomas and Peritumor Neuropil of Rat Brain.” *Acta Neuropathologica* 64 (3). Springer-Verlag: 192–202. doi:10.1007/BF00688109.

Shu, X, A Royant, M Z Lin, T A Aguilera, V Lev-Ram, P A Steinbach, and R Y Tsien. 2009. “Mammalian Expression of Infrared Fluorescent Proteins Engineered From a Bacterial Phytochrome.” *Science* 324 (5928): 804–7. doi:10.1371/journal.pbio.0050077.

Sim, Fraser J, Chao Zhao, Jacques Penderis, and Robin J M Franklin. 2002. “The Age-Related Decrease in CNS Remyelination Efficiency Is Attributable to an Impairment of Both Oligodendrocyte Progenitor Recruitment and Differentiation..” *The Journal of Neuroscience : the Official Journal of the Society for Neuroscience* 22 (7): 2451–59.

Sim, Fraser J, Crystal R McClain, Steven J Schanz, Tricia L Protack, Martha S Windrem, and Steven A Goldman. 2011. “CD140a Identifies a Population of Highly Myelinogenic, Migration-Competent and Efficiently Engrafting Human Oligodendrocyte Progenitor Cells.” *Nature Biotechnology* 29 (10). Nature Publishing Group: 934–41. doi:10.1038/nbt.1972.

Simons, M., and Nave, K.,A. 2016 “Oligodendrocytes: Myelination and Axonal Support.” *Cold Spring Harbour Perspectives in Biol*ogy; 8:a020479

Simons M, Snaidero N, Aggarwal S. 2012. “Cell polarity in myelinating glia: From membrane flow to diffusion barriers.” *Biochemica et Biophysica Acta* 1821: 1146–1153 doi: 10.1016/j.bbalip.2012.01.011

Simpson, Steve, Leigh Blizzard, Petr Otahal, Ingrid Van der Mei, and Bruce Taylor. 2011. “Latitude Is Significantly Associated with the Prevalence of Multiple Sclerosis: a Meta-Analysis..” *Journal of Neurology, Neurosurgery & Psychiatry* 82 (10). BMJ Publishing Group Ltd: 1132–41. doi:10.1136/jnnp.2011.240432.

SkjÃrringe, Tina, Annette Burkhart, Kasper Bendix Johnsen, and Torben Moos. 2015. "Divalent Metal Transporter 1 (DMT1) in the Brain: Implications for a Role in Iron Transport at the Blood-Brain Barrier, and Neuronal and Glial Pathology." ***Frontiers in Molecular Neuroscience*** 8 (June): 41–13. doi:10.3389/fnmol.2015.00019.

Smith, K J, W F Blakemore, and W I McDonald. 1979. "Central Remyelination Restores Secure Conduction.." *Nature* 280 (5721): 395–96.

Smith ME, Eng LF. 1965. "The turnover of the lipid components of myelin." *Journal of the American Oil Chemists Society* 42: 1013–1018.

Smith, Peter M, and Nick D Jeffery. 2006. "Histological and Ultrastructural Analysis of White Matter Damage After Naturally-Occurring Spinal Cord Injury." *Brain Pathology* 16 (2). Wiley/Blackwell (10.1111): 99–109. doi:10.1111/j.1750-3639.2006.00001.x.

Snaidero N, Moebius W, Czopka T, Hekking LHP, Mathisen C, Verkleij D, Goebbels S, Edgar J, Merkler D, Lyons DA, Nave, KA, Simons M. 2014. "Myelin membrane wrapping of CNS axons by PI(3,4,5)P3-dependent polarized growth at the inner tongue." *Cell* 156: 277–290. oi: 10.1016/j.cell.2013.11.044.

Sobottka, Bettina, Urs Ziegler, Andres Kaech, Burkhard Becher, and Norbert Goebels. 2011. "CNS Live Imaging Reveals a New Mechanism of Myelination: the Liquid Croissant Model." *Glia* 59 (12): 1841–49. doi:10.1083/jcb.123.2.443.

Sofroniew, Michael V, and Harry V Vinters. 2009. "Astrocytes: Biology and Pathology." *Acta Neuropathologica* 119 (1): 7–35. doi:10.1201/b13439-63.

Song, Sheng-Kwei, Jun Yoshino, Tuan Q Le, Shiow-Jiuan Lin, Shu-Wei Sun, Anne H Cross, and Regina C Armstrong. 2005. "Demyelination Increases Radial Diffusivity in Corpus Callosum of Mouse Brain." *NeuroImage* 26 (1): 132–40. doi:10.1016/j.neuroimage.2005.01.028.

Song, Sheng-Kwei, Shu-Wei Sun, Michael J Ramsbottom, Chen Chang, John Russell, and Anne H Cross. 2002. "Dysmyelination Revealed Through MRI as Increased Radial (but Unchanged Axial) Diffusion of Water." *NeuroImage* 17 (3): 1429–36. doi:10.1006/nimg.2002.1267.

Song, Sheng-Kwei, Shu-Wei Sun, Won-Kyu Ju, Shiow-Jiuan Lin, Anne H Cross, and Arthur H Neufeld. 2003. "Diffusion Tensor Imaging Detects and Differentiates Axon and Myelin Degeneration in Mouse Optic Nerve After Retinal Ischemia." *NeuroImage* 20 (3): 1714–22. doi:10.1016/j.neuroimage.2003.07.005.

Sormani, Maria Pia, and Matteo Pardini. 2017. "Assessing Repair in Multiple Sclerosis: Outcomes for Phase II Clinical Trials," November. Neurotherapeutics, 1–10. doi:10.1007/s13311-017-0558-3.

Sprinkle, T., J. 1989. “2',3'-cyclic nucleotide 3'-phosphodiesterase, an oligodendrocyte-Schwann cell and myelin-associated enzyme of the nervous system.” Criticle Reviews Neurobiology. 1989;4(3):235-301.

Stanisz, Greg J, Ewa E Odrobina, Joseph Pun, Michael Escaravage, Simon J Graham, Michael J Bronskill, and R Mark Henkelman. 2005. “T1, T2 Relaxation and Magnetization Transfer in Tissue at 3T.” *Magnetic Resonance in Medicine* 54 (3). Wiley-Blackwell: 507–12. doi:10.1002/mrm.20605.

Stankoff, Bruno, Leorah Freeman, Marie-Stéphane Aigrot, Audrey Chardain, Frédéric Dollé, Anna Williams, Damien Galanaud, et al. 2011. “Imaging Central Nervous System Myelin by Positron Emission Tomography in Multiple Sclerosis Using [Methyl-11C]-2-(4’-Methylaminophenyl)- 6-Hydroxybenzothiazole.” *Annals of Neurology* 69 (4): 673–80. doi:10.1002/ana.22320.

Stevenson, Valerie L, Mary L Gawne-Cain, Gareth J Barker, Alan J Thompson, and D H Miller. 1997. “Imaging of the Spinal Cord and Brain in Multiple Sclerosis: a Comparative Study Between Fast Flair and Fast Spin Echo.” *Journal of Neurology* 244 (2). Springer-Verlag: 119–24. doi:10.1007/s004150050060.

Stidworthy, Mark F, Stephane Genoud, Ueli Suter, Ned Mantei, and Robin J M Franklin. 2003. “Quantifying the Early Stages of Remyelination Following Cuprizone-Induced Demyelination..” *Brain Pathology* 13 (3): 329–39.

Stuve, O, N P Dooley, J H Uhm, G S Francis, J P Antel, G Williams, and V Y Yong. 1996. “Interferon Beta-1b Decreases the Migration of T Lyphocytes in Vitro: Effects on MMP-9” 40 (January): 1–11.

Suzuki, Takahiro, Shinsuke Usuda, Hiroshi Ichinose, and Satoshi Inouye. 2007. “Real-Time Bioluminescence Imaging of a Protein Secretory Pathway in Living Mammalian Cells Using Gaussialuciferase.” *FEBS Letters* 581 (24): 4551–56. doi:10.1016/j.febslet.2007.08.036.

Takano, Akihiro, Fredrik Piehl, Jan Hillert, Andrea Varrone, Sangram Nag, Balázs Gulyás, Per Stenkrona, et al. 2013. “In Vivo TSPO Imaging in Patients with Multiple Sclerosis: a Brain PET Study with [18F]FEDAA1106..” *EJNMMI Research* 3 (1). SpringerOpen: 30. doi:10.1186/2191-219X-3-30.

Tannous, Bakhos A, Jan Grimm, Katherine F Perry, John W Chen, Ralph Weissleder, and Xandra O Breakefield. 2006. “Metabolic Biotinylation of Cell Surface Receptors for in Vivo Imaging.” ***Nature Methods*** 3 (5). Nature Publishing Group: 391–96. doi:10.1038/nmeth875.

Targett M, P, J Sussmant, M T O'Leary, A Compston, and W F Blakemore. 1996. *Failure to Acheive Remyalination of Demyelinated Rat Axons Follwing Transplantation of Glial Cells Obtained From Adult Human Brain*. Neuropathology and Applied Biology.

Taveggia, Carla, Antonella Pizzagalli, Ernesta Fagiani, Albee Messing, M Laura Feltri, and Lawrence Wrabetz. 2004. “Characterization of a Schwann Cell Enhancer in the Myelin Basic Protein Gene.” *Journal of Neurochemistry* 91 (4): 813–24. doi:10.1111/j.1471-4159.2004.02745.x.

Tillema, J_M.,, and I., Pirko. 2013. “Neuroradiological Evaluation of Demyelinating Disease..” *Therapeutic Advances in Neurological Disorders* 6 (4): 249–68. doi:10.1177/1756285613478870.

Timmler, Sebastian, and Mikael Simons. 2019. “Grey Matter Myelination.” *Glia* 28 (Pt 2). John Wiley & Sons, Ltd: 549–8. doi:10.1002/glia.23614.

Toledano, Michel, Brian G Weinshenker, and Andrew J Solomon. 2015. “A Clinical Approach to the Differential Diagnosis of Multiple Sclerosis.” *Current Neurology and Neuroscience Reports* 15 (8): 543. doi:10.1212/CPJ.0000000000000030.

Tomassy, Giulio Srubek. 2017. “How Big Is the Myelinating Orchestra? Cellular Diversity Within the Oligodendrocyte Lineage: Facts and Hypotheses,” January, 1–11. doi:10.3389/fncel.2014.00201/abstract.

Tomer, Raju, Li Ye, Brian Hsueh, and Karl Deisseroth. 2014. “Advanced CLARITY for Rapid and High-Resolution Imaging of Intact Tissues.” *Nature Protocols* 9 (7): 1682–97. doi:10.1016/S0006-3495(99)77063-3.

Trapp BD, Nishiyama A, Cheng D, Macklin W. 1997. “Differentiation and death of premyelinating oligodendrocytes in developing rodent brain.” *Journal of Cell Biology* 137: 459– 468.

Tripathi, R B, L E Clarke, V Burzomato, N Kessaris, P N Anderson, D Attwell, and W D Richardson. 2011. “Dorsally and Ventrally Derived Oligodendrocytes Have Similar Electrical Properties but Myelinate Preferred Tracts.” *Journal of Neuroscience* 31 (18): 6809–19. doi:10.1523/JNEUROSCI.6474-10.2011.

Tu, Tsang-Wei, Rashida A Williams, Jacob D Lescher, Neekita Jikaria, L Christine Turtzo, and Joseph A Frank. 2016. “Radiological-Pathological Correlation of Diffusion Tensor and Magnetization Transfer Imaging in a Closed Head Traumatic Brain Injury Model.” *Annals of Neurology* 79 (6). Wiley-Blackwell: 907–20. doi:10.1002/ana.24641.

Uhlenbrock, D, and S Sehlen. 1989. “The Value of T1-Weighted Images in the Differentiation Between MS, White Matter Lesions, and Subcortical Arteriosclerotic Encephalopathy (SAE).” *Neuroradiology* 31 (3). Springer-Verlag: 203–12. doi:10.1007/BF00344344.

Umemori H, Sato S, Yagi T, Aizawa S, Yamamoto T. 1994. “Initial events of myelination involve Fyn tyrosine kinase signalling.” *Nature* 367: 572–576.

Vallstedt, Anna, Joanna M Klos, and Johan Ericson. 2005. “Multiple Dorsoventral Origins of Oligodendrocyte Generation in the Spinal Cord and Hindbrain.” *Neuron* 45 (1): 55–67. doi:10.1016/j.neuron.2004.12.026.

Van Evercooren, A Baron, V Avellana Adalid, A Ben Younes-Chennoufi, A Gansmuller, B Nait Oumesmar, and L Vignais. 1996. “Cell-Cell Interactions During the Migration of Myelin-Forming Cells Transplanted in the Demyelinated Spinal Cord.” *Glia* 16 (2). Wiley-Blackwell: 147–64. doi:10.1002/(SICI)1098-1136(199602)16:2<147::AID-GLIA7>3.0.CO;2-0.

van Montfoort, J E, B Stieger, D K Meijer, H J Weinmann, P J Meier, and K E Fattinger. 1999. “Hepatic Uptake of the Magnetic Resonance Imaging Contrast Agent Gadoxetate by the Organic Anion Transporting Polypeptide Oatp1..” *The Journal of Pharmacology and Experimental Therapeutics* 290 (1): 153–57.

van Waesberghe, J H T M, W Kamphorst, C J A De Groot, M A A van Walderveen, J A Castelijns, R Ravid, G J Lycklama a Nijeholt, et al. 1999. “Axonal Loss in Multiple Sclerosis Lesions: Magnetic Resonance Imaging Insights Into Substrates of Disability,” October, 1–8.

Vellinga, Machteld M, Raoul D Oude Engberink, Alexandra Seewann, Petra J W Pouwels, Mike P Wattjes, Susanne M A van der Pol, Christiane Pering, et al. 2008. “Pluriformity of Inflammation in Multiple Sclerosis Shown by Ultra-Small Iron Oxide Particle Enhancement.” *Brain* 131 (3): 800–807. doi:10.1002/(SICI)1097-4547(19980601)52:5<549::AID-JNR7>3.0.CO;2-C.

Vignais, L, B Nait-Oumesmar, F Mellouk, O Gout, G Labourdette, A Baron-Van Evercooren, and M Gumpel. 1993. “Transplantation of Oligodendrocyte Precursors in the Adult Demyelinated Spinal Cord: Migration and Remyelination..” *International Journal of Developmental Neuroscience : the Official Journal of the International Society for Developmental Neuroscience* 11 (5): 603–12.

Wake H, Lee PR, Fields RD. 2011. “Control of local protein synthesis and initial events in myelination by action potentials.” *Science* 333: 1647–1651. doi: 10.1126/science.1206998

Wang, Yong, Qing Wang, Justin P Haldar, Fang-Cheng Yeh, Mingqiang Xie, Peng Sun, Tsang-Wei Tu, et al. 2011. “Quantification of Increased Cellularity During Inflammatory Demyelination.” *Brain* 134 (12): 3590–3601. doi:10.1016/j.neuroimage.2010.11.087.

Warf, Benjamin C, Juin Fok-Seang, and Robert H Miller. 1991. “Evidence for the Ventral Origin of Oligodendrocyte Precursors in the Rat Spinal Cord.” *Journal of Neuroscience*, September, 1–12.

Wáng, Yì Xiáng J, and Jean-Marc Idée. 2017. "A Comprehensive Literatures Update of Clinical Researches of Superparamagnetic Resonance Iron Oxide Nanoparticles for Magnetic Resonance Imaging." *Quantitative Imaging in Medicine and Surgery* 7 (1): 88–122. doi:10.21037/qims.2017.02.09.

Wei, Qiou, W Keith Miskimins, and Robin Miskimins. 2003. "Cloning and Characterization of the Rat Myelin Basic Protein Gene Promoter." ***Gene*** 313 (August): 161–67. doi:10.1016/S0378-1119(03)00675-9.

Weigert, Roberto, Natalie Porat-Shliom, and Panomwat Amornphimoltham. 2013. "Imaging Cell Biology in Live Animals: Ready for Prime Time." *The Journal of Cell Biology* 201 (7): 969–79. doi:10.1002/ar.1091200115.

Weissleder, Simonova, Bogdanova, Bredow, Enochs, Bogdanov, Jr (1997) "MR imaging and scintigraphy of gene expression through melanin induction." ***Radiology*** 204;7 doi.org/10.1148/radiology.204.2.9240530

Weissleder, Ralph, Anna Moore, Umar Mahmood, Rajeev Bhorade, Helene Benveniste, E Antonio Chiocca, and James P Basilion. 2000. "In Vivo Magnetic Resonance Imaging of Transgene Expression." ***Nature Medicine*** 6 (3). Nature Publishing Group: 351–54. doi:10.1038/73219.

White R, Gonsior C, Kramer-Albers EM, Stohr N, Huttelmaier S, Trotter J. 2008. "Activation of oligodendroglial Fyn kinase enhances translation of mRNAs transported in hnRNP A2-dependent RNA granules." *Journal of Cell Biology* 181: 579 – 586. doi: 10.1083/jcb.200706164.

Winklewski, Pawel J, Agnieszka Sabisz, Patrycja Naumczyk, Krzysztof Jodzio, Edyta Szurowska, and Arkadiusz Szarmach. 2018. "Understanding the Physiopathology Behind Axial and Radial Diffusivity Changes—What Do We Know?." *Frontiers in Neurology* 9 (February). Frontiers: 316–16. doi:10.3389/fneur.2018.00092.

Woodruff, Rachel H, and Robin J M Franklin. 1999. "Demyelination and Remyelination of the Caudal Cerebellar Peduncle of Adult Rats Following Stereotaxic Injections of Lysolecithin, Ethidium Bromide, and Complement/Anti-Galactocerebroside: a Comparative Study." *Glia* 25 (3). Wiley-Blackwell: 216–28. doi:10.1002/(SICI)1098-1136(19990201)25:3<216::AID-GLIA2>3.0.CO;2-L.

Woodruff, Rachel H, Marcus Fruttiger, William D Richardson, and Robin J M Franklin. 2004. "Platelet-Derived Growth Factor Regulates Oligodendrocyte Progenitor Numbers in Adult CNS and Their Response Following CNS Demyelination." *Molecular and Cellular Neuroscience* 25 (2): 252–62. doi:10.1016/j.mcn.2003.10.014.

Wren, D, G Wolswijk, and M Noble. 1992. "In Vitro Analysis of the Origin and Maintenance of O-2Aadult Progenitor Cells." *The Journal of Cell Biology* 116 (1): 167–76. doi:10.1083/jcb.116.1.167.

Wu, Qi, Kenji Ono, Hiromi Suzuki, Megumi Eguchi, Shun Yamaguchi, and Makoto Sawada. 2018. "Visualization of Arc Promoter-Driven Neuronal Activity by Magnetic Resonance Imaging." ***Neuroscience Letters*** 666 (February). Elsevier: 92–97. doi:10.1016/j.neulet.2017.12.041.

Xie, Mingqiang, Jennifer E Tobin, Matthew D Budde, Chin-I Chen, Kathryn Trinkaus, Anne H Cross, Dennis P McDaniel, Sheng-Kwei Song, and Regina C Armstrong. 2010. "Rostrocaudal Analysis of Corpus Callosum Demyelination and Axon Damage Across Disease Stages Refines Diffusion Tensor Imaging Correlations with Pathological Features." *Journal of Neuropathology & Experimental Neurology* 69 (7): 704–16. doi:10.1097/NEN.0b013e3181e3de90.

Yamout, Bassem, Roula Hourani, Haytham Salti, Wissam Barada, Taghrid El-Hajj, Aghiad Al-Kutoubi, Aline Herlopian, et al. 2010. "Bone Marrow Mesenchymal Stem Cell Transplantation in Patients with Multiple Sclerosis: a Pilot Study." *Journal of Neuroimmunology* 227 (1-2). Elsevier B.V.: 185–89. doi:10.1016/j.jneuroim.2010.07.013.

Yokoyama, Akiko, Aiko Sakamoto, Kenji Kameda, Yoshinori Imai, and Junya Tanaka. 2006. "NG2 Proteoglycan-Expressing Microglia as Multipotent Neural Progenitors in Normal and Pathologic Brains." *Glia* 53 (7). Wiley-Blackwell: 754–68. doi:10.1002/glia.20332.

Yoshida, Mika, and Wendy B Macklin. 2005. "Oligodendrocyte Development and Myelination in GFP-Transgenic Zebrafish." *Journal of Neuroscience Research* 81 (1). Wiley-Blackwell: 1–8. doi:10.1002/jnr.20516.

Young KM, Psachoulia K, Tripathi RB, Dunn SJ, Cossell L, Attwell D, Tohyama K, Richardson WD. 2013. "Oligodendrocyte dynamics in the healthy adult CNS: evidence for myelin remodeling." Neuron 77:873–85. doi: 10.1016/j.neuron.2013.01.006.

Zalc, B, D Goujet, and D Colman. 2017. "The Origin of the Myelination Program in Vertebrates." *Current Biology* 18 (12): 1–2.

Zappia, E. 2005. "Mesenchymal Stem Cells Ameliorate Experimental Autoimmune Encephalomyelitis Inducing T-Cell Anergy." *Blood* 106 (5): 1755–61. doi:10.1182/blood-2005-04-1496.

Zawadzka, Malgorzata, Leanne E Rivers, Stephen P J Fancy, Chao Zhao, Richa Tripathi, Françoise Jamen, Kaylene Young, et al. 2010. "CNS-Resident Glial Progenitor/Stem Cells Produce Schwann Cells as Well as Oligodendrocytes During Repair of CNS Demyelination." *Cell Stem Cell* 6 (6): 578–90. doi:10.1016/j.stem.2010.04.002.

Zhang, Chunchao, Angela K Walker, Robert Zand, Mario A Moscarello, Jerry Mingtao Yan, and Philip C Andrews. 2012. "Myelin Basic Protein Undergoes a Broader Range of Modifications in Mammals Than in Lower Vertebrates." *Journal of Proteome Research* 11 (10): 4791–4802. doi:10.1021/pr201196e.

Zhang, Hui, Andrew A Jarjour, Amanda Boyd, and Anna Williams. 2011. “Central Nervous System Remyelination in Culture — a Tool for Multiple Sclerosis Research.” *Experimental Neurology* 230 (1). Elsevier Inc.: 138–48. doi:10.1016/j.expneurol.2011.04.009.

Zhao, Chao, Padraig M Strappe, Andrew M L Lever, and Robin J M Franklin. 2003. “Lentiviral Vectors for Gene Delivery to Normal and Demyelinated White Matter.” *Glia* 42 (1): 59–67. doi:10.1002/glia.10195.

Zhao, Chao, Wen-Wu Li, and Robin J M Franklin. 2006. “Differences in the Early Inflammatory Responses to Toxin-Induced Demyelination Are Associated with the Age-Related Decline in CNS Remyelination.” *Neurobiology of Aging* 27 (9): 1298–1307. doi:10.1016/j.neurobiolaging.2005.06.008.

Zivadinov, Robert, and Thomas P Leist. 2006. “Clinical-Magnetic Resonance Imaging Correlations in Multiple Sclerosis.” *Journal of Neuroimaging* 15 (suppl 1): 10S–21S. doi:10.1046/j.1468-1331.2002.00476.x.

Zurkiya, Omar, Anthony W S Chan, and Xiaoping Hu. 2008. “MagA Is Sufficient for Producing Magnetic Nanoparticles in Mammalian Cells, Making It an MRI Reporter.” ***Magnetic Resonance in Medicine*** 59 (6): 1225–31. doi:10.1002/mrm.21606.

Appendices

Appendix 1: Active Clinical Trials

Appendix 2: MRI Gene Reporters

Appendix 3: Media Recipes

Appendix 4: Antibodies

Appendix 5: Expected Fragments from Restriction Digestions

Appendix 6: Promoter Sequences

1 Active Clinical Trials

Title	Status	Intervention	Location	Clinical Trials Identifier
Nanocrystalline Gold to Treat Remyelination Failure in Chronic Optic Neuropathy In Multiple Sclerosis	Not yet recruiting	Drug: CNM-Au8 (A gold nanocrystal suspension)	University of Sydney	NCT03536559
Impact of Vitamin D Supplementation in Patients With Multiple Sclerosis	Recruiting	Drug: Vitamin D	•University Medical Centre Maribor, Maribor, Slovenia	NCT03385356
Allogenic Mesenchymal Stem Cells And Physical Therapy for MS Treatment	Recruiting	Biological: Umbilical cord derived Mesenchymal Stem Cells - intrathecally	•Cell Therapy Center, University of Jordan, Amman, Jordan •Cell Therapy Center, Amman, Jordan	NCT03326505
Safety Study of Human Neural Stem Cells Injections for Secondary Progressive Multiple Sclerosis Patients	Active, not recruiting	Biological: hNSC - intraventricular	IRCCS, Italy Azienda OSMdT, Italy Neurocentro della Svizzera Italiana, Switzerland	NCT03282760
Neural Stem Cell Transplantation in Multiple Sclerosis Patients	Enrolling by Invitation	Biological: fetal derived hNSC - intrathecally	IRCCS Ospedale San Raffaele, Milan. Italy	NCT03269071
Effect of MD1003 in Progressive Multiple Sclerosis (SPI2)	Active not recruiting	Drug: MD1003 *(high dose biotin)*	MedDay Pharmaceuticals, San Francisco	Nct02936037

Thyroid Hormone for Remyelination in Multiple Sclerosis (MS): A Safety and Dose Finding Study	Recruiting	Liothyronine Sodium	Oregon Health and Science University. Oregon. USA	NCT 02760056
Pilot Trial of Domperidone in Relapsing-Remitting Multiple Sclerosis (RRMS)	Enrolling by invitation	Drug: Domperidone, D2 anatagonist	University of Calgary Canada	NCT02493049
Domperidone in Secondary Progressive Multiple Sclerosis (SPMS)	recruiting	Drug: Domperidone, D2 anatagonist	University of Calgary Canada	NCT02308137
Effect of MD1003 in Spinal Progressive Multiple Sclerosis	Active not recruiting	Drug: MD1003 100mg capsule	Hopital Maison Blanche, Reims, France	NCT02220933
Effect of MD1003 in Chronic Visual Loss Related to Optic Neuritis in Multiple Sclerosis	Active not recruiting	Drug: MD1003 100mg capsule	Hopital Maison Blanche	NCT02220244
Safety and Tolerability of Quetiapine in Multiple Sclerosis	Recruiting	Drug: Extended-release quetiapine fumarate	University of Calgary	NCT02087631
Idebenone for Primary Progressive Multiple Sclerosis	Enrolling by invitation	Drug: Idebenone	National Institutes of Health Clinical Center,	NCT01854359
Role of Vitamin D in Reducing the Relapse Rate in Patients With Multiple Sclerosis	Unknown	Supplemented VitD3	King Saud University.	NCT01753375
Mesenchymal Stem Cells for Multiple Sclerosis	Unknown	Bone marrow mesenchymal stem cells autologous	Karolinska Insitute	NCT01730547

Vitamin D Supplementation in Multiple Sclerosis	Recruiting	Drug: Vitamin D3	Johns Hopkins University	NCT01490502
Cytotron® Delivered Rotational Field Quantum Nuclear Magnetic Resonance Therapy for Multiple Sclerosis	Unknown	Cytotron	The Centre for Advanced Research & Development, India.	NCT01220830
Double Blind Placebo-Controlled Phase I/II Clinical Trial of Idebenone in Patients With Primary Progressive Multiple Sclerosis (IPPoMS)	Active not Recruiting	Drug: Idebenone small molecule analogue of CoEnzyme Q10 - antioxidant	National Institutes of Health Clinical Center	NCT00950248
Mesenchymal Stem Cells for the Treatment of MS	unknown	Biological: Autologous Bone Marrow Transplantation - intrathecal	Hadassah University Hospital, Ein Kerem, Jerusalem, Israel	NCT00781872
Stem Cell Therapy for Patients With Multiple Sclerosis Failing Alternate Approved Therapy- A Randomized Study	Active, not recruiting	Biological: Autologous Bone Marrow Transplantation	Northwestern University, Feinberg School of Medicine	
Neurologic Stem Cell Treatment Study	Recruiting	Procedure: Intravenous BMSC •Procedure: Intranasal BMSC	The Healing Institute, Margate, Florida, United States Al Zahra Hospital, Dubai, United Arab Emirates	NCT02795052
Outpatient Hematopoietic Grafting in Multiple Sclerosis Employing Autologous Peripheral Blood Stem Cells	Enrolling by invitation	Procedure: Hematopoietic stem cell transplantation	-	NCT02674217

Multiple Sclerosis - Simvastatin Trial 2	Recruiting	Drug: Simvastatin *disease modifying anti cholesterol medication*	University College London	ISRCTN82598726
MINERAL (Magnetic-resonance Image of Nutraceutical Efficacy on Relapsing-ms Autoimmune Lesions) study: a novel nutraceutical formula NEUROASPIS PLP10® for the treatment of relapsing-remitting multiple sclerosis	Active, not recruitign	Drug: NEUROASPIS PLP10: *proposed disease modifying neutraceutical*	The Cyprus Institute of Neurology and Genetics Nicosia	ISRCTN06166891
Cell Based therapies delivered by Intravenous Infusion				
Autologous Bone Marrow Derived Stem Cells for the Treatment of Multiple Sclerosis.	Active, not recruiting	Biological: Stem Cell Transplantation	Chicago, Illinois, United States, 60611	NCT03069170
Allogeneic Stem Cell Transplantation for the Treatment of Multiple Sclerosis	Active, not recruiting	Biological: Autologous Bone Marrow Transplantation	University of Louisville	NCT00497952
Safety and Efficacy of Umbilical Cord Mesenchymal Stem Cell Therapy for Patients With Progressive Multiple Sclerosis and Neuromyelitis Optica	Unknown	Biological: human umbilical cord mesenchymal stem cells	Nanjing University Medical College Affiliated Drum Tower Hospital	NCT01364246
Mesenchymal Cells From Autologous Bone Marrow, Administered Intravenously in Patients Diagnosed With Multiple Sclerosis	Recruiting	Bone marrow mesenchymal stem cells autologous	University Regional Hospital Carlos Haya	NCT01745783
Assessment of Bone Marrow-derived Cellular Therapy in Progressive Multiple Sclerosis (ACTiMuS)	Recruiting	Biological: Autologous Bone Marrow Transplantation	North Bristol NHS Trust	NCT01815632

Safety and Efficacy of an Immunoablative Nonmyeloablative Conditioning Protocol for Autologous Bone Marrow Transplantation (BMT) in Patients With Multiple Sclerosis (MS)	Unknown	Biological: Autologous Bone Marrow Transplantation	Hadassah University Hospital, Ein Kerem, Jerusalem, Israel	NCT02529839
Autologous Mesenchymal Stromal Cells for Multiple Sclerosis	Active not recruiting	Biological: BM-MSC	Hospital Vall Hebron Barcelona, Spain,	NCT02495766
MEsenchymal StEm Cells for Multiple Sclerosis	Recruiting	Mesenchymal stem cells	Purpan Hospital Toulouse, France	NCT02403947
Reduced-intensity Immunoablation and Autologous Hematopoietic Stem Cell Transplantation (AHSCT) for Multiple Sclerosis	Recruiting	Autologous haematopeitic stem cells	Makati Medical Centre, Phillipines	NCT 03113162
Repeat Infusion of Autologous Bone Marrow Cells in Multiple Sclerosis	Active not recruiting	Biological: Autologous Bone Marrow Transplantation	University Bristol North Birstol NHS trust	NCT01932593
Safety and Efficacy of BMMNC in Multiple Sclerosis (MS)	Unknown	Biological: Autologous Bone Marrow Transplantation	Chaitanya Hospital	NCT01883661
MEsenchymal StEm Cells for Multiple Sclerosis	Unknown	Biological: Autologous Bone Marrow Transplantation	University of Genova	NCT01854957
Tolerogenic Dendritic Cells as a Therapeutic Strategy for the Treatment of Multiple Sclerosis Patients (TOLERVIT-MS)	recruiting	VitD3 tolerogenic monocyte derived dendritic cells loaded with myelin peptides	Hospital Universitari Germans TRias, Barcelona, Spain.	NCT 02903537

- Source: NIH www.ClinicalTrials.gov

Search Criteria : Multiple Sclerosis

Inclusion Criteria :

Status : Recruiting, Not Yet Recruiting, Active Not Recruiting, Enrolling by invitiaion, Unknown Status
Study Type: Interventional (clinical Trial)
Age: Adult
Sex: All
Therapy: Cell Transplants, Pro regenerative, remyelination therapies

Exlusion Criteria:

Status: Trial Suspended, Terminated, Completed, Withdrawn
Study Type: Observational, Patient register
Age: Under 17years old, Over 65 years old
Therapy: Anti Inflammatory treatment, Immunomodulatory

-Source: www.isrctn.com

Search Criteria: Multiple Sclerosis

Inclusion Criteria:

Status: Ongoing
Study Type: Interventional (Clinical Trial)
Age: Adult
Sex: All
Therapy: Cell Transplants, Pro-regenerative, remyelination therapies

2. MRI Reporter Genes

Gene Reporter	Substrate	Form of Contrast	Affect on Contrast	Promoter	Vector	Limitations	Source
Creatinine Kinase	Phospho-Creatinine Endogenous or supplemented	^{31}Phosphorous NMR	23 fold increase in Phosphocreatine/ATP peaks in comparison to *in vivo* control	Transthyretin Liver specific promoter	Plasmid	Spectroscopy therefore low resolution and specificity	(Koretsky et al. 1990)
Tyrosinase	Endogenous Iron	T_2	1.35 fold increase *in vivo*	Cytomegalovirus	Plasmid	Low contrast levels	(Weissleder *et al* 1997)
Transferrin Receptor	Iron Oxide Nano Particles	T_2	5.3 fold decrease in signal (AU) in vivo	hTR	Plasmid	Negative Contrast	(Weissleder et al. 2000)
LacZ	EGadMe	T_1	57% enhancement *in vivo*	-	mRNA	Intracellular injection	(Louie et al. 2000)
Arginine Kinase	Endogenous Argenine	^{31}Phosphorous NMR	50% increase *in vivo*	Cytomegalovirus	Adenovirus	Spectroscopy therefore low resolution and specificity. Takes 12-13 days to achieve expression	(Walter, Barton, and Sweeney 2000)
Transferrin Receptor	Iron Oxide Nano Particles	T_2	2.4 fold decrease in T2	Tet-Off	Plasmid	Negative Contrast	(Moore *et al* 2001)
Creatinine Kinase	Phospho-Creatinine Endogenous or supplemented	^{31}Phosphorous NMR	-	Cytomegalovirus	Adenovirus	Spectroscopy therefore low resolution and specificity	(Auricchio et al. 2001)
Tyrosinase	Endogenous Iron	T_2/ T_1	36% decrease in T2, 26% increase in T1 in vivo	Cytomegalovirus	Plasmid	Negative Contrast	(Alfke *et al* 2003)
Ferritin	Endogenous Iron	T_2	12% increate in $(T_2)^{-1}$	Tet-Off	Plasmid	Negative Contrast	(Cohen et al. 2005)

Gene Reporter	Substrate	Form of Contrast	Affect on Contrast	Promoter	Vector	Limitations	Source
Ferritin	Endogenous Iron	T_2	2.5 fold increase in R2 in vitro	Cytomegalovirus	Adenovirus	Negative Contrast	(Genove et al. 2005)
LacZ	2-Fluoro-4-nitrophenol-β-d-galactopyranoside (OFPNPG)	^{19}Fluorine	-	Cytomegalovirus	Plasmid	Substrate directly injected in to tissue	(Kodibagkar et al. 2006)
Ferritin & Transferrin Receptor	Supplemented Iron	T_2	21% increate in $(T_2)^{-1}$ ex vivo	SV-40	Plasmid	Negative contrast, Requires electroporation	(Deans et al. 2006)
Biotinalated Acceptor Peptides for cell surface receptors	bis-5-HT- DTPA(Gd) / Streptavidin-MNP / streptavidin– Alexa 680	T_2/ T_1	2 fold increase in R2, 3.3 fold R1	Cytomegalovirus	Lentivirus	Study only reports an n of 1	(Tannous et al. 2006)
Vacuolar Transporter Chaperone	Inorganic polyphosphates	^{31}Phosphorous NMR	-	Gal 1	Plasmid	Spectroscopy therefore low resolution and specificity. Non mammalian cells used	(Ki 2006)
LacZ	OFPNPG	^{19}Fluorine	SNR 20-30 (after direct injection into tumour)	Cytomegalovirus	Plasmid	Spectroscopy therefore low resolution and specificity.	(Liu et al. 2007)
Lysine Rich Protein	Endogenous contrast	Chemical Exchange Saturation Transfer	8.2% enhancement vs 3.5 % for control	Cytomegalovirus	Plasmid	Low signal to noise ratio	(Gilad et al. 2007)
Mag A	Supplemented Iron	T_2	3-4 fold increase in $(T_2)^{-1}$ *in vitro*	Cytomegalovirus	Lentivirus	Negative Contrast	(Zurkiya, Chan, and Hu 2008)
Carboxypeptidase G2	Hyperpolarised 3,5-DFBGlu	^{13}Carbon NMR	-	-	-	Experiments done in solution	(Jamin et al. 2009)

Gene Reporter	Substrate	Form of Contrast	Affect on Contrast	Promoter	Vector	Limitations	Source
LacZ	S-Gal	T_2	3.5 fold decrease in signal	Cytomegalovirus	Plasmid	Negative Contrast. Substrate directly injected in to tissue	(Cui et al. 2010)
Amino-Acylase	hyper-polarised [1-13C]N- Acetyl-L-methionine	^{13}Carbon NMR	-	Cytomegalovirus	pcDNA 3.1	No evidence can work in vivo	(Chen et al. 2010)
LacZ	S-Gal & ^{19}Fluorine S-Gal	^{19}Fluorine T_2	36% increase in R2, (intratumoural injection) 19F didn't work in vivo	Cytomegalovirus	Plasmid	Uses direct intratumoural injection, and low contrast levels	(Yu et al. 2012)
Membrane bound Biotinylated G.luciferase	^{111}Indium-DTPA-biotin, coelenterazine, magnetic nanoparticles	T2, PET, bio-luminescence	2 fold increase in $(T_2)^{-1}$ *in vivo*	Cytomegalovirus	Lentivirus	Negative contrast T2 enhancement is seen in absence of contrast agent, suggesting necrosis.	(Niers et al. 2012)
DMT1	Manganese Chloride	T_1	1.6-1.8 fold increase in R1	CAG	Plasmid and Lentivirus	Systemic background MnCl potentially toxic	(Bartelle et al. 2012)
HSV-TK	5-methyl-5,6-dihydrothymidine	CEST	Change of 2% in magnetization Transfer Ratio	Cytomegalovirus	Lentivirus	Minimal change, MTR variable across machines etc.	(Bar-Shir et al. 2013)
OATP1a1	gadoxetate	T1	6.8 fold increase in signal	PGK	Lentivirus	Uses linear Gd3+chealtor associated with basal ganglia accumulation	(Patrick et al. 2014)
Timd2	Manganese Apoferrtin	T1 and T2	3 fold increase in R1 in vivo and doubling of R2	Phosphoglycerate Kinase	Lentivirus	Manganese loaded ferrtin is toxic	(Patrick et al. 2016)
Ferritin	Supplemented iron	T2 and r2	-	Ubiquitin	Lentivirus with Tet-on	Negative contrast	(He et al. 2016)

3. Media Recipes

8.3i HALF

5L solution:

150.1mg Glycine (Sigma; G6201),

9.8MG L-ALANINE L-Arginine hydrochloride (Sigma; A92600),

4.12mg L- Asparagine-H2O (Sigma; A0884),

12.06mg L-Cysteine hydrochloride-H_2O (Sigma; C7880),

209.6mg L-Histidine hydrochloride-H_2O (Sigma; H8125),

526.1mg L- Isoleucine (Sigma; I2752),

526.1mg L-Leucine (Sigma; L8000),

583.3mg L-Lysine hydrochloride (Sigma; L5626),

149.9mg L-Methionine (Sigma; M9625),

330.4mg L- Phenylalanine (Sigma; P2126),

38.569 L-Proline (Sigma; P0380),

210mg L-Serine (Sigma; S4500),

474.8mg L-Threonine (Sigma; T8625),

79.6mg L-Tryptophan (Sigma; T0254),

360.6mg L-Tyrosine disodium salt dihydrate (Sigma; T1145),

470.6mg L-Valine (Sigma; V0500),

19.55mg Choline Chloride (Sigma; 26980),

9.53mg D-Calcium pantothenate (Sigma; C8731),

18.3mg Niacinamide (Sigma; 1462006),

20.6mg Pyridoxine hydrochloride (Sigma; P9755)

420.7MG Pyridoxine hydrochloride (Sigma; P9755),

16.9mg Thiamine hydrochloride (Sigma; T4625),

36mg i-Inositol (Sigma; I5125),

0.5mg Ferric Nitrate (Sigma; 254223),

1997.9MG Potassium Chloride (Sigma; P3911),

369.9 Sodium Bicarbonate (Sigma; S5761),

25810mg Sodium Chloride (Sigma; S9888),

543.6mg Sodium Phosphate dibasic anhydrous (Sigma; 71640),

0.9633mg Zinc Sulfate (Sigma; Z4750),

22525mg D-Glucose (Sigma; g8270),

124.9 Sodium Pyruvate (Sigma; P2256),

13465mg MOPS (Sigma M1254).

Media was pH adjusted to 7.30 and filtered sterilized (Millipore; SCVPU02RE).

8.3ii SATO

50mL of SATO Stock Solution:

50mL DMEM/F12,

33mg/mL BSA fraction V (Sigma; A4919),

4µg/mL Selenite (Sigma; S5261),

1.61 mg/mL Putrescine (Sigma; P7505),

4µg/mL Progesterone (Sigma; P0130).

8.3iii Miltenyi Washing Buffer (modified)

500ml of modified MWB:

PBS (Thermo Fisher; 70011-044),

5ml (2mM final concentration) Na-Pyruvate (Life Technologies 11360-039)

0.2ml (2mM final concentration) EDTA (Thermo Fisher; 15575-020),

10µg/mL Insulin (Thermo Fisher 12585-014)

0.5% BSA

8.3iv nOPC media

100mL solution:

95.4mL of DMEM/F12 (Thermo Fisher; 11039-021),

2mL (1.5mM final concentration) Na-Pyruvate (Thermo Fisher; 11360-070),

5mg (50ug final concentration)Apo-Transferrin (Sigma; T2036),

1.35mL 10% D(+)Glucose (25mM final concentration) (Sigma; G8644),

1mL SATO Stock Solution (*see 8.3ii)*,

10ug/ml Insulin (Thermo Fisher; 12585-014).

8.3v Slice Culture Media

250mL solution:

120ml BME (Life Technologies 21010046)

60ml HBSS (Life Technologies 24020-091)

60ml Heat Inactivated Horse Serum

2.5ml 100x Glutamax (Life Technologies 35050)

7ml 10%D(+)Gluose (Sigma G8644)

0.5ml Mycozap (Lonza V2A2021)

8.3vi Mixed Glia Media

(Per 500mL solution)

50ml Fetal Bovine Serum (Biosera 280010)

5ml PenStrep (Sigma P4333)

445ml DMEM (Life Technologies 41966029)

8.3vii Selective LB Broth

Per 500ml

LB Broth (Thermo Fischer **10855021)**

100ug/ml Ampicillin

8.3viii LB Selective Agar Plates

For 1L of microbial culture media :

35g LB Agar (Sigma: L2897)

1L dH_2O

Autoclave solution at 121°C for 15 minutes

Cool 40°C then add 100ug/ml Ampicillin (Sigma A0166)

8.3ix Dissociation solution (MACS)

4ml/brain

4mL HALF (*see 8.3i*)

2mM Pyruvate (Life Technologies 11360-039)

2%B27 (Thermo Fisher 17504-001)

34units/mL filtered Papain (Worthington LS003126)

20ug/ml DNAse

8.3x Dissociation Solution (Mixed Glia)

3ml per T75 flask

1 :100 DNAase

1 :500 Papain

3ml HALF

8.3xi Cryoprotectant Solution

per 1L solution :

300g Sucrose (Sigma S9378)

10g Polyvinylpyrrolidone (Sigma PVP40)

500ml of 0.1M Phosphate Buffer (Sigma P5244)

300ml Ethylene Glycol (Merck 109621)

8.4 Antibodies Used

8.4i In vitro staining:

Primaries

Antibody	Concentration	Source
A2B5 (mouse)	1:500	Millipore (MAB312)
Cd11b (mouse)	1:500	Serotec MCA275R)
CNPase (mouse)	1:400	Abcam (6319)
GFAP (rabbit)	1:2000	Dako (Z0334)
NG2	1:200	Millipore MAB5384
MBP (rat)	1:500	Serotec (MCA409S)
O4	1:1000	Millipore 1326
Olig2	1:500	Millipore (AB9610)
RFP (rabbit)	1:1000	Abcam ab34771
Sox10 (goat)	1:500	Santacruz SC17342

Secondaries

Antibody	Concentration	Source
Alexa 488 donkey α goat	1:500	Life technologies (A1055)
Alexa 488 donkey α mouse	1:500	Life technologies (A21202)
Alexa 647 donkey α goat	1:500	Life technologies (A21147)
Alexa 594 donkey α rabbit	1:500	Life technologies (A21207)
Alexa 488 donkey α chicken	1:500	Life technologies (A11039)
Alexa 488 donkey anti rat	1:500	Life technologies (A21208)
Alexa 647 donkey α mouse	1:500	Life technologies (A31571)
Alexa 594 (streptavidin)	1:500	Life technologies (S32356)

8.4ii Organotypic Slice Culture Staining

Primaries

Antibody	Concentration	Source
CC1 (rabbit)	1:200	Abcam (15270)
CNPase (mouse)	1:400	Abcam (6319)
GFAP (rabbit)	1:2000	Dako (Z0334)
MBP (rat)	1:500	Serotec (MCA409S)
Neurofilament (mouse)	1:1000	Sigma (N5389)
Sox10 (goat)	1:200	Santacruz SC17342

Secondaries

Antibody	Concentration	Source
Alexa 488 donkey α goat	1:500	Life technologies (A1055)
Alexa 647 donkey α goat	1:500	Life technologies (A21147)
Alexa 594 donkey α rabbit	1:500	Life technologies (A21207)
Alexa 488 doneky anti rat	1:500	Life technologies (A21208)
Alexa 647 donkey α mouse	1:500	Life technologies (A31571)
Alexa 594 (streptavidin)	1:500	Life technologies (S32356)

5. Predicted digestion products from restriction digests of plasmids

	EcoR1	BamH1	Hind3	Nde1	Nco1	Pvu2	PsT1	Bgl1	EcoR1/Hind3	BH1	Bspe1
PGK:OATP:mSt					3.4/3/3/1.7/0.2		8.8/1.5/0.4/0.8				7.2/4.3
MBP:OATP:mSt					*		*				*
pMDL	4.4/4.3/0.4	8/0.8	3.8/3.6/0.9/0.6								
RSV-Rec						2.9/1.3		2.6/1.6	3.1/0.6/0.3		
VSVG	4.1/1.7			3.6/1.5/0.6	3.8/1.5/0.5						

6. Promoter Sequences

6i PGK Promoter:

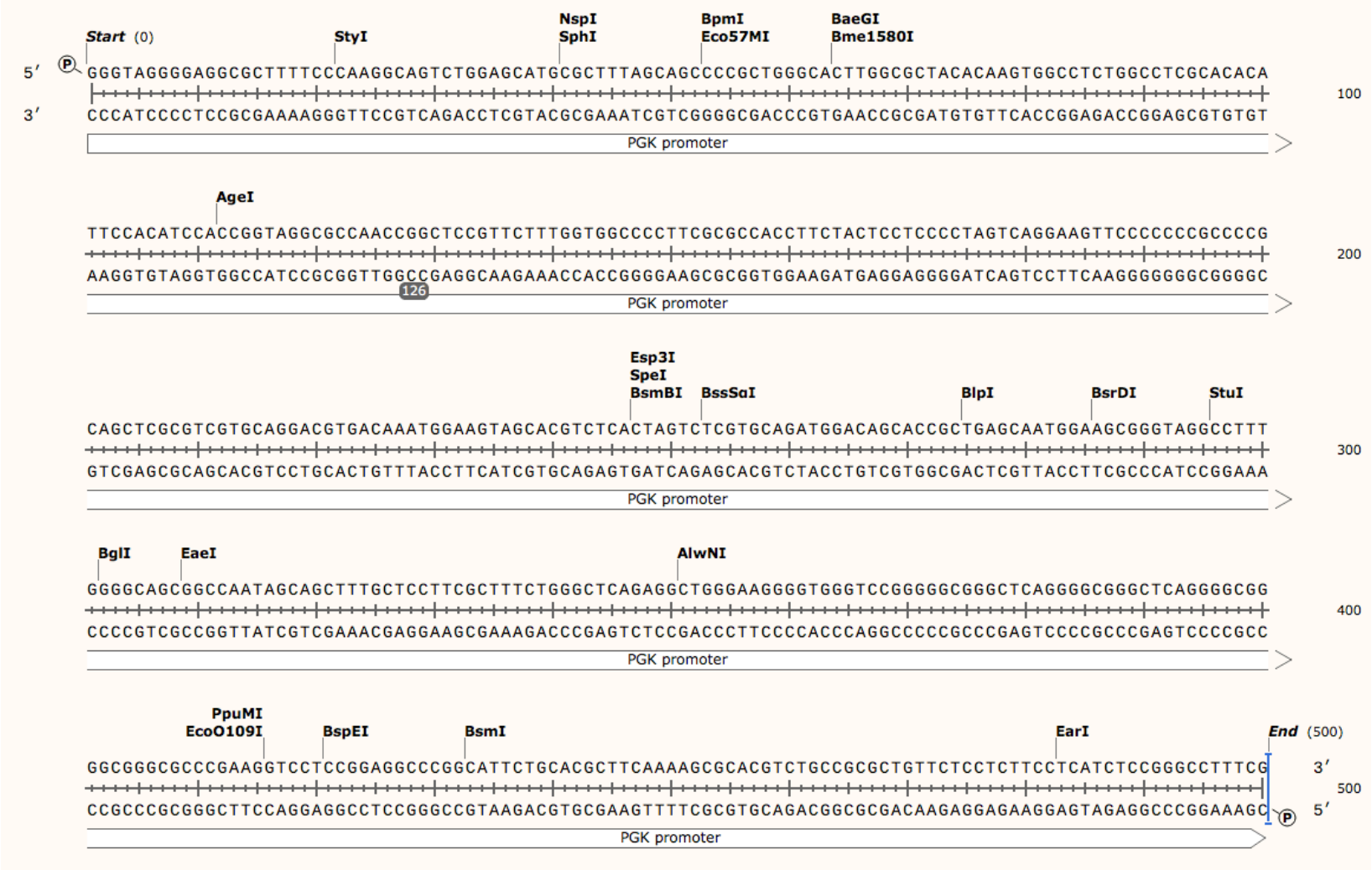

6ii MBP Promoter: